

博士論文

論文題目 Curved Shell Plates'
 Manufacturing Support Framework
(曲がり外板の加工支援フレームワークに関する研究)

氏 名 孫 晶 鈺

(余白)

Content Table

PART I INTRODUCTION AND STATE	21
Chapter 1 Introduction	24
1.1. Background	24
1.1.1. Two-stages manufacturing process of curved shell plate	26
1.1.2. Problems in traditional manufacturing process and possible approaches	31
1.1.3. Problems in OJT knowledge dissemination	33
1.2. Objective.....	34
1.3. Approach	36
1.4. Outline	38
Chapter 2 Related researches	40
2.1. Overview	40
2.2. Curved shell plates' accuracy evaluation system using laser scanners.....	40
2.2.1. System overview.....	40
2.2.2. Problems existing in measurement flow and evaluation standard	42
2.3. Researches on curved shell plate's manufacturing	45
2.3.1. Full automatic machining process of curved shell plate	45
2.3.2. Problems existing in full automatic machining.....	47
2.4. Researches on usage of laser scanner and point cloud data	47
2.4.1. Surface extraction from the point cloud data	49
2.4.2. Surface registration of the point cloud data	52
2.4.3. Problems existing in laser scanner's practical usage in shipyard	52
2.5. Researches on knowledge elicitation and dissemination.....	53
2.5.1. Knowledge elicitation: progresses, interfaces.....	53
2.5.2. Knowledge dissemination: interfaces, storages.....	55
2.5.3. Problems of knowledge elicitation and dissemination in manufacturing.	58
2.6. Originalities of this thesis	58

Chapter 3 Component technologies	60
3.1. Overview	60
3.2. 3D measurement equipment and features.....	60
3.2.1. Laser scanner	60
3.2.2. Kinect	61
3.2.3. Point cloud data	62
3.3. Point cloud processing	63
3.3.1. Edge detection	63
3.3.2. Region growing.....	64
3.3.3. k-Nearest Neighbor.....	65
3.3.4. Plane fitting.....	66
3.3.4.1. Basic plane fitting.....	67
3.3.4.2. Weighted plane fitting	69
3.3.5. Curve fitting.....	71
3.3.5.1. Lagrange interpolation.....	72
3.3.5.2. B-Spline interpolation	73
3.3.6. Iterative closest point.....	75
3.3.7. Real object’s virtualization and selection using polygons	76
3.3.8. Curvature estimation.....	79
3.4. Knowledge engineering.....	80
3.4.1. Ripple down rules.....	80
PART II PROPOSAL AND CONTRIBUTION.....	82
Chapter 4 Curved shell plate’s manufacturing support framework	85
4.1. Investigation and problem clarification during traditional manufacturing....	85
4.1.1. Strategy of this study.....	85
4.1.2. Interview on the traditional manufacturing process	86
4.1.3. Problems existing in the conventional manufacturing process	89
4.2. Supported manufacturing process.....	90
4.3. Layout of the proposed framework.....	94
4.3.1. Requirement definition	94

4.3.2.	Problem definition for common pre-processing	98
4.3.3.	Problem definition for cold forming supporting	99
4.3.4.	Problem definition for heating forming supporting	101
4.3.5.	Problem definition for knowledge elicitation and dissemination.....	104
4.3.6.	Automation of measurement and analysis flow	106
4.4.	Software architecture of the proposed framework	106
Chapter 5 Common pre-processing		109
5.1.	Measured data with irregular obstacles and variable density	109
5.2.	Overview of curved shell plate's measurement	110
5.2.1.	Plate extraction prototype	110
5.2.1.1.	Continuous domain extraction	111
5.2.1.2.	Separated domain recognition.....	112
5.2.2.	Originalities for higher speed and lower failure	113
5.3.	Float region growing candidate selecting and plane fitting	115
5.4.	Weighted normal vector calculation considering point cloud's density	117
5.5.	Judgment standards of the common domain recognition	118
5.6.	Registration method with direction pre-setting.....	121
5.7.	Development of MS.....	124
5.8.	Summary.....	125
Chapter 6 Cold forming supporting		127
6.1.	Overview of the cold forming supporting framework.....	127
6.2.	Pre-process and registration.....	129
6.3.	Press evaluation method	130
6.4.	Perimeter evaluation method	131
6.5.	Development of PSS.....	132
6.6.	Summary.....	133
Chapter 7 Heating forming supporting		135
7.1.	Overview of the heating forming supporting framework.....	135
7.1.1.	Virtual template prototype	137
7.1.1.1.	Virtual template generating.....	138

7.1.1.2.	Registration of the virtual template and plate's point cloud	140
7.1.1.3.	Curvature error calculation.....	140
7.1.2.	Originalities for the practical usage in shipyard	142
7.2.	Automatic template arrangement method.....	143
7.3.	Curvature error based heating grade suggesting	146
7.4.	Development of VTS	147
7.4.1.	2D roller line's matching with 3D design data	147
7.4.2.	User interface of VTS.....	150
7.5.	Summary.....	154
Chapter 8 Knowledge elicitation and dissemination		156
8.1.	Overview of the manufacturing knowledge management	156
8.2.	Raw knowledge interrelated database	160
8.3.	Knowledge base design.....	160
8.4.	Knowledge elicitation process.....	161
8.5.	Knowledge dissemination process	164
8.6.	Development of KBS	165
8.7.	Summary.....	166
PART III EVALUATION		168
Chapter 9 Evaluation of common pre-processing		172
9.1	Overview	172
9.1	Experiment configuration.....	173
9.2	Evaluation of component extraction.....	174
9.2.1.1.	Extraction of the plates which are divided by wooden templates	176
9.2.1.2.	Extraction of the plates which are divided by worker's shadow	177
9.2.1.3.	Extraction of the plates which are divided by wires and hoses.....	178
9.2.1.4.	Extraction of the plates which are divided by water and other obstacles 179	
9.2.1.5.	Relationship between the section curves and the data.....	180
9.2.2.	Weighted region growing evaluation	181
9.2.3.	Extraction effectiveness and efficiency analysis	182

9.3	Evaluation of component registration	183
9.3.1.	Comparison of the proposed method and the general methods	183
9.3.2.	Registration of the plate' point cloud with defects	184
9.3.2.1.	Registration of plate with small defects	185
9.3.2.2.	Registration of plate with big defects	186
9.4	Summary	188
Chapter 10	Cold forming support experiment	190
10.1.	Overview of cold forming support experiment	190
10.2.	Experiment design	192
10.3.	Experiment configuration in shipyard	194
10.4.	Experiment 1 : Plate "Regular 1"	199
10.4.1.	Plate measurement	199
10.4.2.	Press Evaluation Result	200
10.4.2.1.	Plate 1	201
10.4.2.2.	Plate 2	203
10.4.3.	Perimeter Evaluation Result	204
10.5.	Experiment 2 : Plate "Large 1"	205
10.5.1.	Plate measurement	205
10.5.2.	Press Evaluation Result	206
10.5.2.1.	1 st scan	207
10.5.2.2.	2 nd scan	207
10.5.3.	Perimeter Evaluation Result	208
10.6.	Summary	209
Chapter 11	Heating forming support experiment	211
11.1.	Overview of heating forming support experiment	211
11.2.	Experiment design	213
11.3.	Experiment configuration in shipyard	213
11.4.	Design data used in the experiment	223
11.5.	Preliminary experiment	224
11.5.1.	Curved shell plate extraction	224

11.5.2.	Evaluation results' comparison of one single processing step	225
11.6.	Experiment 1 : Plate "Bowl 1"	228
11.6.1.	Objective	228
11.6.2.	Design data reforming and loading.....	228
11.6.3.	Analysis results for one manufacturing step	231
11.6.3.1.	Plate measurement	231
11.6.3.2.	Plate analysis	233
11.6.3.3.	Manufacturing plan design and manufacturing.....	234
11.6.4.	Manufacturing plans for all the steps	236
11.6.5.	Manufacturing results	237
11.7.	Experiment 2 : Plate "Bowl 2"	241
11.7.1.	Objective	241
11.7.2.	Design data reforming and loading.....	241
11.7.3.	Analysis results for one manufacturing step	243
11.7.3.1.	Plate measurement	243
11.7.3.2.	Plate analysis	245
11.7.3.3.	Manufacturing plan design and manufacturing.....	246
11.7.4.	Manufacturing plans for all the steps	248
11.7.5.	Manufacturing results	249
11.8.	Experiment 3 : Plate "Hybrid 1"	254
11.8.1.	Objective	254
11.8.2.	Design data reforming and loading.....	255
11.8.3.	Analysis results for one manufacturing step	257
11.8.3.1.	Plate measurement	257
11.8.3.2.	Plate analysis	258
11.8.3.3.	Manufacturing plan and manufacturing results of this step	260
11.8.4.	Manufacturing plans for all the steps	262
11.8.5.	Manufacturing results	263
11.9.	Summary	268
Chapter 12	Evaluation of knowledge elicitation and dissemination	271

12.1.	Overview of knowledge based system evaluation	271
12.2.	Line heating analysis with curvature error view	271
12.2.1.	Original rule base	272
12.2.2.	Knowledge elicitation process and results	273
12.3.	Complicated heating technic analysis with torsion evaluation view.....	276
12.3.1.	Plate analysis.....	276
12.3.2.	Elicited rules	277
12.3.3.	Elicited rules' adaption	279
12.4.	Knowledge model with different views.....	280
12.4.1.	Usage of knowledge model with curvature evaluation view.....	280
12.4.2.	Usage of knowledge model with torsion evaluation view	282
12.5.	Views for different observation purposes	287
12.6.	Summary	289
PART IV	DISCUSSION AND CONCLUSION.....	290
Chapter 13	Discussion	292
13.1.	Overview.....	292
13.2.	Problems existing in the proposed framework	292
13.2.1.	Imprecise perimeter evaluation with low density.....	292
13.2.2.	Scanner failure under high temperature	295
13.3.	Innovations in the proposed framework.....	296
13.3.1.	Manufacturing on vertical direction.....	296
13.3.2.	Knowledge dissemination's innovation	298
13.3.3.	Discussions on the proposed framework and the renovated manufacturing process	299
13.4.	Values of this work.....	306
13.4.1.	Cost impact	306
13.4.2.	Academic values.....	307
Chapter 14	Conclusion	310
14.1.	Conclusion	310
14.2.	Future work.....	313

REFERENCES	314
ACKNOWLEDGE	325
APPENDIX	329
A.1 Automation engine and configurations in shipyard	329
A1.1 Overview of the automation engine.....	329
A1.2 Automation flow setting.....	331
A1.3 Macro design for multiple system detection and control	331
Automatic UI configuration	331
Operation configuration	334
Path configuration and external system configuration.....	336
Tolerance value setting for different plates	337
Relations between the heating conditions and the contraction	340
A.2 Possible usage of the accumulated data in the future	346
A.2.1 Element storing of situation and action	348
A.2.2 Knowledge elicitation after data accumulation	350
A.2.3 Knowledge dissemination after data accumulation.....	351
PUBLICATIONS	353
Overview.....	353
A) Awards.....	353
B) Contributed Article	353
C) Journals	354
D) International Conferences (With peer reviews)	354
E) International Conferences (Without peer reviews)	355
F) National Conferences.....	356

Figures

<i>Figure 1-1 Curved shell plates on the bow (Ikeda, Y. et al 2009)</i>	24
<i>Figure 1-2 Curved shell plates on the bow and stern (Ikeda, Y. et al 2009)</i>	25
<i>Figure 1-3 Curved shell plates on the bow and stern (Ikeda, Y. et al 2009)</i>	25
<i>Figure 1-4 Press machine for cold forming</i>	27
<i>Figure 1-5 Heating forming with gas burner and water hose</i>	27
<i>Figure 1-6 Patterns of the heating bending</i>	28
<i>Figure 1-7 Manufacturing plan's design using wooden templates</i>	29
<i>Figure 1-8 Perspective line of wooden templates</i>	29
<i>Figure 1-9 Wooden template fixing and observing</i>	30
<i>Figure 2-1 Working accuracy management system of curved shell plate (Nakagaki, N. et al 2011)</i>	42
<i>Figure 2-2 Error definition using signed distances</i>	44
<i>Figure 2-3 Principle of line-heating</i>	44
<i>Figure 2-4 IHI-α (Tango, Y. et al 2011)</i>	46
<i>Figure 2-5 Curved surface machining robot (BUAA 2007)</i>	46
<i>Figure 2-6 Waterline marked with black and white targets for registration of multiple laser scanners (Biskup, K. 2007)</i>	48
<i>Figure 2-7 The standard deviation values along the deck of the ship (Biskup, K. 2007)</i>	48
<i>Figure 2-8 Segmentation and surface extraction of point cloud based on edge detection (Yang, M. 1999)</i>	50
<i>Figure 2-9 Segmentation and surface extraction of point cloud based on region growing (Rabbania, T. 2006)</i>	51
<i>Figure 2-10 Segmentation and surface extraction of point cloud based on 3D grids (Woo, H. 2001)</i>	51
<i>Figure 2-11 Switch operators' decision variables and decision attributes for engine assignment</i>	

<i>(Robinson, S. 2012)</i>	54
<i>Figure 2-12 Example of display view of the hot test model (Robinson, S. 2012)</i>	54
<i>Figure 2-13 Bridge Resource Management simulator training (Kakuta, R. 2007)</i>	55
<i>Figure 2-14 Knowledge based building reconstruction process (Pu, S., Vosselman, G. 2009)</i> 56	
<i>Figure 2-15 Knowledge base and dissemination interface for the feature extractions (Pu, S., Vosselman, G. 2009)</i>	57
<i>Figure 2-16 RDR tree for English tagging knowledge (Nguyen, D. Q. 2015)</i>	57
<i>Figure 3-1 Terrestrial laser scanner FARO (FARO 2011)</i>	61
<i>Figure 3-2 Kinect structure (Microsoft 2012)</i>	62
<i>Figure 3-3 Point cloud data structure</i>	62
<i>Figure 3-4 Edge detection</i>	63
<i>Figure 3-5 The basic region growing method</i>	65
<i>Figure 3-6 Kd-tree (k = 2)</i>	66
<i>Figure 3-7 Feature points of virtual template</i>	73
<i>Figure 3-8 Feature points of virtual template</i>	74
<i>Figure 3-9 Projection to the designed NURBS surface</i>	76
<i>Figure 3-10 Feature points of virtual template</i>	77
<i>Figure 3-11 Real object's virtualization and selection using polygons</i>	78
<i>Figure 3-12 Chord & Normal Vector (Zhang et al. 2008)</i>	79
<i>Figure 3-13 Curve radius estimation</i>	80
<i>Figure 3-14 Ripple-Down Rules sample (Compton, P. et al 1993)</i>	81
<i>Figure 4-1 Traditional manufacturing process using wooden templates</i>	87
<i>Figure 4-2 Convention of manufacturing plans' design</i>	89
<i>Figure 4-3 Conventional manufacturing process</i>	90
<i>Figure 4-4 Supported manufacturing process</i>	91
<i>Figure 4-5 Supported manufacturing process by proposed framework</i>	93
<i>Figure 4-6 Layout of the proposed framework</i>	96
<i>Figure 4-7 Pre-processing</i>	98
<i>Figure 4-8 Cold forming supporting</i>	101
<i>Figure 4-9 Heating forming supporting</i>	103

<i>Figure 4-10 Knowledge elicitation and dissemination</i>	105
<i>Figure 4-11 Automation engine</i>	106
<i>Figure 4-12 Software architecture</i>	107
<i>Figure 4-13 Pulpit user interface</i>	108
<i>Figure 5-1 Measured data with irregular obstacles</i>	110
<i>Figure 5-2 Plate extraction prototype</i>	111
<i>Figure 5-3 Flow of developed plate extraction prototype</i>	113
<i>Figure 5-4 Continuous domain extraction</i>	113
<i>Figure 5-5 Separated domain judgement</i>	114
<i>Figure 5-6 Float normal vector calculation window</i>	115
<i>Figure 5-7 Points used to do plane fitting (Sun, J.Y., IJCC, 2014)</i>	117
<i>Figure 5-8 Normal vector calculation considering point cloud's density (Sun, J.Y., IJCC, 2014)</i>	118
<i>Figure 5-9 Measured data with irregular obstacles (Sun, J.Y., IJCC, 2014)</i>	119
<i>Figure 5-10 Common domain judgment (Sun, J.Y., IJCC, 2014)</i>	120
<i>Figure 5-11 Fitted curve and measured curve (Sun, J.Y., IJCC, 2014)</i>	120
<i>Figure 5-12 Extraction process of plates separated by obstacles</i>	121
<i>Figure 5-13 Registration flow</i>	122
<i>Figure 5-14 Inverted registration result (Sun, J.Y., IJCC, 2014)</i>	123
<i>Figure 5-15 Inertia principal axes (Sun, J.Y., IJCC, 2014)</i>	124
<i>Figure 5-16 User interface of MS</i>	125
<i>Figure 6-1 Convention of cold forming evaluation using wooden template</i>	127
<i>Figure 6-2 Overview of the Press Support System (PSS)</i>	128
<i>Figure 6-3 Point cloud thinning</i>	129
<i>Figure 6-4 Distance error calculation</i>	130
<i>Figure 6-5 Perimeter calculation flow</i>	131
<i>Figure 6-6 Press evaluation user interface</i>	132
<i>Figure 6-7 Press evaluation user interface</i>	133
<i>Figure 6-8 Generated interfaces for observation of cold forming manufacturing</i>	134
<i>Figure 7-1 Convention of the heating forming decision making using wooden templates</i>	135

<i>Figure 7-2 Overview of Virtual Template System (VTS)</i>	137
<i>Figure 7-3 Virtual template prototype (Sun, J.Y., ICCAS2013)</i>	138
<i>Figure 7-4 Virtual templates generating (Sun, J.Y., IJASM, 2014)</i>	139
<i>Figure 7-5 Curvature error definition (Sun, J.Y., IJASM, 2014)</i>	141
<i>Figure 7-6 Torsion observation and evaluation (Sun, J.Y., IJASM, 2014)</i>	144
<i>Figure 7-7 Automatic virtual template arrangement</i>	144
<i>Figure 7-8 Part division of the virtual templates' frames and measured frames</i>	145
<i>Figure 7-9 Torsion detection result</i>	146
<i>Figure 7-10 Curvature error based heating grade suggesting</i>	147
<i>Figure 7-11 Roller lines and perimeters' vertexes information in DXF ship design file</i>	148
<i>Figure 7-12 2D roller line's matching with 3D frame design data</i>	149
<i>Figure 7-13 2D roller lines and 2D perimeters</i>	149
<i>Figure 7-14 Cross points of 2D roller lines and 2D perimeters</i>	150
<i>Figure 7-15 Match 2D roller lines with 3D frame lines</i>	150
<i>Figure 7-16 Virtual templates' operation interface</i>	151
<i>Figure 7-17 Cursor position judgement</i>	152
<i>Figure 7-18 User interface of VTS</i>	152
<i>Figure 7-19 Displacement evaluation histograms</i>	154
<i>Figure 7-20 Generated interfaces for observation during the manufacturing</i>	155
<i>Figure 8-1 Convention of deciding manufacturing plans</i>	156
<i>Figure 8-2 Knowledge elicitation and dissemination for manufacturing suggestions</i>	157
<i>Figure 8-3 Overview of NRDR interview-based knowledge model (Sun, J.Y, ISPE, 2014)</i>	159
<i>Figure 8-4 Nested Ripple Down Rule Trees (Sun, J.Y, ISPE, 2014)</i>	161
<i>Figure 8-5 Knowledge Elicitation using Nested Ripple-Down Rules (Sun, J.Y, ISPE, 2014)</i>	163
<i>Figure 8-6 Rule base modification based on observation of the interfaces</i>	164
<i>Figure 8-7Nested ripple down rule base (Sun, J.Y, ISPE2014)</i>	165
<i>Figure 8-8 The Xml-based Rule Sets (Sun, J.Y, ISPE, 2014)</i>	166
<i>Figure 8-9 Rules Relation View and Rule's Detail View (Sun, J.Y, ISPE, 2014)</i>	166
<i>Figure 9-1 Plate conditions in the shipyard</i>	175
<i>Figure 9-2 Curved shell plate extraction results separated by domains</i>	176

<i>Figure 9-3 Plate's point cloud divided by worker's shadow</i>	178
<i>Figure 9-4 Plate's point cloud divided by wires and hoses</i>	179
<i>Figure 9-5 Plate's point cloud divided by water</i>	179
<i>Figure 9-6 Panel extraction result (a) region growing (b) weighted region growing</i>	181
<i>Figure 9-7 Curved shell plate registration results. (1) Measured point cloud and design data (a) Parallel registration (b) registration without direction presetting (c) registration with direction presetting</i>	183
<i>Figure 9-8 Registration result for plate A (defect rate 10.3%)</i>	186
<i>Figure 9-9 Registration result for plate B (defect rate 52.5%)</i>	187
<i>Figure 10-1 Cold forming experiment flow</i>	192
<i>Figure 10-2 Layout of the experiment in the shipyard</i>	195
<i>Figure 10-3 Scan spot A (Press machine)</i>	195
<i>Figure 10-4 Scan spot B (After every press step)</i>	196
<i>Figure 10-5 Scanner parameter setting</i>	196
<i>Figure 10-6 Measurement of Plate "Regular 1"</i>	200
<i>Figure 10-7 Press design data of Plate "Regular 1"</i>	200
<i>Figure 10-8 Evaluation result of Plate "Regular 1" (plate 1)</i>	201
<i>Figure 10-9 Exaggerative evaluation result of Plate "Regular 1" (plate 1)</i>	202
<i>Figure 10-10 Evaluation histogram of Plate "Regular 1" (plate 1)</i>	202
<i>Figure 10-11 Evaluation result of Plate "Regular 1" (plate 2)</i>	203
<i>Figure 10-12 Exaggerative evaluation result of Plate "Regular 1" (plate 2)</i>	203
<i>Figure 10-13 Evaluation histogram of Plate "Regular 1" (plate 2)</i>	204
<i>Figure 10-14 Perimeter evaluation result of Plate "Regular 1"</i>	205
<i>Figure 10-15 Measurement of Plate "Large 1"</i>	206
<i>Figure 10-16 Press design data of Plate "Large 1"</i>	206
<i>Figure 10-17 Evaluation result of Plate "Large 1" during manufacturing</i>	207
<i>Figure 10-18 Evaluation result of Plate "Large 1" after cold forming</i>	208
<i>Figure 10-19 Evaluation histogram of Plate "Large 1" after cold forming</i>	208
<i>Figure 10-20 Perimeter evaluation result of Plate "Large 1"</i>	209
<i>Figure 11-1 Heating forming experiment flow</i>	213
<i>Figure 11-2 Heating forming support framework layout in shipyard</i>	214

<i>Figure 11-3 Heating forming process support scene in shipyard</i>	215
<i>Figure 11-4 Scanner setting with motor and gear</i>	215
<i>Figure 11-5 Scanner setting with crane (height 4650mm)</i>	216
<i>Figure 11-6 Scan spots at the heating forming area</i>	216
<i>Figure 11-7 Scan spot 1</i>	217
<i>Figure 11-8 Scan spot 2</i>	217
<i>Figure 11-9 Scan spot 3</i>	218
<i>Figure 11-10 Scan spot 4</i>	218
<i>Figure 11-11 Scan spot 5</i>	219
<i>Figure 11-12 Scan spot 6</i>	219
<i>Figure 11-13 Scan spot 7</i>	220
<i>Figure 11-14 Generated UI of the heating forming support framework</i>	222
<i>Figure 11-15 curved shell plate extraction in preliminary experiment</i>	225
<i>Figure 11-16 Curvature evaluation view and torsion evaluation view in preliminary experiment</i>	225
<i>Figure 11-17 SAT design data of Plate “Bowl 1”</i>	229
<i>Figure 11-18 DXF file containing 2D roller line data of Plate “Bowl 1”</i>	229
<i>Figure 11-19 DAT file containing frame design data of Plate “Bowl 1”</i>	230
<i>Figure 11-20 Registered design data of Plate “Bowl 1”</i>	230
<i>Figure 11-21 Virtual template generation of Plate “Bowl 1”</i>	231
<i>Figure 11-22 Extraction of Plate “Bowl 1” (Step1)</i>	232
<i>Figure 11-23 Registration result of Plate “Bowl 1” (Step1)</i>	232
<i>Figure 11-24 Distance error analysis result of Plate “Bowl 1” (Step1)</i>	233
<i>Figure 11-25 Torsion analysis results of Plate “Bowl 1” (Step1)</i>	234
<i>Figure 11-26 Curvature error analysis results of Plate “Bowl 1” (Step1)</i>	234
<i>Figure 11-27 Designed manufacturing plan for “Bowl 1” (Step1)</i>	235
<i>Figure 11-28 Displacement color map before and after this manufacturing step (“Bowl 1”)</i>	235
<i>Figure 11-29 Manufacturing actions of Plate “Bowl 1” (all the steps)</i>	237
<i>Figure 11-30 Manufacturing result of Plate “Bowl 1” (all the steps)</i>	238
<i>Figure 11-31 Plate’s evaluation results for all the manufacturing steps (“Bowl 1”)</i>	240

<i>Figure 11-32 design data of Plate “Bowl 2”</i>	242
<i>Figure 11-33 Virtual template generation of Plate “Bowl 2”</i>	243
<i>Figure 11-34 Extraction of Plate “Bowl 2” (Step1)</i>	244
<i>Figure 11-35 Registration result of Plate “Bowl 2” (Step1)</i>	244
<i>Figure 11-36 Distance error analysis results of Plate “Bowl 2” (Step1)</i>	245
<i>Figure 11-37 Torsion analysis results of Plate “Bowl 2” (Step1)</i>	246
<i>Figure 11-38 Curvature error analysis results of Plate “Bowl 2” (Step1)</i>	246
<i>Figure 11-39 Designed manufacturing plan for “Bowl 2” (Step1)</i>	247
<i>Figure 11-40 Displacement color map before and after this manufacturing step (“Bowl 2”)</i>	247
<i>Figure 11-41 Manufacturing actions of Plate “Bowl 2” (all the steps)</i>	249
<i>Figure 11-42 Manufacturing result of Plate “Bowl 2” (all the steps)</i>	250
<i>Figure 11-43 Plate’s evaluation results for all the manufacturing steps (“Bowl 2”)</i>	254
<i>Figure 11-44 NURBS design data of Plate “Hybrid 1”</i>	255
<i>Figure 11-45 Design data of Plate “Hybrid 1”</i>	256
<i>Figure 11-46 Virtual template generation results of Plate “Hybrid 1”</i>	257
<i>Figure 11-47 Extraction of Plate “Hybrid 1” (Step1)</i>	257
<i>Figure 11-48 Registration result of Plate “Hybrid 1” (Step1)</i>	258
<i>Figure 11-49 Distance error analysis results of Plate “Hybrid 1” (Step1)</i>	259
<i>Figure 11-50 Torsion analysis results of Plate “Hybrid 1” (Step1)</i>	259
<i>Figure 11-51 Curvature error analysis results of Plate “Hybrid 1” (Step1)</i>	260
<i>Figure 11-52 Designed manufacturing plan for “Hybrid 1” (Step1)</i>	260
<i>Figure 11-53 Displacement color map before and after this manufacturing step (“Hybrid 1”)</i>	261
<i>Figure 11-54 Manufacturing actions of Plate “Hybrid 1” (all the steps)</i>	263
<i>Figure 11-55 Final manufacturing result of Plate “Hybrid 1” (checked by system)</i>	263
<i>Figure 11-56 Manufacturing result of Plate “Hybrid 1” after every step</i>	264
<i>Figure 11-57 Plate’s evaluation results for all the manufacturing steps (“Hybrid 1”)</i>	267
<i>Figure 11-58 Final manufacturing result of Plate “Hybrid 1” (checked by real wooden template)</i>	267
<i>Figure 11-59 Manufacturing steps and count of heating actions under real wooden templates</i>	

<i>and the proposed framework</i>	269
<i>Figure 12-1 Manufacturing steps of the curved shell plate</i>	272
<i>Figure 12-2 The original rule base</i>	272
<i>Figure 12-3 Plan comparison</i>	273
<i>Figure 12-4 Knowledge base after step 2</i>	274
<i>Figure 12-5 Knowledge base after step 3</i>	274
<i>Figure 12-6 Knowledge base after step 5</i>	275
<i>Figure 12-7 The Situation and Manufacturing Area of the Curved Shell Plate</i>	277
<i>Figure 12-8 Rule base for line heating (Sun, J.Y, ISPE2013)</i>	277
<i>Figure 12-9 Nested ripple down rule base (Sun, J.Y, ISPE2014)</i>	278
<i>Figure 12-10 Manufacturing based on constructed Knowledge Base</i>	279
<i>Figure 12-11 Curvature evaluation view for one manufacturing step</i>	281
<i>Figure 12-12 Heating lines' designed by a worker</i>	282
<i>Figure 12-13 Heating lines' designed by another worker</i>	282
<i>Figure 12-14 Displacement color map</i>	283
<i>Figure 12-15 Horizontal virtual templates (plate view)</i>	284
<i>Figure 12-16 Horizontal virtual templates (perspective view)</i>	285
<i>Figure 12-17 Vertical virtual templates (plate view)</i>	285
<i>Figure 12-18 Horizontal virtual templates (side view)</i>	286
<i>Figure 12-19 Horizontal virtual templates (perspective view)</i>	287
<i>Figure 12-20 Result of the designed manufacturing action</i>	287
<i>Figure 13-1 Procedure of edge fitting (Hiekata, K., Yamato, H., Sun, J., Matsubara 2014)</i> .	294
<i>Figure 13-2 Result of measurement of edge shape in an experiment with a surface plate</i> ..	294
<i>Figure 13-3 Scanner failure example (a)</i>	295
<i>Figure 13-4 Scanner failure example (b)</i>	296
<i>Figure 13-5 Vertical curvature evaluation using the vertical virtual templates</i>	297
<i>Figure 13-6 Heating lines on the vertical directions</i>	297
<i>Figure 13-7 Conventional manufacturing method (Tanaka, Y., 2004)</i>	300
<i>Figure 13-8 Renovated manufacturing process and the effects</i>	301
<i>Figure 13-9 Decrease of the setback (long heating manufacturing time) on cold forming</i>	302

<i>Figure 13-10 Decrease of time cost and physical effort on heating forming</i>	303
<i>Figure 13-11 Rate of failure (%) on heating forming</i>	304
<i>Figure 13-12 Change of accuracy distribution on heating forming</i>	305
<i>Figure 13-13 Panel extraction result</i>	308
<i>Figure 13-14 Improvement in knowledge engineering</i>	309
<i>Figure a1-1 Overview of automatic engine</i>	330
<i>Figure a1-2 Automation engine UI configuration file</i>	332
<i>Figure a1-3 Details of automation engine UI configuration</i>	333
<i>Figure a1-4 Generated user interface</i>	334
<i>Figure a1-5 Operation configuration file</i>	335
<i>Figure a1-6 Details of operation configuration</i>	336
<i>Figure a1-7 External system configuration</i>	337
<i>Figure a1-8 Path configuration</i>	337
<i>Figure a1-9 Correlation between tolerance setting and the ship part</i>	338
<i>Figure a1-10 Customized numeric keyboard</i>	339
<i>Figure a1-11 Laser scanner located at the cold forming spot</i>	339
<i>Figure a1-12 Generated UI of the cold forming support framework</i>	339
<i>Figure a1-13 Scan scope setting and tolerance value setting</i>	340
<i>Figure a1-14 Relation between the plate's thickness and the contraction of the plate (Refrigeration by water)</i>	342
<i>Figure a1-15 Relation between the refrigeration method, heating direction and the contraction of the plate (Plate's thickness: 14mm)</i>	343
<i>Figure a1-16 Relation between the plate's thickness and the contraction of the plate (Heating speed: 170mm/min; Heating from upper side)</i>	344
<i>Figure a1-17 Relation between the heating speed and the contraction of the plate (Plate's thickness: 14mm; Heating from upper side)</i>	344
<i>Figure a2-1 Process modeling (Sun, J.Y, ISPE, 2015)</i>	347
<i>Figure a2-2 Subsequent manufacturing analyzing (Sun, J.Y, ISPE, 2015)</i>	347
<i>Figure a2-3 Process knowledge model (Sun, J.Y, ISPE, 2015)</i>	348
<i>Figure a2-4 Ontology of situations</i>	349

Figure a2-5 Ontology of actions 349
Figure a2-6 Paring of element situation and element action..... 351
Figure a2-7 Fuzzification process (Sun, J.Y, ISPE, 2015) 352

Tables

<i>Table 1.1 Problems existing in the manufacturing process</i>	32
<i>Table 9.1 Server features</i>	173
<i>Table 9.2 Faro Focus 3D</i>	174
<i>Table 9.3 Scanner parameter setting</i>	174
<i>Table 9.4 Parameter setting of the MS system</i>	175
<i>Table 9.5 Automatic extraction</i>	176
<i>Table 9.6 Extraction results for plates divided by worker' shadows</i>	178
<i>Table 9.7 Extraction results for plates divided by wires and hoses</i>	179
<i>Table 9.8 Extraction results for plates divided by water</i>	180
<i>Table 9.9 Comparison of the extracted result with an without weighted region growing</i>	182
<i>Table 9.10 Comparison between general methods (a) (b) and new presented method (c)</i>	184
<i>Table 9.11 Registration results of the plate A with and without defect</i>	186
<i>Table 9.12 Registration results of the plate B with and without defect</i>	188
<i>Table 10.1 Faro Focus 3D X series</i>	191
<i>Table 10.2 Server features</i>	191
<i>Table 10.3 Experiment scenario of the cold forming support framework</i>	198
<i>Table 10.4 Perimeters of Plate "Regular 1"</i>	205
<i>Table 10.5 Perimeters of Plate "Large 1"</i>	209
<i>Table 10.6 Cold forming support experiment result summary</i>	210
<i>Table 11.1 Faro Focus 3D 120 series</i>	212
<i>Table 11.2 Server features</i>	212
<i>Table 11.3 Experiment scenario of the heating forming support framework</i>	221
<i>Table 11.4 Torsion evaluation for curved shell plate A</i>	226
<i>Table 11.5 Experiment conditions in the general experiments</i>	227
<i>Table 11.6 Plate evaluation results before and after this manufacturing step (A1*S)</i>	236
<i>Table 11.7 Plate evaluation results after each manufacturing step ("Bowl 1")</i>	239

<i>Table 11.8 Plate evaluation results before and after this manufacturing step (“Bowl 2”) _</i>	<i>248</i>
<i>Table 11.9 Plate evaluation results after each manufacturing step (A1*P) _____</i>	<i>251</i>
<i>Table 11.10 Plate evaluation results before and after this manufacturing step (“Hybrid 1”)_____</i>	<i>262</i>
<i>Table 11.11 Plate evaluation results after each manufacturing step (“Hybrid 1”)_____</i>	<i>265</i>
<i>Table 11.12 Heating forming experiment result summary (Sun, J.Y., JASNAOE, 2014) ___</i>	<i>270</i>
<i>Table 12.1 Importance of views for different purposes _____</i>	<i>288</i>
<i>Table 13.2 Result of measurement of edge length in an experiment with a surface plate (mm)</i>	<i>295</i>
<hr/>	
<i>Table 13.3 Curved shell plates’ manufacturing scenario in shipyard S _____</i>	<i>306</i>
<i>Table a1.1 Correlation between tolerance setting and the plate thickness _____</i>	<i>338</i>
<i>Table a1.2 Experiments in different manufacturing conditions _____</i>	<i>341</i>
<i>Table a1.3 Experiment conditions in the general experiments _____</i>	<i>345</i>
<hr/>	

PART I INTRODUCTION AND STATE

PART I INTRODUCTION AND STATE	21
Chapter 1 Introduction	24
1.1. Background	24
1.1.1. Two-stages manufacturing process of curved shell plate	26
1.1.2. Problems in traditional manufacturing process and possible approaches	
31	
1.1.3. Problems in OJT knowledge dissemination	33
1.2. Objective.....	34
1.3. Approach	36
1.4. Outline	38
Chapter 2 Related researches	40
2.1. Overview	40
2.2. Curved shell plates' accuracy evaluation system using laser scanners.....	40
2.2.1. System overview.....	40
2.2.2. Problems existing in measurement flow and evaluation standard	42
2.3. Researches on curved shell plate's manufacturing	45
2.3.1. Full automatic machining process of curved shell plate	45
2.3.2. Problems existing in full automatic machining.....	47
2.4. Researches on usage of laser scanner and point cloud data	47
2.4.1. Surface extraction from the point cloud data	49
2.4.2. Surface registration of the point cloud data	52
2.4.3. Problems existing in laser scanner's practical usage in shipyard	52
2.5. Researches on knowledge elicitation and dissemination.....	53
2.5.1. Knowledge elicitation: progresses, interfaces.....	53
2.5.2. Knowledge dissemination: interfaces, storages.....	55
2.5.3. Problems of knowledge elicitation and dissemination in manufacturing.	58
2.6. Originalities of this thesis	58
Chapter 3 Component technologies	60
3.1. Overview	60
3.2. 3D measurement equipment and features.....	60
3.2.1. Laser scanner	60
3.2.2. Kinect	61

3.2.3. Point cloud data	62
3.3. Point cloud processing	63
3.3.1. Edge detection	63
3.3.2. Region growing.....	64
3.3.3. k-Nearest Neighbor.....	65
3.3.4. Plane fitting.....	66
3.3.4.1. Basic plane fitting.....	67
3.3.4.2. Weighted plane fitting	69
3.3.5. Curve fitting.....	71
3.3.5.1. Lagrange interpolation.....	72
3.3.5.2. B-Spline interpolation	73
3.3.6. Iterative closest point.....	75
3.3.7. Real object's virtualization and selection using polygons	76
3.3.8. Curvature estimation.....	79
3.4. Knowledge engineering.....	80
3.4.1. Ripple down rules.....	80

Chapter 1 Introduction

1.1. Background

The round contours and elegant hulls of a ship resemble a woman's figure. That might be why ships have been classified as feminine objects in gender-specific languages since antiquity. What gives a ship its shapely exteriors are the curved shell plates which are made from large, thick plates of steel as shown in Figure 1-1 and Figure 1-2, covering the entire ship from stern to bow with complex three-dimensional curve surfaces.

To ensure the good watertight keeping, increase the strength of the hull and meet the propulsive performance of the vessel, the curved surfaces of the plates are always extremely complex and designed in different shapes. There are only 2 curved shell plates constituting the left and right side of the vessel which can have exactly the same shape among over 200 plates of one ship.



Figure 1-1 Curved shell plates on the bow (Ikeda, Y. et al 2009)



Figure 1-2 Curved shell plates on the bow and stern
(Ikeda, Y. et al 2009)



Figure 1-3 Curved shell plates on the bow and stern
(Ikeda, Y. et al 2009)

Even though the curved shell plates' shapes are various, they can be broadly classified as following:

- (1) Trumpet type: No vertical bending in the plate's width direction
- (2) Bowl Type: vertical bending, center falls
- (3) Saddle Type: vertical bending, center rises
- (4) Twist Type: diagonal areas are higher / are lower than the other diagonal areas

In addition, in shipbuilding industry, considering the low-volume production caused by individual orders, it is necessary to design different bending scheme for the curved shell plates of every different ship.

1.1.1. Two-stages manufacturing process of curved shell plate

As a method for bending a steel plate, there is a two-stages bending process consisting of cold forming and heating bending. The cold forming process is to deform a certain bending shape of the curved shell plates by applying load using a press machine as shown in Figure 1-4. This cold forming process can make a large deformation degree in a relatively short time. However, it cannot achieve accurate bending requirement. Hence, after the cold forming process, the heating forming as shown in Figure 1-5 is processed by human using the repeated plastic deformation due to the cooling of the water and the heating of the gas burner.



Figure 1-4 Press machine for cold forming



Figure 1-5 Heating forming with gas burner and water hose

Since the 3D shapes of the curved shell plates can be extremely arbitrary and considering the large size of them, they can only be plastically deformed by various heating patterns such as triangle heating or even grilled point bending as shown in Figure 1-6. The decisions (manufacturing plans) of these heating patterns and the locations of the heating areas are based on the wooden bending template (Kikata) check with human eyes (Hayashi, S. 2004). The wooden templates used in this process to evaluate the curved surface of a curved shell plate are made up of bottom line and perspective stick from the ship's design data. As known by now, this process has no clear-cut methodology and carries great risks for the subsequent heat sealing process.

During the processing, the parameters (e.g. the angles between wooden templates' perspective sticks as shown in Figure 1-7 and Figure 1-8, the grade of the gap between the wooden templates' bottom line and the curved shell plate, etc.) which are required for the design of processing plan based on a personal check-with-eyes result are quantitatively immeasurable. Individual difference is among the manufacturing plans designed by the workers, and the variation in after-processing shapes arises due to the heavy depending on the tacit knowledge, skill and experiences of the craftsmen during the processing.

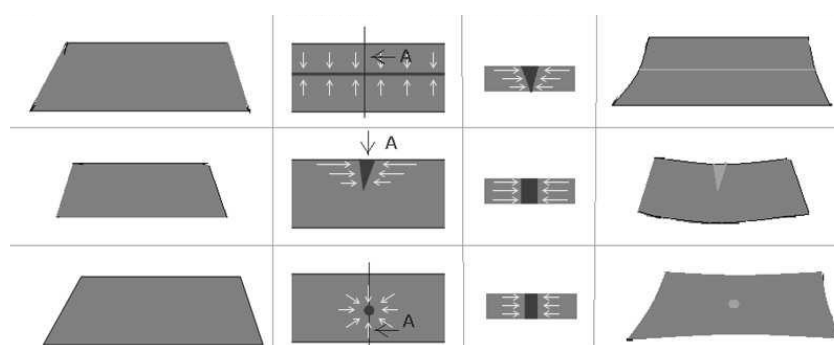


Figure 1-6 Patterns of the heating bending



Figure 1-7 Manufacturing plan's design using wooden templates



Figure 1-8 Perspective line of wooden templates

Before the construction of a ship, about four to eight wooden templates consisting of the bottom line and perspective stick are made from the ship's design data for every curved shell plate (totally about 500 wooden templates per ship). This wooden templates' producing process costs a lot of time and money, and may contain inaccuracies.

In addition, as shown in Figure 1-9, for every step during the manufacturing process, to put these wooden templates on the appropriate position on the curved shell plates (for the perspective line's check, etc.), a considerable amount of time and physical strength is required of the worker.



Figure 1-9 Wooden template fixing and observing

1.1.2. Problems in traditional manufacturing process and possible approaches

As introduced in 1.1.1, during the curved shell plates' manufacturing process, the parameters (e.g. the angle between wooden templates' perspective sticks, the grade of the gap between the wooden templates' bottom lines and the curved shell plate, etc.), which are required for the design of the following manufacturing plan, are based on a manual check by eye and results are always quantitatively immeasurable. During the curved shell plate's manufacturing process, problems listed in Table 1.1 exist. Because the observed results are always obscure, how to decide the heating and cooling areas of the following processing is still uncertain. Even if a consensus is reached on the situation of the curved shell plate, different workers may give totally different manufacturing plans of the next manufacturing step because there is a lot of tacit knowledge such as the processing rules and habits which are hardly discovered or educated during the processing. Thus, individual differences arise among the manufacturing plans designed by the worker, and also in the after-processing shapes, due to the heavy dependency on tacit knowledge, skill and experience of the craftsmen during the processing. Besides, since the manufacturing scene cannot be effectively reproducible by using video or paper record, beginning workers have to learn all of the tacit knowledge through real practice after they have mastered a certain degree of the manufacturing techniques. It usually takes about two years of training to produce one qualified worker.

In nowadays' shipbuilding industry, there is only a few expert workers with the knowledge and skills of the curved shell plate's manufacturing serving each shipyard. In summer, the manufacturing spot could be over 40 degrees. The workers holding the water hose and gas burner have to repeat the process of heating and cooling until the shape corresponds with the design. Besides, they have to put the heavy wooden templates on the curved shell plate one by one, and then fix them to observe necessary parameters for designing the next-step's manufacturing plans. Under this situation, saving the unnecessary time and physical effort by suggesting the relatively efficient manufacturing plans is of great importance for them. However, in reality, the manufacturing plans for every single step are obscure and cannot be guaranteed to be the most proper ones to optimize the

following manufacturing.

Table 1.1 Problems existing in the manufacturing process

stage	Manufacturing content	Problems
Cold Forming	<ol style="list-style-type: none"> 1. Press operation and adjustment using press roller 2. Perimeter check using tape-measure 	<ol style="list-style-type: none"> A) Plate's sections without wooden templates cannot be evaluated. B) Forming quality dispersion (lead to in-expectable time consuming in the after-processing). C) Perimeter check cost time, sometimes inaccuracy
Line Heating Bending	<ol style="list-style-type: none"> 1. Heating operation for bending 2. Shape confirmation at every step of the manufacturing process using wooden templates 	<ol style="list-style-type: none"> A) Plate's sections without wooden templates cannot be evaluated. B) Considerable amount of time and physical strength are required of workers. C) Check is based on human eyes, precise parameters such as the angles and displacement cannot be taken, individual differences exist. D) Individual differences exist in the manufacturing plans. E) A lot of tacit knowledge exist in the inference process from the wooden templates' confirming results to the manufacturing plans

1.1.3. Problems in OJT knowledge dissemination

In addition, because both the curved shell plates and the wooden templates have 3D shapes, the placement angles of the wooden templates and the displacement between them are very difficult to be recorded and conveyed by 2D medium such as video or papers. As a conventional means for training the young workers, OJT (On The Job Training) are usually carried out in shipyard. The OJT, in which the skilled expert workers and the beginner workers collaborate, focus on disseminating knowledge during the practical manufacturing. However, in many cases errors and inefficiency cannot be allowed even in OJT. Hence, 3D virtualized training and even 3D reproducible manufacturing environment are desired. Also, the demand of the effective knowledge elicitation and dissemination approach in the virtualized environment comes out.

The possible approaches noted so far for extracting the knowledge in curved shell plates' manufacturing process aim to produce appropriate manufacturing plans (output) for some certain situations of curved shell plate (input) like the "situation specific model" discussed by Clancey et al in 1985 and 1992. As of now, only some general introductions have been extracted by conducting interviews with the workers due to the lack of effective manufacturing data acquisition system. But once the manufacturing data and the manufacturing process itself can be effectively evaluated and recorded, some knowledge elicitation mechanism should be taken into consideration. A famous knowledge elicitation method named Ripple-Down Rules proposed by Compton et al in 1989 and 1992 can be used to incrementally build a set of appropriate and validated links between the conditions of curved shell plate and the manufacturing plans designed by workers instead of the basic general introductions.

On the other hand, modern engineering has begun to use non-contact 3D scanning technique using laser scanners. Laser scanners emit laser and receive reflections to collect a real-world object's shape information. The distance between every point of the object and laser scanner is calculated by measuring the laser pulse's travel time. By combining this distance and the radiation direction, 3D positional coordinates can be obtained. Measured results are formatted in point

cloud data which include three-dimensional coordinates representing the points of the measured object's surface, the reflection intensity and color information. According to Kobayashi et al.(2008), door assembly in the motor vehicle industry is measured by a handy laser scanner to obtain point cloud data-based on the circular holes, elongated holes or normal vectors on the door panels, point cloud data is superimposed on the CAD data and the error is expressed with a color map. As an application of laser scanners to shipbuilding, Biskup, K. et al. calculated the surface displacement of a 40-meter vessel. The vessel was measured by a laser scanner from multiple positions. The measured multiple point clouds were registered, wrapped with polygonal meshes, surfaced with NURBS (Piegl, L., Tiller, W. 1996) and then the displacement was calculated. All of these technologies give us a chance to record the existing manufacturing process in the 3D virtual environment for the workers to observe and analyze the manufacturing efficiently not just OJT but also after the manufacturing.

1.2. Objective

Sun (2013) developed a virtual template prototype to virtualize the virtual templates and generate the manufacturing plans for the heating forming process of the curved shell plates in the shipyard. This prototype is a set of some classic point cloud processing algorithms showing the possibility of replacing the real wooden templates with the virtual manufacturing environment.

However, in the research mentioned above,

- How to introduce this system to the shipyard was not considered. The methods and algorithms can rarely satisfy the practical usage in shipyard without significant improvements and appropriate combinations.
- Not only the heating forming process, but also the whole manufacturing process including the cold forming process is expected to be supported too.

- To support the beginner workers, the experienced workers' knowledge should be elicited and disseminated in an efficient way for the supporting of the beginner workers.

The aim of this research is

1. To facilitate the whole manufacturing process of the curved shell plate by proposing a practical framework.
 - To propose manufacturing evaluation method for achieving high and stable quality of the cold forming.
 - To develop a visual environment for facilitating the heating forming stage by replacing the wooden templates with the virtualized templates of high evaluation accuracy and usability.
 - To propose knowledge models for preserving the convention in the curved shell plate's manufacturing.
2. To evaluate the proposed framework by conducting multiple manufacturing experiments in the shipyard.

The manufacturing convention including the concept of how to decide the manufacturing areas, the way to arrange and observe the wooden templates, and how to choose the manufacturing technics and decide if a plate is finished or not based on the observation results is expected to be totally preserved in the following ways:

- To manufacture and evaluate the plate based on the interfaces of proposed framework.
- To store and reproduce every single step of the manufacturing process.
- To conduct interviews based on the recorded scenarios for the knowledge elicitation.

1.3. Approach

In this thesis, laser scanner is used for capturing the curved shell plate's 3D shape before and after every manufacturing step.

As a pre-processing of vital importance, the 3D shape of the measured plate is extracted efficiently from the raw measured point cloud data from laser scanner which contains a lot of irregular obstacles.

The cold forming is supported by the efficient accuracy evaluation and perimeter measurement of the plate. The evaluation results are used to decide if the plate is deformed good enough to be passed to the heating forming stage to enhance the manufacturing efficiency.

The heating forming is supported by virtualizing the whole manufacturing process on computer. The wooden templates are totally replaced by the virtualized templates. The necessary parameters including the displacement, angles which are difficult to be observed quantitatively using the real wooden templates are calculated automatically before each manufacturing step to help the workers make the manufacturing decision.

To support the beginner workers who cannot decide the manufacturing plans alone, the expert workers' knowledge is elicited by conducting interviews or data analysis based on the recorded 3D manufacturing scenarios. The advanced manufacturing suggestions including special heating technics (point heating and curve heating) or heating lines' combinations are outputted by the system.

Furthermore, through the interviews towards to the workers who used the framework proposed in this thesis, the virtualized manufacturing process and the elicited knowledge is evaluated, and the effectiveness of the proposed framework can be set forth.

Specifically, by achieving the following items, the whole manufacturing process of curved shell plates is facilitated.

- Common pre-processing: Efficient curved shell plate's 3D shape extraction and registration

Redesign the classic algorithms to achieve the high processing speed and low failure. Develop an independent Plate Measurement System (PMS) as a sub-system of the manufacturing support framework which is responsible for extracting the plates from the raw point cloud data including obstacles.

- Cold forming support: accuracy evaluation and perimeter measurement

Develop a Press Support System (PSS). Locate the measured shape of the curved shell plates onto the press design data after cold forming. Calculate the displacements and virtualize the errors using color maps and histograms for the workers to grasp the plate's situation during and after cold forming process.

- Heating forming support: Effective manufacturing environment virtualization

Develop a Virtual Template System (VTS) which is also a sub-system of the manufacturing support framework. Automate the preparation of the input ship design data. Virtualize both the wooden templates and the manufacturing plan design process. Automatically calculate the necessary parameters for the manufacturing plan design. Develop an interface for the workers to observe the heating grade suggestion result more easily.

- Knowledge elicitation and dissemination

Develop a Knowledge Based System (KBS) including one knowledge models: the interview-based knowledge model for explicit knowledge elicitation. Capture the correlations between the 3D parameters describing the curved shell plate's situations and the relevant manufacturing plans designed by the expert workers. Virtualize and disseminate the elicited knowledge on computer.

- Evaluation of the whole manufacturing support framework

Conduct the case studies of each component subsystem using the real data measured in shipyard to verify every subsystem's effectiveness. Manufacture multiple kinds of curved shell plates in practical overall evaluation experiments.

At last, develop the automation engine (AE) which can be customized according to the environment of the shipyard and the different processing flows even when there are needs to control some external systems. Automatize the whole measurement and analysis flow of the framework.

1.4. Outline

This thesis consists of 4 parts, 13 chapters.

The first part gives an introduction and state of this research.

The second part proposes the framework and clarifies the contribution.

The third part evaluates the proposed framework.

The last part is the discussion and conclusion.

To be specifically,

Next chapter reviews related literature on the curved shell plates' manufacturing.

Originalities of this study are introduced.

Chapter 3 introduces the component technologies which are used in this thesis.

Part 2 is from Chapter 4 to Chapter 8.

Chapter 4 gives the lay-out of the whole proposed framework for facilitating the entire process of the curved shell plate's manufacturing. Four systems constitute the proposed framework.

Chapter 5 develops the first sub system – curved shell plate's Measurement System (MS) for the pre-processing of the framework.

Chapter 6 explicates the development of the second sub system – Press Supporting System (PPS) for the cold forming supporting.

Chapter 7 develops the third sub system – Virtual Template System (VTS) for the heating forming supporting.

Knowledge based system (KBS) is presented in Chapter 8.

Part 3, Evaluation and optimization, are in Chapter 9 – Chapter 12. The cold forming supporting process, the heating forming supporting process and the knowledge elicitation and dissemination are evaluated in the experiments.

Part 4 is from Chapter 13 to Chapter 14.

Some discussions are made in Chapter 13.

This thesis is concluded in Chapter 14. Prospects for further study are also discussed in Chapter 14

Chapter 2 Related researches

2.1. Overview

In this chapter, the precedence researches on the curved shell plate's manufacturing process are discussed. First, the working accuracy management system of curved shell plate based on the displacement measured by laser scanner is introduced. Then, the current state of researches in the world about the laser scanning and the curved shell plate's manufacturing is summarized. Finally, the originalities of this thesis are presented.

2.2. Curved shell plates' accuracy evaluation system using laser scanners

Nowadays, the curved shell plate's manufacturing still relies heavily on the workers' experience and knowledge. And the accuracy evaluation can only be performed on the portion where the wooden templates are put; overall surface cannot be quantitatively evaluated. To evaluate the accuracy of the curved shell plate's whole surface, the curved shell plate's accuracy evaluation system based on 3D measured data has been developed by Hiekata, K. et al. from The University of Tokyo.

2.2.1. System overview

The system calculated the surface displacement of curved shell plates. Curved shell plates are measured by laser scanners (Hiekata, K., Yamato et al 2011). Curved shell plates' accuracy is computed by registering the measured point cloud data of curved shell plates and the design data in NURBS and calculating the displacement of these two data points. The system's flow is as shown in Figure 2-1.

In order to clarify the originality of this thesis, the outline of this previous system is discussed here.

The input data of this accuracy evaluation system includes the curved shell plate's design data representing the 3D CAD shape of the hull and the point cloud

data measured by laser scanners representing the shape of the real curved shell plate. The design data is represented by the NURBS surfaces of the ship and a combination of the trimmed curves for cutting out the shape of the curved shell plate. Because the point cloud data obtained by laser scanners includes variations and noise comparing with the real shape of the curved shell plate, the moving least-squares method is conducted to smooth the raw data, and then the outliers are removed based on the distances from the reference plane too. Furthermore, by applying the region growing method, the unnecessary parts of the ground and the real wooden templates are also removed. After extracting the curved shell plate from the raw data by applying these pre-processing above, the calculation of the principal axes of inertia and the center of gravity is performed towards the edge of the extracted curved shell plate, and then the coordinate transformation is performed so that they can match the design data. The signed distances between the transformed design data in the format of NURBS and the measured point cloud data are defined as the work errors. The working accuracy is defined by the calculation using Newton method and is outputted as histogram and color map (Nakagaki, N. et al 2011 and 2013).

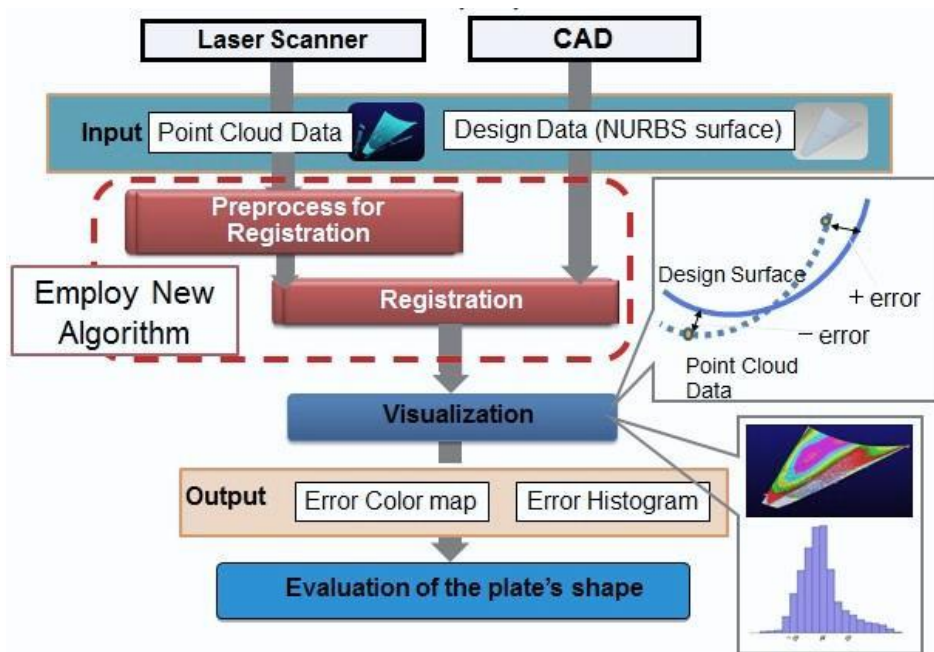


Figure 2-1 Working accuracy management system of curved shell plate (Nakagaki, N. et al 2011)

By introducing this system into shipyard, a number of problems are found. In the following sections, the problems existing in measurement flow and evaluation standard are described.

2.2.2. Problems existing in measurement flow and evaluation standard

Problems existing in the measurement flow are listed as below:

- a. The part of the component cannot be extracted efficiently due to irregular obstacles endogenous to manufacturing workshops and their shadows divide the component's measured point cloud data into several separated domains. Manual extraction and integration of these separated domains waste a lot of time and is a barrier for practical application. The well-known methods for calculating smooth surfaces from noisy point cloud such as moving least squares (MLS) projection (Pauly et al., 2002) has the same problem that the whole component cannot be extracted at one time when the component is separated by the obstacles' shadows.
- b. PCA registration has a lot of failure when the measured point cloud is with

variable density or is not complete. ICP (Iterative Closest Point) algorithm is expected to be used to conduct a registration between the measured point cloud data and the design data. However, due to the features of the ICP algorithm, without a clear registration direction presetting, the registration of the two data sets could go in the wrong direction and lead to improper registration results.

- c. An intolerable amount of time in shipyard (over 1 hour per plate) is cost during the manufacturing due to many manual processes such as extracting and combing the separated parts of the curved shell plate, some processing is so difficult even impossible for the workers to conduct on computer.

As a result, existing point cloud processing methods (the basic region growing method and ICP registration method) can rarely satisfy the accuracy evaluation target in shipbuilding without significant improvements and appropriate combination (Hiekata, K., JASNAOE, 2012).

Problems existing in the evaluation standard applying are listed as below:

- a. Although the displacement between curved shell plate's surface and design surface as shown in Figure 2-2 can be virtualized using color maps by this system, the manufacturing plan (where to do the next heating) for the following heating step is still unclear. The principle used to bend a curved shell plate by line-heating is as shown in Figure 2-3, at the location where to apply the heat, the upper side of the plate shrinks, and the underside of the plate expands, while the neutral axis is assumed to be constant. Therefore, the heating area should be decided based on the curvature differences instead of the signed distance errors.

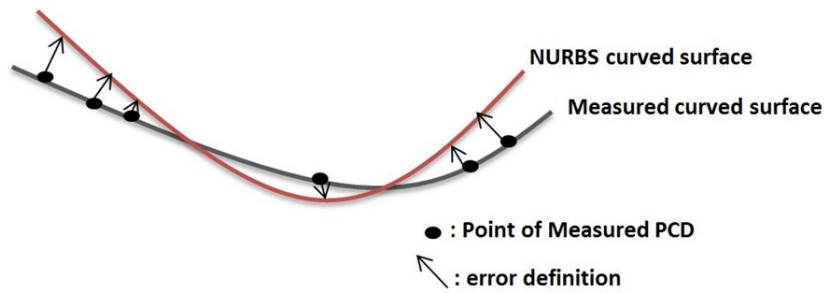


Figure 2-2 Error definition using signed distances

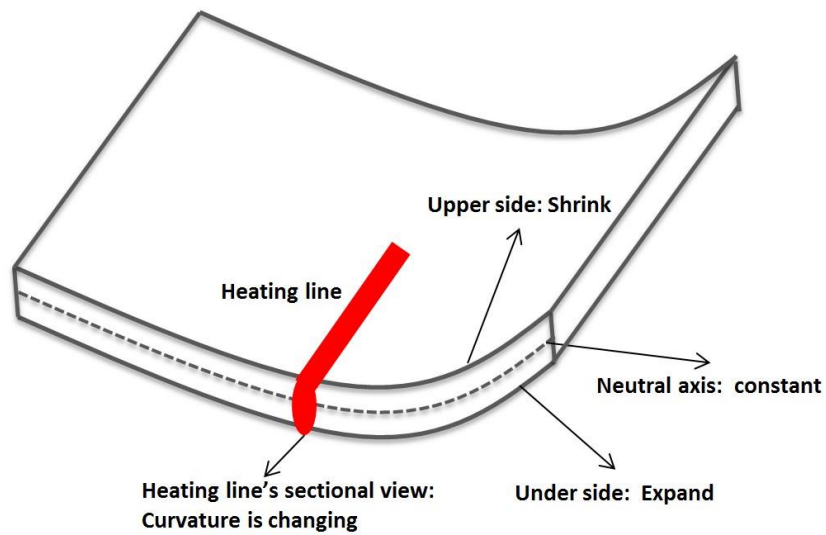


Figure 2-3 Principle of line-heating

- b. This system is only designed to be used to do the final evaluation of the curved shell plates after they are considered to be completed. Also, each manufacturing step cannot be reproduced on the computer to help us do the knowledge elicitation.

This thesis aims at reforming the prior system by solving the problems above, and presenting an effective curved shell plate's manufacturing facilitating framework based on the reformed system.

2.3. Researches on curved shell plate's manufacturing

Curved shell plate's manufacturing relies heavily on the workers' experiences and skills; at least 10 years could be cost to become a full-fledged expert. Even though over 99% of the curved shell plates in the world are still manufactured manually, nowadays studies to quantitatively automate the manufacturing process have been carried out, and among them some results were presented. In this section, the current state of the curved shell plate's manufacturing automation and the practical application of these studies are discussed (Park, J.S, Shin, J.G, Ko, K.H. 2007).

2.3.1. Full automatic machining process of curved shell plate

The full automatic machining of curved shell plate is based on the premise that the connection between the machining plans consisting of the parameters (such as the heating line's location, the thickness and width of the plate and the heating velocity) and the plate's target situation can be accurately determined (Okumoto, T. 2009).

In curved shell plate's manufacturing, as mentioned in 2.2.2, the deformation using the extension and contraction at the heating area is used. This process is a complex non-linear problem, to determine the automatic machining parameters, simulations and experimental methods are often used.

In Japan, the IHI Marine United Inc. started the studies about fully automated machining of curved shell plates in 1990, and has developed a first unit "IHI- α " shown in Figure 2-4 in 1997 (Fujimura, K. 2009). In 2011, they greatly improved the first unit, and developed the new unit "IHIMU- α " which can automatically complete some plates' machining process. In order to calculate the machining plans, "IHIMU- α " used the elasticity FEM (Finite Element Method) based on the inherent strain theory to output the heating position, heating order and heating rate after input the desired shape and the plate's thickness.



Figure 2-4 IHI- α (Tango, Y. et al 2011)



Figure 2-5 Curved surface machining robot (BUAA 2007)

In Korea, Shin et al. also developed a fully automated machining system for curved shell plates named “iCALM”. This system can do the curved shell plate’s modeling for ships, provide the heating parameters and evaluate the work accuracy.

As shown in Figure 2-5, the large complex curved surface machining robot was developed by the Beijing University of Aeronautics and Astronautics and Tsinghua University. It can predict the machining parameters based on certain situation of the curved shell plates, a part of this project has been introduced into the shipyard.

2.3.2. Problems existing in full automatic machining

Although, a lot of studies and experiments about the automatic machining of curved shell plates have been carried out, almost all of the curved shell plates in the world are still manufactured manually using the line-heating technique from last century 1960s (Wang, Z., 2007). The problems existing in the full automatic machining are listed as below:

- a. These studies are intended to focus on the deformation parameter prediction from the flat steel plate straightly to the desired shape (Matsuoka, K. 2004). The studies dealing with the accuracy evaluation of each machining step and the calculation about the secondary heating correction are rare.
- b. Moreover, in current state of the automatic machining for curved shell plates, large equipment is required, and the enormous energy consuming is also a remaining problem.
- c. Also, because the researches about the automatic machining tend to not employ the conventional way to do the manufacturing using wooden templates, it becomes entirely different processing technique even for an expert worker. That leads to the extremely difficult secondary heating correction once the shape of the curved shell plate being manufacturing goes wrong.

2.4. Researches on usage of laser scanner and point cloud data

Although not like the manufacturing process supporting in the industry, there are still some samples using the laser scanner in other fields too. Laser scanner provides a big chance for both the measurement of the existing component and the reverse engineering of the measured object.

Laser scanning is also used for structural engineering (Gordon, S. 2004), mining industry and modelling in the shipbuilding (Gutiérrez, 2006; Arias, P. 2006).

For reverse engineering of the building models, Pu, S., Vosselman, G. (2009) proposed a knowledge based reconstruction of building models from terrestrial laser

scanning data. While for the deformation detection, Park, H. S., Lee, H. M.(2007) proposed a new approach for health monitoring of structures using TLS (terrestrial Laser Scanning), and Monserrat, O., Crosetto, M. (2008) gave a method for the deformation measurement using the point cloud data obtained by laser scanner and the least squares 3D surface matching.

Here some examples of the laser scanner usage are illustrated, and the problems existing in point cloud processing will be discussed later.

Biskup, K. (2007) gives an example of the usage of laser scanner in shipbuilding. The surface displacement of a 40-meter vessel was calculated as an evaluation result as shown in the figures below. The vessel was measured by a laser scanner from multiple positions. The measured multiple point clouds were registered, wrapped with polygonal meshes, surfaced with NURBS and then the displacement was calculated.



Figure 2-6 Waterline marked with black and white targets for registration of multiple laser scanners (Biskup, K. 2007)

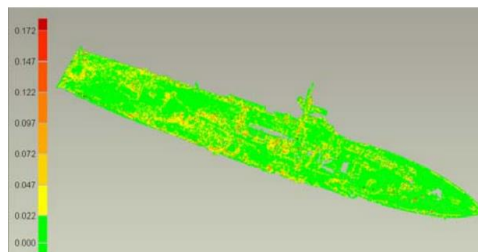


Figure 2-7 The standard deviation values along the deck of the ship (Biskup, K. 2007)

Because the processing contains too much manual parts, time cost was pointed out to be a vital problem. Firstly, the measurement procedure followed for the data collection took approximately 7 working hours, scanning both elements of the boat, the hull and the deck. Even some time, the system works fine; it was time-consuming because of the enormous quantity of points. Sometimes the computer works very slowly, especially in cases of the component's surface extraction. (Biskup, K. 2007) For the manual filtering process, a certain degree of skill and experience are needed to avoid removing too much data with the consequent loss of information, or too little data with the obstacles staying in the point cloud.

2.4.1. Surface extraction from the point cloud data

As we know, surface extraction from the point cloud is a task of vital importance for the reverse engineering and object measuring using laser scanner (Varady, T 2000). The manual surface extraction from the point cloud data is considered as a time-consuming and risky task for the subsequent processing. Some researches work on the automatic and high accurate surface recognition using the segmentation by fitting curves or surfaces in order to extract some useful geometric information. Wani, M. A. (2003). developed a parallel edge region-based segmentation algorithm targeted at reconfigurable MultiRing network. Sithole, G.(2003) proposed an automatic structure detection method in a point-cloud of an urban landscape based on point cloud segmentation and classification.

Current approaches for surface extraction methods mainly have two categories:

(1) The most basic approach for surface extraction from point cloud is based on edge detection. Yang, M., published in Journal of CAD a computational boundary detection method by comparing the principal curvatures at the neighborhood points to facilitate the partitioning of the point cloud. The neighborhood connecting algorithm was used after the edge points were detected. The different kinds of detected edges are shown in Figure 2-8.

As the main shortage of this edge-detection surface extraction approach, Woo, H. (2001) pointed out that these fitting processes take too much time and since the

representative edge data of the surface cannot always be extracted due to the irregular obstacles or discrete points in the point cloud.

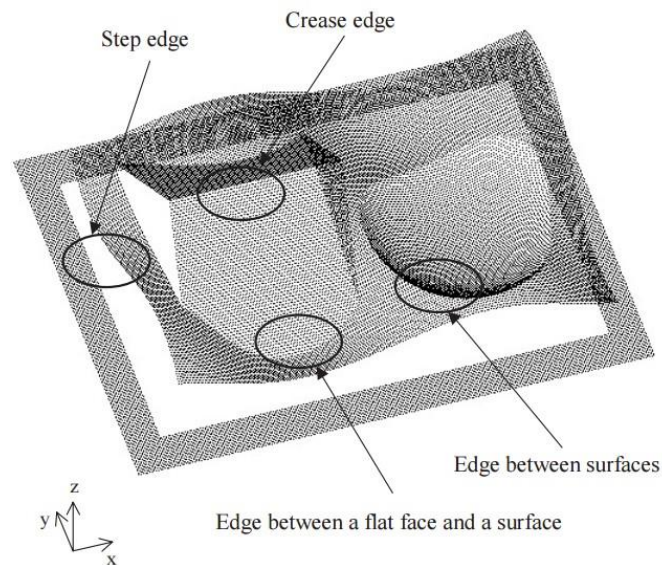


Figure 2-8 Segmentation and surface extraction of point cloud based on edge detection (Yang, M. 1999)

(2) Region growing is another approach trying to detect the continuous surfaces with the word “continuous” meaning the similar geometrical properties such as the similar normal vector’s values between the neighborhood points. Rabbania, T. (2006) proposed a surface extraction method containing two steps, the normal estimation and the region growing as shown in Figure 2-9. The region growing step uses the calculated normal vectors of the points, in accordance with user specified parameters to group points trying to avoid over-segmentation. Two constrains are applied to this step: the local connectivity which is enforced by using only the neighborhood points in KNN, and the surface smoothness which is checked through a threshold on the differences between the current seed points and the points being evaluated. As shown in Figure 2-9

According to the definition of region growing method, it cannot be applied to the measured objects which are not continuous.

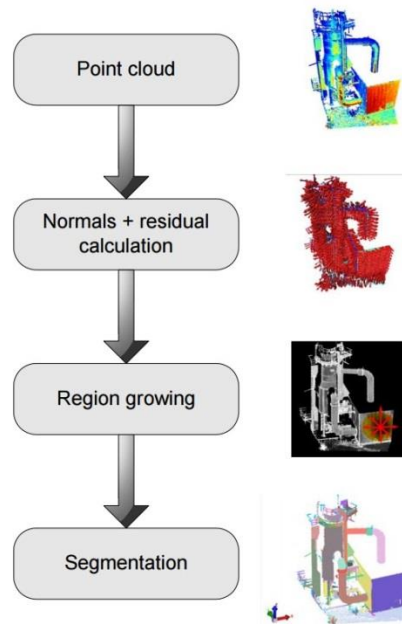


Figure 2-9 Segmentation and surface extraction of point cloud based on region growing (Rabbania, T. 2006)

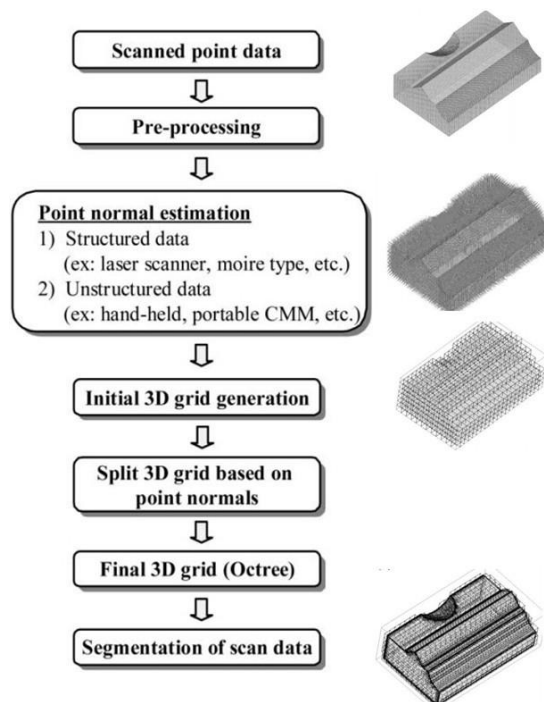


Figure 2-10 Segmentation and surface extraction of point cloud based on 3D grids (Woo, H. 2001)

Some hybrid segmentation methods are also developed to solve the problems mentioned above. Instead of conducting curve and surface fitting directly toward the point cloud, as shown in Figure 2-10, Woo, H. (2001) proposed a new method for segmenting the point cloud data, and fitting surface after that. The normal vectors of the points are estimated at first. Then the 3D grids are generated towards the point cloud. The standard deviation σ of points' normal vectors in each cell indicates the changes in the shape within this cell. Threshold is set on σ to decide if the cell should be divided into more cells or not. Then the edges of the surfaces are detected at the highly curved areas with high densities of cells.

2.4.2. Surface registration of the point cloud data

A relatively new approach of surface registration is from Yun, D. (2015) who proposed an automated registration method of multi-view point clouds using sphere targets. From this research, they also find that in most of the existing methods for the accurate registration of point clouds, the overlapping regions between two point clouds should be detected. However, in most of the cases the overlap region and direction can only be detected manually, which becomes a vital problem for the automatic measurement using laser scanner. They proposed a method using targets which are put on the object manually to solve this problem.

2.4.3. Problems existing in laser scanner's practical usage in shipyard

The researches about the point cloud processing methods introduced above show a lot of possibilities of the merits which the laser scanner could bring us. However, problems for the practical usage of laser scanner in shipyard still exist.

- a. There are a lot of irregular obstacles such as the floor, workers, water hoses and the wooden templates existing in the point clouds measured in the shipyard.
- b. The plate part in the measured point cloud is usually separated irregularly by the water which cannot reflect the laser and the shadows of the obstacles.
- c. The manual segmentation method cost too much time when extract the plate

part due to the enormous numbers of the points in the point cloud.

- d. The registration process can cost a lot of time and may give wrong results without presetting of the direction (the pre-overlap of the design data and the point cloud).

This thesis will work on these problems' solutions by proposing a method which can extract the separated plate's surface from the point cloud with obstacles and a registration method with pre-settings of the registration direction.

2.5. Researches on knowledge elicitation and dissemination

A lot of researches work on the knowledge elicitation and dissemination in different fields. Cheung, C.F. (2011) proposed a multi-faceted and automatic knowledge elicitation system (MAKES) for managing unstructured information". Hiekata, K., Yamato, H. (2007) developed a ship design educational framework using ShareFast.

Especially with the consideration on the interfaces and progresses of the knowledge elicitation and dissemination, Robinson, S. (2012) focused on the effect of visual representation and model parameters when doing the simulation based knowledge elicitation, while Pu, S., Vosselman, G. (2009) proposed a knowledge based reconstruction method of building models using 3D laser scanner point cloud.

In this subsection, some representative examples will be introduced, and the problems existing in the knowledge elicitation and dissemination during the active curved shell plates' manufacturing will be clarified.

2.5.1. Knowledge elicitation: progresses, interfaces

An example for the knowledge elicitation considering the interfaces, the visual representation and the model parameters is from Robinson, S. (2012). This research proposes a visual interactive simulation (VIS) as a means for eliciting experts' decision-making by getting them to interact with a visual simulation of the real system in which they used to work. Experiment with decision-makers in Ford Motor Company engine assembly plant was conducted to prove the effectiveness and

efficiency of the visual representation interface. 2D and 3D views and the model parameter settings will be provided by the system.

Decision variables	Decision attributes
(1) Set path option at junction J to conveyor B or C, or automatic	(1) Quantity of engines on each section of the conveyor
(2) Switch hot test cell/waiting stand on or off	(2) Type of engine on each section of the conveyor (2.1 or 2.4.1)
	(3) Type of engine currently being/last tested in each hot test cell
	(4) Type of engine parked on each waiting stand
	(5) Operational status of each hot test cell (free, busy, broken)
	(6) Quantity of engines tested by each hot test cell operator

Figure 2-11 Switch operators' decision variables and decision attributes for engine assignment (Robinson, S. 2012)

The decision attributes are in the figure above.

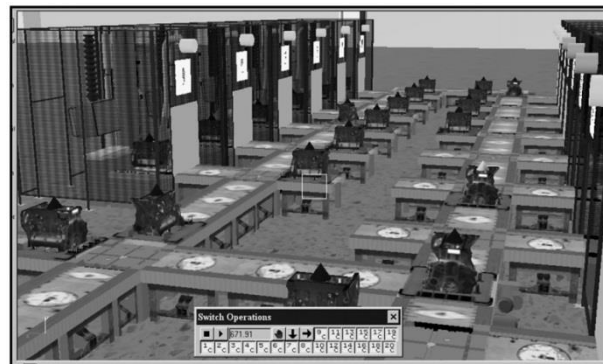


Figure 2-12 Example of display view of the hot test model (Robinson, S. 2012)

For each visual representation the experts first worked with the model shown in the figure above with unadjusted parameters and then with adjusted parameters. The decision variables they used were recorded in a fixed sequence.

As pointed in this research, all the switch operators worked through the models in a fixed sequence which means the consequences of these decisions can be estimated and calculated. However, in the active curved shell plates' manufacturing, the manufacturing sequence varies every time after each single manufacturing step.

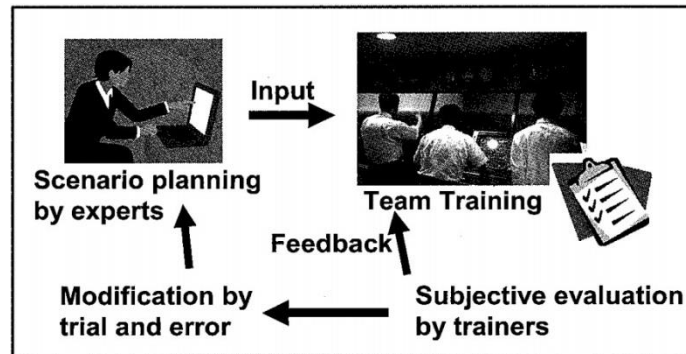


Figure 2-13 Bridge Resource Management simulator training (Kakuta, R. 2007)

Another research about the knowledge extraction and the training of the beginner crews on ship is provided by Kakuta, R.(2007). As shown in Figure 2-13, firstly, experts plan and input the scenarios into the training simulator. After that, visualization of scenario progression as Gantt chart and evaluation of the crew size change effect on watch keeping performance are conducted by the simulator. Crews give the feedback to the system after the training. A lot of data is inputted into the training system including the navigation environment, scenario event, own ship information and the crew team design. After the training process, the system can output the team performance in form of Gantt chart, and knowledge about the team design, scenario design can be extracted though the output information. Three training scenarios are used to evaluate this approach, it is confirmed that useful knowledge to quantify and control scenario difficulty is obtained though these experiments.

2.5.2. Knowledge dissemination: interfaces, storages

An example for the combination research of the knowledge base and the laser scanner, knowledge based reconstruction of building models from terrestrial laser scanning data, is from Pu, S., Vosselman, G. (2009). They present an automatic method for reconstruction of building facade models from terrestrial laser scanning data. Firstly, the point cloud of the building is obtained from the laser scanner. Then least squares fitting, convex hull fitting and concave polygon fitting is conducted toward the obtained point cloud. After the outline polygon of the features

is generated, the general knowledge is used to assume the occluded parts of the object from the polygons. Finally, a polyhedron building model can be reconstructed and virtualized.

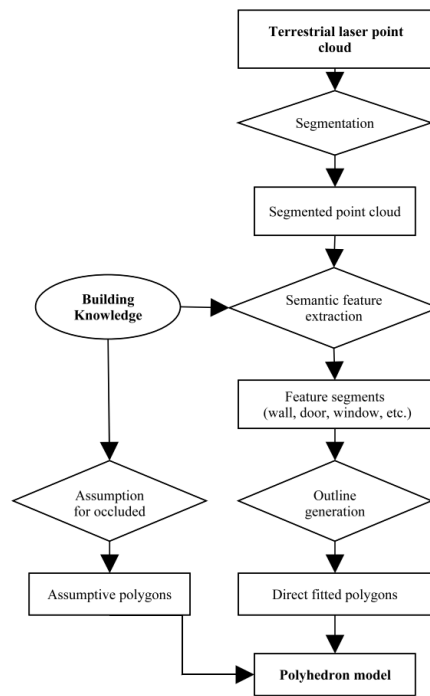


Figure 2-14 Knowledge based building reconstruction process (Pu, S., Vosselman, G. 2009)

In Pu, S. 's research, the knowledge for extracting the features such as ground, wall and roof is stored in a formulated feature constraints base as shown in Figure 2-15. When trying to disseminate the knowledge, each segment displayed on the interface shown in the figure is checked through these stored constraints to determine whether or not it is irrelevant, if relevant, which semantic feature it represents.



Figure 2-15 Knowledge base and dissemination interface for the feature extractions (Pu, S., Vosselman, G. 2009)

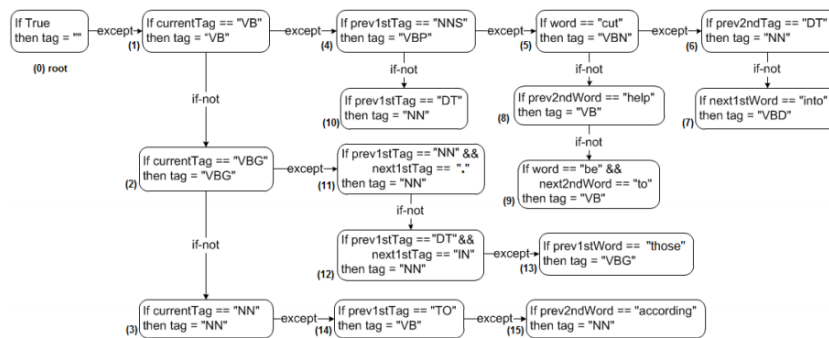


Figure 1.: An example of a SCRDR tree for English POS tagging.

Template	Example
#2: if previous1 st Word == "object.previous1 st Word" then tag = "correctTag"	(13)
#3: if word == "object.word" then tag = "correctTag"	(5)
#4: if next1 st Word == "object.next1 st Word" then tag = "correctTag"	(7)
#10: if word == "object.word" && next2 nd Word == "object.next2 nd Word" then tag = "correctTag"	(9)
#15: if previous1 st Tag == "object.previous1 st Tag" then tag = "correctTag"	(4)
#20: if previous1 st Tag == "object.previous1 st Tag" && next1 st Tag == "object.next1 st Tag" then tag = "correctTag"	(11)

Figure 2-16 RDR tree for English tagging knowledge (Nguyen, D. Q. 2015)

Nguyen, D. Q. (2015) proposed a new method for constructing a transformation rule base for the Part-of-Speech tagging task in which the tagging knowledge is represented in the form of Ripple-Down Rules as shown in Figure 2-16. Bindoff, I. (2014) developed a ripple-down rules based clinical decision support system to detect drug-related problems by determine if the problems are clinically relevant or not according to the rule base.

2.5.3. Problems of knowledge elicitation and dissemination in manufacturing

According to the researches introduced above, the knowledge elicitation and dissemination with the 3D virtualized environment is effective for most of the conditions.

However, knowledge elicitation and dissemination during the curved shell plates' manufacturing should also consider the following points:

- a. To avoid the time-consuming OJT (on the job training), the manufacturing process should be recorded and represented in a comprehensible way. 3D interfaces are considered to be helpful in this case
- b. Since the manufacturing process is not fixed but active, the parameters representing the real time situation should be able to be calculated, measured and represented too.
- c. The process to elicit the knowledge based on the 3D represented interfaces should be defined. The knowledge is going to be stored in the format of Ripple-Down Rules.

2.6. Originalities of this thesis

On the basis of 2.2 2.3 2.4 and 2.5, three originalities in this thesis can be described as follows:

- (1) To propose and develop interfaces with high accuracy and high usability for facilitating the curved shell plates' manufacturing and preserving the manufacturing convention.
- (2) To propose an efficient method for eliciting and disseminating the manufacturing knowledge existing in the manufacturing processes based on the data recorded by the proposed interface in (1).
- (3) To propose original point cloud processing methods supporting (1) for extracting the plates' point clouds which are separated by irregular obstacles and for registering them with the design data.

The whole manufacturing framework will be constructed based on the above original proposals, and at the end of this thesis the effectiveness of these originalities will be concluded.

Chapter 3 Component technologies

3.1. Overview

In this chapter, the component technologies concerning the developed framework will be introduced. Specifically, there are the 3 dimensional measurement equipment and features, the basic point cloud processing technologies and the knowledge engineering technology.

In the practice, a lot of improvements are made toward these general technologies, the reasons and the implementation of these improvements will be introduced in the later chapters. In this chapter the general technologies will be introduced.

3.2. 3D measurement equipment and features

3.2.1. Laser scanner

Non-contact 3D scanning by laser scanner has started to spread dramatically in recent years and its performance has been improving immensely. The laser scanner measures the distance by calculating the time in which a laser pulse travels back and forth between the object to be measured and the light-receiving sensor. It then combines the distance and the direction of radiation, thus the 3D positional coordinates are obtained. The laser scanner is able to measure a multiple number of points at a time. In this study, the laser scanner is used to measure the shape of the curved shell plate.

Specifically, as shown in Figure 3-1(left), the terrestrial laser scanner provides a 3D visualization of a scene by measuring distances to object surfaces in a spherical coordinate system, it records two angles (horizontal angle θ and vertical angle \varnothing) of laser beams transmitted with regular vertical and horizontal increment, and a distance r of the measured point on the object surface as shown in Figure 3-1(right), regarding the laser scanner as the center of the coordinate system. By rotating the irradiation port, (θ, \varnothing) is changed rapidly so that a large amount of points' positional information can be measured in a short time.

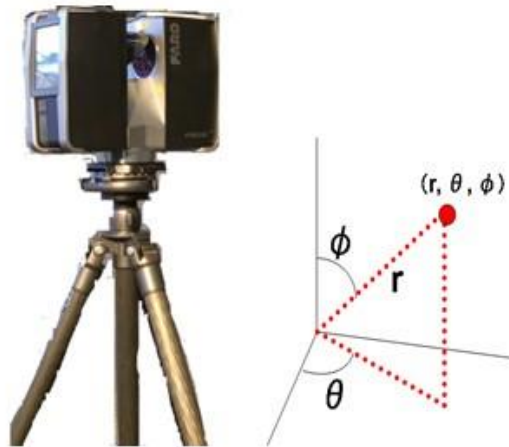


Figure 3-1 Terrestrial laser scanner FARO (FARO 2011)

3.2.2. Kinect

Kinect (codenamed in development as Project Natal) is a line of motion sensing input devices by Microsoft. The main utility of Kinect is to detect the human motions, but it can also record a set of 3D points of the object. As shown in Figure 3-2, the device features an "RGB vision camera, 3D depth sensor, motorized tilt and multi-array microphone running proprietary software", which provide full-body 3D motion capture, facial recognition and voice recognition capabilities.

An IR projector and an IR camera constitute the 3D depth sensor. The IR projector used in Kinect is an IR laser that passes through a diffraction grating and turns into a lot of IR dots. Each of those points is unique and the IR camera sees how it distorts and the distance to that point. By combining that data with the color image from the camera and the transforming algorithm, the 3D point cloud data can be obtained.

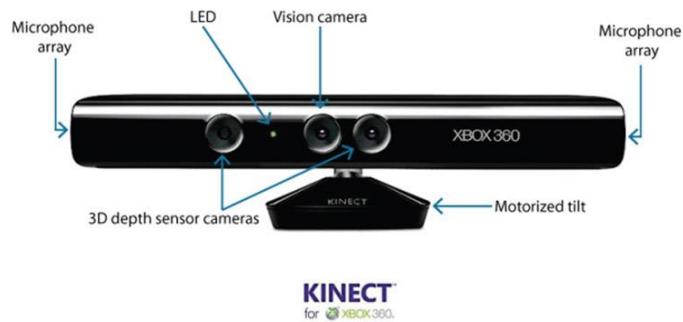


Figure 3-2 Kinect structure (Microsoft 2012)

3.2.3. Point cloud data

The Coordinate system, color system, data structure and data format of point cloud data depend on the manufacturer of the laser scanner. The Cartesian coordinate system, RGB color system and text data format are used in this system. As shown in Figure 3-3, every row represents a point, the first 3 columns are (x, y, z) coordinates, the following column is the reflection intensity of each point, the last 3 columns are (R, G, B) respectively.

```

2  -13.98610000  6.09780000  -5.83700000  321 148 148 148
3  -13.98250000  6.10140000  -5.83630000  193 140 140 140
4  -13.97850000  6.10420000  -5.83540000  161 138 138 138
5  -13.96760000  6.10500000  -5.83170000  81 133 133 133
6  -13.97270000  6.11260000  -5.83470000  -95 122 122 122
7  -13.96690000  6.11480000  -5.83310000  -143 119 119 119
8  -13.96330000  6.11830000  -5.83240000  -223 114 114 114
9  -13.96540000  6.12430000  -5.83410000  -79 123 123 123
10 -13.96140000  6.12750000  -5.83320000  -143 119 119 119
11 -13.95640000  6.13050000  -5.83190000  -143 119 119 119
12 -13.95420000  6.13450000  -5.83180000  -95 122 122 122
13 -13.95410000  6.13940000  -5.83260000  -111 121 121 121
14 -13.94990000  6.14280000  -5.83170000  -63 124 124 124
15 -13.95000000  6.14740000  -5.83240000  -31 126 126 126
16 -13.94250000  6.14890000  -5.83010000  -47 125 125 125
17 -13.94680000  6.15640000  -5.83280000  -31 126 126 126
18 -13.94350000  6.16010000  -5.83220000  -47 125 125 125
19 -13.94180000  6.16450000  -5.83230000  -47 125 125 125

```

Figure 3-3 Point cloud data structure

3.3. Point cloud processing

The point cloud processing technologies concerning this thesis is introduced in this subsection.

3.3.1. Edge detection

Edge detection in point cloud processing is the name for a set of mathematical methods which aim at identifying points in a point cloud at which point features (color, brightness or normal vector) changes sharply or, more formally, has discontinuities. The points at which image point features change sharply are typically organized into a set of curved line segments termed edges.

In general, under successful edge detection, the relatively unimportant information will be eliminated, and the subsequent processing can be greatly simplified. In this study, in order to extract the curved shell plates' separated domains divided by the shades of the obstacles, it is necessary to identify the edges of each domain which has been already extracted. And the edge detection is also used to reduce the continuous domain's extraction time.

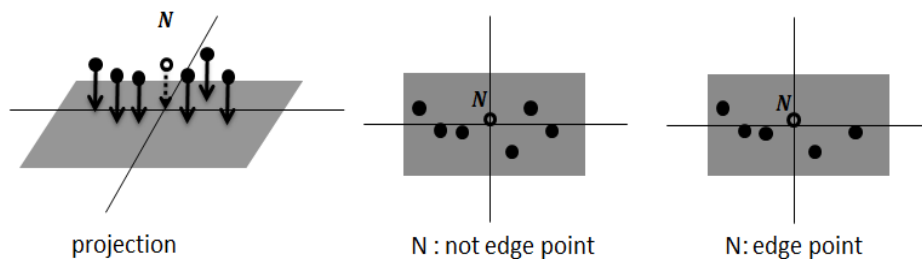


Figure 3-4 Edge detection

The statistical curvature evaluation technique from Kalogerakis in 2009 is used in this study. And as a pre-processing step to edge detection, a smoothing stage, typically Gaussian smoothing, is almost always applied (see also noise reduction). To extract the edge in this process, as shown in Figure 3-4, a plane is fitted using the principal component analysis. The points used to do plane fitting is the neighbor

points of seed point N searched by k -NN method. Then the neighbor points are projected to the plane. If not all of the 4 quadrants have neighbor points as shown in the right image of Figure 3-4, the point N is considered as the edge.

Specifically, the algorithm of this method is as below:

- a. For a point N , the neighbor points is searched, and plane fitting is performed to the searched neighbors.
- b. The neighbor points are projected onto the fitted plane.
- c. If not all of the 4 quadrants have neighbor points, the point N is considered as the edge.
- d. The above operation is performed toward every point belonging to the extracted domain.

And depending on the tangible issues, the 4 quadrants can be changed into 6 or 8.

3.3.2. Region growing

As a crucial pre-process conducted toward the measured curved shell plate's point cloud data, all of the noise should be removed and the separated domains belonging to the same component should be extracted efficiently.

The proposed component extraction method is based on a basic point cloud processing method called region growing method according to Forsyth et al., which repeats the process of calculating the normal vector at each neighbor point of the seed point, extracting the neighbor point which has a similar normal vector as the seed point and setting the extracted neighbor point as the next seed point. Figure 3-5 shows the main flow of the region growing method. The growing process ends when the normal vectors have relatively dramatic changes.

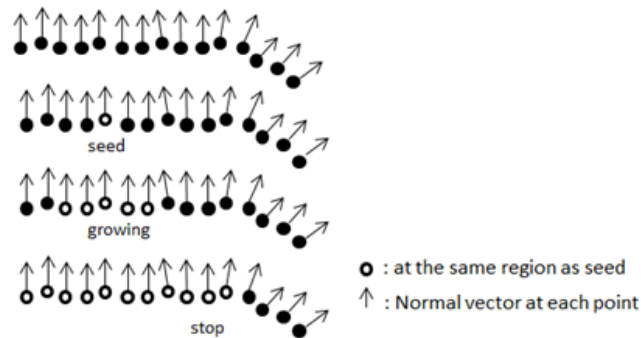


Figure 3-5 The basic region growing method

The algorithm of the basic region growing method is as below:

- A) The seed point which belongs to the curved shell plate is selected.
- B) The neighboring points of the seed point are detected.
- C) Among the detected neighboring points, the ones satisfying certain features (Normal vector similarity in this case) are extracted and added to the domain.
- D) Step B) and C) are repeated until the growth stops.

To make the neighbor search more efficient here, a space-partitioning data structure, Kd-tree (Gross et al., 2007), is constructed using the scanned point cloud data for organizing points in a k-dimensional space recursively. The normal vector at each point is first calculated using Least-squares regression (which will be introduced in later subsection), then normalized. And the comparison of the points' features is conducted by calculating the inner product of the normal vectors.

3.3.3. k-Nearest Neighbor

In pattern recognition, the k-Nearest Neighbor algorithm (KNN) is a method for classifying objects based on the closest training examples in the feature space. KNN is a type of instance-based learning, or lazy learning where the function is only approximated locally and all computation is deferred until classification (Jeffrey S. Beis and David G. Lowe. 1997). The KNN algorithm is amongst the simplest of all machine learning algorithms: an object is classified by a majority

vote of its neighbors, with the object being assigned to the class most common amongst its k nearest neighbors (k is a positive integer, typically small). If $k = 1$, then the object is simply assigned to the class of its nearest neighbor.

In this study, KNN is used to search the k nearest neighbor points from the point cloud for a certain seed point. Kd-tree is used as the basic data structure.

Kd-tree has a similar structure to the binary tree, all nodes are divided along with one axis (Hill, M.1990). As a common method of generating Kd-tree, a super n -dimensional space containing all of the elements is prepared, and then a recursive 2-division with respect to an axis is performed (Gross et al., 2007). During this process, the numbers of the elements in the two divided spaces remain the same. Also, as shown in Figure 3-6, instead of repeatedly division with respect to every axis, the division relative to the largest axis is performed.

Once a Kd-tree is constructed, for neighbor points search, it is possible to exclude the majority of the tree nodes by some simple test, and result in a high speed search. Though Kd-tree has the disadvantage that little difference in speed comparing to all points search would exist, it is still fast in point cloud because the k is defined into 3 in this case. In this study, the kNNBBF which is an efficient k -Nearest Neighbor search technique is used.

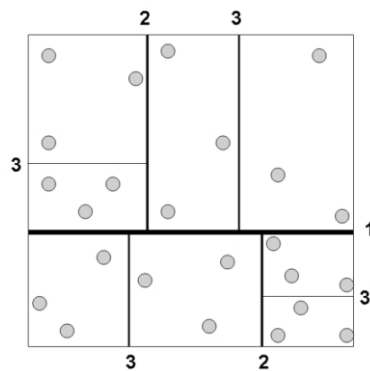


Figure 3-6 Kd-tree ($k = 2$)

3.3.4. Plane fitting

In this study, as an important component technology, the proper plane fitting

method is of vital importance during the region growing introduced last subsection.

3.3.4.1. Basic plane fitting

The definition of the plane fitting in 3D point cloud is : within the points in the point cloud, the regression plane $ax + by + cz + d = 0$ is calculated using the neighbor points $\{P_i\}(i = 1, \dots, n)$ of the seed point of which the normal vector $\mathbf{n} = (a \ b \ c)^T$ is demanded.

Firstly, the condition that the regression plane should satisfy is to minimize the equation (3.1) .

$$J = \sum_i (ax_i + by_i + cz_i + d)^2 \rightarrow \min \quad (3.1)$$

The conditions to minimize equation (3.1) are equations (3.2) - (3.5).

$$\frac{\partial J}{\partial a} = \sum_i 2x_i(ax_i + by_i + cz_i + d) = 0 \quad (3.2)$$

$$\frac{\partial J}{\partial b} = \sum_i 2y_i(ax_i + by_i + cz_i + d) = 0 \quad (3.3)$$

$$\frac{\partial J}{\partial c} = \sum_i 2z_i(ax_i + by_i + cz_i + d) = 0 \quad (3.4)$$

$$\frac{\partial J}{\partial d} = \sum_i 2(ax_i + by_i + cz_i + d) = 0 \quad (3.5)$$

By dividing both sides of Equation (3.5) with n, Equation (3.6) and (3.7) are obtained; the regression plane passes though the center of gravity $\mathbf{G} = (\bar{x} \ \bar{y} \ \bar{z})^T$ of the points of which the regression plane is being calculated.

$$a \cdot \frac{1}{n} \sum_i x_i + b \cdot \frac{1}{n} \sum_i y_i + c \cdot \frac{1}{n} \sum_i z_i + d \cdot \frac{1}{n} \sum_i 1 = 0 \quad (3.6)$$

$$a\bar{x} + b\bar{y} + c\bar{z} + d = 0 \quad (3.7)$$

$$d = -(a\bar{x} + b\bar{y} + c\bar{z}) \quad (3.8)$$

Then by dividing both sides of Equation (3.2) with n and organizing the result with Equation (3.8), Equation (3.12) is obtained. S_{pq} is the covariance of p and q .

$$a \cdot \frac{1}{n} \sum_i x_i^2 + b \cdot \frac{1}{n} \sum_i x_i y_i + c \cdot \frac{1}{n} \sum_i z_i x_i + d \cdot \frac{1}{n} \sum_i x_i = 0 \quad (3.9)$$

$$a\overline{x^2} + b\overline{xy} + c\overline{zx} - (a\bar{x} + b\bar{y} + c\bar{z})\bar{x} = 0 \quad (3.10)$$

$$(\overline{x^2} - \bar{x}^2)a + (\overline{xy} - \bar{x} \cdot \bar{y})b + (\overline{zx} - \bar{z} \cdot \bar{x})c = 0 \quad (3.11)$$

$$S_{xx}a + S_{xy}b + S_{zx}c = 0 \quad (3.12)$$

Similarly, Equation (3.13) and (3.14) can be obtained from Equation (3.3) and (3.4) respectively.

$$S_{xy}a + S_{yy}b + S_{yz}c = 0 \quad (3.13)$$

$$S_{zx}a + S_{yz}b + S_{zz}c = 0 \quad (3.14)$$

Equation (3.15) is obtained summarizing Equation (3.12) - (3.14).

$$\begin{pmatrix} S_{xx} & S_{xy} & S_{zx} \\ S_{xy} & S_{yy} & S_{yz} \\ S_{zx} & S_{yz} & S_{zz} \end{pmatrix} \begin{pmatrix} a \\ b \\ c \end{pmatrix} = \mathbf{0} \quad (3.15)$$

At last, the eigenvector for the smallest eigenvalue of the coefficient matrix $\mathbf{\Sigma}$ of the Equation (3.15) coincides with the normal vector $\mathbf{n} = (a \ b \ c)^T$. Here $\mathbf{\Sigma}$ is the variance-covariance matrix of $\{\mathbf{P}_i\}$.

3.3.4.2. Weighted plane fitting

Because of the problems discussed in the beginning of this subsection, in order to remove such high frequency noise, the regression plane is obtained toward the points which have already been weighted using the distances between them and the seed point. In this case, condition the regression plane should satisfy is to minimize the Equation (3.16). As shown in Equation (3.17) the weight w_i is calculated for each point so as points closer to the point being calculated has greater influence when the plane is fitted. Here d is the distance between each point and the point being calculated and h is the average interval of the point cloud points.

$$J_w = \sum_i w_i(ax_i + by_i + cz_i + d)^2 \rightarrow \min \quad (3.16)$$

$$w_i = \exp\left(-\frac{d^2}{h^2}\right) \quad (3.17)$$

The conditions to minimize equation (3.16) are equations (3.18) - (3.21).

$$\frac{\partial J_w}{\partial a} = \sum_i 2w_i x_i(ax_i + by_i + cz_i + d) = 0 \quad (3.18)$$

$$\frac{\partial J_w}{\partial b} = \sum_i 2w_i y_i(ax_i + by_i + cz_i + d) = 0 \quad (3.19)$$

$$\frac{\partial J_w}{\partial c} = \sum_i 2w_i z_i(ax_i + by_i + cz_i + d) = 0 \quad (3.20)$$

$$\frac{\partial J_w}{\partial d} = \sum_i 2w_i(ax_i + by_i + cz_i + d) = 0 \quad (3.21)$$

By dividing both sides of Equation (3.21) with $\sum_i w_i$, Equation (3.22) is obtained; the regression plane passes through the weighted center of gravity $\mathbf{G}_w = (\bar{x}_w \ \bar{y}_w \ \bar{z}_w)^T$ of the points of which the regression plane is being calculated.

Each coordinate of the weighted center of gravity is shown as Equation (3.25) - (3.27).

$$a \cdot \frac{1}{\sum_i w_i} \sum_i w_i x_i + b \cdot \frac{1}{\sum_i w_i} \sum_i w_i y_i + c \cdot \frac{1}{\sum_i w_i} \sum_i w_i z_i + d \cdot \frac{1}{\sum_i w_i} \sum_i w_i = 0 \quad (3.22)$$

$$a\bar{x}_w + b\bar{y}_w + c\bar{z}_w + d = 0 \quad (3.23)$$

$$d = -(a\bar{x}_w + b\bar{y}_w + c\bar{z}_w) \quad (3.24)$$

$$\bar{x}_w = \frac{1}{\sum_i w_i} \sum_i w_i x_i \quad (3.25)$$

$$\bar{y}_w = \frac{1}{\sum_i w_i} \sum_i w_i y_i \quad (3.26)$$

$$\bar{z}_w = \frac{1}{\sum_i w_i} \sum_i w_i z_i \quad (3.27)$$

Then by dividing both sides of Equation (3.18) with $\sum_i w_i$ and organizing the result with Equation (3.24), Equation (3.31) is obtained. S_{pq_w} is the weighted covariance of p_i and q_i .

$$a \cdot \frac{1}{\sum_i w_i} \sum_i w_i x_i^2 + b \cdot \frac{1}{\sum_i w_i} \sum_i w_i x_i y_i + c \cdot \frac{1}{\sum_i w_i} \sum_i w_i z_i x_i + d \cdot \frac{1}{\sum_i w_i} \sum_i w_i x_i = 0 \quad (3.28)$$

$$a\overline{x^2_w} + b\overline{xy_w} + c\overline{zx_w} - (a\bar{x}_w + b\bar{y}_w + c\bar{z}_w)\bar{x}_w = 0 \quad (3.29)$$

$$(\overline{x^2_w} - \bar{x}_w^2)a + (\overline{xy_w} - \bar{x}_w \cdot \bar{y}_w)b + (\overline{zx_w} - \bar{z}_w \cdot \bar{x}_w)c = 0 \quad (3.30)$$

$$S_{xx_w}a + S_{xy_w}b + S_{zx_w}c = 0 \quad (3.31)$$

S_{pq_w} is the weighted covariance of p_i and q_i .

$$\begin{aligned}
 S_{pq_w} &= \frac{1}{\sum_i w_i} \sum_i w_i (p_i - \bar{p}_w)(q_i - \bar{q}_w) \\
 &= \frac{1}{\sum_i w_i} \sum_i (w_i p_i q_i - w_i p_i \bar{q}_w - w_i \bar{p}_w q_i + \bar{p}_w \bar{q}_w) \\
 &= \bar{p} \bar{q}_w - \bar{p}_w \bar{q}_w - \bar{p}_w \bar{q}_w + \bar{p}_w \bar{q}_w = \bar{p} \bar{q}_w - \bar{p}_w \bar{q}_w
 \end{aligned} \tag{3.32}$$

Similarly, Equation (3.33) and (3.34) can be obtained from Equation (3.19) and (3.20) respectively.

$$S_{xy_w} a + S_{yy_w} b + S_{yz_w} c = 0 \tag{3.33}$$

$$S_{zx_w} a + S_{yz_w} b + S_{zz_w} c = 0 \tag{3.34}$$

Equation (3.35) is obtained summarizing Equation (3.31), (3.33) and (3.34).

$$\begin{pmatrix} S_{xx_w} & S_{xy_w} & S_{zx_w} \\ S_{xy_w} & S_{yy_w} & S_{yz_w} \\ S_{zx_w} & S_{yz_w} & S_{zz_w} \end{pmatrix} \begin{pmatrix} a \\ b \\ c \end{pmatrix} = 0 \tag{3.35}$$

At last, the eigenvector for the smallest eigenvalue of the coefficient matrix $\boldsymbol{\Sigma}_w$ of the Equation (3.35) coincides with the normal vector $\mathbf{n} = (a \ b \ c)^T$. Here $\boldsymbol{\Sigma}$ is the weighted variance-covariance matrix of $\{\mathbf{P}_i\}$.

3.3.5. Curve fitting

In this study, both the wooden templates' design data and the measured curved shell plates are in the form of point cloud data. To do the comparison and evaluation of the curvatures at the position of the frames (where the templates should be put),

these point cloud data should be firstly fitted into curves.

Curve fitting is the process of constructing a curve, or mathematical function that has the best fit to a series of data points, possibly subject to constraints. Curve fitting can involve either interpolation, where an exact fit to the data is required, or smoothing, in which a "smooth" function is constructed that approximately fits the data. In this subsection, Lagrange interpolation and Spline interpolation will be introduced.

3.3.5.1. Lagrange interpolation

In this study, Lagrange interpolation is used to generate the virtual templates' bottom lines. Lagrange interpolation is one of the interpolation methods which make the interpolated curve pass through all of the control points (Gabriel A. et al. 2001).

The Lagrange interpolating polynomial in 3D point cloud processing is the polynomial $Y(x)$ and $Z(x)$ of degree $\leq (n - 1)$ that passes through the n points (x_1, y_1, z_1) , (x_2, y_2, z_2) , ..., (x_n, y_n, z_n) , and is given by:

$$Y(x) = \sum_{i=1}^n Y_i(x) \quad (3.36)$$

$$Z(x) = \sum_{k=1}^n Z_k(x) \quad (3.37)$$

where

$$Y_i(x) = y_i \prod_{\substack{j=1 \\ j \neq i}}^n \frac{x - x_j}{x_i - x_j} \quad (3.38)$$

$$Z_k(y) = z_k \prod_{\substack{l=1 \\ l \neq k}}^n \frac{x - x_l}{x_k - x_l} \quad (3.39)$$

The formula was first published by Waring (1779), rediscovered by Euler in 1783,

and published by Lagrange in 1795 (Jeffreys and Jeffreys 1988).

Lagrange interpolating polynomials are implemented in Mathematica as `Interpolating Polynomial[data, var]`. They are used, for example, in the construction of Newton-Cotes formulas.

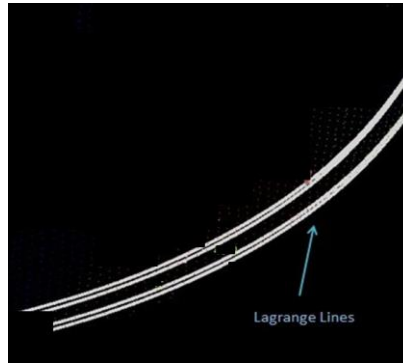


Figure 3-7 Feature points of virtual template

The fitted template's bottom lines are shown as the figure above.

3.3.5.2. B-Spline interpolation

In this study, B-Spline interpolation is used to estimate the measured curved shell plates' frame lines. B-Spline curve is defined by a series of parameters $t(\{t_0, t_1, t_2, \dots\})$. The "B" of B-Spline is the initial letter of "basis". B-Spline does not have to pass through all of the control points, and is a smooth curve defined from the given multiple control points. Because it is expressed by the piecewise polynomial and generally not passes through the control point other than the end points, even some control points are changed, the influence on the whole curve is limited. Therefore, B-Spline interpolation is widely utilized in the cases that not all the control points represent the exact part of the expected curve. (Catmull, E. and Clark, J. 1978)

$$\mathbf{S}(t) = \sum_{i=0}^{m-n-2} \mathbf{P}_i b_{i,n}(t), \quad t \in [t_n, t_{m-n-1}] \quad (3.40)$$

$$\begin{aligned}
 b_{j,0} &= 1 \quad \text{if } t_j \leq t \leq t_{j+1} \quad \text{where } j = 0, \dots, m-2 \\
 b_{j,0} &= 0 \quad \text{if } t > t_{j+1} \quad \text{or } t < t_j \quad \text{where } j = 0, \dots, m-2 \\
 b_{j,n}(t) &= \frac{t - t_j}{t_{j+n} - t_j} b_{j,n-1}(t) + \frac{t_{j+n+1} - t}{t_{j+n+1} - t_{j+1}} b_{j+1,n-1}(t) \\
 &\quad \text{where } j = 0, \dots, m-n-2
 \end{aligned}$$

The B-Spline curve of one segment can be expressed by Equation (3.40). t_i which are called “knot” are a series of real numbers. Also $b_{i,n}$ are referred to B-Spline basis functions, and is defined by the recurrence formula of de Boor Cox.

In a 2D B-Spline curve, the basis function is as below:

$$\begin{aligned}
 \mathbf{S}_i(t) &= [t^2 \quad t \quad 1] \frac{1}{2} \begin{bmatrix} 1 & -2 & 1 \\ -2 & 2 & 0 \\ 1 & 1 & 0 \end{bmatrix} \begin{bmatrix} \mathbf{P}_{i-1} \\ \mathbf{P}_i \\ \mathbf{P}_{i+1} \end{bmatrix} \\
 &\quad t \in [0, 1], i = 1, 2, \dots, m-2
 \end{aligned} \tag{3.41}$$

In this study, the B-Spline basis functions are as follows:

$$\begin{aligned}
 \mathbf{S}_i(t) &= [t^3 \quad t^2 \quad t \quad 1] \frac{1}{6} \begin{bmatrix} -1 & 3 & -3 & 1 \\ 3 & -6 & 3 & 0 \\ -3 & 0 & 3 & 0 \\ 1 & 4 & 1 & 0 \end{bmatrix} \begin{bmatrix} \mathbf{P}_{i-1} \\ \mathbf{P}_i \\ \mathbf{P}_{i+1} \\ \mathbf{P}_{i+2} \end{bmatrix} \\
 &\quad t \in [0, 1], i = 1, 2, \dots, m-2
 \end{aligned} \tag{3.42}$$

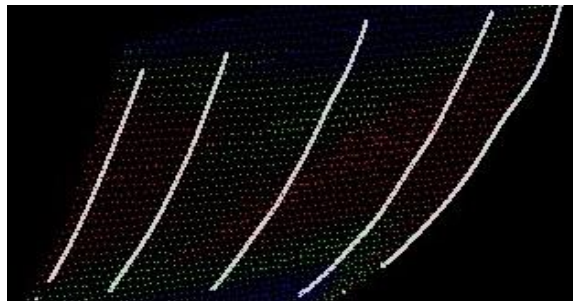


Figure 3-8 Feature points of virtual template

The fitted measured frame line of the curved shell plate is shown as the figure above.

3.3.6. Iterative closest point

In shipbuilding, components' design data is often expressed in SAT format, a standard file format of ACIS. In SAT files, surfaces and curves are expressed as NURBS (Non-Uniform Rational B-Spline). To evaluate the accuracy of the component or to provide any farther manufacturing advice, as an important pre-process, a registration between the design data and the extracted component's point cloud data should be conducted efficiently.

In this study, Iterative closest point algorithm is used to do the registration between the design data and the extracted component's point cloud data.

After a parallel transformation using the center of gravity, a basic ICP algorithm is conducted for the registration of the point cloud and the design data. The design curved surface $S(u, v) = (x(u, v), y(u, v), z(u, v))$ is a rational equation using the B-Spline basis functions which represent the homogeneous coordinate system projection results of the non-constant spacing knots (Piegl et al., 1996).

$$\mathbf{r}(u, v) = \mathbf{S}(u, v) - \mathbf{P} \quad (3.43)$$

$$\mathbf{r}(u, v) \cdot \mathbf{S}_u(u, v) = 0 \quad (3.44)$$

$$\mathbf{r}(u, v) \cdot \mathbf{S}_v(u, v) = 0 \quad (3.45)$$

As defined in Equation (3.43), the projection vector can be obtained by subtracting the measured point \mathbf{P} 's position vector from the design curve surface $\mathbf{S}(u, v)$. Therefore, $\mathbf{r}(u, v)$ satisfies the Equations (3.44) and (3.45). Here, the $\mathbf{S}_u(u, v)$ and $\mathbf{S}_v(u, v)$ are the u -direction's and the v -direction's partial derivatives of the designed curved surface respectively. Projection vector $\mathbf{r}(u, v)$ as shown in Figure 3-9 can be calculated by solving these three equations. Here \mathbf{Q} is the projection point.

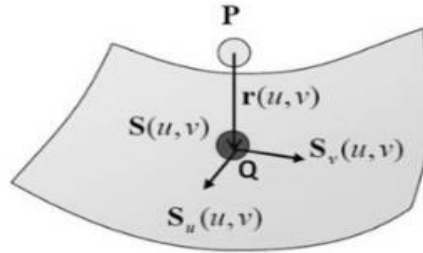


Figure 3-9 Projection to the designed NURBS surface

Next, the coordinate transformation of the measured point cloud using the motion vector \mathbf{t} and the rotation matrix \mathbf{R} is conducted to reduce the displacement of the design curved surface and the measured point cloud (Okuda et al., 2004 and Besl et al., 1992). \mathbf{P}' in Equation (3.46) is the transformed measured point. To estimate \mathbf{R} and \mathbf{t} , the displacement $E(\mathbf{R}, \mathbf{t})$ expressed in Equation (3.47) is minimized (Cristobal et al., 2011). This process is repeated until $E(\mathbf{R}, \mathbf{t})$ is smaller than the threshold (Zhang et al., 1994).

$$\mathbf{P}' = \mathbf{R}\mathbf{P} + \mathbf{t} \quad (3.46)$$

$$E(\mathbf{R}, \mathbf{t}) = \sum_{i=1}^n \|Q_i - \mathbf{R}\mathbf{P}_i - \mathbf{t}\| \quad (3.47)$$

In this study, some improvements are made toward the basic ICP algorithm to solve some practical issues. The reasons and the implementation of these improvements will be introduced in later chapters.

3.3.7. Real object's virtualization and selection using polygons

The wooden templates which are a set of prototypes made for the confirmation and evaluation of industrial products are basically made of wood. One of the reason why wood is chose is that wood is relatively affordable, durable and easy to be cut. As introduced in the first chapter, a wooden template for one frame line of the plate

consists of a curved bottom surface, a perspective stick and two support sticks. Conventionally, judgment of manufacturing accuracy of the curved shell plate is based on the observation on the perspective plane formed by the perspective sticks of wooden templates which are put on the plate.

In this subsection, the technique for representing the wooden template on a computer by virtualizing it using polygons will be introduced.

Polygon originally referred to the shape with multiple angles, in 3D computer science it refers to the elements when representing an object with a combination of triangular or rectangular (under some situations, maybe more than pentagon). Practically, when drawing a map with geographical information system (GIS), the outlines of the regions are described in the form of polygon, while a road or a railway is represented in the form of polyline. Objects constructed in polygons essentially only consists straight lines and planes, by a combination of processes such as smooth shading which subdivide the curve and curved surface, the curved surface can also be expressed (Makoto, S.,2008,2010,2012).

In this study, the feature points of the wooden template are first defined as shown in Figure 3-10. These points are specified as the end points of the polygons so that the virtual template can be constituted

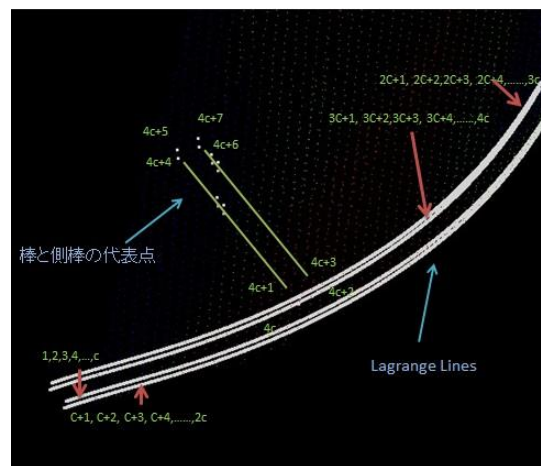


Figure 3-10 Feature points of virtual template

For one wooden template, the feature points are defined as following:

The points of the four base lines forming the wooden template's bottom surface are obtained using Lagrange interpolation to the design point cloud of the frame line, and are arranged as below:

- i. $(1, 2, 3, \dots, c)$
- ii. $(c + 1, c + 2, c + 3, \dots, 2c)$
- iii. $(2c + 1, 2c + 2, 2c + 3, \dots, 3c)$
- iv. $(3c + 1, 3c + 2, 3c + 3, \dots, 4c)$

The end points of the perspective stick:

- i. Upper $(4c + 4, 4c + 5, 4c + 6, 4c + 7)$
- ii. Bottom $(4c + 1, 4c + 2, 4c + 3, 4c + 4)$

The end points of the support sticks:

- i. Left stick $(4c + 8, 4c + 9, 4c + 12, 4c + 13, 4c + 16, 4c + 17, 4c + 18, 4c + 19)$
- ii. Right stick $(4c + 10, 4c + 11, 4c + 14, 4c + 15, 4c + 20, 4c + 21, 4c + 22, 4c + 23)$

The polygons constituting one wooden template are defined above. One side surface of the perspective stick is defined in four points $(4c+5, 4c+7, 4c+1, 4c+3)$. One side surface of the bottom of the template is defined by a set of four points $\{(i+k, i+k+1, c+i+k, c+i+k+1)\}$ ($k=1, 2, 3, \dots, c$ $i=1, 2, 3, 4$)

The virtualized wooden template represented by a set of polygons is shown in Figure 3-11. The adjacent surfaces are printed in different colors to emphasis the 3D effect.

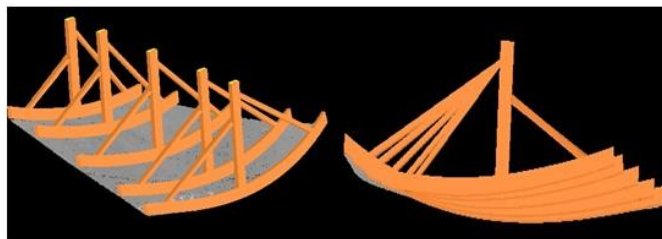


Figure 3-11 Real object's virtualization and selection using polygons

3.3.8. Curvature estimation

In this study, in order to generate the proper manufacturing plans by comparing the curvatures at each frame point between the virtual templates bottom lines and the measured frame lines, it is necessary to estimate the partial curvatures at these points. The curvature estimation method in point cloud from Zhang et al.(2008) is used.

This method employs neighbor normal vector and osculating circle. The advantage of this method is that it is simple enough to use and sensitive only to the neighbor points in the point cloud of the seed point.

As shown in Figure 3-12, for each seed point \mathbf{p} at which the curvature is to be estimated, let \mathbf{N} be its' normal vector. Then only the coordinates of the neighbor points are enough to calculate the curvatures at point \mathbf{p} . m points ($m = 2, 3, \dots$) in the neighbor are found. One of them is \mathbf{q}_i . \mathbf{N} and \mathbf{M}_i are the normal vectors corresponding to \mathbf{p} and \mathbf{q}_i respectively. Transform the coordinates of these points to the local coordinates system $(\mathbf{p}, \mathbf{X}, \mathbf{Y}, \mathbf{N})$, and then the \mathbf{q}_i should be (x_i, y_i, z_i) , \mathbf{M}_i should be $(n_{x,i}, n_{y,i}, n_{z,i})$. At last, a circle passing through \mathbf{p} and the neighbor points is fitted to get the curvature at \mathbf{p} .

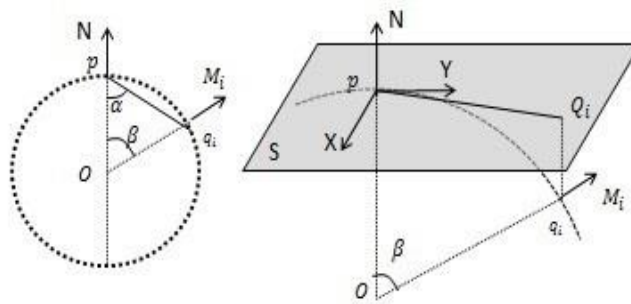


Figure 3-12 Chord & Normal Vector (Zhang et al. 2008)

The normal curvature can be estimated with the following equations.

$$K_p = \left(\sum_{i=1}^m \frac{\sin \beta}{|\mathbf{pq}_i| \sin \alpha} \right) / m \quad (3.48)$$

$$\mathbf{p}: \{0, 0, 0\} \quad \mathbf{q}_i: \{x_i, y_i, z_i\}$$

$$\mathbf{M}_i: \{n_{x,i}, n_{y,i}, n_{z,i}\}$$

$$\frac{\sin \beta}{|pq_i| \sin \alpha} = \frac{\frac{x_i \cdot n_{x,i} + y_i \cdot n_{y,i}}{\sqrt{x_i^2 + y_i^2}}}{\sqrt{n_{xy}^2 + n_z^2} \cdot \sqrt{x_i^2 + y_i^2}} \quad (3.49)$$

The fitted circles is shown in the following figure.

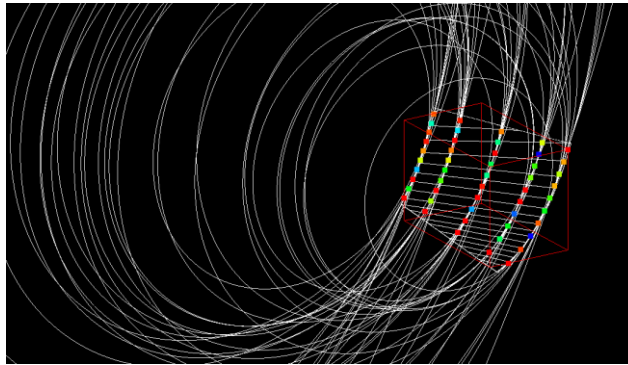


Figure 3-13 Curve radius estimation

3.4. Knowledge engineering

In this sub-section, the technology used in knowledge management in this study will be introduced.

3.4.1. Ripple down rules

Differences between the manufacturing plan suggested by the proposed system and the manufacturing plan actually used by workers exist. In order to extract the tacit knowledge during the heating process, interview investigation about these differences in different cases was conducted. The knowledge in specific situations during the manufacturing process is extracted and represented using the RDR (Ripple-Down Rules) (Catlett, J. 1992).

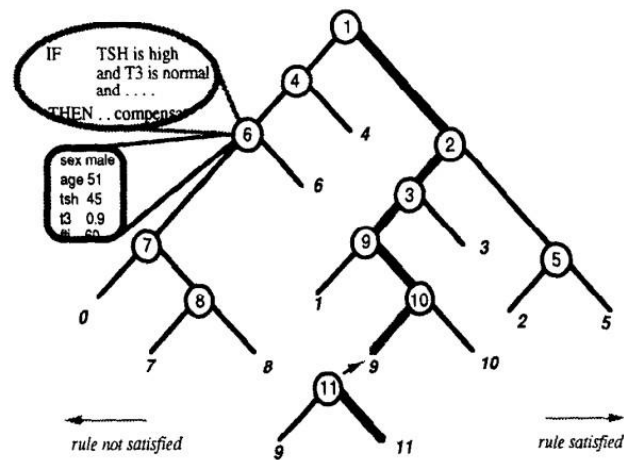


Figure 3-14 Ripple-Down Rules sample (Compton, P. et al 1993)

RDR, which was proposed by Compton and Jansen based on experience maintaining the expert system GARVAN-ES1 (Compton, P. et al 1993 and 1994; Gaines, B.R. 1995), is a method for extracting and representing knowledge. In the RDR framework, the human expert's knowledge is acquired based on the current context and is added incrementally into a binary decision tree in the format of a set of independent rules (if .. elsif rules) as shown in Figure 3-14. In other words, RDR adds new rules when the existing ones cannot satisfy the situation of current context. The correct description of the current situation is very crucial to extract proper rules and avoid duplication. So it is conceivable that a lot of time and effort can be saved by using the virtual manufacturing plan design environment because more precise and recordable parameters describing curved shell plates' situations become more accessible. The workers can get an immediate and visualized image about the curved shell plate's situation by checking these parameters.

PART II PROPOSAL AND CONTRIBUTION

PART II PROPOSAL AND CONTRIBUTION	82
Chapter 4 Curved shell plate’s manufacturing support framework	85
4.1. Investigation and problem clarification during traditional manufacturing....	85
4.1.1. Strategy of this study.....	85
4.1.2. Interview on the traditional manufacturing process	86
4.1.3. Problems existing in the conventional manufacturing process	89
4.2. Supported manufacturing process.....	90
4.3. Layout of the proposed framework.....	94
4.3.1. Requirement definition	94
4.3.2. Problem definition for common pre-processing	98
4.3.3. Problem definition for cold forming supporting	99
4.3.4. Problem definition for heating forming supporting	101
4.3.5. Problem definition for knowledge elicitation and dissemination.....	104
4.3.6. Automation of measurement and analysis flow	106
4.4. Software architecture of the proposed framework	106
Chapter 5 Common pre-processing	109
5.1. Measured data with irregular obstacles and variable density	109
5.2. Overview of curved shell plate’s measurement.....	110
5.2.1. Plate extraction prototype	110
5.2.1.1. Continuous domain extraction	111
5.2.1.2. Separated domain recognition.....	112
5.2.2. Originalities for higher speed and lower failure	113
5.3. Float region growing candidate selecting and plane fitting	115
5.4. Weighted normal vector calculation considering point cloud’s density	117
5.5. Judgment standards of the common domain recognition	118
5.6. Registration method with direction pre-setting.....	121
5.7. Development of MS.....	124
5.8. Summary.....	125
Chapter 6 Cold forming supporting	127
6.1. Overview of the cold forming supporting framework.....	127
6.2. Pre-process and registration.....	129
6.3. Press evaluation method	130

6.4. Perimeter evaluation method	131
6.5. Development of PSS.....	132
6.6. Summary.....	133
Chapter 7 Heating forming supporting	135
7.1. Overview of the heating forming supporting framework.....	135
7.1.1. Virtual template prototype	137
7.1.1.1. Virtual template generating	138
7.1.1.2. Registration of the virtual template and plate's point cloud	140
7.1.1.3. Curvature error calculation.....	140
7.1.2. Originalities for the practical usage in shipyard	142
7.2. Automatic template arrangement method.....	143
7.3. Curvature error based heating grade suggesting	146
7.4. Development of VTS	147
7.4.1. 2D roller line's matching with 3D design data.....	147
7.4.2. User interface of VTS.....	150
7.5. Summary.....	154
Chapter 8 Knowledge elicitation and dissemination	156
8.1. Overview of the manufacturing knowledge management	156
8.2. Raw knowledge interrelated database	160
8.3. Knowledge base design.....	160
8.4. Knowledge elicitation process.....	161
8.5. Knowledge dissemination process	164
8.6. Development of KBS.....	165
8.7. Summary.....	166

Chapter 4 Curved shell plate's manufacturing support framework

In this chapter, the design of the framework developed for facilitating curved shell plate's manufacturing will be described in detail. First, based on the investigations performed towards the curved shell plate's manufacturing process in 4.1, the necessary functions, the main possible problems on the algorithm level and the solutions are clarified for the proposed framework. Next, a layout of the proposed framework is described in 4.3, while the decided sub-systems are designed in the following sub sections.

4.1. Investigation and problem clarification during traditional manufacturing

A survey about the current curved shell plate's manufacturing problems is conducted in shipyard, the problems and the challenges existing in solving these problems are found.

4.1.1. Strategy of this study

An interview about the difficulty of the full automatic machining was conducted first. As introduced in Chapter 2, that all of the information not only about the plate but also about the manufacturing environment is extremely difficult to be obtained for every manufacturing step is the main difficult point for the full automatic machining. Therefore, the workers need to do the manufacturing with the inadequate information and parameters observed from the wooden templates which means the manufacturing relies on both the wooden template and the human worker. To provide the effective framework for facilitating the manufacturing and preserving the manufacturing knowledge, the virtualized version of the wooden template can be a good choice for providing more accurate evaluation results. And the analysis of the convention during the manufacturing should also be conducted. The problems existing in the traditional manufacturing process are analyzed and

expected to be solved in this study, too.

4.1.2. Interview on the traditional manufacturing process

Another interview on the current curved shell plate's manufacturing process using the traditional wooden templates was conducted. The correlation between the ship's design data and the manufacturing process using wooden templates is as shown in Figure 4-1. First, after the shape of each curved shell plate is designed in consideration of the whole ship's performance, the wooden templates are produced based on each curved shell plate's design data. During this process, a lot of money and time has already been consumed before the formal shipbuilding process starts. Next, each curved shell plate is cut from the plane steel plate and pressed into a shape which is close to the design shape to some extent using a press machine. Then the heating manufacturing process conducted by human started. During the whole manufacturing process, the following items are given to the workers:

- a. Plane steel plates with frame line (where to put the wooden templates) painted on it
- b. Wooden templates representing curved shell plate's design shape
- c. Gas burner and water hose to bend the plates (for heating forming stage)
- d. Press machine (for cold forming stage)

The heating and pressing areas are decided by trying to deform the smooth curved surface which matches a and b using c and d. Specifically, workers consider the manufacturing plans (the heating and pressing areas) by putting and rotating b on a and observing the situations such as the displacement between them and the angles between the perspective sticks of the arranged wooden templates. After deciding the manufacturing plans they use the c and d to implement them. The experiences and intuitions of the workers are needed during this manufacturing process, and of course the individual differences exist. The manufacturing time and qualities can vary dramatically between different workers such as the experienced ones and the beginners.

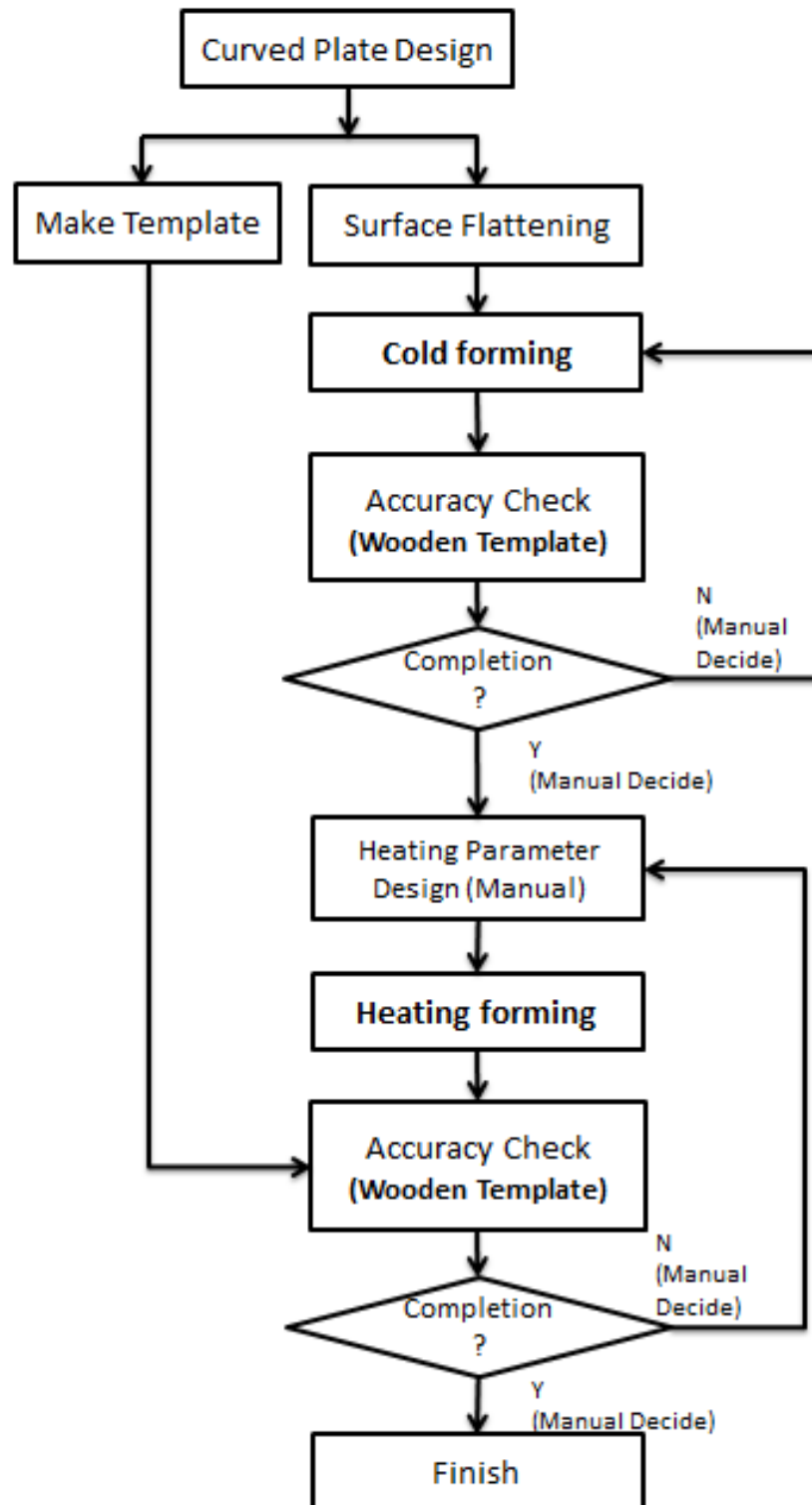


Figure 4-1 Traditional manufacturing process using wooden templates

There are some common principles existing in the manufacturing process. Because the cold forming using press machine is more efficient than heating forming performed by human, workers usually try to bend the plates using press machine to minimize the heating processing time before start the heating forming process. Also, to form a 3D curved surface, the adjustments on vertical direction to correct the torsion are usually performed after the horizontal bending which is responsible to form a certain degree of curvature. As shown in Figure 4-3, the specific process of the manufacturing is summarized as following:

- A) Deform the curved shell plate to some extent using press machine
- B) Check the perimeters and press result of the curved shell plate using wooden templates for press, if not a big inaccuracy exists, Go to C)
- C) Put the wooden templates for heating on predetermined location of the pressed plate
- D) Observe the perspective line formed by the perspective sticks' endpoint of the wooden templates to grasp the situation of the curvature and torsion situation of the current plate
- E) Decide the heating areas (usually heating lines) based on the displacements of the plate and wooden templates
- F) Perform the heating forming using gas burner and water hose
- G) Repeat C) - F) until getting close enough to the design shape

During the manufacturing, the parameters of the wooden templates and the plate shown in Figure 4-2 are observed for deciding the next step's manufacturing plan including the heating finishing judging, the heating areas, the heating grades and the heating technics selecting.

- Gaps between plate and wooden templates
- Smoothness of the plate by touching
- Extent of the shaking of wooden templates
- Angles between wooden templates' sticks
- Distance between wooden templates tops and upper plane
- Displacement between the ends of the wooden templates and plate

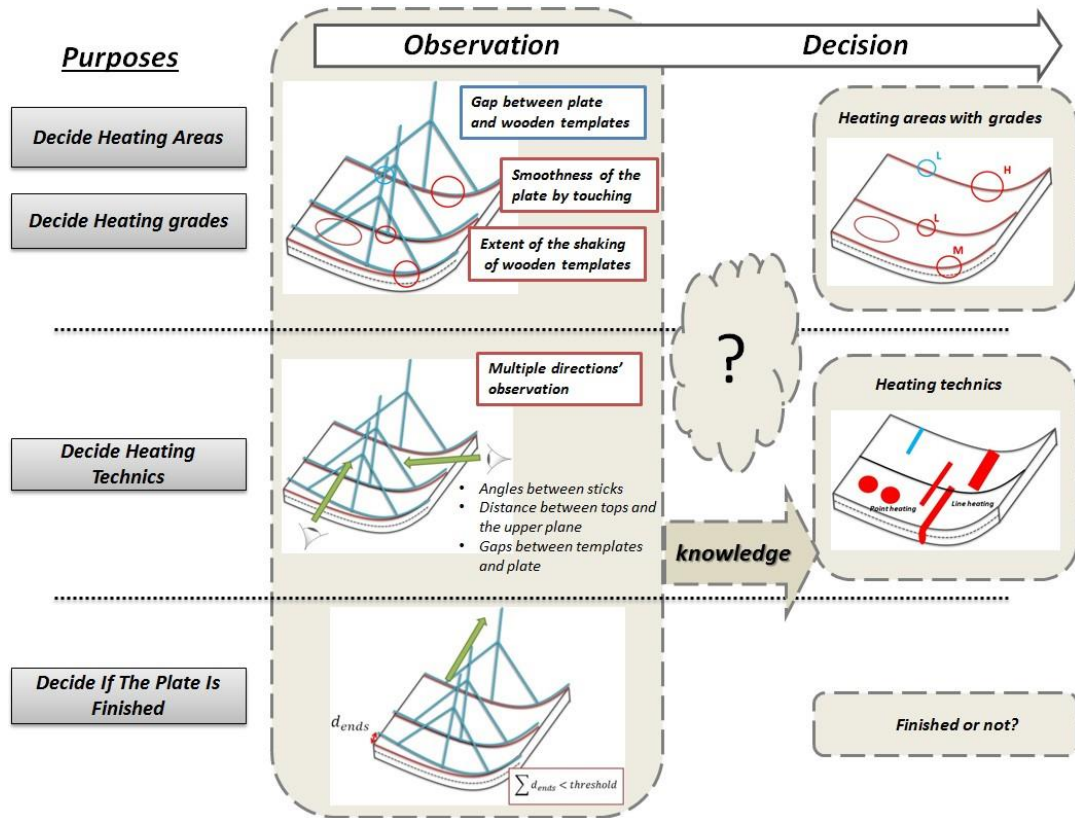


Figure 4-2 Convention of manufacturing plans' design

4.1.3. Problems existing in the conventional manufacturing process

As summarized in Table 1.1 of Chapter 1, there are many problems existing in this manufacturing process shown in Figure 4-3 obstructing the progress of the efficient manufacturing and the automation.

- The dramatic physical effort and time cost when trying to put and fix wooden templates onto the plate
- The inaccurate observing results of the wooden templates' parameters.
- The difficulty for understanding the expert's knowledge without real time specific example analysis (OJT)
- The controversial manufacturing plans for one plate from multiple experts

Especially, during the current manufacturing process, parameters such as the angles, locations and rotation of the wooden templates are not specified

quantitatively. Sometime even an experienced worker cannot explain why they design the heating plans which are different from others. When there are multiple heating plans from different workers, there is not a quantitative way to determine which one is the best.

Quantitative expresses of the wooden templates' parameters become necessary to solve the above problems. And it is considered a desirable framework for performing and recording the manufacturing processes in an accurate virtual environment. Also, the knowledge model will be needed to support the beginner workers.

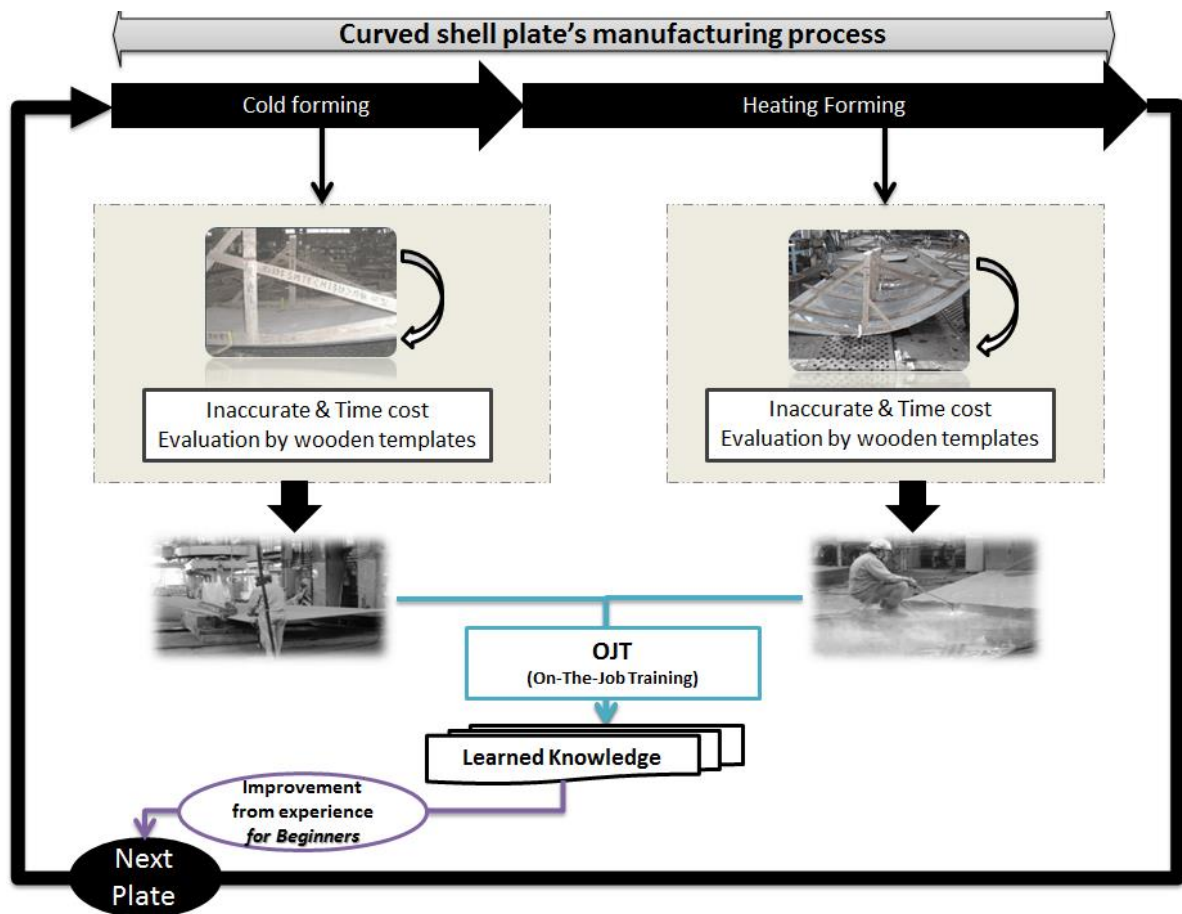


Figure 4-3 Conventional manufacturing process

4.2. Supported manufacturing process

The manufacturing process which is expected to be supported by the proposed framework is illustrated in Figure 4-4.

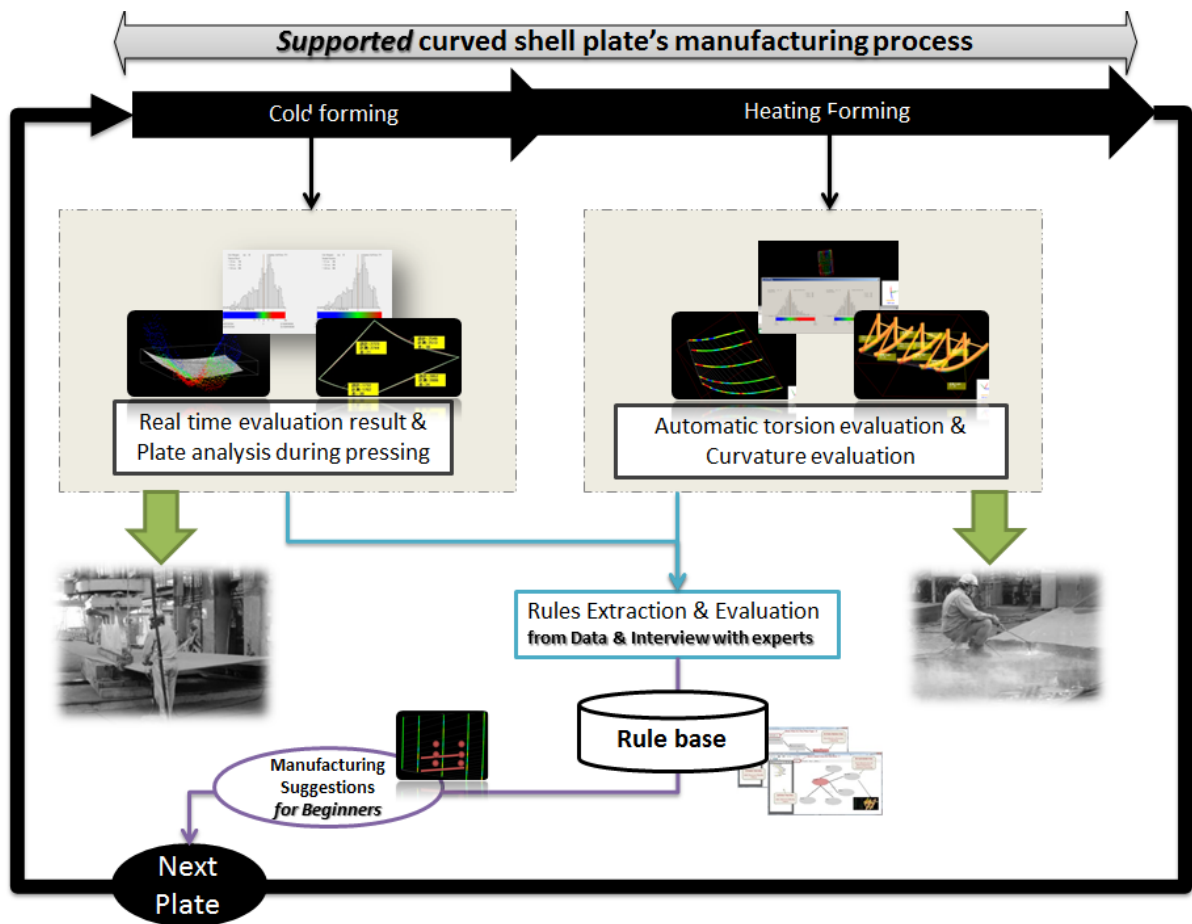


Figure 4-4 Supported manufacturing process

Instead of the manual evaluation of the plate during the cold forming and heating forming stage, the evaluation should be performed automatically on computer, and to conserve the conventional manufacturing habits and knowledge, the wooden templates are going to be totally virtualized in 3D virtual environment as well as the measured plate's 3D point cloud data. The parameters needed for the manufacturing plan's design for every manufacturing step are expected to be calculated based on the generated virtual templates and the measured plates automatically and provided for the workers efficiently. The knowledge elicitation and learning should not only be conducted during the manufacturing (OJT), but also after the manufacturing based on the recorded 3D manufacturing scenario.

As shown in Figure 4-5, the supported specific process of the manufacturing is

summarized as following:

- A) Deform the curved shell plate to some extent using press machine
- B) Check the perimeters and press result (automatically calculated) of the curved shell plate, If OK then go to C)
- C) Observe the curvature evaluation view and the torsion evaluation view (automatically calculated) from VTS to decide the heating technics
- D) Perform the heating forming using gas burner and water hose
- E) Repeat C) – D)until getting close enough to the design shape

For the knowledge elicitation from experts, the manufacturing scenarios including the templates' observations and the manufacturing plans' design are accumulated and analyzed based on the interviews with the expert workers after every manufacturing step.

For the knowledge dissemination, the special heating technics and heating lines' combinations are suggested from the KBS for the beginner workers to manufacture some complicated plates.

The whole support process on computer is totally automatized.

By facilitating the plate's measurement, wooden template's fixing and observing, the whole manufacturing process is expected to be more efficient by using this framework. And with the high accurate evaluation results after each manufacturing step, the manufacturing plans designed by the workers are more effective.

The beginner workers are expected to be supported during the manufacturing by using KBS proposed in this thesis. The training of the beginner workers can be conducted not only on job, but also after the manufacturing because a lot of 3D manufacturing scenarios are going to be accumulated by using the proposed framework.

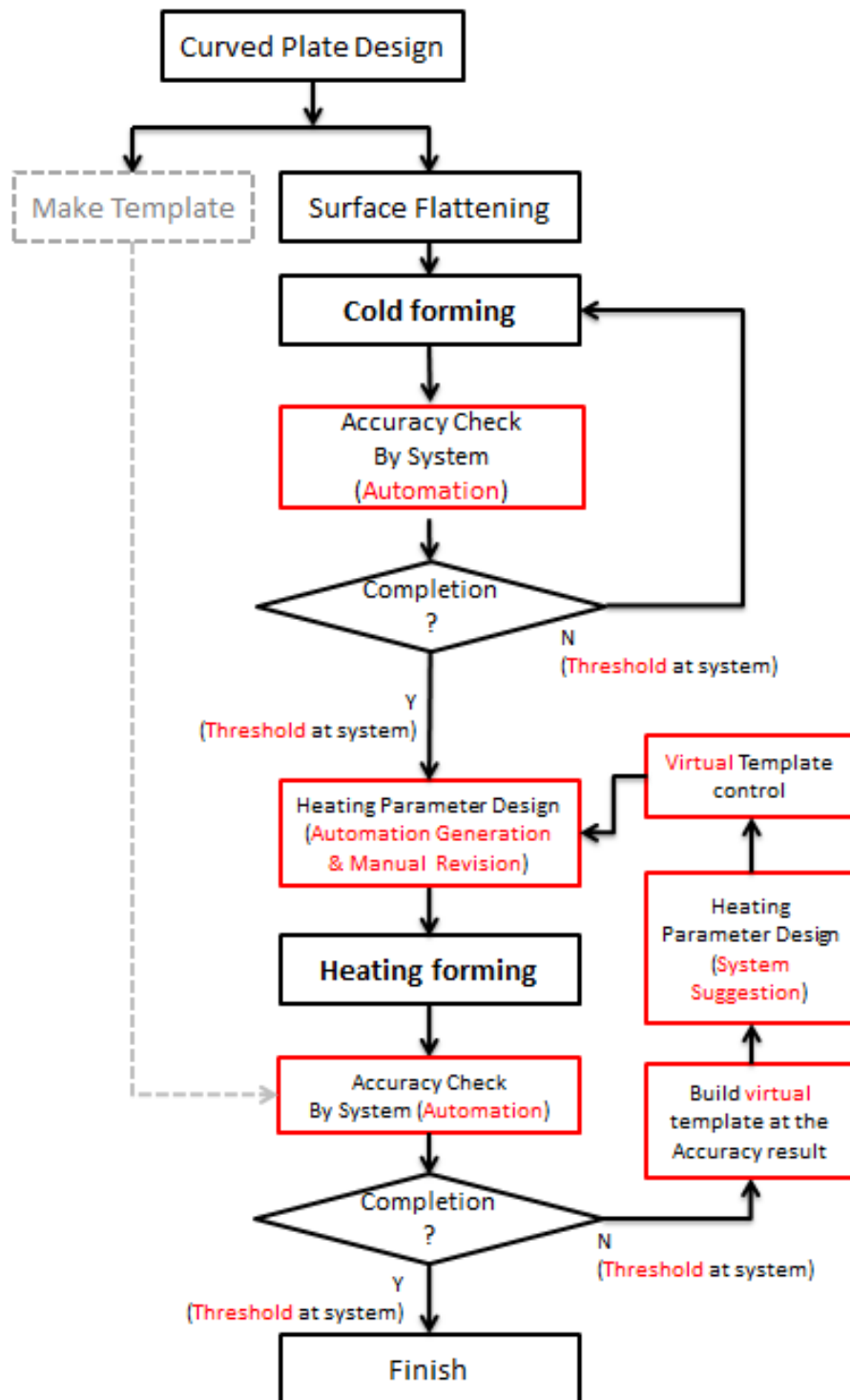


Figure 4-5 Supported manufacturing process by proposed framework

4.3. Layout of the proposed framework

Based on the investigations conducted in 4.1 and the expected supported manufacturing process, the framework proposed in this thesis constructs 4 systems to support the 2 stages (Cold forming process and Heating forming process) of the curved shell plate's manufacturing process and the knowledge elicitation and dissemination during the manufacturing process for the beginner workers. In this subsection, the layout of the proposed framework will be discussed.

4.3.1. Requirement definition

This thesis aimed at proposing a curved shell plate's manufacturing support framework which could facilitate the manufacturing of the curved shell plate in the shipyard by providing the necessary manufacturing information and suggestions about the plate automatically and efficiently. The real tools using in the conventional manufacturing such as the wooden template and rulers are virtualized based on the ship's design data for the automatic measurement and analysis of the plate before and after every manufacturing step.

As shown in Figure 4-6, in this thesis, laser scanner is used for capturing the curved shell plate's 3D shape before and after every manufacturing step.

- As a pre-processing of vital importance, the 3D shape of the measured plate is extracted efficiently from the raw measured point cloud data measured by laser scanner and registered automatically to the design surface.
- The cold forming is supported by the efficient accuracy evaluation and perimeter measurement of the plates' point cloud. The workers decide if the plate reaches the press design shape according to the evaluation results and whether to forward it to the heating forming.
- The heating forming is supported by virtualizing the whole manufacturing process on computer. The necessary parameters for the design of manufacturing plan are provided automatically. The workers can operate the virtual templates in the traditional way as they used to.
- Furthermore, to support the beginner workers who cannot decide the

manufacturing plans alone, the expert workers' knowledge is elicited by conducting interviews or data analysis based on the recorded 3D manufacturing scenarios. The advanced manufacturing suggestions including special heating technics (point heating and curve heating) or heating lines' combinations are outputted by the system.

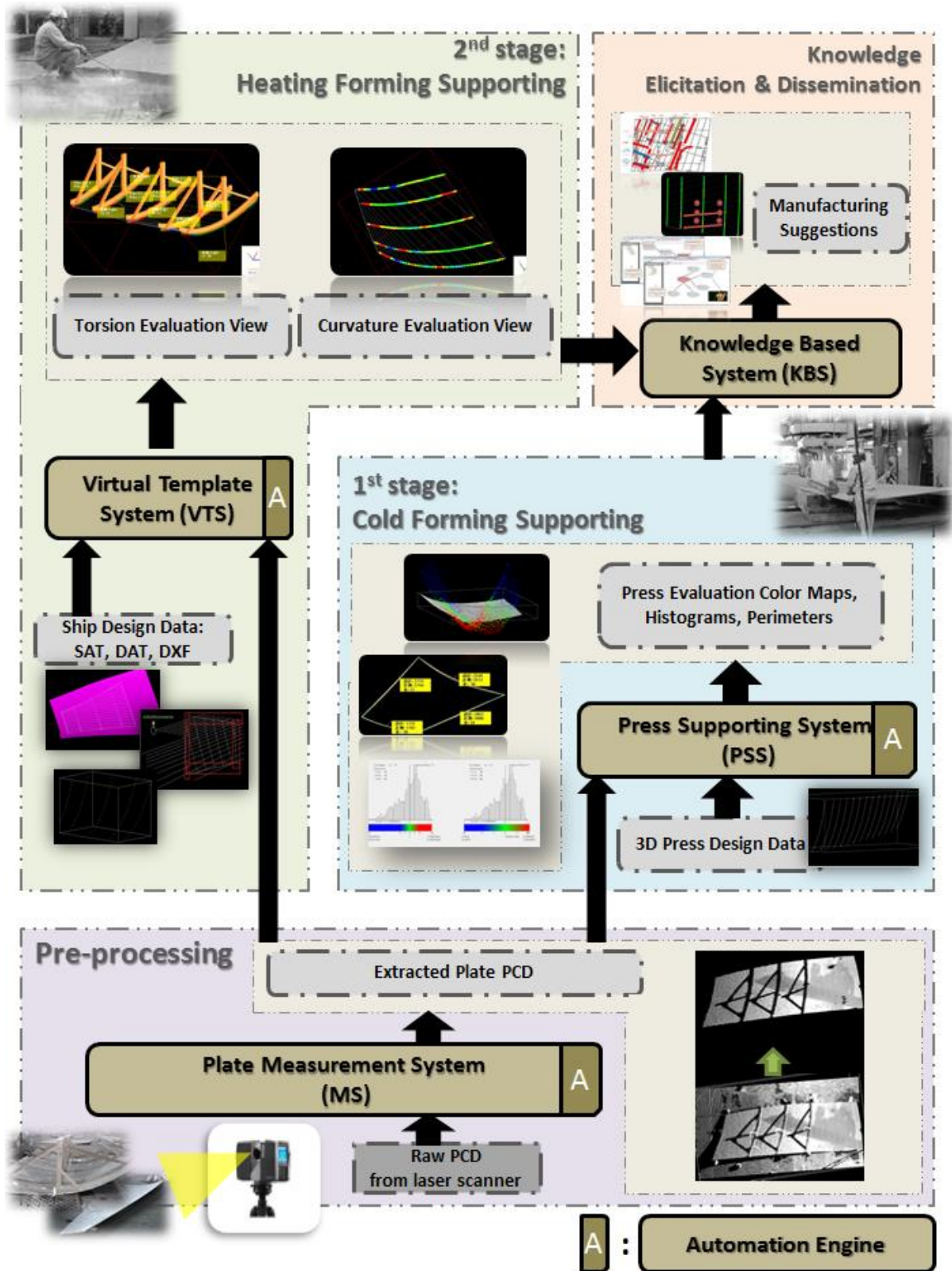


Figure 4-6 Layout of the proposed framework

As that will be introduced in the following sub sections, the curved shell plate's support framework consists of 4 systems: Plate Measuring System (MS), Press Supporting System (PSS), Virtual Template System (VTS) and Knowledge Based System (KBS). Besides these 4 systems, there is an Automation Engine (AE) which is responsible to improve the usability of the 4 systems. The construction of the framework and how the sub systems support the whole manufacturing process are described as below:

- Common pre-processing:
 - ✓ Plate Measuring System deals with the raw point cloud data obtained from laser scanner and outputs the 3D point cloud of the curved shell plate. It outputs the plate's part of the point cloud even when the plate is divided into multiple domains.
- Cold forming supporting:
 - ✓ Press Supporting System is responsible for providing the distance error and perimeter evaluation results after each press step during the 1st stage (cold forming process). It helps workers to know if the curved shell plate has reached the press design shape to reduce the time consuming in the after-processing.
- Heating forming supporting:
 - ✓ Virtual Template System generates a virtual environment by virtualizing the wooden templates and the traditional manufacturing process. It is responsible to provide a totally virtualized manufacturing environment and give the necessary parameters for manufacturing plan's design including the torsion evaluation results and curvature evaluation results of the plate. The experienced workers are able to work under this virtual environment without using the real wooden templates
- Knowledge elicitation and dissemination:
 - ✓ Knowledge Based System elicits and disseminates the knowledge existing in the manufacturing process of the relatively difficult plates. It should be able to suggest the advanced manufacturing plans including the special heating technics (point heating, curve heating) and the

combinations of heating lines for the beginner workers.

4.3.2. Problem definition for common pre-processing

In shipbuilding, depending on the conditions in the factory, the laser scanner measured results of components (Figure 4-7) cannot satisfy the accuracy evaluation requirement due to the following factors:

(1) The measured point cloud data always includes a lot of needless noise, such as the floor, the workers and some wooden templates which are necessary templates for the manufacturing.

(2) The measured point cloud data are usually divided into multiple separated domains by these obstacles' shadows. Manual extraction and integration of these separated domains wastes a lot of time.

(3) The measured point cloud data always has a large amount of points which slow down the extraction process dramatically longer than the preferred time limit of several minutes.

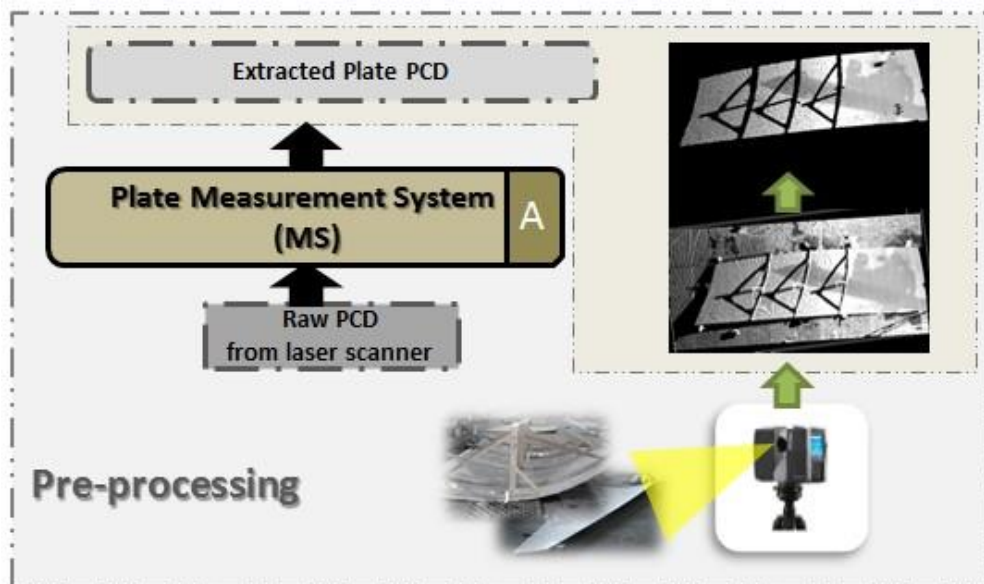


Figure 4-7 Pre-processing

As a crucial pre-process, all of the noise should be removed and the separated domains belonging to the same component should be extracted efficiently as shown in Figure 4-7.

The objective of Plate Measurement System is to extract only the part of the curved shell plate from the 3D measured point cloud data which contain a lot of obstacles and are obtained from laser scanner. In this paper, the component extraction consists of two main processes: the continuous domain extraction which extracts the small separated domains from one single seed point and the separated domain recognition which decides if an extracted domain is from the same component (plate) as the other ones. The small domains divided by the obstacles should be recognized sequentially. The inference steps are hierarchized to accomplish the sequential recognition.

To solve the problem (1) and (3) gaining higher extracting speed and lower extracting failure during the continuous domain's recognition, the improvements based on the classic region growing method are made.

- ✓ To save the normal vector calculation and comparison time for the continuous domain's region growing, in this study, the point candidates for the next growing seed are carefully selected following the float region growing window.
- ✓ To avoid improper growing into points that are too far from the seed such as the floor near the component, points which are used to do the plane fitting are seriously selected under certain constraints.
- ✓ When the point cloud's density varies dramatically, to calculate the normal vector of a seed point using its neighbor points, weighted plane fitting is applied.

To solve the problem (2) achieving efficient plate extraction when the plate is divided into multiple separated domains, the following method is used.

- ✓ For the divided domain recognition, new judgement standards of the common domain are discussed which is aimed to the efficient and effective recognition and extraction of all the domains which belong to the plate under different conditions.

4.3.3. Problem definition for cold forming supporting

As introduced in 1.1.2, two main problems existing in the cold forming process (press process) of the curved shell plates:

- a. Forming quality dispersion exists (lead to in-expectable time consuming in

the after-processing).

- b. Perimeter check cost time, sometimes cause inaccuracy

To solve these problems, this paper develops a software system Press Support System for evaluating the curve shell plate's shape and perimeter automatically by using laser scanner. The system registers pre-processed measured data and design data together, calculates the distance errors between them and virtualizes the errors into a gradation color map and histograms as shown in Figure 4-8. Besides, the perimeters of the measured data and design data are also calculated and virtualized in the 3D view for the workers to check.

There are 2 problems should be solved on the algorithm level.

- (1) The density in both the design point cloud and measured point cloud varies dramatically which could lead to inaccurate registration and evaluation results.
- (2) Because the design data of press process is also point cloud, the distance error cannot be calculated directly to the two point clouds when the density of the point cloud is low.

There are 2 originalities in the proposed algorithms solving the problems mentioned above respectively.

- ✓ Due to the varying density existing in both the design point cloud and measured point cloud, to avoid the improper registration result, the average density thinning of the two data is conducted
- ✓ In this thesis, a plane is fitted towards to the nearest points of the measured point cloud from the design point being evaluated using the basic plane fitting method. Then the distance between the design point being evaluated and the fitted design plane is calculated as the displacements

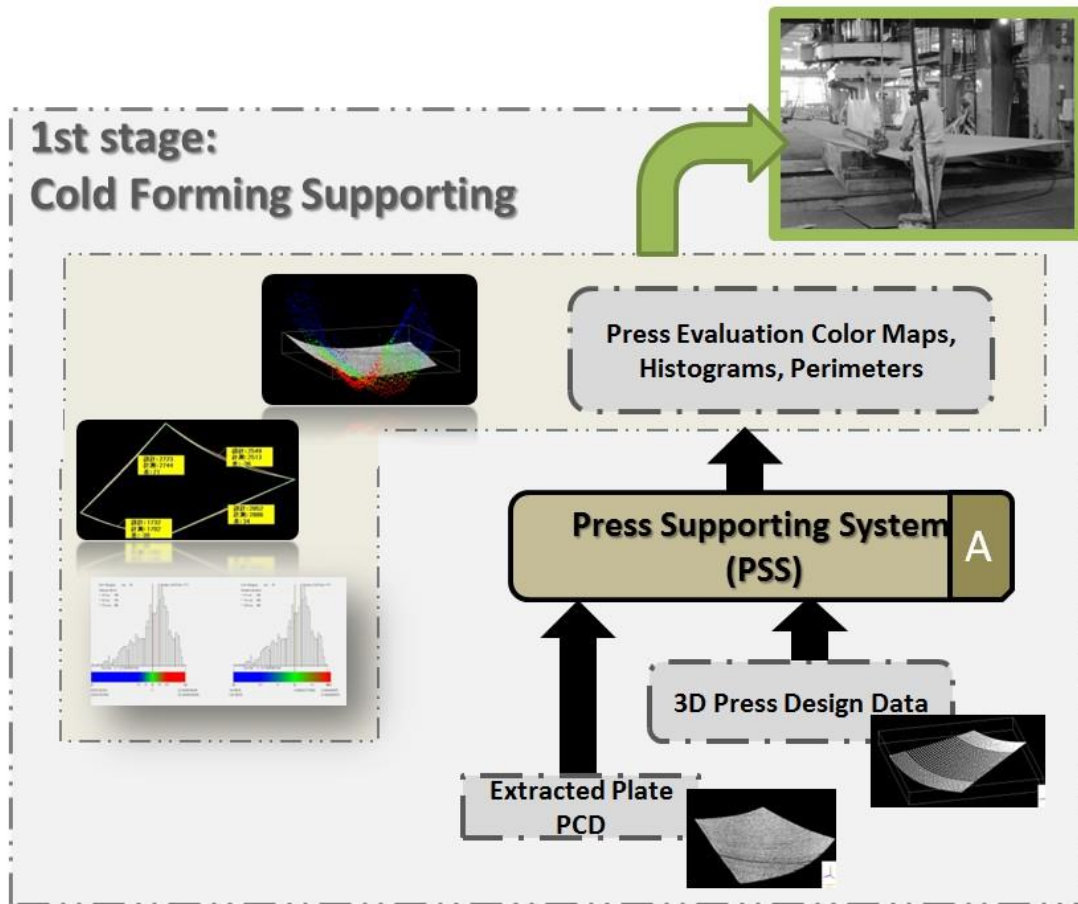


Figure 4-8 Cold forming supporting

4.3.4. Problem definition for heating forming supporting

Plastically deforming of heating and water-cooling based on the wooden template (Kigata) check with human eyes is used to produce these curved shell plates with extremely arbitrary 3D shapes. As mentioned in the first chapter, this process has no clear-cut methodology and carried great risks for the subsequent heat sealing process. About five to eight wooden templates consisting bottom line and perspective stick are made from curved shell plates' design data for every curved shell plate before the construction of the ship. This wooden templates' producing process cost a lot of time and money, and may already create inaccuracy. During the curved shell plates' processing, after the wooden templates are located on the curved shell plates' frame lines (the lines showing the design data), the angle between their perspective sticks, the grade of the gap between the wooden templates' bottom line

and the curved shell plate are strictly observed by workers. Based on the quantitatively immeasurable check-with-eyes results, how to decide the heating and cooling areas of the following processing is still uncertain. Different people may have different answers here because a lot of tacit knowledge such as the processing rules and habits which are hardly discovered or educated exist. Therefore, the variation in after-processing shapes arises and may cause the gaps between the curved shell plates for the following heating sealing process, and the construction schedule's extension.

This thesis presents a software system, Virtual Template System for virtualizing curved shell plate's manufacturing process using virtual templates and laser scanner. The system generates design data-based virtual templates which have the same shape as the real wooden templates, extracts curved shell plate from 3D point cloud data measured by laser scanner using system MS. Then the generated virtual templates are located onto the extracted point cloud, and finally two views including curvature evaluation view and torsion evaluation view which help the workers to decide the heating area for the following processing are provided as shown in Figure 4-9. Besides, the whole process is automated.

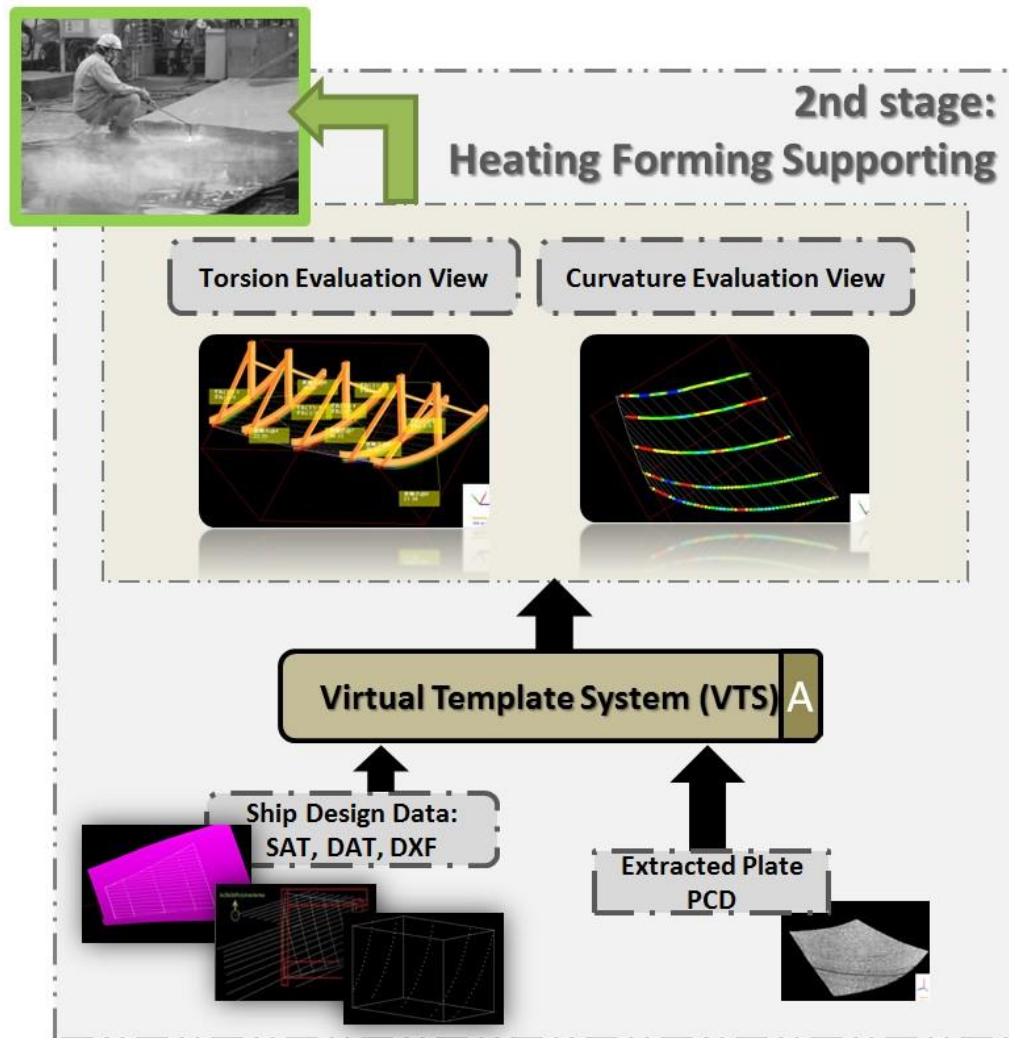


Figure 4-9 Heating forming supporting

The main difficult points in the proposed method above are as below.

- (1) During the registration process, applying ICP algorithm directly to the virtual templates and the measured point cloud may cause the wrong matching directions of the two data.
- (2) Even knowing the areas which have relatively big curvature errors, how to arrange the heating lines is still unknown.
- (3) It cost too much time to arrange the virtual templates onto the proper positions on the plate.
- (4) The heating grade at each heating area is unknown.
- (5) It is too hard for the workers to operate the virtual templates on computer.

There are many improvements based on the classic algorithms in the proposed framework solving the problems mentioned above respectively.

- ✓ This research proposes a registration direction pre-setting method before applying the ICP registration method.
- ✓ Since the roller lines are designed along with the torsion of the curved shell plate, it is effective to apply heating along with the roller lines to keep the right torsion. Therefore, this research matches the 2D roller lines onto the extracted plate's point cloud to help the workers design the right heating lines.
- ✓ This research proposes an automatic template arrangement and torsion evaluation method which dramatically reduces the template arrangement time of every manufacturing step.
- ✓ Heating lines with heating grades (heating time of each heating line) by using a float points-window for the curvature error calculating of each frame is provided.
- ✓ A virtual template operation interface is developed to help the workers operate the virtual templates as they used to do with the real wooden templates and observe the automatically analyzed results more easily.

4.3.5. Problem definition for knowledge elicitation and dissemination

A major problem in the curved shell plates' manufacturing is that the design of the manufacturing plan heavily depends on the implicit knowledge, habits and experience of the workers. Manufacturing plans including different heating technics (point heating, curve heating, and line heating) and complicated heating combinations vary according to the knowledge and skills of the craftsman in charge of the plate even for the same design shape. In other words, the current practice highly depends on the individuals and there is a risk to lose the knowledge and skills at the time of their retirement. Also to avoid inaccurate distorted output shapes and troubles in the subsequent heat sealing process, the tacit knowledge and

skills for bending plates must be elicited, shared and reused in daily operation.

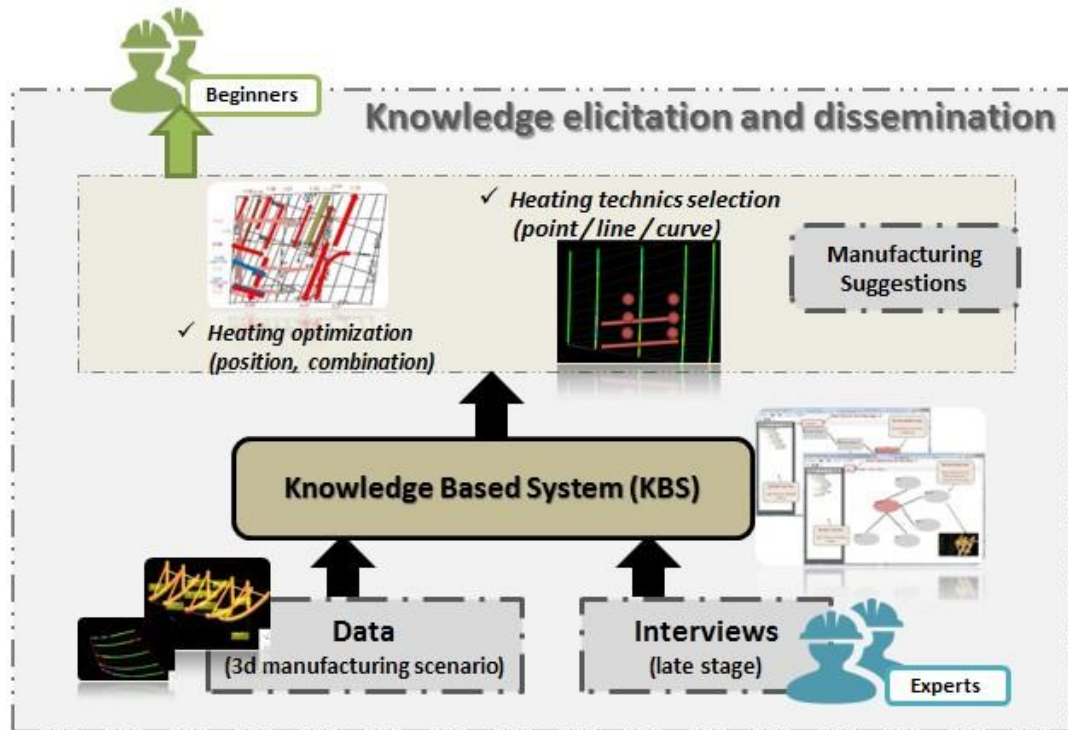


Figure 4-10 Knowledge elicitation and dissemination

The main problems existing in the curved shell plates' manufacturing process can be divided as below:

- (1) The common guidelines such as which kind of heating technic should be used under certain situation.
- (2) The interviews for the knowledge elicitation cannot be conducted during the manufacturing for most of the times.

This thesis developed an interview based RDR knowledge model working with the virtualized manufacturing scenarios solving the problems above respectively:

It aims at capturing the correlations between the 3D parameters describing the curved shell plate's situations and the relevant manufacturing plans designed by the expert workers. The extracted rules can be virtualized as shown in Figure 4-10.

4.3.6. Automation of measurement and analysis flow

In order to make the whole framework easier to be used by workers, the automation engine of measurement / analysis flow sends every system operation command instead of manually using the function of operation system. Therefore it can detect and control both the system and the scanner, and makes the system completely automated.

The engine's workflow follows the setting files which are prepared by the shipyard's administrator. As shown in Figure 4-11; what the workers need to do is just select a few items by pushing some buttons. The design and the development of this engine are specifically explained in the appendix of this thesis.

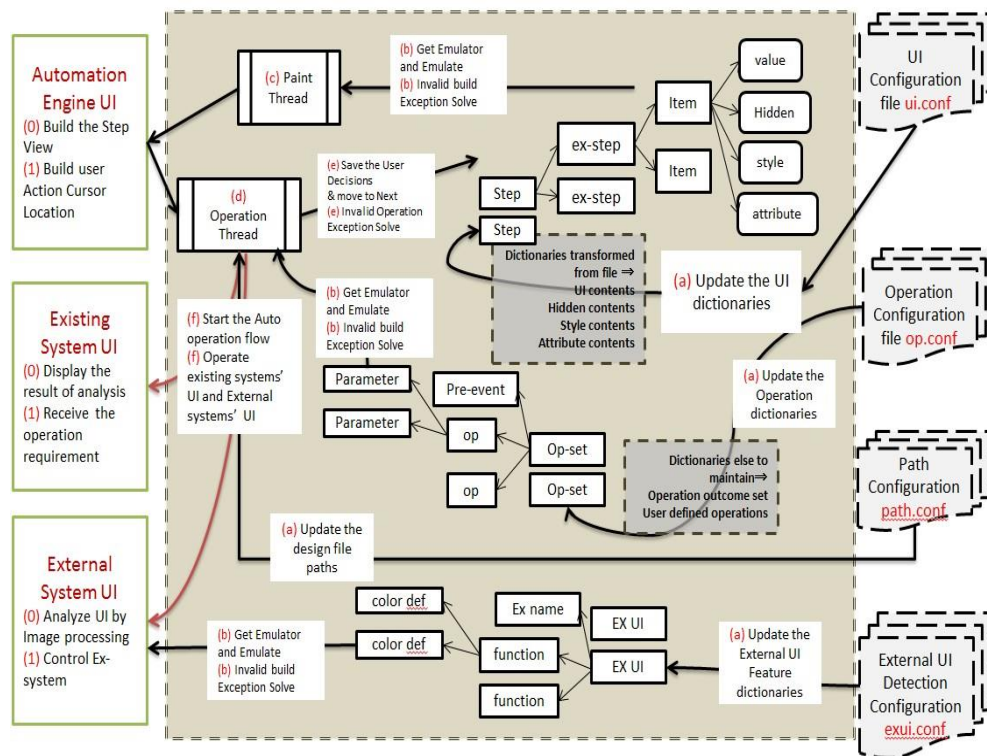


Figure 4-11 Automation engine

4.4. Software architecture of the proposed framework

The proposed systems are all embedded in a 3D point cloud platform called Pupilpit

developed in C# provided by UNICUS Co., Ltd.. The user can explicitly change the parameters to adjust the balance between the processing accuracy and the efficiency.

As shown in Figure 4-12, the Pupulpit has mainly 2 functions:

- 3D point cloud viewer
- 3D polygon mesh viewer

The MS, PSS and VTS as well as the AE all work on the basis of Pupulpit's 2 viewers. They exchange the measured plate's point cloud data and the designed shape's NURBS data with the viewers provided by Pupulpit to display them. There are also some other plugins which do not belong to our proposed framework working on Pupulpit.

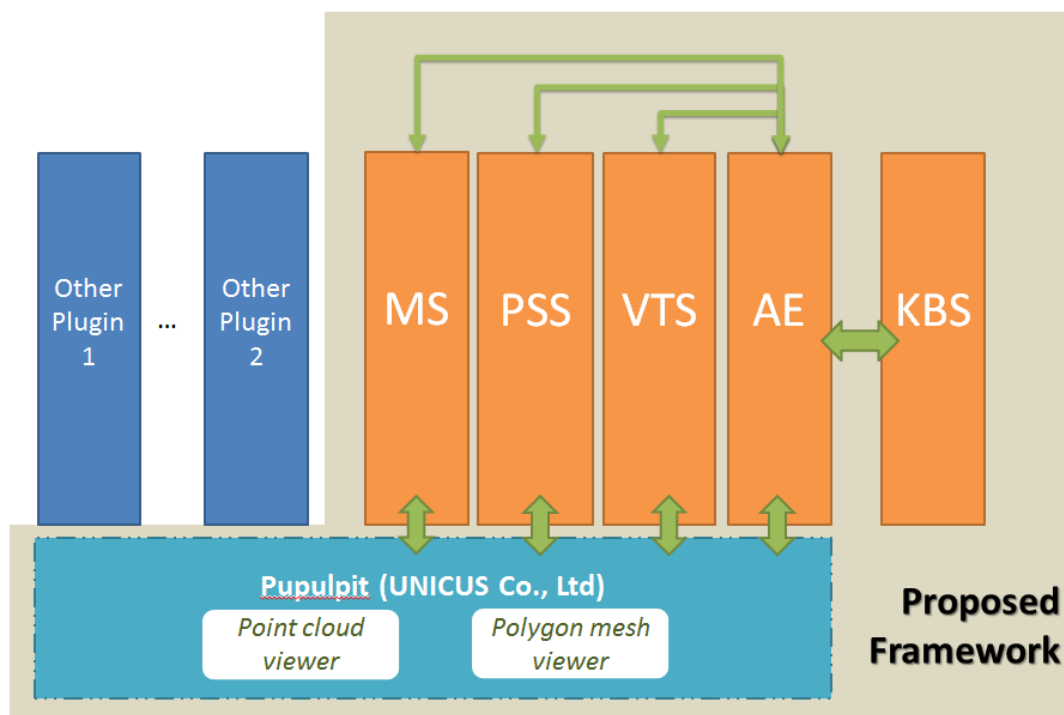


Figure 4-12 Software architecture

AE also exchanges data and commands directly with MS, PSS and VTS to control them automatically.

KBS works as an independent system but receives necessary manufacturing scenario data from AE.

The 2 viewer are based on the library called GLsharp which is a C# version of OpenGL. As an out-standing platform, Pupulpit has a customizable user interface. Figure 4-13 illustrates the customized user interface of Pupulpit for the proposed framework.

- (A) The workspace for the file list being displayed.
- (B) The 3D view for the 3D models which can be moved and rotated on this view
- (C) The properties of the selected model including the points' count, visibility
- (D) The plugin executive window

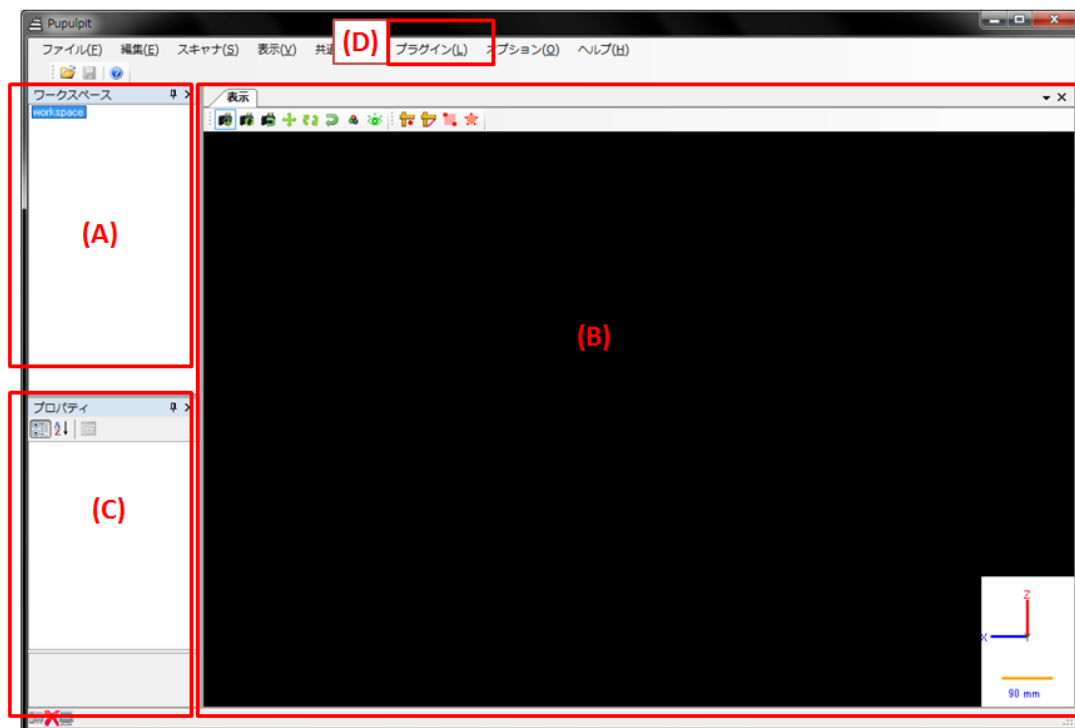


Figure 4-13 Pupulpit user interface

The user interfaces of each system proposed in this thesis will be illustrated in later chapters respectively.

Chapter 5 Common pre-processing

5.1. Measured data with irregular obstacles and variable density

When measured by laser scanners in the shipyard during the real manufacturing process, the 3D point clouds of the curved shell plates usually contain a lot of obstacles such as the shadow of wooden templates, the support wood and sometimes the workers who are standing on the plate while scanning.

Within about 200 sets of the measurement results obtained in the shipyard, there are over 120 sets which are divided into multiple domains by the obstacles. The point cloud segmentation techniques such as the basic region growing method as introduced in 3.3.2 cannot be applied directly to these data. It is necessary to extract and integrate these domains one by one manually.

The obstacles are not the only problem existing in the plate measurement process, due to the relative position of the plate and the laser scanner and the scan angles of the laser, the density could vary dramatically in the point cloud which causes the improper plate extraction results.

Also, the shipyard requires high measurement and analysis speed to reduce the time cost during the manufacturing. However, every single shot of one curved shell plate including obstacles could have over 5,000,000 points, only to prepare the normal vectors of all the points as a pre-process of the region growing can cost a lot of time.

Though as introduced in Chapter 2, different kinds of registration method of the point cloud and design surface is developed in the related researches. There is still not a fully automatic registration when there is not a clear overlap between the two data.

An automatic, efficient and effective plate measurement system which can extract the point cloud of the plane from the measured data with obstacles, and a fully automatic registration method with the automatic overlap pre-setting are expected.

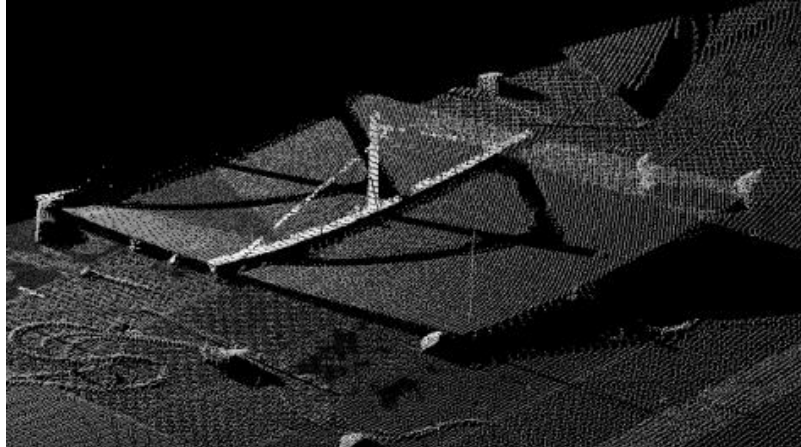


Figure 5-1 Measured data with irregular obstacles

5.2. Overview of curved shell plate's measurement

To construct an environment which can capture and store the manufacturing scenarios for the subsequent manufacturing plan analysis, the optimization and labor saving during the measurement are required.

As a basic image processing algorithm, the region growing method introduced in Chapter 3 can only extract continuous domains, and the integration of these separated domains is manual. It is necessary to develop a more efficient and effective plate extraction method which can also recognize the multiple domains of the curved shell plate's point cloud data divided by the obstacles or the shades of the obstacles. The process should be totally automated and fast enough to support every manufacturing step within the workers' toleration (1 - 3 minutes).

In addition, the fully automatic registration method of the measured point cloud and the plate's design surface is also an important pre-process of the plate's measurement.

5.2.1. Plate extraction prototype

As shown in Figure 5-2, this thesis proposes a plate extraction prototype (Sun, J.Y. PLM2014) consisting of two main processes: the continuous domain extraction which extracts the small separated domains from one single seed point and the

separated domain recognition which decides if an extracted domain is from the same component as the other ones.

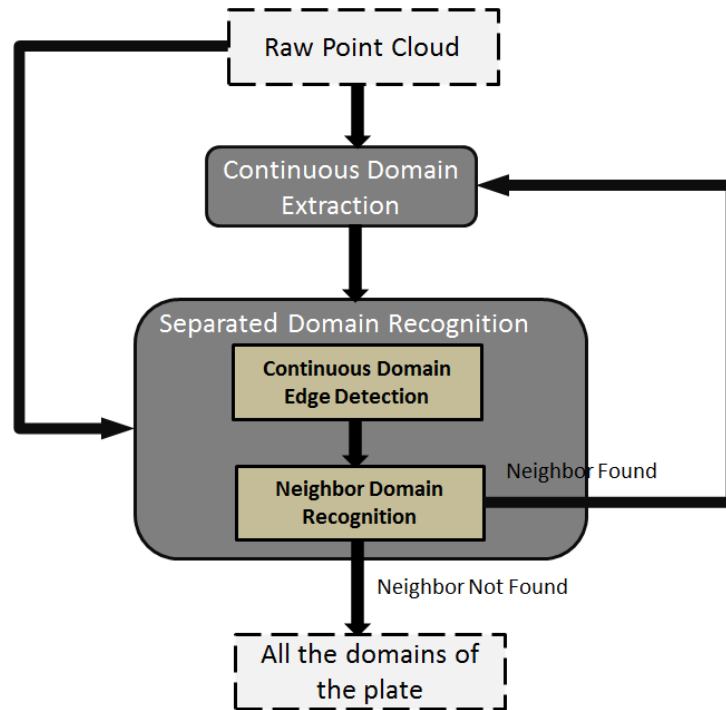


Figure 5-2 Plate extraction prototype

5.2.1.1. Continuous domain extraction

The continuous regions are extracted by the region growing method introduced in 3.3.2. Region growing method is generally executed for meshed point cloud. However meshing point cloud requires more computational time. So in this system, the method is executed directly towards point cloud data.

The count $N_{neighbor}$ of the neighborhood points searched for the next growing is set to 20, 30 or 40. For every scan setting, 10 sets of point clouds are measured. And then region growing using different $N_{neighbor}$ is conducted. The final $N_{neighbor}$ is selected in the ones which result into the right extraction result. When there are two or more $N_{neighbor}$ qualified, the biggest one will be chosen.

After the right $N_{neighbor}$ is decided, the threshold of the similarity of the normal vectors TH_{normal} is set to 0.995, 0.996, 0.997 or 0.998. Also, for every scan setting,

10 sets of point clouds are measured. And region growing using different TH_{normal} is conducted. The final TH_{normal} is selected in the ones which result into the right extraction result without failure. When multiple TH_{normal} are qualified, the biggest one will be chosen.

The limit of the region growing times (recursions) is set to 1000 considering the biggest plate under high density.

5.2.1.2. Separated domain recognition

To recognize the neighbor domain which belongs to the curved shell plate too, the edges of the already extracted domains are detected first. Then the neighbor points of these edges from the point cloud are judged under some constraints to see if they belong to the curved shell plate. Once a qualified neighbor point is found, the continuous domain extraction will be conducted toward this point. This process repeats itself until there is no neighbor point.

The figure below shows the flow of the developed plate extraction engine. The common domain judgment is conducted here to decide if any neighbor domain is of the same component as the continuous domain extracted firstly.

The basic region growing method introduced in 3.3.2 is used to do the continuous domain extraction, and 4th curve surface fitting of the neighbor points is used to decide the right region growing seed for the next domain (Hiekata, K., Sun, J. JASNAOE2011).

Multiple problems exist in the engine mentioned above,

- Cost too much time when the point cloud data is too big.
- Accidently grow into wrong area which is not part of the curved shell plate.

In this study, a lot of improvements are made to solve these problems from different sides.

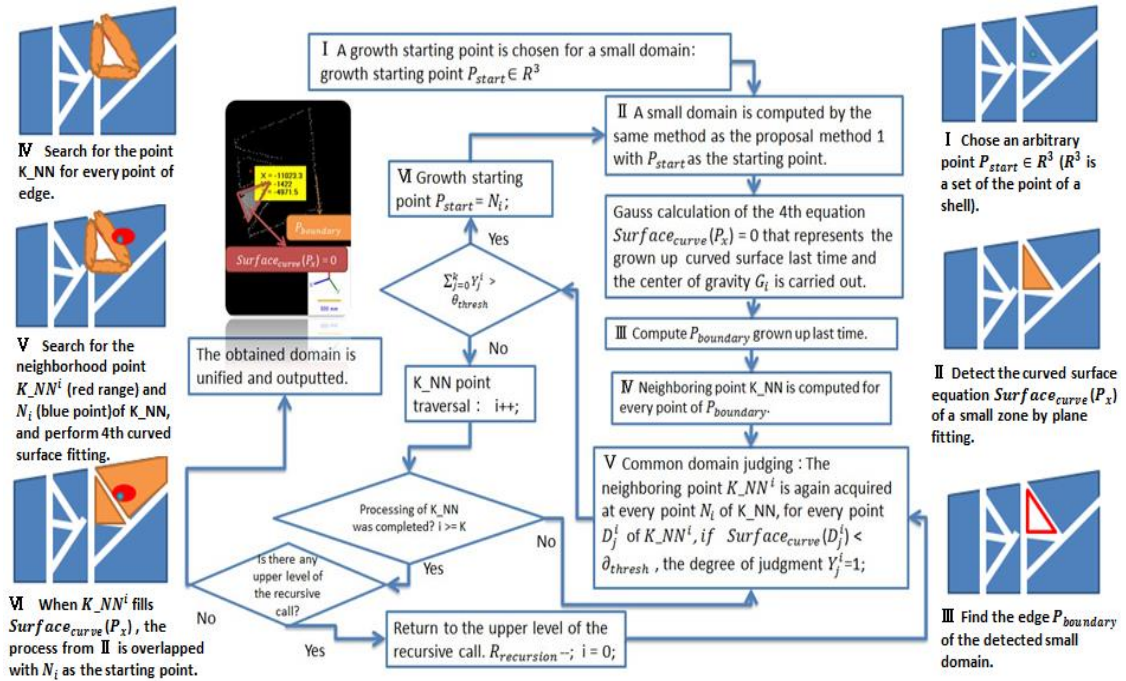


Figure 5-3 Flow of developed plate extraction prototype

5.2.2. Originalities for higher speed and lower failure

In this research, a lot of improvements based on the classic region growing method and the curved surface common domain recognition is made to make the extraction more effective and fast.

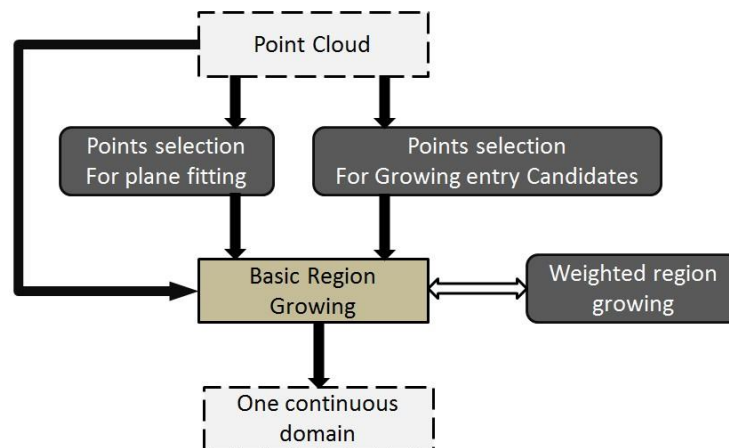


Figure 5-4 Continuous domain extraction

As shown in Figure 5-4, the proposed continuous domain extraction method is based on a basic point cloud processing method called region growing method discussed in 5.2.1, which repeats the process of calculating the normal vector at each neighbor point of the seed point, extracting the neighbor point which has a similar normal vector as the seed point and setting the extracted neighbor point as the next seed point. The growing process ends when the normal vectors have relatively dramatic changes. To make the neighbor search more efficient here, a space-partitioning data structure, k-d tree, is constructed using the scanned point cloud data for organizing points in a k-dimensional space recursively.

As a necessary pre-process of the basic region growing method, normal vector calculation of every points existing in the measured point cloud was conducted. In this section, a specially designed float normal vector calculation window is used to shorten the calculation time.

When the point cloud's density varies dramatically, to calculate the normal vector of a seed point using its neighbor points, plane fitting method using all the neighbors equally may cause unrepresented results. Normal vector calculation method considering point cloud's density is developed.

Also, to avoid improper growing into points that are too far from the seed such as the floor near the component, points which are used to do the plane fitting have to be seriously selected under certain constraints.

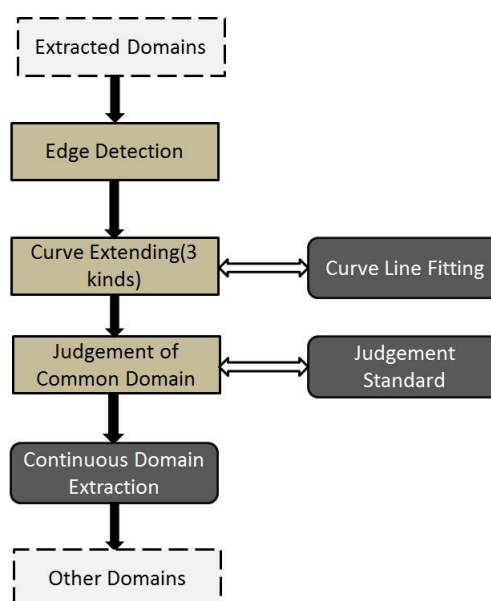


Figure 5-5 Separated domain judgement

At last, as shown in Figure 5-5, to better recognize the neighbor domain, the judgement standards of the separated domains are redefined into the extend curve fitting and comparison as an extension the 4th curved surface fitting and comparison.

5.3. Float region growing candidate selecting and plane fitting

To save the normal vector calculation and comparison time for the continuous domain's region growing, in this study, the point candidates for the next growing seed are carefully selected following the following procedure.

As shown in the figure below, distance from the gravity center G_n of the candidate neighbors, distance from the gravity center G_e of extracted points PCD_e and distance from the fitted plane of PCD_e are considered when select the candidate seed for the next growing step.

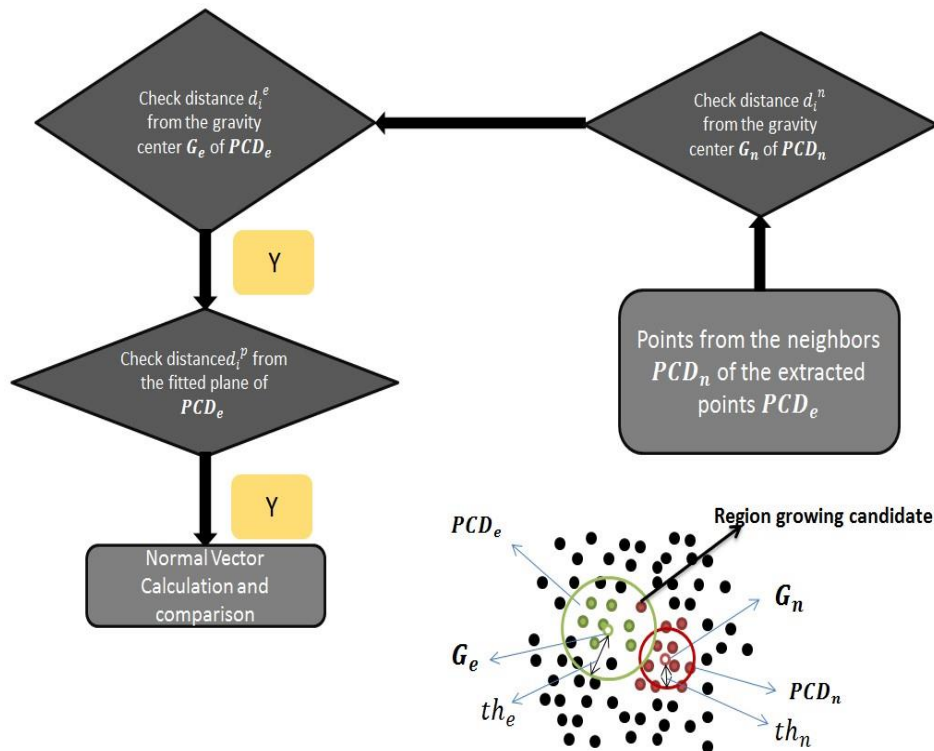


Figure 5-6 Float normal vector calculation window

Only the points which are relatively outside of the neighbors and relatively close to the

extracted point cloud are considered to be the next growing entry candidates. Thus, as shown in Figure 5-6, the gravity point \mathbf{G}_e of the extracted points and the gravity point \mathbf{G}_n of the neighbors are calculated, and the distances d_i^n , d_i^e and d_i^p are computed for every point \mathbf{P}_i of the neighbors. Support there are totally m points in the neighbors and l points in the extracted points, only when

$$d_i^n > b_{thresh} \times \sum_1^m d_k^n / m \quad (1)$$

$$d_i^e < b_{thresh} \times \sum_1^l d_k^e / l \quad (2)$$

$$d_i^p < b_{thresh} \times \sum_1^l d_k^p / l \quad (3)$$

is the point \mathbf{P}_i considered to be the next growing entry. b_{thresh} is a thresh value between 0 and 1. In this thesis, b_{thresh} is set to 0.74 according to the extraction test to 3 sample data measured under the designed experiment condition. .

In this research, the normal vector calculation window is floatable while the region growing, and only the normal vectors belong to or close to the plate are calculated, therefore, the calculation time is dramatically reduced than the normal region growing method.

To avoid improper growing into points that are too far from the seed such as the floor near the component, points which are used to do the plane fitting have to be seriously selected under certain constraints. The distance d between the point being evaluated and the extracted points is checked to decide if this point should be considered to be part of the domain or not. In this paper, two planes are fitted for the normal vector calculation and the distance d 's calculation respectively as shown in Figure 5-7. The point \mathbf{P}_j is the point being evaluated. Since *plane1* is used to calculate the normal vector of the point \mathbf{P}_j , it is fitted using all the neighbor points \mathbf{R}_1 with no concern about whether they are already recognized as part of the domain or not. Normal vector comparison can only evaluate the direction trend here at \mathbf{P}_j . The distance d should also be considered to avoid growing to an area not part of the domain but only has a slight difference in normal vector comparison result. *plane2*, which is used to evaluate the distance d , is calculated using only the points \mathbf{R}_2 which are already recognized as part of the domain.

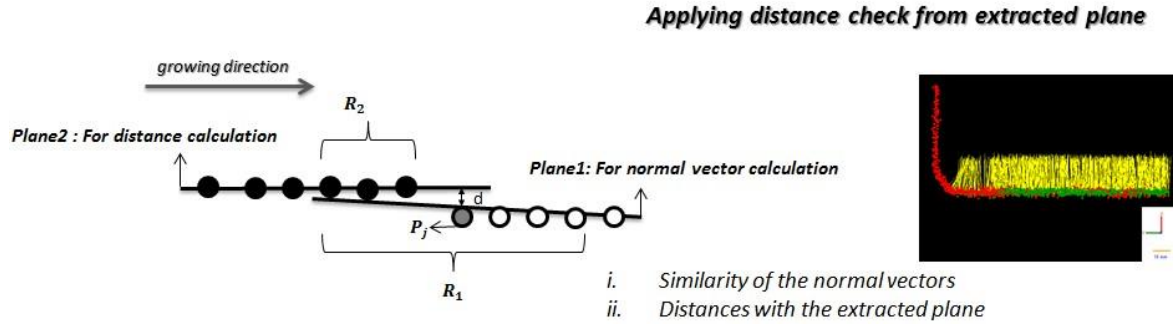


Figure 5-7 Points used to do plane fitting (Sun, J.Y., IJCC, 2014)

5.4. Weighted normal vector calculation considering point cloud's density

When the point cloud's density varies dramatically, to calculate the normal vector of a seed point using its neighbor points, plane fitting method using all the neighbors equally may cause unrepresented results.. As shown in Figure 5-8, to determine whether P_4 belongs to the same region as P_i ($i = 1,2,3$), normal vector calculation is performed on it. Since the density at P_i ($i = 5,6,7$) is lower than that at P_i ($i = 1,2,3$), the normal vector of no weighted plane (plane 3) will be outputted as in Fig. 3. Obviously, it cannot represent the normal vector at P_4 , and is dramatically differed from the normal vector at P_2 . Therefore, the growing is terminated without P_4 being included while P_4 actually belongs to the same region as P_i ($i = 1,2,3$).

And according to Enomoto, M. (2012), the errors of the laser scanner follow the Gaussian distribution. Thus, to calculate the normal vector at each neighbor point and the seed point, weighted plane fitting (plane 4) conducted in this paper. By using the weighted plane fitting, the weighted sensitivities based on the distances from the point being evaluated are applied to the points which are used to fit the plane. This subsection used both the basic plane fitting using least square regression discussed in 3.3.4.1 when the point cloud's density is invariant, and the weighted plane fitting introduced in 3.3.4.2 when the point cloud's density varies dramatically. $\exp(-\frac{d^2}{h^2})$ is used to calculate the weight w_i . Here d is the distance between the point being evaluated P_{eva} and the points which used to fit the plane for calculate the normal vector. h is decided as the 2 to 4 times of the average

intervals in the point cloud. The qualified h is decided by conducting about 10 sets of measurement and extraction. Within the ones which can result into proper extraction results, the smallest one is chosen.

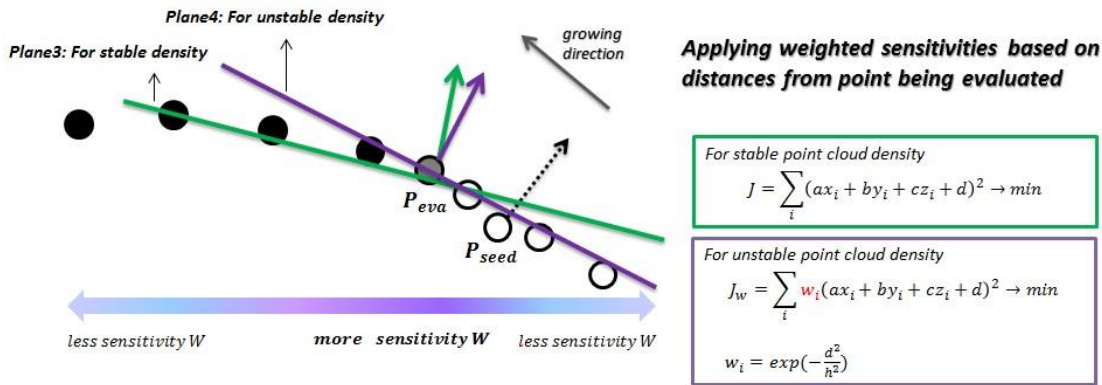


Figure 5-8 Normal vector calculation considering point cloud's density (Sun, J.Y., IJCC, 2014)

5.5. Judgment standards of the common domain recognition

Figure 5-9 shows the flow of the redesigned common domain judgment process. First, one single seed P_{seed} on the component is selected randomly, and then the continuous domain is computed by a region growing method illustrated above. The second step, highlighted in gray, has the same processing as the process discussed in 5.3, and 5.4. Neighbor points $R_{neighbors}$ are calculated for every point of the extracted continuous domain's boundary $P_{boundary}$. Then the neighbor points $R_{neighbors}^i$ are obtained for point N_i in $R_{neighbors}$. For all the points D_j^i in $R_{neighbors}^i$, the common domain judgment, which will be introduced later, is performed to decide whether N_i can be chosen as a seed point of another domain of this component. Also, this process is recursively repeated until all the points of the component are extracted successfully.

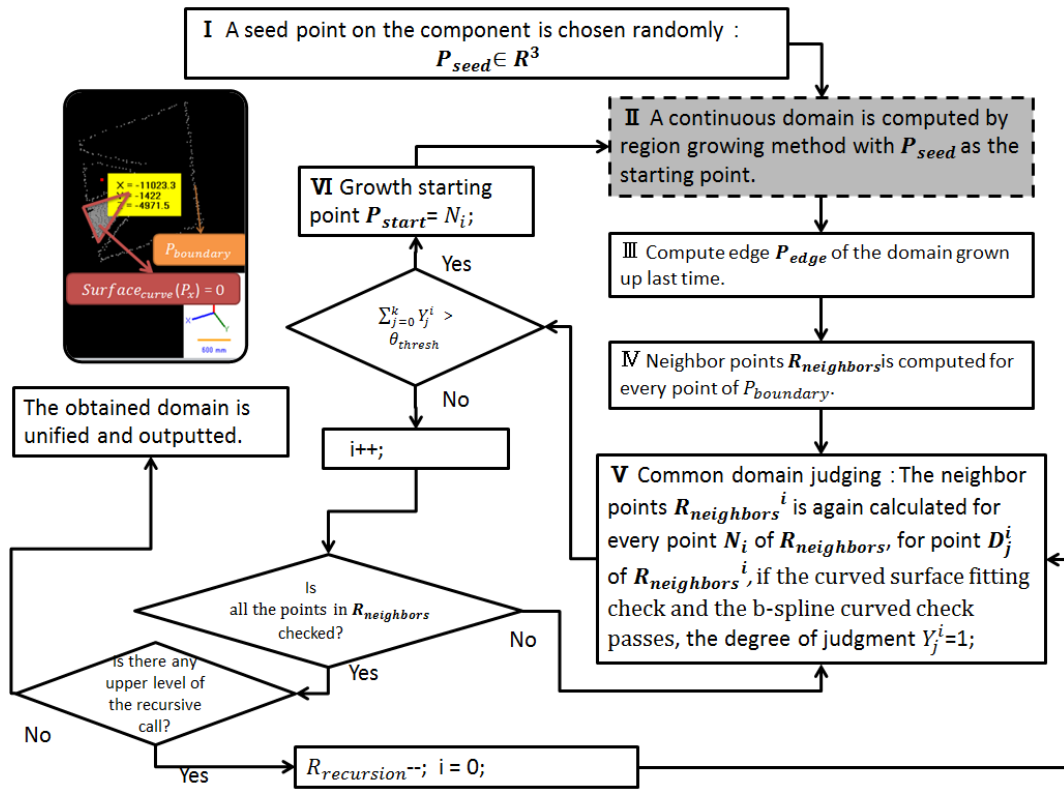


Figure 5-9 Measured data with irregular obstacles (Sun, J.Y., IJCC, 2014)

Figure 5-10 illustrates how common domain judgment works. Domain A is first recognized by the method in 2.1. For every edge point of domain A, 4th curved surface fitting and b-Spline curve fitting, which is widely used in designing free-form surface of ships, are performed to decide if the degree of judgment Y_j^i of point D_j^i is true (1) or false (0). Only when the sum of all Y_j^i is greater than the threshold, is the point N_i selected as a seed point to start another domain's (domain B) growing process.

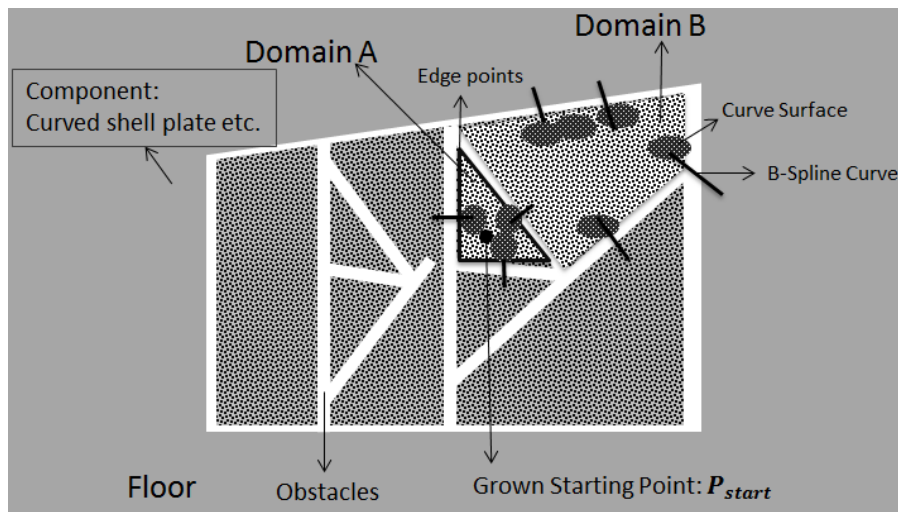


Figure 5-10 Common domain judgment (Sun, J.Y., IJCC, 2014)

As shown in Figure 5-11, in this process, 4th curved surface equation is used to fit the curved surface around the edge point of the extracted domain A. D_j^i is checked to see whether it belongs to the curved surface S_{fitted} or not.

If only D_j^i passes the curved surface check, the b-spline curved line check is conducted. Here P_i is the control point.

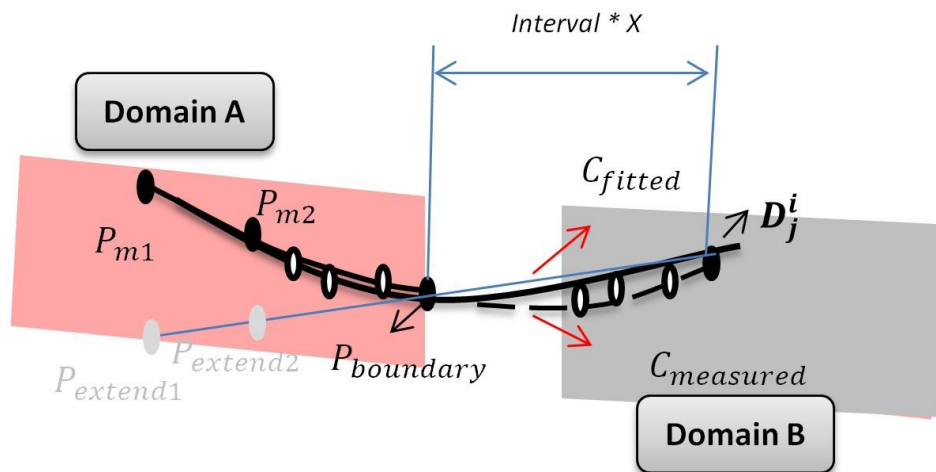


Figure 5-11 Fitted curve and measured curve (Sun, J.Y., IJCC, 2014)

Four points ($D_j^i, P_{edge}, P_{m1}, P_{m2}$) are taken as the control points of the b-spline line. $P_{extend1}$ and $P_{extend2}$ are two points on the extension line of $|D_j^i P_{edge}|$, and P_{m1}, P_{m2} are

their nearest points in domain A. After b-spline curve C_{fitted} is calculated out, the nearest points in domain B are obtained for the points of C_{fitted} . The group of these nearest points is C_{measured} . Only if the average of every pair's distance between C_{fitted} and C_{measured} is smaller than the threshold, can the degree of judgment Y_j^i of D_j^i be set to true.

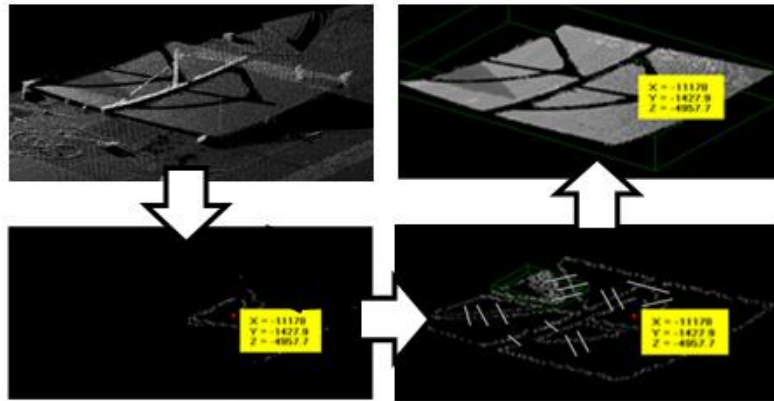


Figure 5-12 Extraction process of plates separated by obstacles

The extraction process of the plates which are separated by obstacles is shown in Figure 5-12. A seed point is firstly selected from a single domain of the plate so that this continuous separated domain can be extracted. Then the edges of this domain are detected and curves are extended from these edge points to their neighborhood points on the neighbor domains. Only when the neighbor domains pass the common domain judgement standard, the neighbor domains can be recognized as also parts of the plates. This loop repeats itself until all the domains of the plate are extracted successfully.

The count TH_{judge} of the sum of all Y_j^i is set to 0.71, 0.72, 0.73, 0.74 or 0.75. For every scan setting, 10 sets of point clouds are measured. And then region growing using different TH_{judge} is conducted. The final TH_{judge} is selected in the ones which result into the right extraction result. When there are two or more TH_{judge} qualified, the smallest one will be chosen.

5.6. Registration method with direction pre-setting

As shown in Figure 5-13, this thesis proposes an efficient registration method involving parallel transformations using the center of gravity of the two data sets,

the pre-setting of the registration direction and the traditional ICP registration, an algorithm employed to minimize the difference between two clouds of points.

To register the measured point cloud to the designed data, a parallel transformation using the center of gravity of both data sets is conducted using the equation below. Here the \mathbf{P} represents the point from the measured data. \mathbf{G}_d and \mathbf{G}_m are the centers of gravity of the designed perimeter and measured perimeter respectively.

$$\mathbf{P}' = \mathbf{P} + (\mathbf{G}_d - \mathbf{G}_m) \quad (3)$$

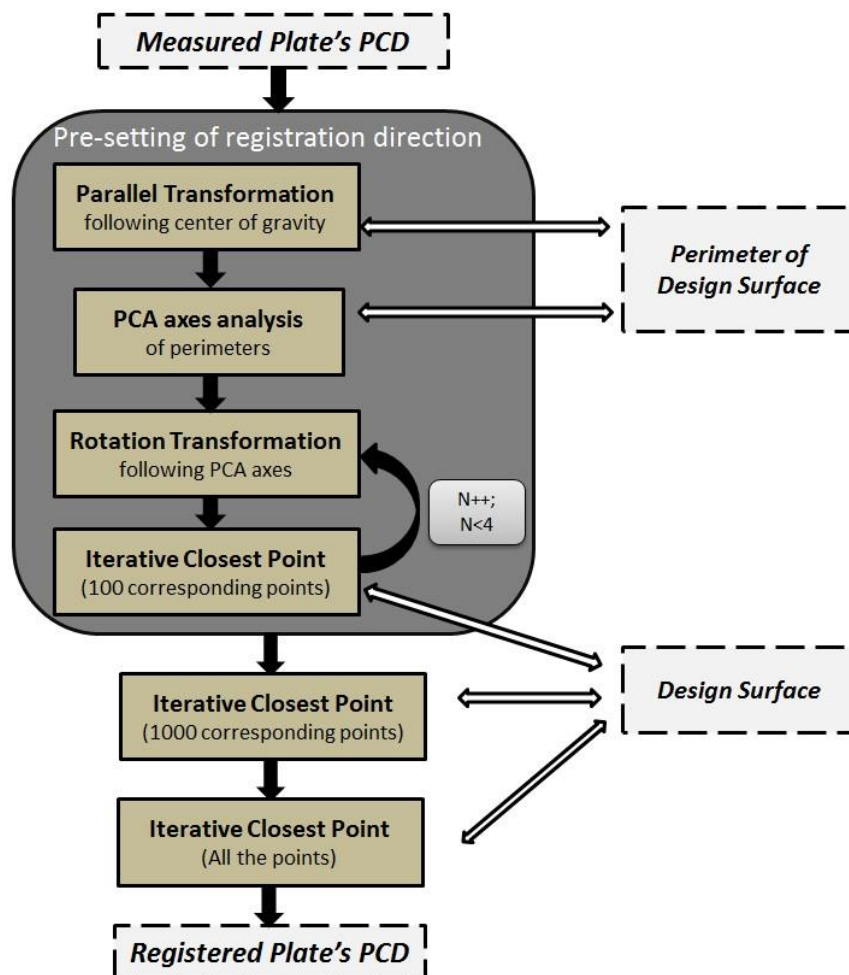


Figure 5-13 Registration flow

In practice, as shown in Figure 5-14, the registration method Iterative Closest Point stands a good chance of getting an obviously wrong output if the registration

is started from an improper direction.

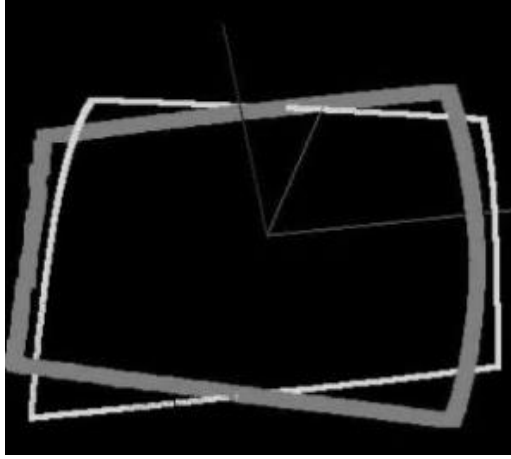


Figure 5-14 Inverted registration result (Sun, J.Y., IJCC, 2014)

To solve this problem, before ICP algorithm is conducted, after three directions of the inertia principal axes are calculated to find the proper registration start direction with the minimum displacement. Firstly, the inertia tensor \mathbf{I} is calculated. The three eigenvectors of \mathbf{I} are the inertia principal axes as shown in Figure 5-15.

As expressed in the following equation, the measured point cloud P is registered to the design data according to multiple ways. The registration direction with the minimum displacement is chosen to be the original direction to conduct the ICP algorithm. Here \mathbf{R}_d and \mathbf{R}_m are the eigenvectors' set of the design data's and the measured data's inertia tensor \mathbf{I} respectively.

$$\mathbf{I} = \begin{bmatrix} \sum_{i=0}^{n-1} m_i(|\mathbf{P}_i|^2 - x_i^2) & -\sum_{i=0}^{n-1} m_i x_i y_i & -\sum_{i=0}^{n-1} m_i x_i z_i \\ -\sum_{i=0}^{n-1} m_i x_i y_i & \sum_{i=0}^{n-1} m_i(|\mathbf{P}_i|^2 - y_i^2) & -\sum_{i=0}^{n-1} m_i y_i z_i \\ -\sum_{i=0}^{n-1} m_i x_i z_i & -\sum_{i=0}^{n-1} m_i y_i z_i & \sum_{i=0}^{n-1} m_i(|\mathbf{P}_i|^2 - z_i^2) \end{bmatrix} \quad (4)$$

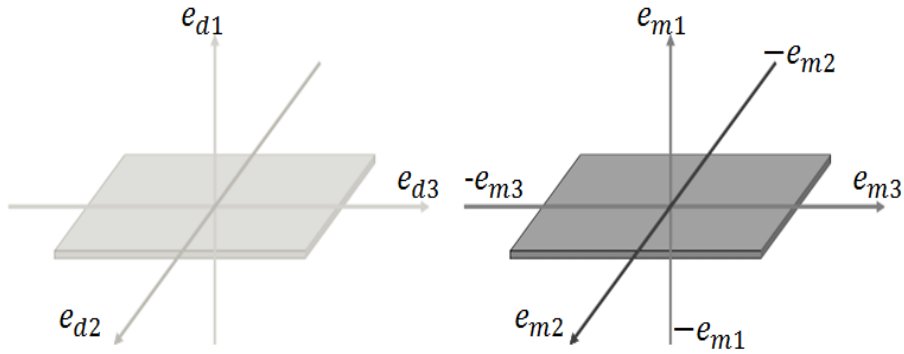


Figure 5-15 Inertia principal axes (Sun, J.Y., IJCC, 2014)

$$\mathbf{P}' = \mathbf{R}_d^T \times \mathbf{R}_m \times \mathbf{P} \quad (5)$$

$$\mathbf{R}_d = (\mathbf{e}_{d1}, \mathbf{e}_{d2}, \mathbf{e}_{d3}) \quad , \quad \mathbf{R}_m = (a\mathbf{e}_{m1}, b\mathbf{e}_{m2}, c\mathbf{e}_{m3}) \quad a = \{1, -1\}, b = \{1, -1\}, c = \{1, -1\}$$

To save the calculation time of ICP, the ICP is firstly conducted toward 100 corresponding points, and then 1000. At last, all the points in the point cloud are used. The corresponding points of the measured points are found by doing the projection of these points onto the design surface of the plate.

5.7. Development of MS

The parameter setting interface for the plate measurement system is as shown in Figure 5-16. How to set these parameters are discussed in the sub-sections above. For every scan setting, parameters that can be customized are as below:

- The count of the neighbor points used in the region growing method $N_{neighbor}$
- The value h used to calculate the weighted plane (the Gaussian's attenuation degree)
- The threshold of the similarity of the normal vectors TH_{normal}
- The b_{thresh} in 5.3
- Whether to calculate the normal vectors
- The limit of the region growing times
- Whether to recognize the separated domains
- The threshold of the sum of all Y_j^i in 5.5 TH_{judge}
- Whether to display the progress of the separated domain recognition

- The start seed point of the region growing method

For one fixed scan spot, there is no need to change the parameters listed above every time. If the administrator of the shipyard relocated the scanner or the scan spot, they can just modify the configuration files which will be illustrated in Appendix to adapt the new environment.

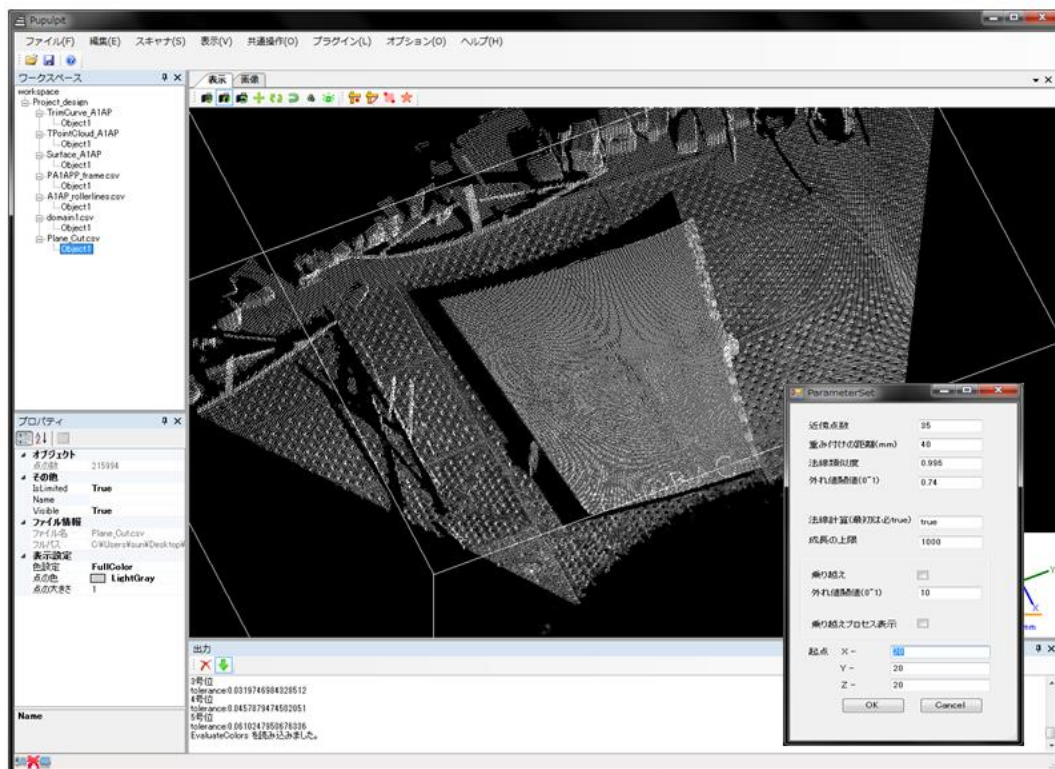


Figure 5-16 User interface of MS

5.8. Summary

In this chapter, the features of the measured curved shell plates' point clouds and the problems existing in the curved shell plates' extraction are explained at first. Then the developed plate extraction prototype which uses plain region growing method and common domain recognition is introduced. To achieve higher speed and reduce the failure rate during the extraction, huge improvements are made as below:

For the continuous domain extraction, the float normal vector calculation window is used instead of calculating the normal vectors of all the points. Also the

region growing seed candidates are carefully selected to reduce the calculation time to an acceptable level in the shipyard. On the other hand, to reduce the failure rate during the extraction such as accidentally growing into the points which do not belong to the plate, different points selection method are applied to the plane fitting of different purposes. And to avoid improper stop during the failure caused by variable density existing in the point cloud, the normal vector calculation in consideration of the point cloud's density is introduced.

For the separated domains recognition, the judgement standards of the common domain are discussed which is aimed to the efficient and effective recognition and extraction of all the domains which belong to the plate under different conditions.

Chapter 6 Cold forming supporting

6.1. Overview of the cold forming supporting framework

As shown in Figure 6-1, the convention method of evaluating the plate’s shape during the cold forming is to check the gaps between the wooden templates and the plate when trying to fix them on the plate. The ends’ displacements of the wooden templates and the plates are observed, when the sum of these displacements is smaller than the threshold, the plate is judged as finished and forwarded to the subsequent heating forming.

Three main problems as below exist in nowadays’ cold forming process of the curved shell plate.

- The evaluation of the curved shell plate’s shape after every press step using wooden templates cost a lot of time and efforts.
- Only the frame areas can be evaluated by using the wooden templates. Areas without frames (where wooden template is fixed) cannot be evaluated.
- The evaluation of the curved shell plate’s perimeter may be not accurate and also cost time and efforts.

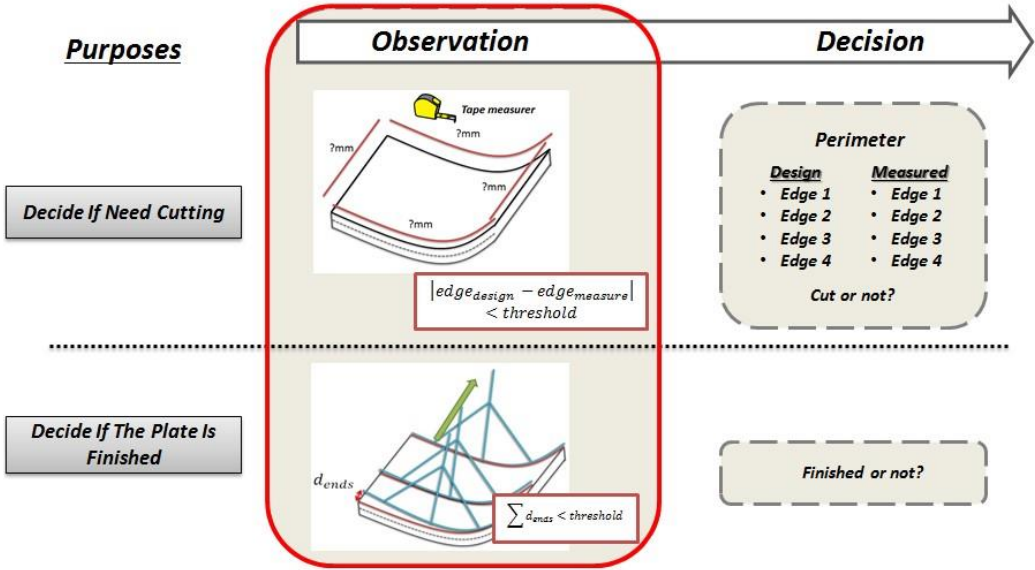


Figure 6-1 Convention of cold forming evaluation using wooden template

Therefore, the Press Support System (PSS) cooperating with the Plate Measurement System (MS) is developed to solve these two problems.

As shown in Figure 6-2, the developed PSS has two kinds of input data:

- The extracted plate's point cloud
- The design target point cloud of the cold forming process

The plate's point cloud is firstly extracted using the MS, and the design target point cloud of the cold forming process represents about 70% ~ 80% curvature degree of the final shape of the curved shell plate (the rest 20% ~30% is supposed to be deformed in the heating forming process).

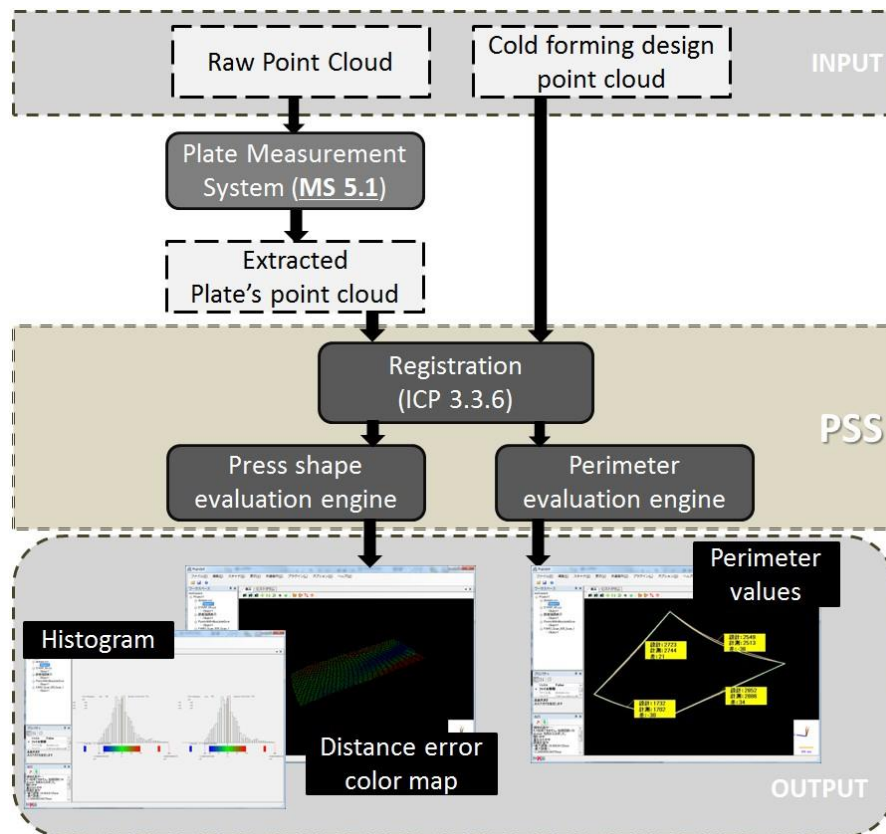


Figure 6-2 Overview of the Press Support System (PSS)

PSS firstly does the registration of the two input data. Then based on the registered design point cloud and measured point cloud, the distance errors between the two data are calculated and transformed into the color map and histogram by

the press evaluation engine for the workers. At the same time, the perimeters of the measured point cloud and design point cloud are calculated by the perimeter evaluation engine and the errors are also displayed in the message box shown in the 3D view of the point cloud.

6.2. Pre-process and registration

The registration of the design point cloud and the measured point cloud uses the ICP method introduced in 3.3.6.

Due to the varying density existing in both the design point cloud and measured point cloud, to avoid the improper registration result, the average density thinning of the two data is conducted as a necessary pre-process as shown in the following figure.

The concrete procedure of thinning is described following.

- a. Principal component of the surface part is analyzed and it is divided into two equal parts by a plane which is vertical to the first principal component vector.
- b. The operation a is repeated for the other divided parts until the number of points from each separated part becomes less than a fixed threshold.
- c. A set of each part's gravity center is considered as thinned points of the surface part.

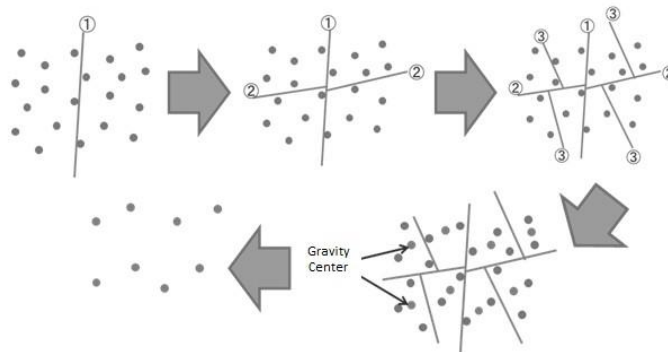


Figure 6-3 Point cloud thinning

6.3. Press evaluation method

The basic concept of the convention of the shape evaluation during the cold forming is to find out the areas with the big displacement from the design surface in form of wooden template. This research proposes a method to calculate these displacements and visualize them in the form of color maps and histograms.

As shown in Figure 6-4 (left), the distance error d_{error} of the design point being evaluated P_e is found by calculating the distance between the nearest point N_e of the measured point cloud from P_e . This method is only effective when the design point cloud and measured point cloud have the similar density, otherwise, the calculated d_{error} cannot represent the distance error between the two data, and the result color map will be as shown in the left bottom of the following figure.

To solve this problem, the design plane is fitted towards to the nearest points of the measured point cloud from the design point being evaluated P_e' using the basic plane fitting method introduced in 3.3.4.1. Then the distance between the design point being evaluated P_e' and the fitted design plane is calculated as the distance error of P_e' . This method can also be applied to the input data with different densities.

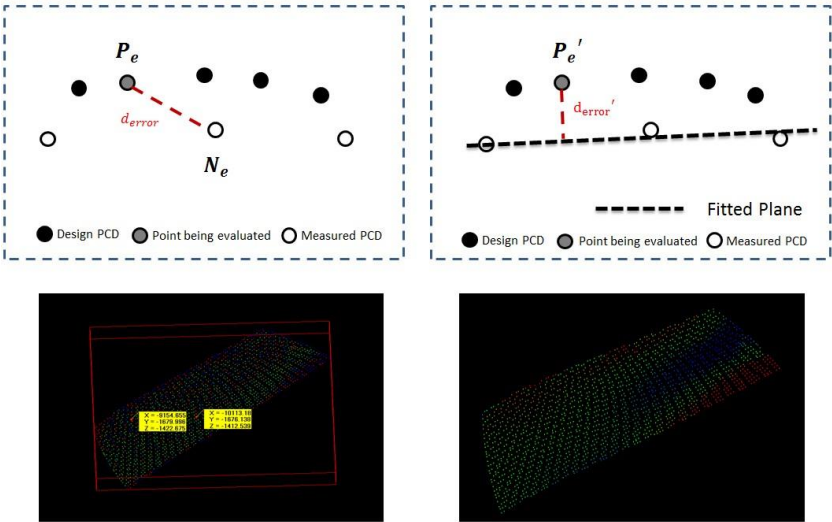


Figure 6-4 Distance error calculation

The developed press evaluation engine outputs the distance color map generated based on the calculated distance errors between the design data and measured data, and the histograms about the distribution of the distance errors as shown in Figure 6-. The color map helps workers to get an intuitive idea of the plate's shape by displaying the distance errors in the gradation way. The mean μ and standard deviation σ are calculated, the one-dimensional gradation is implemented as that the points around μ are displayed in green, the points having the value over $\mu + \sigma$ is always displayed as red, and the points having the value under $\mu - \sigma$ is displayed as blue. The outputted histogram helps the workers to grasp the amount of the errors. The horizontal axis represents the levels of the error; the vertical axis shows the amount of the points corresponding to this level.

The ratio of the points with displacements smaller than the threshold set by workers is used to judge if a plate is finished or not after the cold forming.

6.4. Perimeter evaluation method

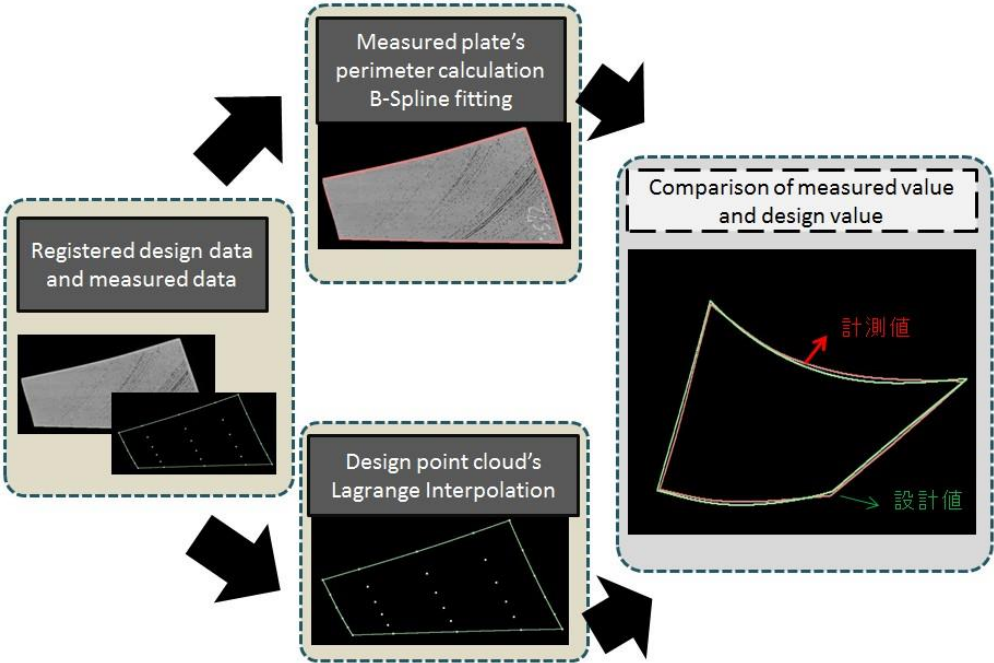


Figure 6-5 Perimeter calculation flow

The perimeter evaluation engine calculates and displays the perimeter values of the measured data and the design data. As shown in Figure 6-5, after the design data and measured data are registered together, the measured plate's perimeter is calculated by fitting a B-Spline curve (3.3.5.2) based on the edges of the point cloud. Then the design shape's perimeter is calculated by interpolating a Lagrange curve (3.3.5.1) based on the edges of the thinned design point cloud.

6.5. Development of PSS

The user interface of the press evaluation engine is as shown below:

The user or the automation engine has to select

- (1) The point cloud to be moved (the design point cloud)
- (2) The point cloud staying at the original position (the measured point cloud)
- (3) The threshold of the displacement

This manual operating can be automatized by using the automation engine introduced in the appendix. The evaluation result is displayed to the workers as shown in the figure below.

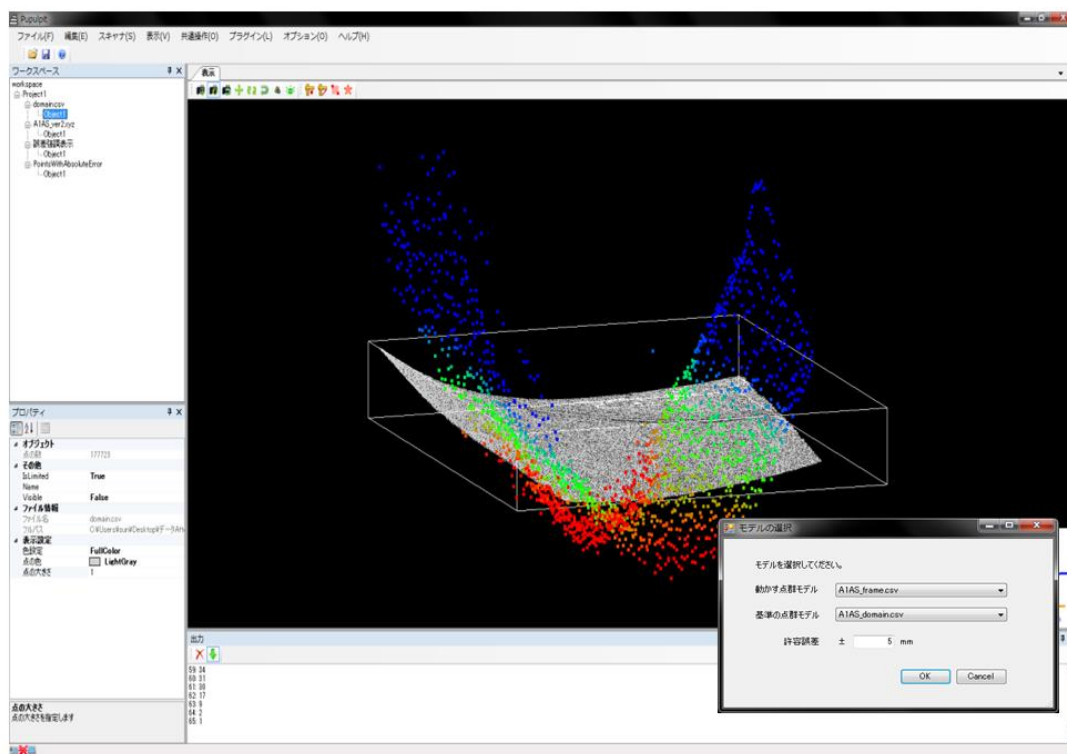


Figure 6-6 Press evaluation user interface

The user interface of the perimeter evaluation engine is as shown below:

The user has to select

- (1) The point cloud to be moved (the design point cloud)
- (2) The point cloud staying at the original position (the measured point cloud)

This manual operating can also be automatized by using the automation engine introduced in the appendix. The evaluation result is displayed to the workers as shown in the figure below.

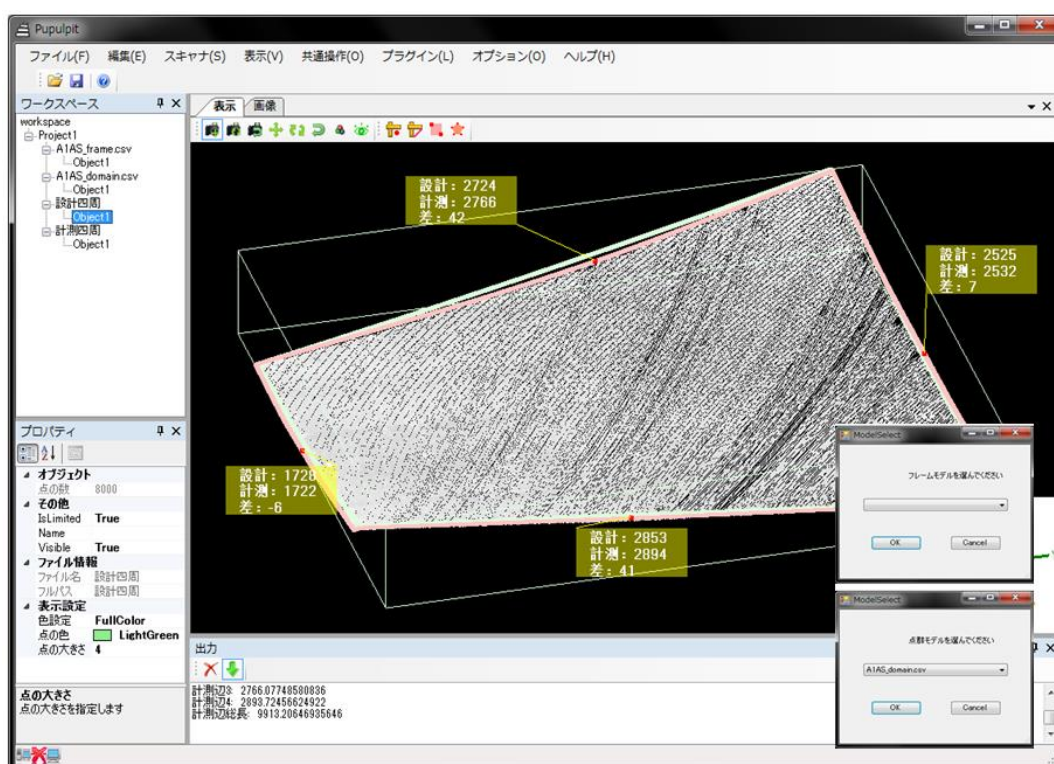


Figure 6-7 Press evaluation user interface

6.6. Summary

In this chapter, the problems existing in the cold forming process (press process) and the expectations of the workers are explained first. Then the pre-process and registration of the design data and the measured data are introduced. Based on the registered data, the displacement errors of the two data are calculated and displayed in the readily comprehensible way; the perimeter values are also

computed and displayed after the edges of the two data are found by curve fitting and curve interpolation.

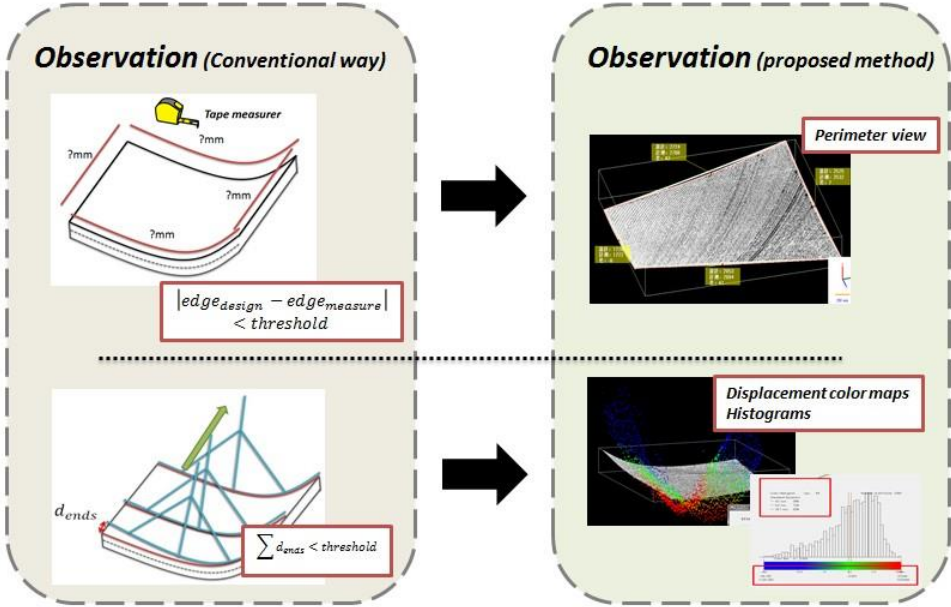


Figure 6-8 Generated interfaces for observation of cold forming manufacturing

By achieving the items mentioned above, the press support system meets most of the conditions in the shipyard’s practical way to use, and as shown in the figure above, the necessary parameters used in the manufacturing convention can all be observed on system instead of using the wooden templates.

Chapter 7 Heating forming supporting

7.1. Overview of the heating forming supporting framework

Figure 7-1 shows the convention of the decision making during the heating forming using the real wooden templates. To decide the heating areas and heating grades, the gaps between plate and wooden templates, the extent of the shaking of each wooden templates and the smoothness of the plate when trying to touch the surface are observed by human eyes. The heating technics are decided by observing the wooden templates which are arranged on the plate through multiple directions. The angles between the templates' sticks, the distances between the tops of the templates and the upper representative plane, and the gaps between the template and the plate are observed. At last, the ends' displacements between the templates and the plates (when the sticks of the templates pass a same plane) are used to decide if the plate is finished or not.

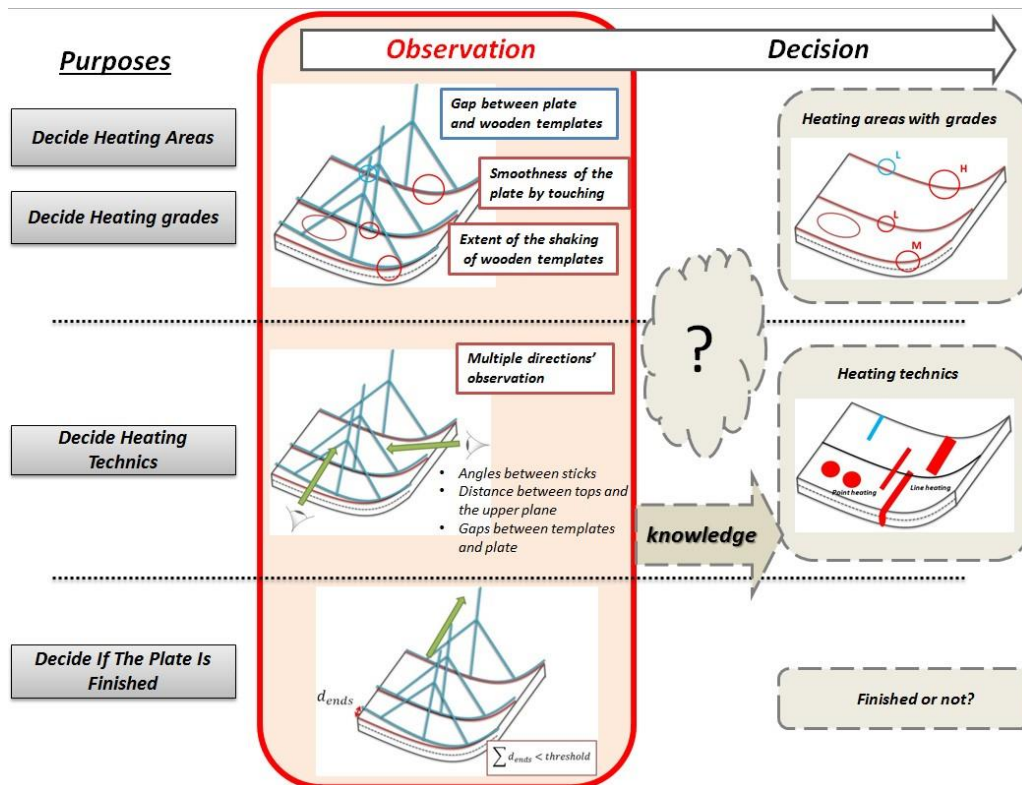


Figure 7-1 Convention of the heating forming decision making using wooden templates

As discussed in 4.1, a lot of problems exist in the heating forming process of the curved shell plates. To solve these problems, this research virtualizes the heating forming process on computer in real time for every manufacturing step of the curved shell plates. As shown in Figure 7-2, there are three input data for the Virtual Template System:

- Frame design point cloud
- Raw measured point cloud of curved shell plate
- 2D roller line design point cloud

The frame design point cloud represents the 3D design shape of the curved shell plate where the wooden templates are put. The 2D roller line point cloud represents the lines along which the heating is usually applied to avoid destroy the right torsion of the curved shell plate. The frame point cloud and the 2D roller line point cloud are both from the ship's design data. And another input data is the measured raw point cloud data which is obtained from the laser scanner.

At first, virtual templates are generated from the frame design point cloud; the plate's point cloud data is extracted from the measured raw point cloud including obstacles using the Plate Measurement System (MS); the 2D roller line data is matched to the registered virtual templates and plate's point cloud. Then the system calculates the simplest manufacturing plan with the heating grade, and automatically arranges the virtual templates on the plate's point cloud to detect the torsion situation of the curved shell plate for every manufacturing step. At last, two views as below are generated for the workers to grasp the situation of the curved shell plate and decide the manufacturing plan (heating plan) for the next manufacturing step.

- Torsion evaluation view
- Curvature evaluation view

In this chapter, the virtual template prototype is developed first by implementing some classic algorithms and the problems existing in importing this prototype into the shipyard are introduced. Then the original points based on these classic methods and the new virtual templates' operation interface will be discussed.

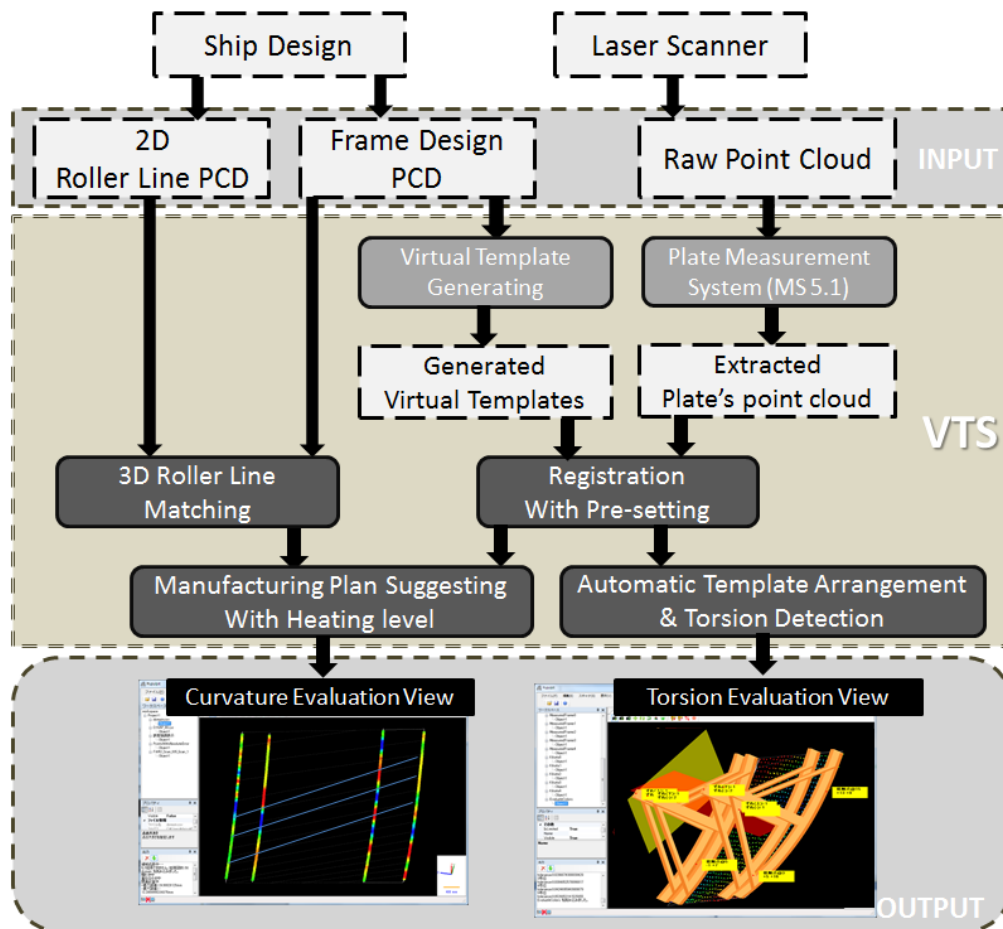


Figure 7-2 Overview of Virtual Template System (VTS)

7.1.1. Virtual template prototype

This thesis proposes a virtual template prototype (Sun, J.Y., ICCAS2013) to virtualize the wooden template on computer and calculate the curvature errors along each frame where the wooden templates are put.

As shown in Figure 7-3, the system involves the extraction of curved shell plate's real shape from the point cloud measured by laser scanner; the virtualization of curved shell plate's wooden template and the manufacturing environment; the automatic suggestion of the manufacturing plan by calculating the curvature differences between the virtual templates' bottom line and the measured data.

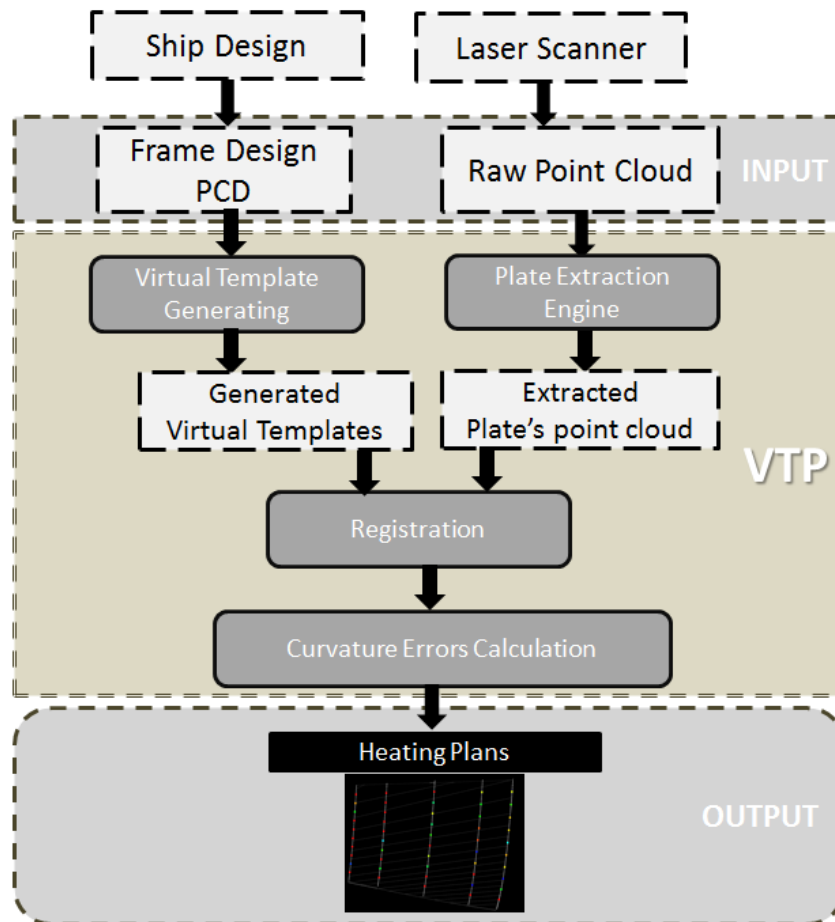


Figure 7-3 Virtual template prototype (Sun, J.Y., ICCAS2013)

7.1.1.1. Virtual template generating

Four to six wooden templates per plate are usually used to do the plate's evaluation and the manufacturing plan's design. Workers put them on the plate and observe the two planes: the plane formed by the upper points of the wooden templates' sticks and the plane formed by wooden templates' sticks themselves. If the plate is finished, these two planes would be perfectly fitted with no gap between it and the sticks. Otherwise, the gaps and angles between the sticks and the plane will be used to design the following manufacturing plan. Virtual template prototype is designed to generate the virtual templates with the same features of the real ones.

The bottom line of the virtual template is generated from the 3D coordinates of

the frame's design data which is part of the ship's design data using 3D Lagrange interpolation. Then the representative upper plane and the perspective plane are defined to determine the position of the virtual template's perspective stick.

The representative upper plane which all the upper endpoints of the virtual templates' perspective sticks pass is firstly generated as shown in Figure 7-4. First, the normal vectors \mathbf{v}_k of the k^{th} frame line's center \mathbf{P}_{mk} are calculated and added. The sum is normalized and multiplied by a fixed distance H and the result is set to be $H\mathbf{V}'$. Next, plane fitting is performed for the curved shell plate's frame point group \mathbf{FL}_k . The representative upper plane of virtual template group is generated by moving the obtained plane using $H\mathbf{V}'$ as shown in Figure 5.

In practice, the evaluation of the curved shell plate in manufacturing is performed by checking the position of the virtual templates' perspective plane. The definition of the perspective plane is made for virtual templates too. The center point \mathbf{p}_{m1} of 1st frame line is projected on the representative upper plane, and projecting point \mathbf{p}_{proj} is obtained. Then the perspective plane is defined by \mathbf{p}_{m1} , \mathbf{p}_{proj} and the center point \mathbf{p}_{m2} of the 2nd frame line. The generated virtual templates with the same perspective plane as a real wooden templates group are drawn on the computer.

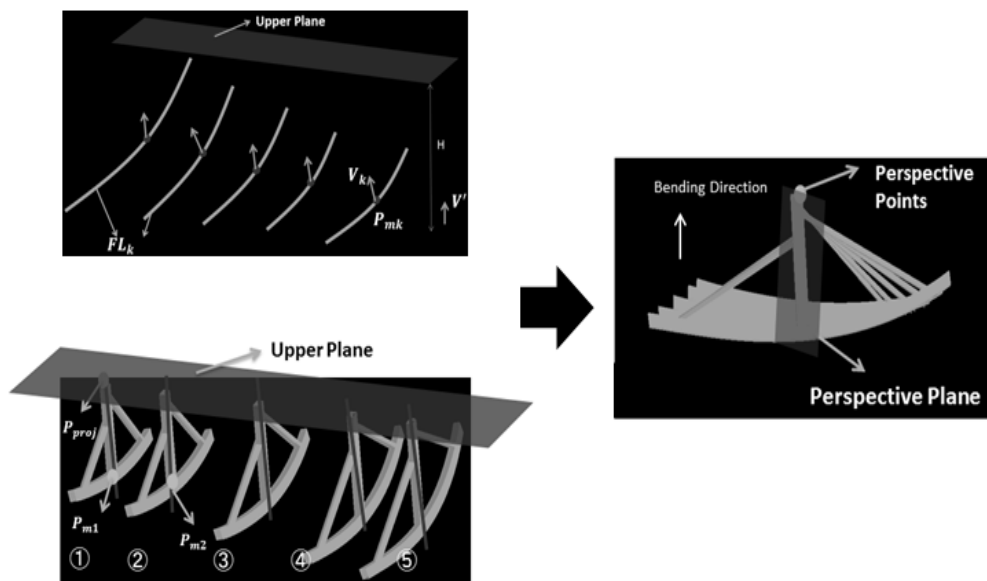


Figure 7-4 Virtual templates generating (Sun, J.Y., IJASM, 2014)

Finally, the generated virtual templates with the same perspective plane as a real wooden templates group are drawn on the computer. During the processing, when virtual templates are rotated respectively, the generated perspective plane is reconstructed. The distances between the reconstructed perspective plane and the virtual templates' sticks are used to check the plate's torsion.

7.1.1.2. Registration of the virtual template and plate's point cloud

The registration of virtual templates and measured curved shell plate's point cloud data is performed using ICP (Iterative Closest Point algorithm) introduced in 3.3.6 which is an algorithm employed to minimize the difference between two clouds of points. Because the plates have been deformed by using the press machine during the cold forming stage, they already have certain curvatures; therefore they can be registered to the design data with a relatively high conformity. To solve some improper registration results happening when there are missing part in the measured plate, the densities vary dramatically, or the obvious differences exist between measured plate and the design shape, a registration method with the registering direction pre-setting will be proposed later in this thesis.

After the generated virtual templates and the plate's point cloud are registered together, the nearest neighbor points in the measured point cloud from the planes fitted using the design frames are extracted. Curves are fitted using the extracted points respectively as the measured frames.

7.1.1.3. Curvature error calculation

In practice, it is easy to understand: that heating should be applied to where the curvature error is relatively large should be considered to be satisfied first (Scully, K. et al 1987). In this paper, the heating factor (manufacturing plan) is basically proposed by finding these locations where have relatively big difference in curvature from the design data (Kevin, S. 1987 and Bisgaard, C.H. 2000). Curvature difference between the virtual template's bottom line and measured

curved shell plate is calculated and colored as the first important output of this system. Since the measured frame line is a discrete point group from measured point cloud, curve fitting is carried out using a B-spline interpolation.

Then, the amount of necessary contraction by heating at each frame point is calculated for every frame line as shown in Figure 7-5. The section of measured frame line and the virtual template's bottom line are shown in Figure 7-5(left). H_p is the plate thickness at this frame line. $1/n$ part of the frame line is shown in Figure 7-5(right). During the plastic deformation, if heat is applied to point P_i , then the length l_i at upper side of plate at point P_i contracts while the lower side of plate expands. And the length l'_i of the neutral axis displayed by a dotted line does not change. Therefore, heat is applied to point P_i until it becomes design shape (i.e., $l_i = l_{oi}$). And the necessary surface contraction by heating at each frame point required for correction processing is expressed as first formula. The value which serves as standard of the necessary thermal at each point of one frame line is computed using second formula (Sun, J.Y., JASNAOE2013).

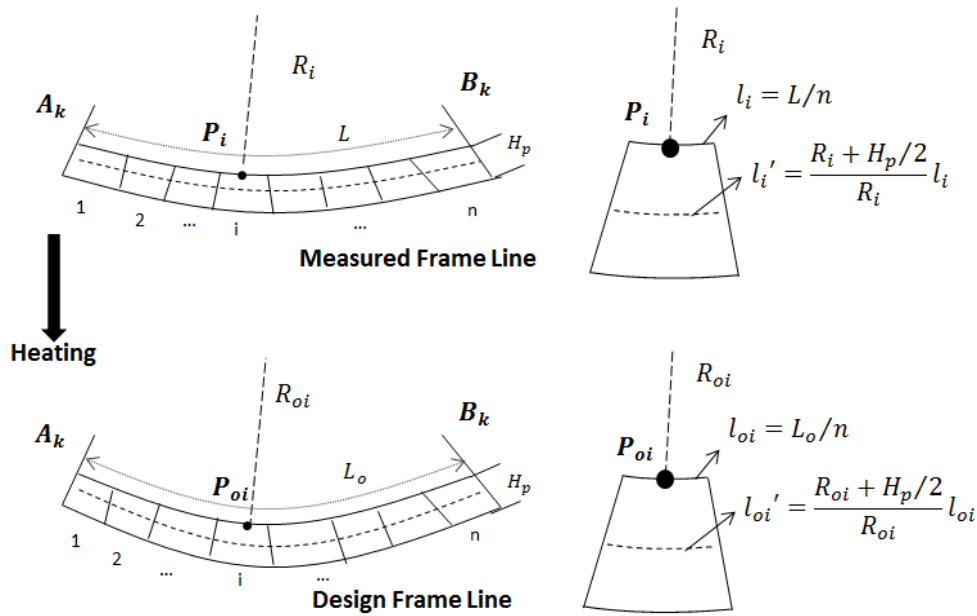


Figure 7-5 Curvature error definition (Sun, J.Y., IJASM, 2014)

$$\Delta l_i = l_i - l_{oi} = \frac{(R_i - R_{oi}) \times \frac{H_p}{2}}{R_i \times (R_{oi} + \frac{H_p}{2})} \times l_i \quad (1)$$

$$\mu = \frac{(R_i - R_{oi}) \times H_p / 2}{R_i \times (R_{oi} + H_p / 2)} > \varepsilon_{thresh} \quad (2)$$

At last, the heating line is located between the points with large curvature error of the adjacent frame lines (e.g. point $P_{k,i}$ and $P_{k+1,j}$ which has μ bigger than the threshold) according to Wang, Z. et al 2007.

7.1.2. Originalities for the practical usage in shipyard

In this research, as shown in Figure 7-2, the Virtual Template System (VTS) makes a lot of original improvements based on the prototype to satisfy the practical use in shipyard.

- ✓ Although the virtual template prototype provided the manual way to arrange the virtual templates to the right location on the measured plates. This manual process is too inefficient and inaccurate. This section proposes an automatic template arrangement and torsion evaluation method which dramatically reduces the template arrangement time of every manufacturing step.
- ✓ Another improvement is to provide heating areas with heating grades (heating time of each heating line) by using a float points-window for the curvature error calculating of each frame.
- ✓ During the registration process, applying ICP algorithm directly to the virtual templates and the measured point cloud may cause the wrong matching directions of the two data. Therefore, this section proposes a registration direction pre-setting method before applying the ICP registration method as introduced in Chapter 5.
- ✓ 2D roller lines' design data is mapped to the extracted plate for helping decide the heating lines. When importing the developed virtual template prototype to the shipyards, the workers found that applying heating along with the heating lines connecting the points with big curvature errors of the adjacent frames may destroy the torsion situation of the plate. Since the roller lines are designed along with the torsion of the curved shell plate, it is

effective to apply heating along with the roller lines to keep the right torsion. Therefore, this section matches the 2D roller lines onto the extracted plate's point cloud to help the workers design the right heating lines.

- ✓ A virtual template operation interface is developed to help the workers control the virtual templates as they used to do with the wooden templates and observe the automatically analyzed results more easily.

By achieving the items listed above, the Virtual Template System can meet the most practical requirements in shipyard.

7.2. Automatic template arrangement method

To produce a curved shell plate with exactly the same shape as design, not only is the curvature situation at each frame necessary, but the whole curved shell plate's torsion should also be taken into serious consideration (Araki, M. et al 1973). In other words, workers can always change their manufacturing plans due to the different situations with the torsion. The correlations between the torsion situation, the extent of curvature error, and the manufacturing plan designed by workers include a lot of tacit knowledge and habits according to Masaki, N. et al (1993).

To totally virtualize the manufacturing process of curved shell plates on computer, the arrangement of the templates which represents curved shell plate's torsion situation should be reproduced in virtual environment as well as the curvature error.

In the case of using real wooden templates, after several times of heating and cooling at each heating area, workers often start to care about whether or not the torsion goes the wrong way. They will rotate the virtual template to a proper position (where the rest parts of template have the minimum sum of distances from curved shell plate) on the frame, and check if the perspective sticks pass a same plane (perspective plane) as shown in Figure 7-6 (left). If the perspective sticks do not pass the perspective plane, it means that improper torsion exists. The improper torsion can be evaluated by checking the degrees of the angles between the perspective sticks. Also as shown in Figure 7-6 (right), the two templates are carefully put on the right location of the plate, then the workers check the angles

between the perspective stick of the virtual templates and the average perspective plane to check the torsion of the curved shell plates.

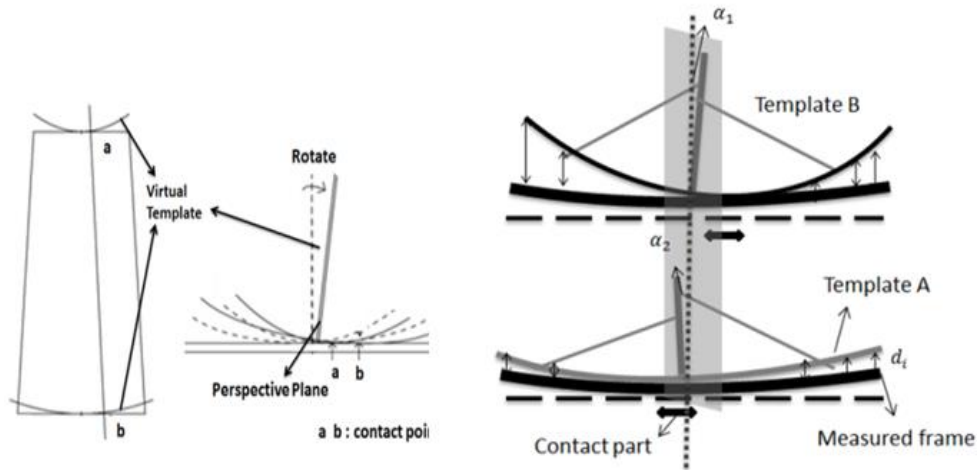


Figure 7-6 Torsion observation and evaluation (Sun, J.Y., IJASM, 2014)

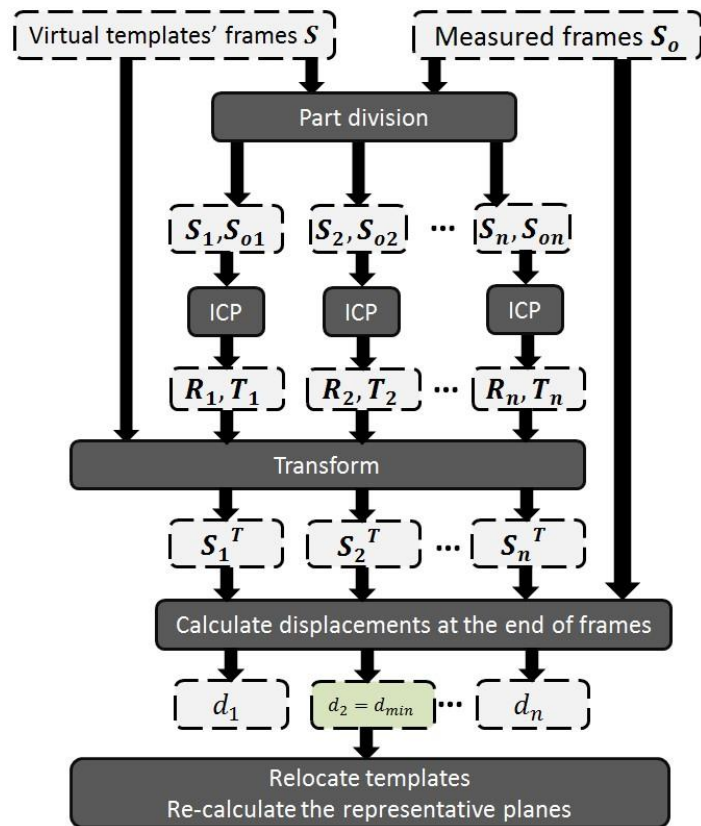


Figure 7-7 Automatic virtual template arrangement

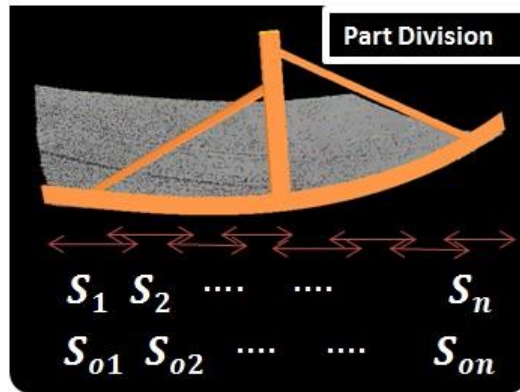


Figure 7-8 Part division of the virtual templates' frames and measured frames

This research developed a method to detect the torsion of the curved shell plates automatically which makes torsion evaluation and observation in virtual environment possible. As shown in Figure 7-7, firstly, virtual templates' bottom lines and the measured frames of curved shell plates are divided into n parts $\{S_1, S_2, \dots, S_n\}$ and $\{S_{01}, S_{02}, \dots, S_{0n}\}$ as shown in Figure 7-8. Then each part of the virtual templates is registered to the location of the corresponding part of the measured frame using ICP algorithm. The rotation matrixes $\{R_1, R_2, \dots, R_n\}$ and the transfer vectors $\{T_1, T_2, \dots, T_n\}$ used in ICP are also applied to the whole virtual template S . Therefore, the virtual templates can be rotated freely on the measured frames by applying the following transformed frames $\{S^T_1, S^T_2, \dots, S^T_n\}$.

Every template is rotated on the frame until the sum of every part's distance d_i between the measured frame and the virtual template's bottom line reaches a minimum. Then the angles α_i between the curved shell plate's sticks and the reconstructed perspective plane are computed and outputted to make the torsion situation clear. Also the distances between them and the upper plane are computed to check the heating situation in a portrait direction. Therefore, these necessary data for the manufacturing plan's design can be reproduced in the virtual environment in an easily understandable way.

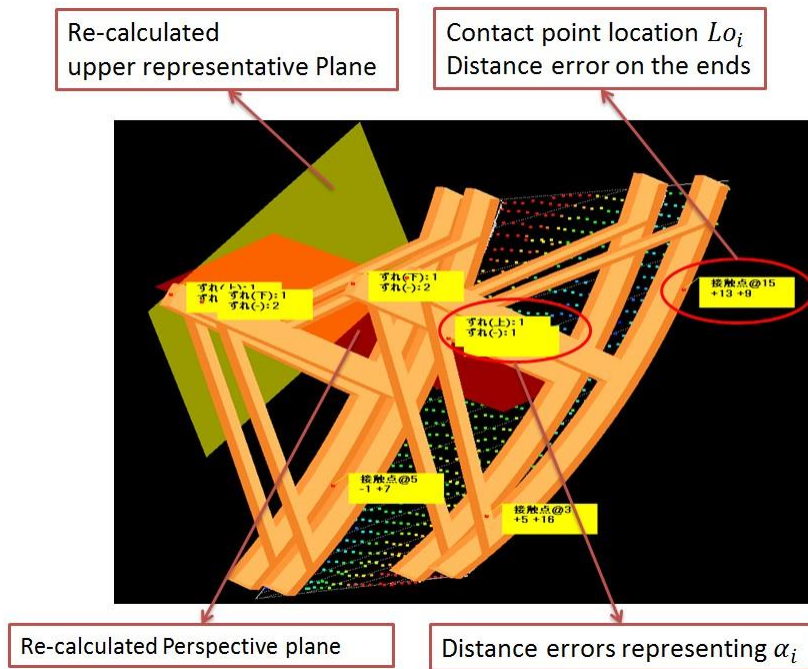


Figure 7-9 Torsion detection result

As shown in Figure 7-9, after the virtual templates are automatically arranged to the right locations on the frames of the curved shell plate, the detected location (contact point between virtual templates and plate's point cloud) is shown in the yellow message box with a yellow line connected to the location. Also, the distance errors on the frame's ends between virtual templates and plate are displayed in the same message box. The upper representative plane and the perspective plane are re-calculated based on the relocated virtual templates. The distances between the end points of the virtual templates' perspective stick and these two planes are displayed in the view too to help the workers grasp the torsion situation of the curved shell plate.

7.3. Curvature error based heating grade suggesting

The virtual template prototype only provides the heating positions of every manufacturing step; this section provides not only the positions but also the heating grades by considering both the degree and distribution of the curvature errors.

A float points-window for calculating the curvature errors is applied. Every

measured frame point's curvature error is calculated and given a normalized value. Then the color map with one dimensional color gradation is outputted. The color map helps workers to get an intuitive idea of the curvature error's degree by displaying the curvature errors in the gradation way. The mean μ and standard deviation σ are calculated, the one-dimensional gradation is implemented as that the points around μ are displayed in green, the points having the value over $\mu + \sigma$ are always displayed as red, and the points having the value under $\mu - \sigma$ are displayed as blue.

The output is as shown in Figure 7-10. The workers are suggested to apply heating on the upper side of the curved shell plate with more time and temperature at the locations with large red area, and to apply heating on the underside of the curved shell plate with more time and higher temperature at the locations with large blue area. And if there are too many red or blue areas, the larger ones are going to be modified first.

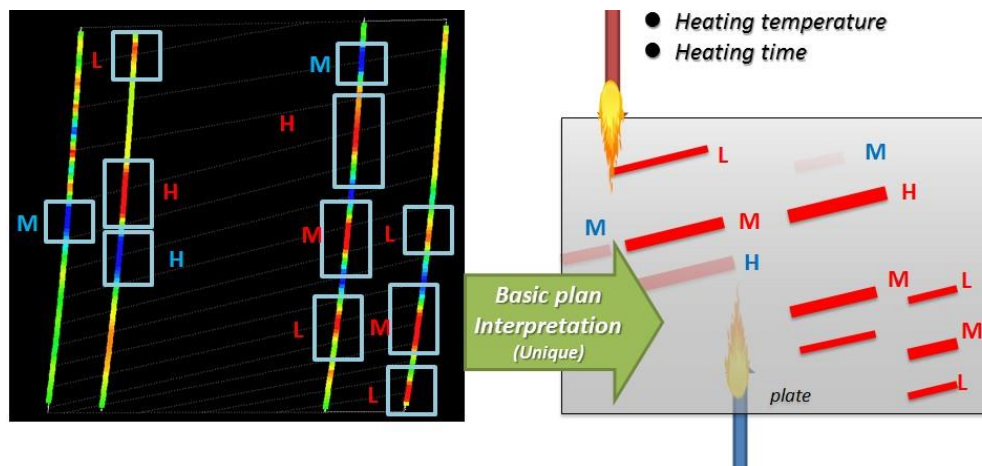


Figure 7-10 Curvature error based heating grade suggesting

7.4. Development of VTS

7.4.1. 2D roller line's matching with 3D design data

When innovating the developed virtual template prototype to the shipyards, the

workers found that applying heating along with the heating lines connecting the points with big curvature errors of the adjacent frames (Sun 2013) may destroy the torsion situation of the plate, and pointed out that to avoid this, the heating should be applied along with the roller lines because the roller lines are designed along with the torsion of the curved shell plate. However, unlike the frame design data, the roller line design data is in 2D dimension due to the design convention of the ship. They are usually stored in the DXF files as shown in Figure 7-11.

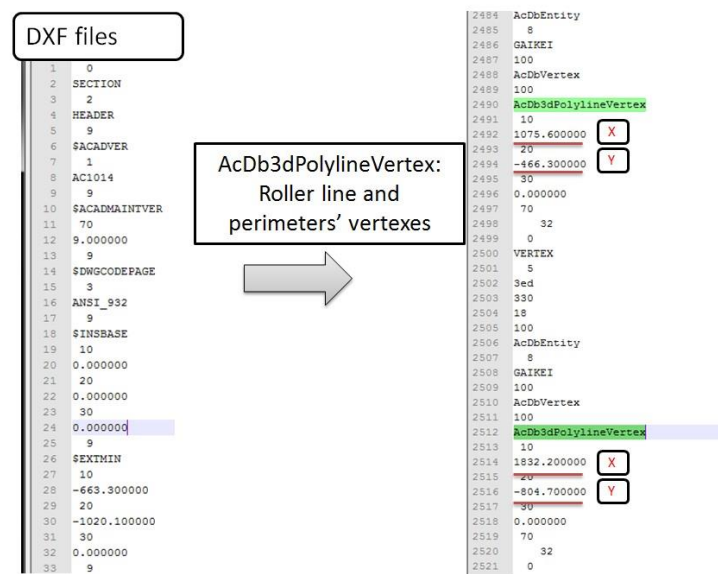


Figure 7-11 Roller lines and perimeters' vertexes information in DXF ship design file

Therefore, this research matches the 2D roller lines onto the 3D frame design data to help the workers design the right heating lines along with the 3D roller lines.

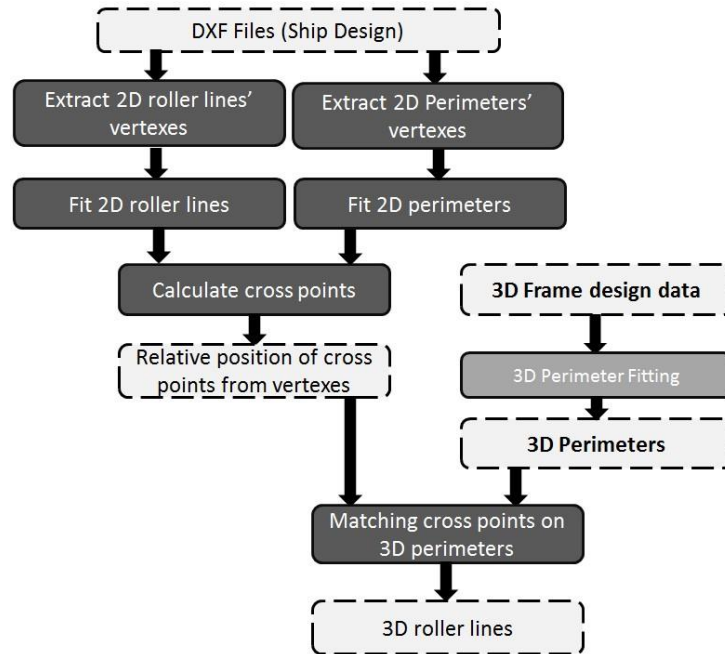


Figure 7-12 2D roller line’s matching with 3D frame design data

As shown in Figure 7-12, firstly, the 2D roller lines and 2D perimeters’ vertexes are extracted from the DXF ship design files, and then 2D roller lines and 2D perimeters are fitted as shown in Figure 7-13.

The cross points are calculated as shown in Figure 7-14. To match each 2D perimeter to the corresponding 3D perimeter, the length of each perimeter is calculated $\{d_1^{2D}, \dots, d_4^{2D}\}$, $\{d_1^{3D}, \dots, d_4^{3D}\}$. The 2D roller lines are matched with the 3D frames as shown in Figure 7-15.

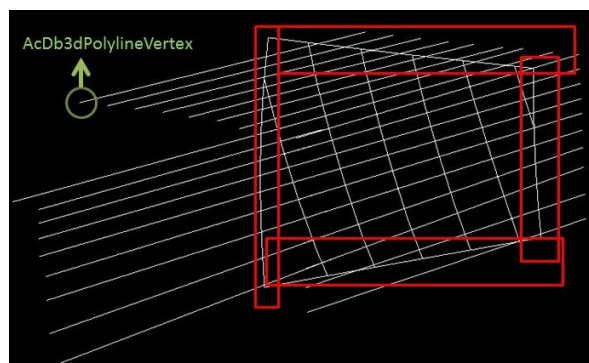


Figure 7-13 2D roller lines and 2D perimeters

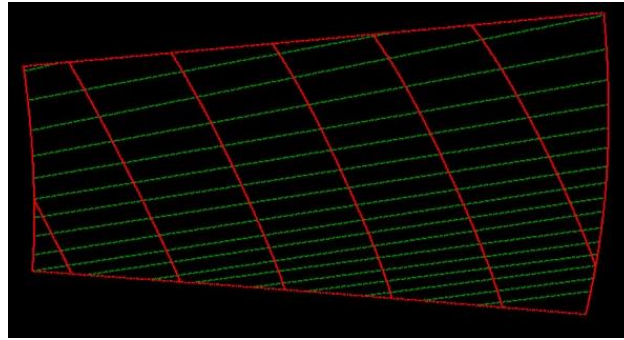


Figure 7-14 Cross points of 2D roller lines and 2D perimeters

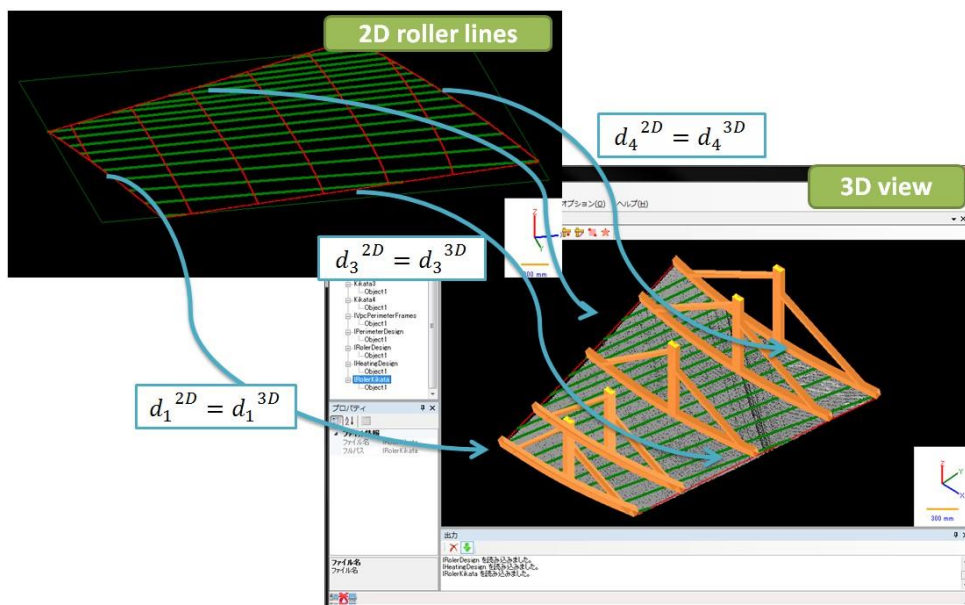


Figure 7-15 Match 2D roller lines with 3D frame lines

7.4.2. User interface of VTS

In this research, a user interface specially designed for the workers in shipyard to operate and observe the virtual templates in 3D environment is developed as shown in Figure 7-16.

There are mainly 3 functions of this user interface:

- Rotate the virtual templates
- Switch visible/invisible status of each virtual template
- Display the parameters of the curved shell plate in real time

By clicking on the side stick of each virtual template, the virtual template can be

rotated a little at once. By clicking on the perspective stick of each virtual template, it can be changed from visible to invisible (half transparent) or in contrary from invisible to visible.

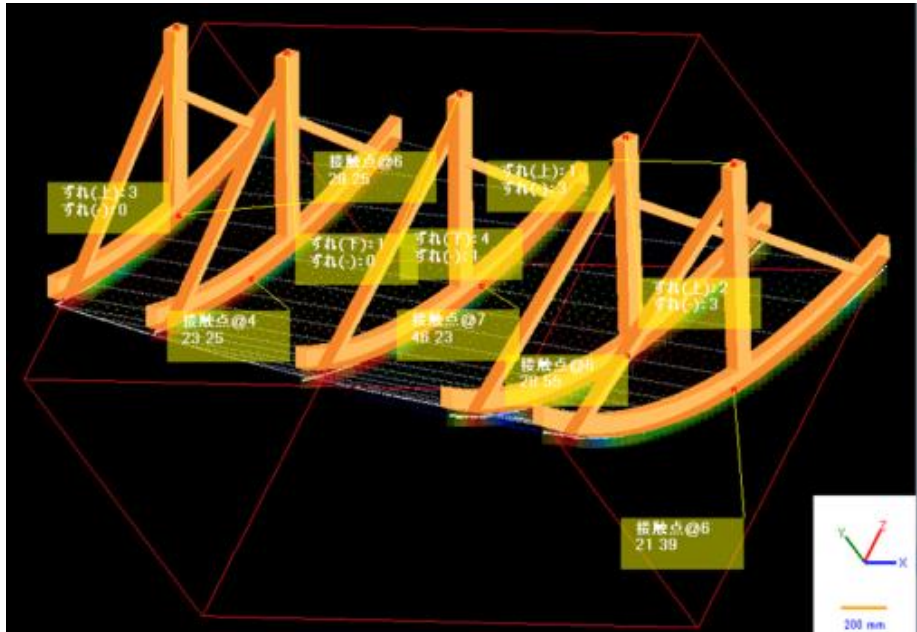


Figure 7-16 Virtual templates' operation interface

Because “click” is a mouse (or track ball) operation, it only has 2D property (X and Y). The virtual templates exist in the 3D environment, thus the cursor's location should be translated into 3D environment with a depth Z property. And since the virtual templates are drawn on computer in the form of polygon, the “click” depth judgement follows the following algorithm:

- a. For every click, the area of the triangles S_{ABO} , S_{ACO} , S_{CBO} , S_{ADO} shown in Figure 7-17.
- b. If $S_{ABO} + S_{ACO} + S_{CBO} + S_{ADO} = S_{ABCD}$, the cursor is considered as float on the polygon.
- c. If multiple polygons are judged clicked, the distances d from the projection point of the cursor and the 3D view camera's position are calculated. The polygon with the smallest d is chosen.

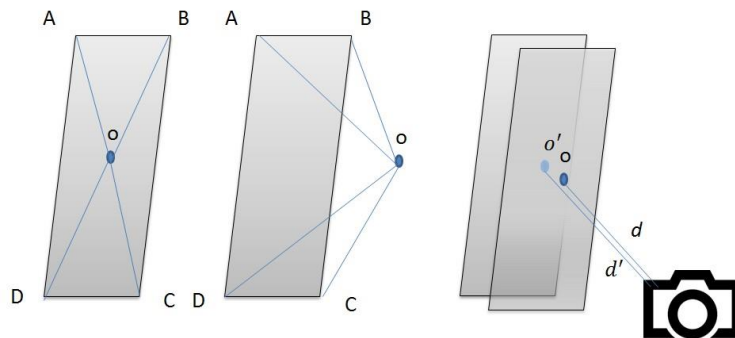


Figure 7-17 Cursor position judgement

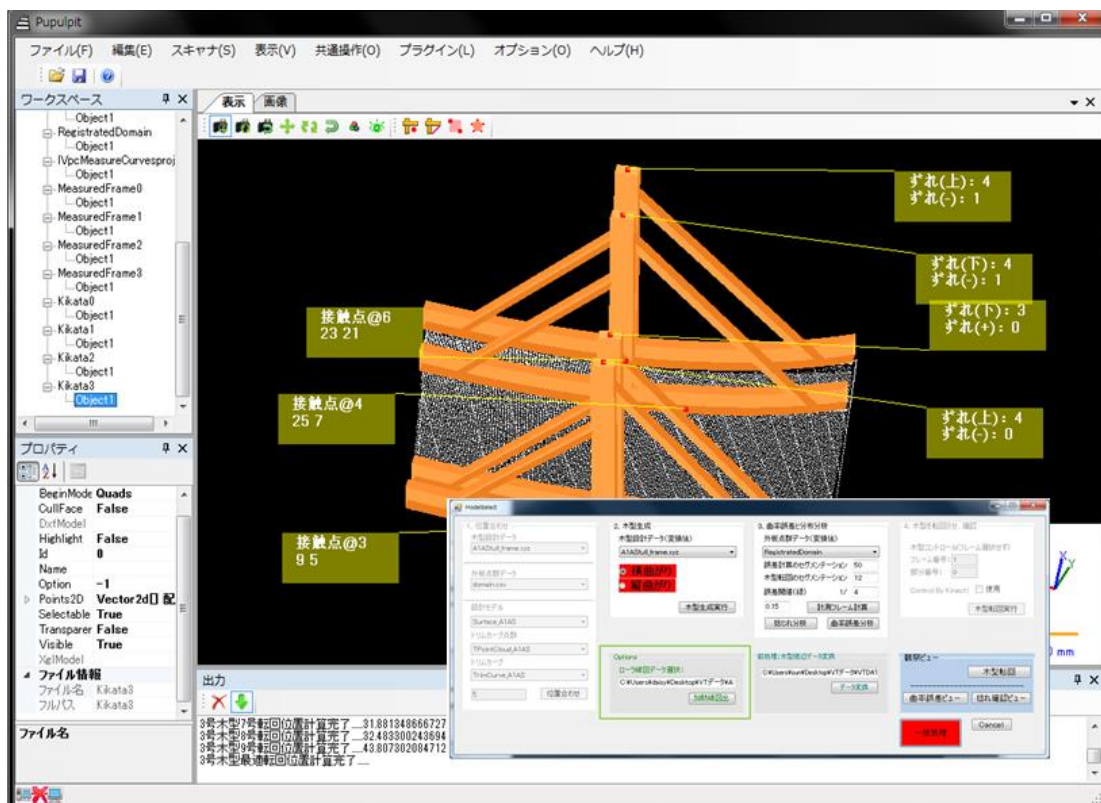


Figure 7-18 User interface of VTS

Figure 7-18 shows the user interface of the developed virtual template system. There are 4 steps' panels and 1 view selection panel and 2 option preparation panels which can be executed from this interface.

The 4 steps' panels are as below:

1. The registration of the design data and extracted measured data

- Frame line design PCD
 - Extracted measured plate's PCD
 - Design model
 - Trim perimeter
 - Coordinate lines
 - Threshold of the registration
2. The generation of the virtual templates
 - Frame line design PCD
 - Vertical direction (direction of the virtual template generation)
 - Horizontal direction (direction of the virtual template generation)
 3. The curvature error and torsion calculation
 - Registered measured plate
 - Segments' count of the frame when calculate the curvature
 - Segments' count of the frame when rotate the template
 - Threshold of the errors
 - Torsion calculation button
 - Curvature error calculation button
 4. The virtual template's rotation and confirmation
 - Target virtual template No
 - Target frame segment No
 - Whether to control by Kinect

The 1 view selection panel contains buttons as below:

- Virtual template keyboard rotation mode selection button
- Curvature error view selection button
- Torsion view selection button

The 2 option preparation panels are as below:

- Roller line converting button (2D DXF to 3D roller line PCD)
- Frame line converting button (DAT to 3D frame line PCD)

Beside the two views, the workers can also check the displacement error of the plate (the displacement between the design data and the measured data) in the form of histograms. As shown in the following figure, the displacement errors are

displayed in two ways: one with absolute error threshold (5mm and 10 mm), the other one with the threshold of the standard deviation. The workers can have an intuitive image about the plate's displacement grade and the error deviation after each manufacturing step.

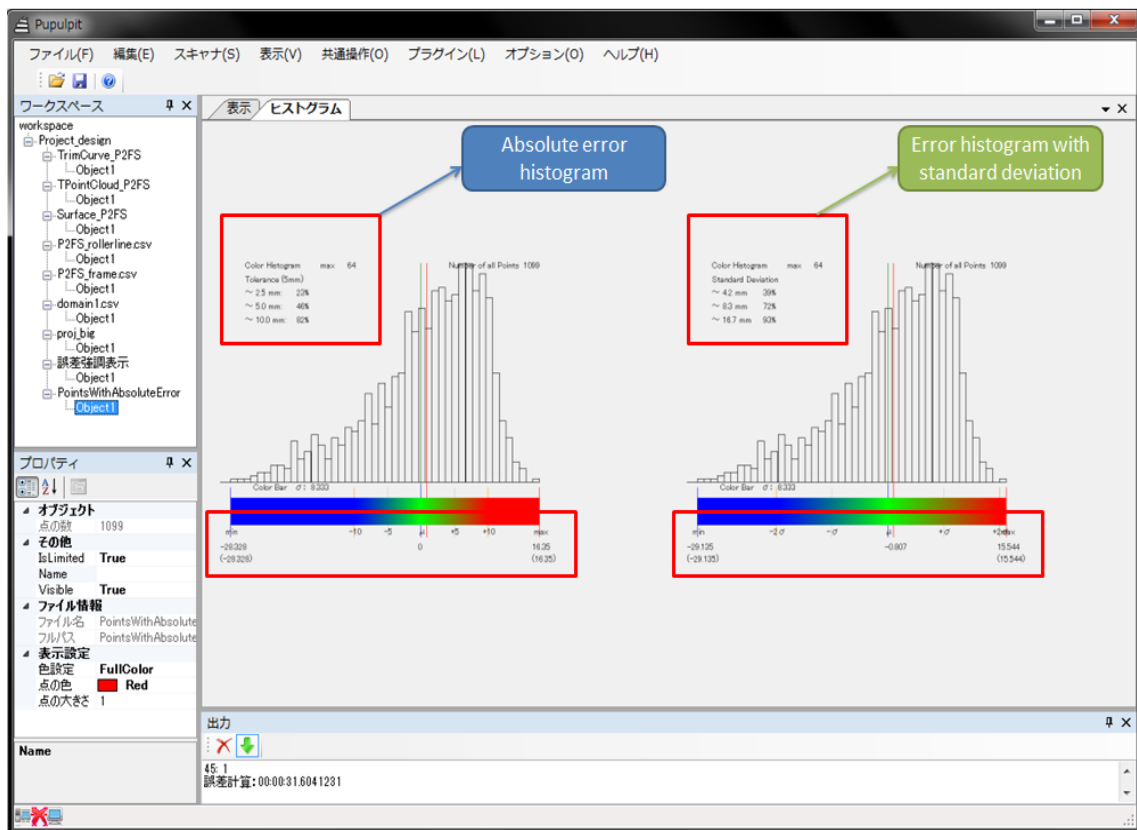


Figure 7-19 Displacement evaluation histograms

7.5. Summary

In this chapter, the overview of the virtual template system is introduced at first. The prototype is introduced firstly. Then the improvements made based on the prototype are illustrated. With direction pre-setting, the registration between the virtual templates and the measured plates are more effective and with lower failure. The automatic template arrangement and torsion detection save a lot of time and effort of the workers who used to do the template arranging manually. The heating lines with not only locations but also grades are suggested by implementing the

gradation color map of the curvature errors. To help the workers match the right position of each heating lines onto the real plate and design the heating line along with the roller lines, the 2D design roller lines are automatically matched with the 3D frame design data. At last, a new virtual templates' operation user interface is developed for the workers to operate the 3D environment more smoothly.

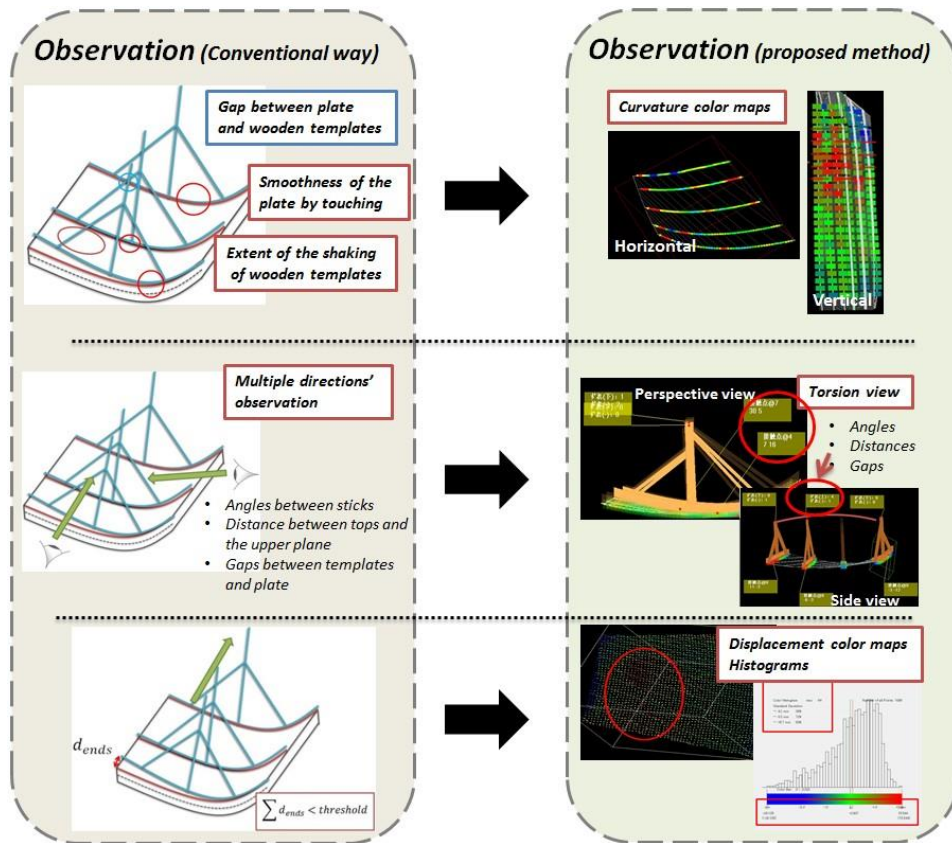


Figure 7-20 Generated interfaces for observation during the manufacturing

By achieving the items mentioned above, the virtual template system meets most of the conditions in the shipyard's practical way to use, and as shown in Figure 7-20, the necessary parameters used in the manufacturing convention can all be observed on system instead of using the wooden templates.

Chapter 8 Knowledge elicitation and dissemination

8.1. Overview of the manufacturing knowledge management

A major problem in the curved shell plates' manufacturing is that the design of the manufacturing plan heavily depends on the implicit knowledge, habits and experience of the workers. As shown in Figure 8-1, the judgement of the decision about how to manufacture the plate in the next step based on the observation results is conducted by the workers individually. Therefore, manufacturing plans varies according to the knowledge and skills of the craftsman who is in charge of the plate even for the same design shape. In other words, the current practice highly depends on the individuals and there is a risk to lose the knowledge and skills at the time of their retirement. Also to avoid inaccurate distorted output shapes and troubles in the subsequent heat sealing process, the tacit knowledge and skills for bending plates must be elicited, shared and reused in daily operation.

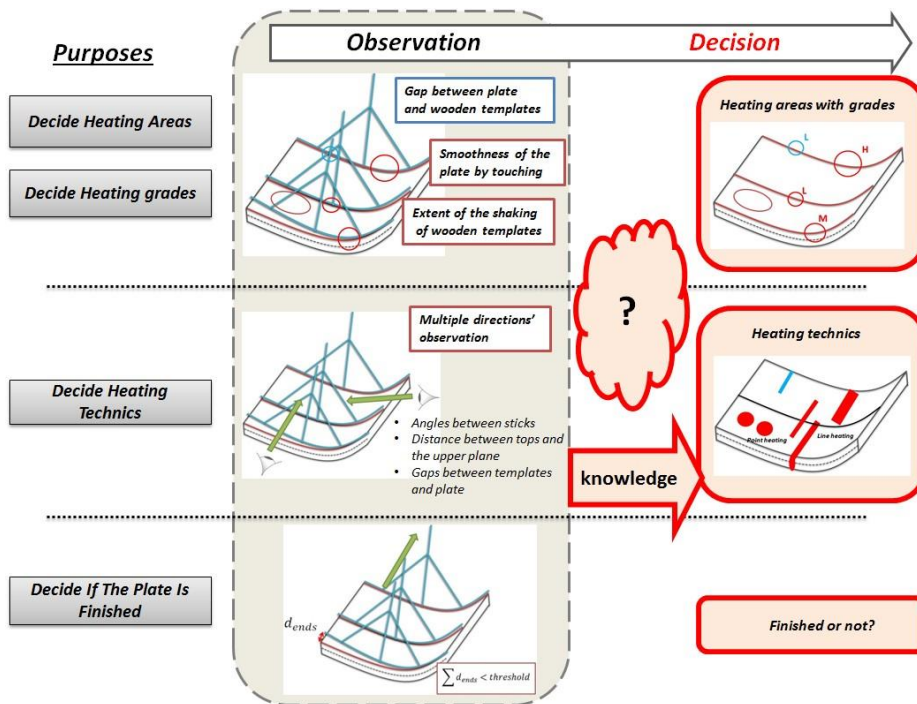


Figure 8-1 Convention of deciding manufacturing plans

As shown in Figure 8-2, this chapter proposes a knowledge-based approach to capture the knowledge and skills for the curved shell plate's manufacturing process based on the recorded 3D manufacturing scenarios and the interviews conducted in shipyard. The knowledge is articulated in NRDR (Nested Ripple Down Rules) tree format and a computer system is developed for facilitating the captured knowledge for reuse. The whole system is on the basis of the software system VTS (Virtual Template System) introduced in the prior chapter which can virtualize the manufacturing process and automatically suggest manufacturing plans.

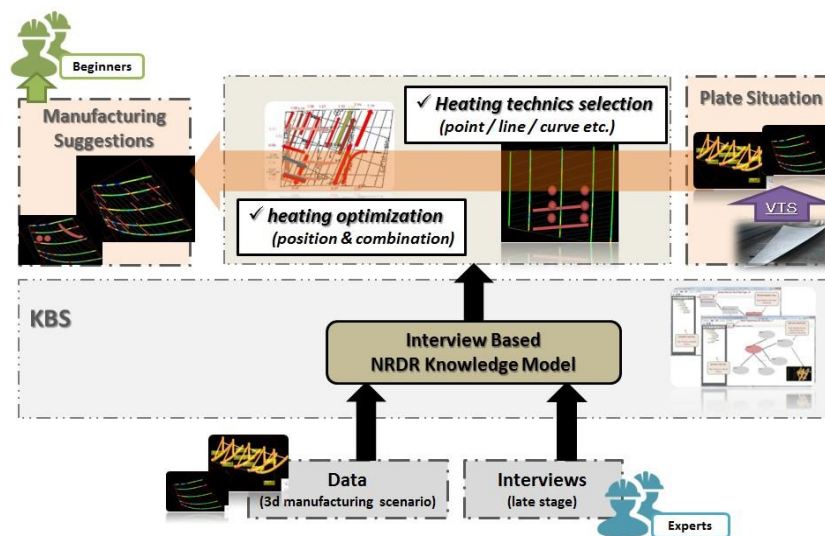


Figure 8-2 Knowledge elicitation and dissemination for manufacturing suggestions

Because the workers always design some different manufacturing plans under some specific situations rather than just considering the curvature differences between the design data and the measured shape which the software mentioned above uses, an interactive system has been designed that incorporates a four faceted knowledge-based framework to provide beginning workers with the capability to quickly design a manufacturing plan about all aspects of the design process as the expert workers. These facets are as follows:

- (1) VTS (Virtual Template System) introduced in the prior chapter generates and record the information from the virtualized manufacturing process including

the curved shell plates' curvature information, torsion information, and the system's suggested basic manufacturing plan.

(2) Raw Knowledge Interrelated Database executes the process of capturing information. In this process, expert analyzes the information and screen out that can lead better insights into the expert workers' opinion.

(3) Knowledge Base software system implements the Nested Ripple-Down Rules to deal with the issues which lead to the special manufacturing plan design (not the system's suggested basic ones). The knowledge are stored and virtualized as rules in this framework.

(4) Knowledge Elicitation analyzes the correlations between the parameters describing the curved shell plate's situations and the relevant manufacturing plans designed by the expert workers, and then translates them into the rules; Knowledge Dissemination provides the relevant instructional rule from the KB based on the automated measurement of the curved shell plate's situation.

The system which integrates the proposed approaches above is evaluated by conducting a series of experiments in the shipyard. The knowledge such as how to manufacture the curved shell plate considering multiple parameters of the plate in one time is elicited by evaluating a couple of parameters' combinations. The tacit knowledge existent in the curved shell plate's different situations during the manufacturing process is proved to be effectively elicited, represented and disseminated.

The overview of the framework which implemented the proposed approach is illustrated in Figure 8-3. The raw knowledge interrelated database captures information from the virtualized manufacturing process including the curved shell plates' curvature information, torsion information, and the system's suggested manufacturing plan from the system VTS from the prior study. The knowledge base system stores and virtualizes the knowledge. To condense the size of RDRs, Nested Ripple Down Rule Trees (NRDR) which is a concept hierarchy using RDR is implemented. A rule-based knowledge which contains a set of validated rules classified by the curved shell plate's situation is constructed. Besides, the rules are visualized to help the workers understand the knowledge.

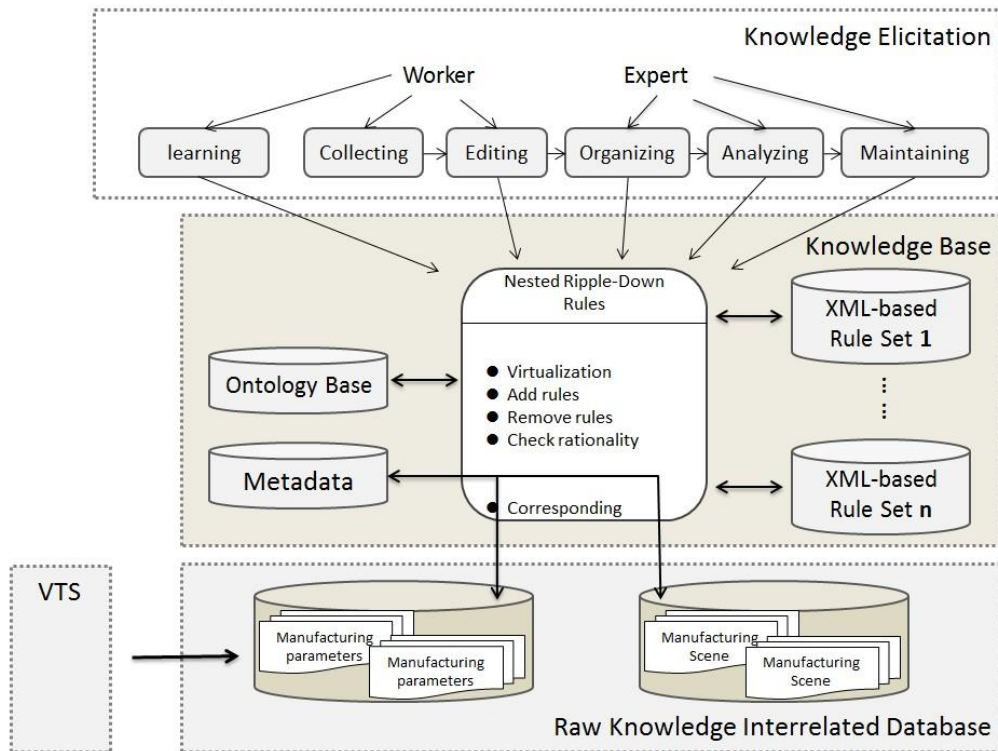


Figure 8-3 Overview of NRDR interview-based knowledge model (Sun, J.Y, ISPE, 2014)

During the knowledge elicitation process, certain correlations between the parameters describing the curved shell plate’s situations and the relevant manufacturing plans designed by the expert workers are elicited and captured into a set of rules. Firstly, workers compare the two manufacturing plans: the system’s suggested plan (basic line heating) and the plan they actually used. If these two plans are not completely the same, interviews are conducted to explain the differences by considering the plate’s parameters. Based on the result of the interview, new rules are added as the captured knowledge.

During the knowledge dissemination process, depending on the curved shell plate’s situation, the framework can give manufacturing samples and diagnosis dealt before. Firstly, after the plate’s measuring of each manufacturing step, whether the VTS system’s suggested basic manufacturing plan can be used or not are evaluated by the worker. If not, the following manufacturing decision should follow the rules’ tree from the constructed knowledge base until the most proper diagnosis is found.

8.2. Raw knowledge interrelated database

As shown in Figure 8-3, the Raw Knowledge Interrelated Database consists of two main kinds of data screened out from the VTS (Virtual Template System): (1) Manufacturing Parameters such as the angles between the virtual templates' sticks and the distance between the virtual templates' bottom lines and the curved shell plate; (2) Manufacturing Scene which is a screenshot of the virtualized template and curved shell plate. These data and scenes screenshot of manufacturing can ensure the following knowledge base construction and knowledge elicitation to be efficiently carried out no matter during or after the manufacturing. The information about the basic manufacturing manual without considering the curved shell plate's situation is stored as the ontology database. And the manufacturing parameters and screenshots are given metadata attributes in each rule's xml file and could be searched from the knowledge base interface.

8.3. Knowledge base design

Mostly there are multiple parameters describing the curved shell plate's situation used to design the next manufacturing plan at a time. With the plain RDRs, the parameters can only be considered one by one which will clearly cause the data redundancy and make the knowledge base intricate to be used. Therefore, the knowledge base software system in this work chooses the NRDR (Nested Ripple Down Rule Trees) which can efficiently represent the knowledge existing in the manufacturing while having a relatively condensed reasonable tree size. The system uses NRDR to define a conceptual hierarchy. With the proper combination of the parameters' values, the system ensures the expert can introduce his/her own vocabulary to express him/herself more naturally. As the example shown in Figure 8-4, the NRDR can condense the size of natural RDRs mentioned in the Chapter 3 as the same concept defined by a lower order RDR tree (C3) may be used multiple times in higher order trees (where the Rule 3.33 is). Also the diagnosis which represents the experts decision is executed after each rule is reached.

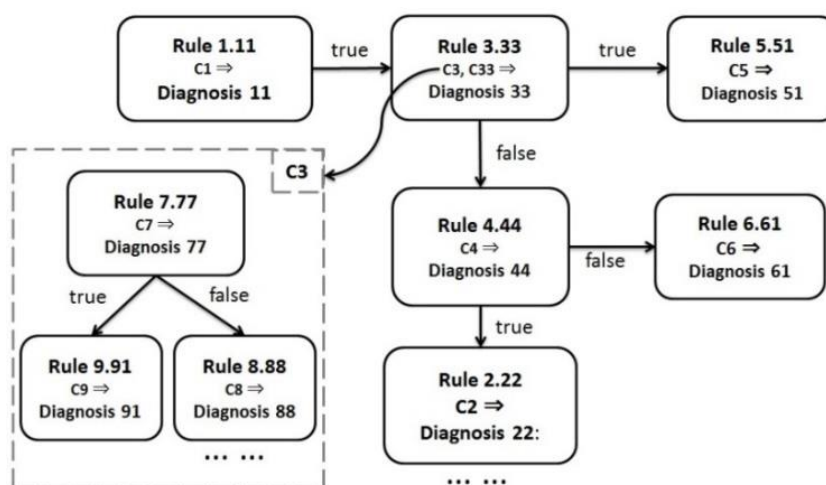


Figure 8-4 Nested Ripple Down Rule Trees (Sun, J.Y, ISPE, 2014)

As shown in Figure 8-4, the data structure is similar to a decision tree. Each node has a rule, the format of this rule is "IF cond1 AND cond2 AND ... AND condN THEN conclusion". Cond1 is a condition (Boolean evaluation), for example "the max distance D from virtual templates' bottom line and the curved shell template > 5mm", which could also be written in "isGreater(D,5)". Each node has exactly two output nodes; these output nodes are connected to another node or another decision tree such as C3 in Figure 8-4 by "TRUE" or "FALSE".

8.4. Knowledge elicitation process

Differences between the manufacturing plan suggested by the existing KB system and the manufacturing plan actually used by workers exist. In order to extract the tacit knowledge during the manufacturing process, interview investigation about these differences in different cases was conducted. The knowledge during the manufacturing process is elicited and disseminated based on the database and system introduced in 8.2 and 8.3.

During the knowledge elicitation, as shown in Figure 8-5, the human expert's knowledge is acquired based on the current context and is added incrementally into a binary decision tree in the format of a set of independent rules (if .. elsif rules). In

the NRDRs framework, the added rules could be a plain rule or contain the other rule's reference. In other words, NRDR adds new rules containing or not containing other rule's reference when the existing ones cannot satisfy the situation of current context. The knowledge elicitation process is as following.

- i. Firstly, Figure 8-5 (upper) is the original description of the knowledge we know before this knowledge elicitation step. The plate is measured and analyzed using VTS system and the knowledge related data (the parameters and manufacturing scenes) are stored in the database introduced before.
- ii. Then interviews are conducted when the VTS's suggested plan cannot be used directly and the existing rule set cannot give a reasonable diagnosis based on the current plate's situation. A new rule (Rule 10.101) is added into the tree.
- iii. As shown in this figure, some different rules (the Rule 7.77 9.91 and 8.88) are the same patterns which need to be considered and processed before the new Rule 10.101 is analyzed to be necessary.
- iv. A new lower level rules' tree C3 is created and reused in both Rule 3.33 and Rule 10.101. The same process repeated in the following elicitation.

For the second step, the current plate's situation is all output in the proposed interfaces as shown in Figure 8-6. The curvature maps replace the hand-drawing heating areas decided by shake the wooden templates on the plate. The torsion view with virtual templates gives the parameters which were observed by human eyes. By reading these information, the workers can grasp the main situation of the plates, and substitute them into the existing rule base and find out if it is necessary to add some new rules to make it be able to output the manufacturing plans which the workers consider as the most proper ones based on the plate's situation.

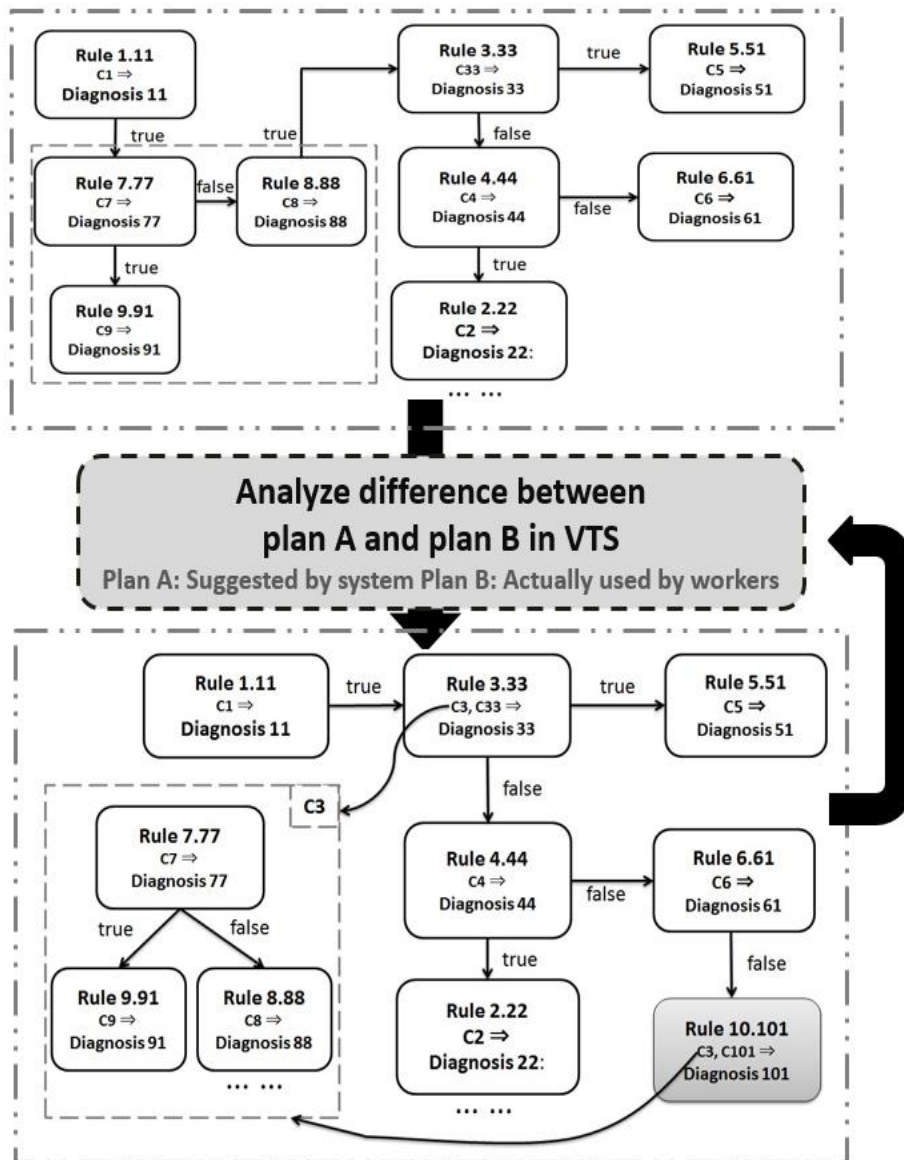


Figure 8-5 Knowledge Elicitation using Nested Ripple-Down Rules (Sun, J.Y, ISPE, 2014)

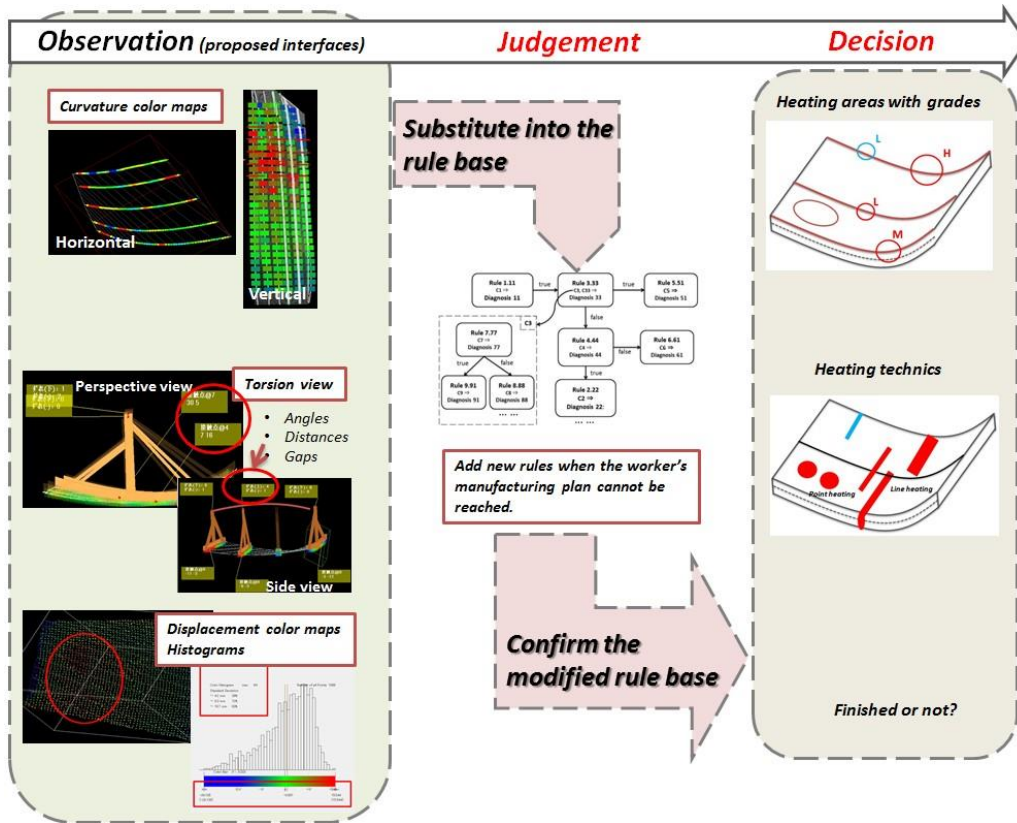


Figure 8-6 Rule base modification based on observation of the interfaces

8.5. Knowledge dissemination process

During the knowledge dissemination, depending on the curved shell plate's situation, the framework can give manufacturing samples (the right diagnosis) dealt before. The knowledge dissemination process is as following.

- i. Firstly, after the plate's measuring of each manufacturing step, whether the VTS system's suggested basic manufacturing plan (The heating lines connecting the red areas) can be used or not are evaluated by the worker.
- ii. If not, the worker starts to search the right diagnosis following the rules' tree constructed during the knowledge elicitation based on the plate's parameters stored in the raw knowledge interrelated database. As show in the Figure above, the diagnosis 101 is reached when the judgments of Rule 1.11, Rule3.33, Rule 4.44 and Rule 6.61are TRUE, FALSE, FALSE and

FALSE.

- iii. Before the diagnosis 101 is carried out, the child tree C3 which contains the pre-checking rules (the Rule 7.77 9.91 and 8.88) should be checked and executed first.

The rule's structure used in this research is as below:

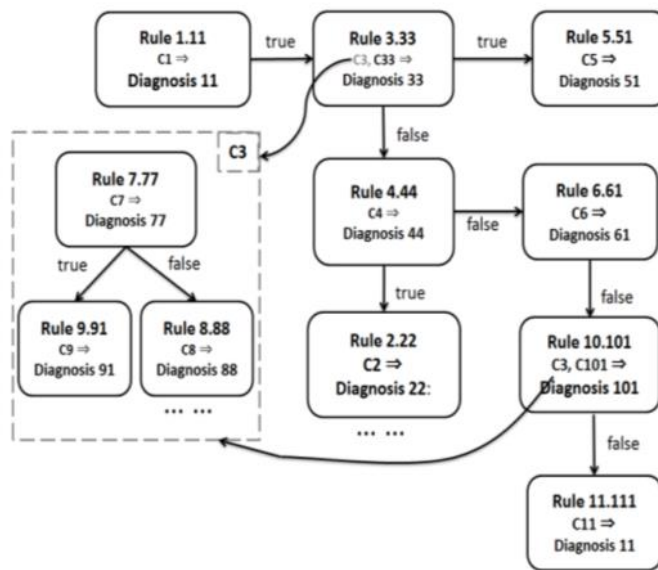


Figure 8-7Nested ripple down rule base (Sun, J.Y, ISPE2014)

8.6. Development of KBS

As shown in Figure 8-8, physically the Knowledge Base in this system is stored as some xml-based rules' sets; the overview of the rules relations are represent in the Rules Relation View as shown in Figure 8-9 (upper) while each rule's details are read from the metadata file and displayed in the Rule's Detail View as shown in Figure 8-9(lower). Each rule's details and the relations between rules are displayed, adjusted, modified or deleted in these visible views. Besides, by clicking the items in the Rules' Tree View, the corresponding rule's detail is displayed in the view to facilitating the knowledge obtaining during the curved shell plate's manufacturing process.

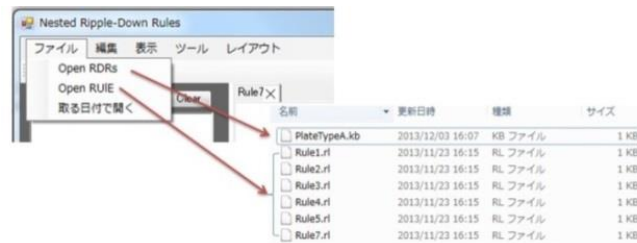


Figure 8-8 The Xml-based Rule Sets (Sun, J.Y, ISPE, 2014)

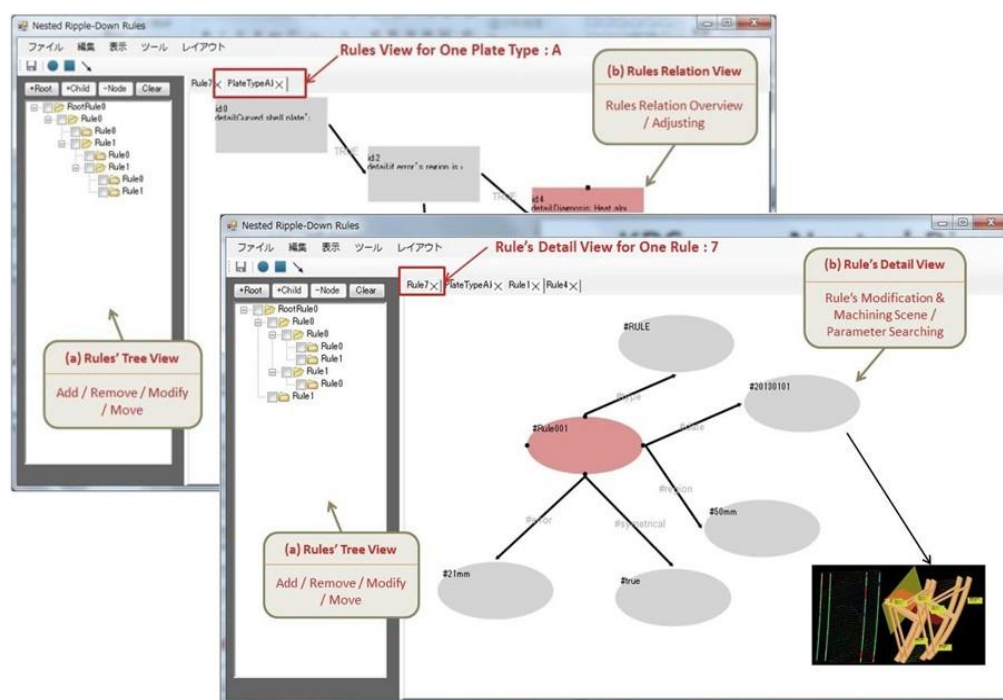


Figure 8-9 Rules Relation View and Rule's Detail View (Sun, J.Y, ISPE, 2014)

8.7. Summary

In this chapter, the problems existing in the process of extracting the knowledge by interviews are introduced. To well model the extracted knowledge by interviews, an interview-based knowledge model is constructed using Nested Ripple Down Rules. Analysis for knowledge elicitation is conducted through the interviews with expert workers when the system-suggested manufacturing plans (heating areas) are found different from that actually used by workers. The parameters used in the

knowledge elicitation are provided in the virtualized environment instead of using the real wooden templates.

For the usage of the knowledge based system, the workers can get the common manufacturing guidelines such like which kind of the heating technics (point heating, curve heating, or straight line heating) to use from the interview-based NRDR knowledge model.

PART III EVALUATION

PART III EVALUATION	168
Chapter 9 Evaluation of common pre-processing	172
9.1 Overview	172
9.1 Experiment configuration.....	173
9.2 Evaluation of component extraction.....	174
9.2.1.1. Extraction of the plates which are divided by wooden templates	176
9.2.1.2. Extraction of the plates which are divided by worker's shadow	177
9.2.1.3. Extraction of the plates which are divided by wires and hoses.....	178
9.2.1.4. Extraction of the plates which are divided by water and other obstacles	179
9.2.1.5. Relationship between the section curves and the data.....	180
9.2.2. Weighted region growing evaluation	181
9.2.3. Extraction effectiveness and efficiency analysis	182
9.3 Evaluation of component registration	183
9.3.1. Comparison of the proposed method and the general methods	183
9.3.2. Registration of the plate' point cloud with defects	184
9.3.2.1. Registration of plate with small defects.....	185
9.3.2.2. Registration of plate with big defects.....	186
9.4 Summary.....	188
Chapter 10 Cold forming support experiment	190
10.1. Overview of cold forming support experiment	190
10.2. Experiment design	192
10.3. Experiment configuration in shipyard	194
10.4. Experiment 1 : Plate "Regular 1".....	199
10.4.1. Plate measurement.....	199
10.4.2. Press Evaluation Result	200
10.4.2.1. Plate 1.....	201
10.4.2.2. Plate 2.....	203
10.4.3. Perimeter Evaluation Result.....	204
10.5. Experiment 2 : Plate "Large 1"	205
10.5.1. Plate measurement.....	205
10.5.2. Press Evaluation Result	206

10.5.2.1.	1 st scan	207
10.5.2.2.	2 nd scan	207
10.5.3.	Perimeter Evaluation Result.....	208
10.6.	Summary	209
Chapter 11	Heating forming support experiment	211
11.1.	Overview of heating forming support experiment	211
11.2.	Experiment design	213
11.3.	Experiment configuration in shipyard	213
11.4.	Design data used in the experiment.....	223
11.5.	Preliminary experiment.....	224
11.5.1.	Curved shell plate extraction	224
11.5.2.	Evaluation results' comparison of one single processing step	225
11.6.	Experiment 1 : Plate "Bowl 1"	228
11.6.1.	Objective	228
11.6.2.	Design data reforming and loading.....	228
11.6.3.	Analysis results for one manufacturing step	231
11.6.3.1.	Plate measurement	231
11.6.3.2.	Plate analysis	233
11.6.3.3.	Manufacturing plan design and manufacturing.....	234
11.6.4.	Manufacturing plans for all the steps.....	236
11.6.5.	Manufacturing results.....	237
11.7.	Experiment 2 : Plate "Bowl 2"	241
11.7.1.	Objective	241
11.7.2.	Design data reforming and loading.....	241
11.7.3.	Analysis results for one manufacturing step	243
11.7.3.1.	Plate measurement	243
11.7.3.2.	Plate analysis	245
11.7.3.3.	Manufacturing plan design and manufacturing.....	246
11.7.4.	Manufacturing plans for all the steps.....	248
11.7.5.	Manufacturing results.....	249
11.8.	Experiment 3 : Plate "Hybrid 1"	254
11.8.1.	Objective	254

11.8.2.	Design data reforming and loading.....	255
11.8.3.	Analysis results for one manufacturing step	257
11.8.3.1.	Plate measurement	257
11.8.3.2.	Plate analysis	258
11.8.3.3.	Manufacturing plan and manufacturing results of this step	260
11.8.4.	Manufacturing plans for all the steps	262
11.8.5.	Manufacturing results	263
11.9.	Summary	268
Chapter 12	Evaluation of knowledge elicitation and dissemination	271
12.1.	Overview of knowledge based system evaluation	271
12.2.	Line heating analysis with curvature error view.....	271
12.2.1.	Original rule base	272
12.2.2.	Knowledge elicitation process and results	273
12.3.	Complicated heating technic analysis with torsion evaluation view	276
12.3.1.	Plate analysis.....	276
12.3.2.	Elicited rules	277
12.3.3.	Elicited rules' adaption	279
12.4.	Knowledge model with different views.....	280
12.4.1.	Usage of knowledge model with curvature evaluation view.....	280
12.4.2.	Usage of knowledge model with torsion evaluation view	282
12.5.	Views for different observation purposes	287
12.6.	Summary	289

Chapter 9 Evaluation of common pre-processing

9.1 Overview

While efficiently evaluating the accuracy of the ship component has been considered important for many years as a necessary part of planning and control of production in shipbuilding, using point cloud data scanned by noncontact 3D laser scanner has only recently been taken into consideration (Biskup et al., 2007) . Most of the existing point cloud processing algorithms cannot be applied directly to the applications in shipbuilding. As discussed in Chapter 5, two vital problems exist here.

(a) The part of the component cannot be extracted efficiently due to irregular obstacles endogenous to manufacturing workshops and their shadows divide the component's measured point cloud data into several separated domains. Manual extraction and integration of these separated domains waste a lot of time and is a barrier for practical application. The well-known methods for calculating smooth surfaces from noisy point cloud such as moving least squares (MLS) projection (Pauly et al., 2002) has the same problem that the whole component cannot be extracted at one time when the component is separated by the obstacles' shadows.

(b) Some general algorithms are used to conduct the registration between the measured point cloud data and the design data. Due to the features of these registration algorithms such as the ICP algorithm, without a clear registration direction presetting which is usually done manually, the registration of the two data sets could go in the wrong direction and lead to improper registration results.

As a result, existing point cloud processing methods (the basic region growing method and general registration method) can rarely satisfy the accuracy evaluation target in shipbuilding without significant improvements and appropriate combination.

This thesis presented a reformative component extraction method solving problem (a) and a reformative component registration method in Chapter 5 solving problem (b) for the component's accuracy evaluation in shipbuilding. First, k-d tree construction is performed on the scanned point cloud data to fasten the neighbor

searching of each point. To extract the continuous domain of the component from the point cloud data, a region growing method is performed on every neighbor point of the seed point. Then the neighbor domain, which is separated by obstacles' shadows or water from the extracted domain, is recognized by conducting curved surface fitting and b-spline curved line fitting at each edge point of the extracted domain. The whole component can be extracted by repeating the above steps. Before registering the extracted point cloud data of the component and the designed data, proper registration direction is decided by performing registration direction analysis on the two kinds of data. And then, ICP (Iterative Closest Point) is applied for the following registration.

In this chapter, the effectiveness and efficiency of the proposed improvements on the component extraction and component registration are evaluated. A set of experiments are conducted in the shipyard to evaluate the performance of the point cloud processing methods proposed above.

9.1 Experiment configuration

About 200 curved shell plates are measured, extracted, registered and evaluated after plastically deformed. In these experiments, laser scanner Faro Focus 3D is used. The features of the server and the scanner used are as shown in the table below:

Table 9.1 Server features

<i>items</i>	<i>values</i>
CPU	Inter(R) Core(TM) i7 CPU L 640 @ 2.13GHz 2.13GHz
OS	Windows 7 64bit
Memory	8.00 GB
Hardware	SSD 128 GB

Table 9.2 Faro Focus 3D

<i>items</i>	<i>values</i>
Range Focus3D	0.6 – 120m
Measurement speed	up to 976,000 points/second
Ranging error	± 2mm
Integr. colour camera	Up to 70 mio. pixel
Laser class	Laser class 1
Weight	5,2kg
Multi-Sensor	GPS, Compass, Height Sensor, Dual Axis Compensator
Size	240 x 200 x 100mm
Scanner control	via touchscreen display and WLAN

The scanner parameters set in this experiment are summarized as below:

Table 9.3 Scanner parameter setting

<i>items</i>	<i>values</i>
Horizontal angle range	97° ~ 201°
Vertical angle range	-64° ~ -17°
Resolution	1/10 ~ 1/8
Speed	122 kpt/sec

9.2 Evaluation of component extraction

As shown in Figure 9-1, over 62% of the measured 203 plates are separated by different kinds of obstacles. Even after the whole support framework is introduced into the shipyard and the wooden template is replaced by the virtual template, the separation by the workers' shadows (10%), the water, cords and hoses (16%) could still happen. In this sub-section, the comparison of the proposed methods and the manual extraction, and the relationship between the extraction parameters and the

plates' conditions will be discussed.

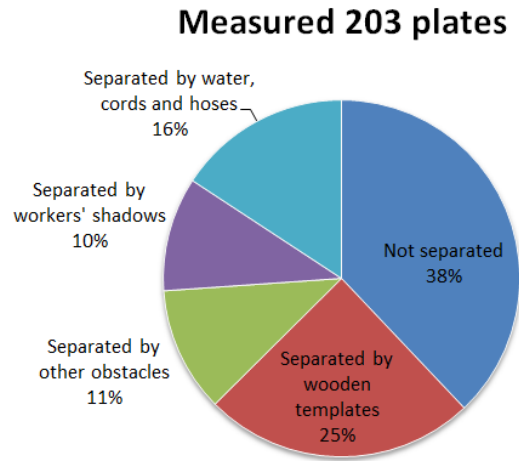


Figure 9-1 Plate conditions in the shipyard

And the parameters used in MS system following the parameter setting rules introduced in Chapter 5 are as below:

Table 9.4 Parameter setting of the MS system

<i>items</i>	<i>values</i>
<i>Count of neighbor points used in the region growing</i>	35
<i>The value h used to calculate the weighted plane (the Gaussian's attenuation degree)</i>	40mm
<i>The threshold of the similarity of the normal vectors</i>	0.996
<i>The b_{thresh} in 5.3</i>	0.74
<i>Whether to calculate the normal vectors following candidate selection</i>	TRUE
<i>The limit of the region growing times</i>	1000
<i>Whether to recognize the separated domains</i>	TRUE
<i>The threshold of the sum of all Y_j^i in 5.5</i>	10
<i>Whether to display the progress of the separated domain recognition</i>	FALSE
<i>The start seed point of the region growing method</i>	Random

9.2.1.1. Extraction of the plates which are divided by wooden templates

Three experiments about component extraction are given in Figure 9-2. The plates are measured with high solution. The Comparison between the manual method and new presented method is summarized in Table 9.5. Detail discussions are made in the following sub-sections.

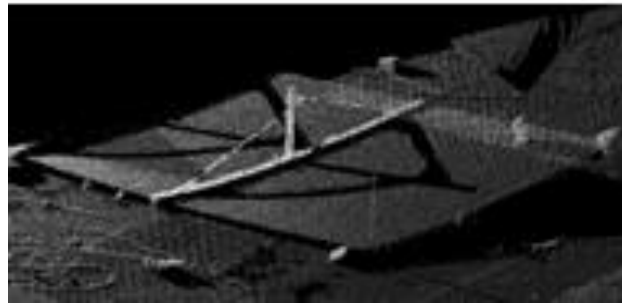


Figure 9-2 Curved shell plate extraction results separated by domains

Table 9.5 Automatic extraction

<i>Plate Size (perimeter)</i>	<i>Points</i>	<i>Component Divided into (domains)</i>	<i>Manually/ Automatically</i>	<i>Extraction (with candidate selection)</i>	<i>Extraction (without candidate selection)</i>
3.4m × 2.6m	1.34 million (from 3.64 million)	7	Auto	143	12m37s
				[183 times growing]	[368 times growing]
				1.35 million normal vectors	3.64 million normal vectors

As shown in Figure 9-2, the curved shell plate is measured with some wooden templates on it. It has about 1.34 million points, and is divided into multiple domains due to the shadows of the wooden templates. Only one single point is selected previously, then according to the curved surface fitting and the B-Spline line fitting (shown as white lines in the figure), the multiple domains are recognized automatically. The time used for extraction in this case is only about 143 seconds.

For all of these experiments, the extraction with candidate selection (5.3) and the

extraction with random candidate selection (general region growing) are compared.

As shown in Table 9.5, the extraction time with candidate selection is obviously reduced to at least 1/10 from the one with random candidate. The reason can be considered as following:

- a. The growing times (growing recursion levels) are reduced. For these three experiments, the growing times all decreased which means the selected candidate is more effective than the random candidates.
- b. The normal vectors' calculation time is reduced. For the plain region growing method, the normal vectors of all of the points including the obstacles are calculated; while for the proposed extraction method with candidate selection, the normal vectors' calculation is only conducted to the points around the selected candidates. Such like experiment (a), because the obstacles existing in the measured point cloud contains over 3 million points, the proposed method saved over 8 minutes on normal vectors' calculation.

The following sub-section will introduce some summarized extraction results of the plates which are divided by the other kinds of obstacles or the shadows of obstacles. And then the relationship between the common domain recognition standards' setting and the features of the measured point cloud will be discussed.

9.2.1.2. Extraction of the plates which are divided by worker's shadow

As shown in Figure 9-3, sometimes plates' point clouds are divided by workers' shadows. Here 5 different plates are extracted successfully from these point clouds. They are all larger than 4 meters \times 2 meters. The details of the extraction results and the plates' point clouds are as shown in Table 9.6. All of the plates are extracted successfully within 2 minutes.

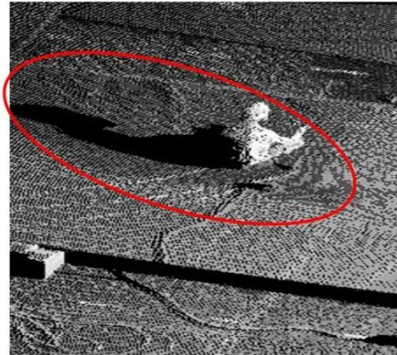


Figure 9-3 Plate's point cloud divided by worker's shadow

Table 9.6 Extraction results for plates divided by worker' shadows

<i>Plate No.</i>	<i>Points (with obstacles)</i>	<i>Points (only plate)</i>	<i>Component Divided into</i>	<i>Max gap between domains (mm)</i>	<i>Effective curve length (mm)</i>	<i>Execution Time (seconds)</i>
1	1,530,000	180,000	2	489	1000	39
2	2,130,000	290,000	2	570	1000	43
3	2,300,000	300,000	4	662	1000	57
4	1,350,000	180,000	3	695	1000	55
5	970,000	170,000	7 (with other obstacles)	592	1000	37

9.2.1.3. Extraction of the plates which are divided by wires and hoses

As shown in Figure 9-4, sometimes plates' point clouds are divided by wires and hoses. Here 5 different plates are extracted successfully from these point clouds. They are all larger than 10 meters \times 2 meters. The details of the extraction results and the plates' point clouds are as shown in Table 9.7. For the plates which are divided into relatively less domains are extracted within 70 seconds.

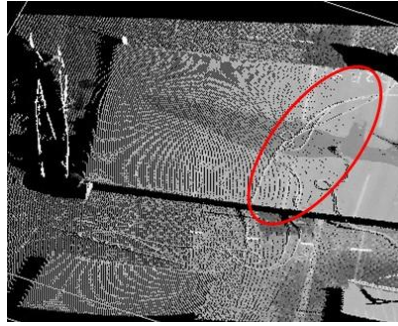


Figure 9-4 Plate's point cloud divided by wires and hoses

Table 9.7 Extraction results for plates divided by wires and hoses

<i>Plate No.</i>	<i>Points (with obstacles)</i>	<i>Points (only plate)</i>	<i>Component Divided into</i>	<i>Max gap between domains (mm)</i>	<i>Effective curve length (mm)</i>	<i>Execution Time (seconds)</i>
1	1,340,000	310,000	5	210	400	57
2	1,670,000	200,000	6	136	200	37
3	1,120,000	270,000	3	177	400	32

9.2.1.4. Extraction of the plates which are divided by water and other obstacles

As shown in Figure 9-5, sometimes plates' point clouds are divided by wires and hoses. Here 5 different plates are extracted successfully from these point clouds. They are all longer than 10 meters and wider than 1.5 meter. The details of the extraction results and the plates' point clouds are as shown in Table 9.8.

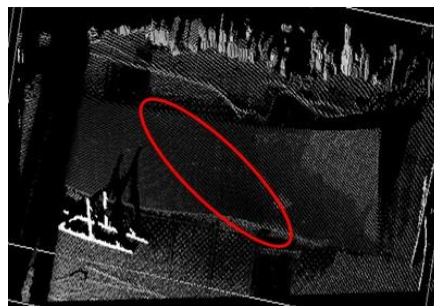


Figure 9-5 Plate's point cloud divided by water

Table 9.8 Extraction results for plates divided by water

<i>Plate No.</i>	<i>Points (with obstacles)</i>	<i>Points (only plate)</i>	<i>Component Divided into</i>	<i>Max gap between domains (mm)</i>	<i>Effective curve length (mm)</i>	<i>Execution Time (seconds)</i>
1	1,740,000	200,000	4	280	400	43
2	1,770,000	180,000	7	699	1000	58
3	1,180,000	190,000	3	378	400	41

9.2.1.5. Relationship between the section curves and the data

As shown in the tables summarized above, the fact that the effective curve lengths for the common domain recognition is in accordance with the gaps between the separated domains. For the gaps from the workers' shadows, the plates are usually divided into 2 or 3 domains, but the gaps between the domains are relatively large. Although it partly depends on the irradiation angles of the laser scanner, the average gap for this kind of data is over 500mm. For this kind of data, the section curve used to do the common domain recognition is usually 1000mm.

For the gaps from the wooden templates and their shadows, the plates are usually divided into at least 3 domains. This kind of data covers over 30% of the measured data. The deviation of the gaps existing in this kind of data is bigger than the other data, ranging from 100mm to 500mm. System uses common domain recognition section curves with the length 400mm and 1000mm to cover this deviation.

For the small gaps from the wires, water hoses and gas burner's cords which exist in more than 20% of the measured data, the effective common domain recognition curves are usually 200mm or 400mm.

At last, not only can curved shell plates be extracted from the measured point cloud using the proposed algorithm, other components, such as the panel or the block's lateral surface (over 10,000,000 points) can use this method.

9.2.2. Weighted region growing evaluation

The plate shown in Figure 9-6 is partly covered by some water which has not been dried completely. Due to the varying reflectivity of the laser from these areas, the densities of the points vary incoherently (points' intervals from 5mm to 25mm). The experiment using region growing method (not weighted) and the proposed weighted region growing method is conducted towards this kind of data.

The result in Table 9.9 shows that the extraction without using the weighted region growing causes serious data defects which can be observed in the figure; while the extraction using the weighted region growing maintains the plate's integrity by successfully extracting all of the points belonging to the plate.

In this case, the defects shown in Figure 9-6 happen on the frame line which means the measured frame line fitted using the extraction result (a) cannot represent the real situation of the plate here. And obvious defects can be observed on the perimeters in the red circle which could cause the inaccuracy perimeter evaluation results.

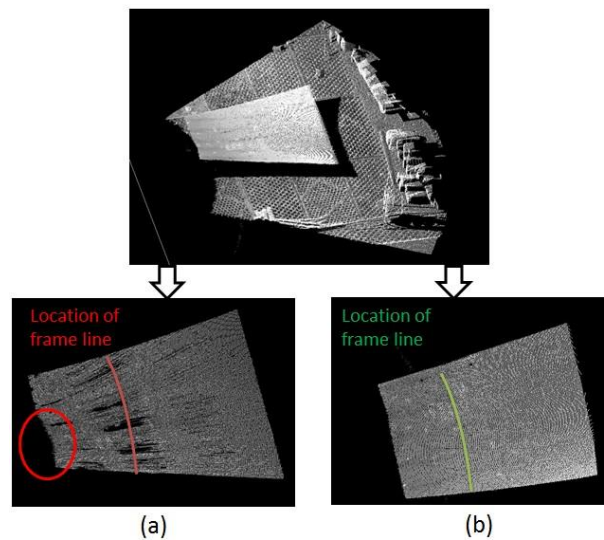
The figure consists of three main parts. At the top is a 3D point cloud visualization of a rectangular plate, showing its surface texture and some irregularities. Two white arrows point downwards from this 3D view to two 2D panels below. Panel (a) on the left shows a 2D point cloud of the plate. A red line is drawn across the plate, labeled 'Location of frame line'. A red circle is drawn around a portion of the left edge, indicating a defect or irregularity in the perimeter. Panel (b) on the right shows the same 2D point cloud. A green line is drawn across the plate, also labeled 'Location of frame line'. The perimeter of the plate in panel (b) appears much smoother and more regular than in panel (a).

Figure 9-6 Panel extraction result (a) region growing (b) weighted region growing

181

Table 9.9 Comparison of the extracted result with an without weighted region growing

	<i>Measured point cloud</i>	<i>Extraction result (a)</i>	<i>Extraction result (b)</i>
Points	359,529	129,306	160,930
Data Integrity	----	Defects found on frame and perimeter	Good

9.2.3. Extraction effectiveness and efficiency analysis

Analysis about the extraction effectiveness and efficiency is conduct under the following three different conditions.

(A) When the plate is separated into over 10 separated domains

There are over 10 plates belonging to this group in the totally 200 plates. For this kind of plates, despite the total points' count, it consumes over 120 seconds (max 200 seconds) to extract these plates. The average extraction time is 103 seconds which is relatively long comparing to the other kinds of data. However, since the gaps are relatively regular, over 90% of the separated domains are extracted successfully only except some small domains of 10 to 100 points.

(B) When the points in the measured point cloud is over two million

There are 7 plates falling into this group (over two million points with obstacles). For this kind of plates, it cost about 100 seconds to 180 seconds to extract these plates. These plates are always with relatively high density but are rarely separated by the obstacles. Thus almost all of the points belonging to the plate can still be extracted within 3 minutes. However, from these plates, it can be seen that the extraction time increases along with the points' count of the plates.

(C) When the obstacles are irregular and multiple

The plates fall into this group when the difference between the largest gap and the smallest gap is over 200mm. For this kind of plates, the extraction speed doesn't

change so much from (B), but a considerable number of the small domains cannot be extracted. The plates in this group are usually required to be scanned again.

9.3 Evaluation of component registration

This sub-section evaluates the registration of the measured plates in 9.2, the comparison of the proposed method and the general methods, evaluation of the registration of the plates with different levels of defects will be conducted.

9.3.1. Comparison of the proposed method and the general methods

A curved shell plate's registration example is given below to illustrate how the proposed component registration method in 5.6 works. As shown in Figure 9-7 (1), the measured point cloud of the curved shell plate and the design data are displayed on the computer. It can be seen that originally they have totally different positions and need to be registered. The results are summarized in Table 9.10.

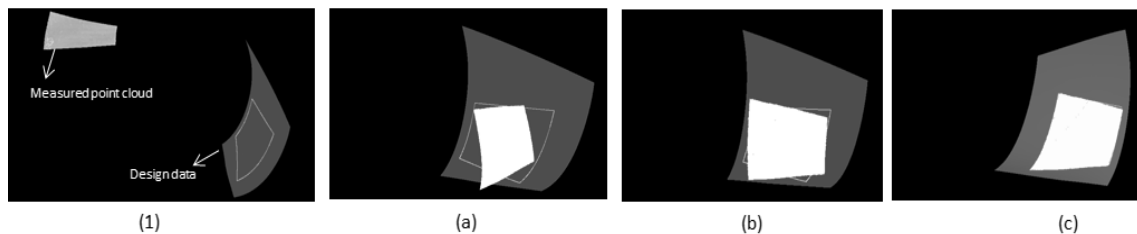


Figure 9-7 Curved shell plate registration results. (1) Measured point cloud and design data (a) Parallel registration (b) registration without direction presetting (c) registration with direction presetting

Result (a). Parallel transformation using only the 3D coordinate of the center of gravity and the PCA axes is performed at first. Figure 9-7 (a) shows the transformation result of this step. As shown in Table 9.10, the displacements detected are over 1 meter, and the overlap of the design data and measured data is obviously in a wrong direction

Result (b). Figure 9-7 (b) shows the result of conducting the ICP algorithm directly from the position in result (a) without direction pre-setting. It turns out

that the registration went into an inverse direction. Obviously, result (b) cannot satisfy the following component evaluation processing due to the large displacement. The max displacement is even over 300mm, and the ICP cost over 5 minutes but not converged.

Result (c). Multiple ways of registration direction are tested before the ICP algorithm is performed. The registration direction with the least displacement is chosen to do the direction pre-setting for the ICP algorithm. As shown in Figure 9-7 (c), with registration direction test and presetting, the registration result goes exactly the right way, and turns out to be capable for the following processing because ICP converged after 42 times of converging, and the differences of ICP converging errors (the sum of the squares of all the points' displacements) between the last two times of converging is 3mm which is smaller than the threshold 5mm. Besides, the standard deviation of the displacements is 3.5mm showing the relatively good quality of the measured plate.

Table 9.10 Comparison between general methods (a) (b) and new presented method

(c)

	<i>ICP Converging Times</i>	<i>ICP Error Converging</i>	<i>Max Displacement (+)</i>	<i>Max Displacement (-)</i>	<i>Standard deviation</i>	<i>Execution Time</i>
(a)	---	---	+1200mm	-1032mm	---	4s
(b)	1000	Not converged	+317mm	-284mm	175mm	5m43s
(c)	42	3mm	+21mm	-12mm	3.5mm	30s

9.3.2. Registration of the plate' point cloud with defects

As introduced before, due to the special conditions in the shipyard, a considerable number of plates are measured with obstacles. Therefore, there are a lot of defects existing in these data. For most of this kind of data in which the defects are found on the areas which have little influence on the evaluation results, the system still try to do the registration of the measured data with defects and the design surface.

In this sub-section, the registration of the measured plate with defect and the design surface will be evaluated from the following aspects:

- a. Can the area with big displacement errors be detected or not.
- b. Is the max displacement acceptable or not.
- c. Is the standard deviation of the displacement acceptable or not.

Two plates are measured twice with and without defect respectively. And the above three evaluation points are summarized at the end.

9.3.2.1. Registration of plate with small defects

Plate A is measured twice and registered with the design surface. As shown in Figure 9-8, measured point cloud A-2 has some defects on the right side, while point cloud A-1 has points covering all over the plate. The defect rate is calculated using the formula below:

$$R_{defect} = \frac{N_{integrity} - N_{defect}}{N_{integrity}} \quad (1)$$

Here $N_{integrity}$ is the number of the points in the point cloud without defect, while N_{defect} is the number of the points in the point cloud with defects. R_{defect} of point cloud A-2 is 10.3% which is relatively small in the 200 measured plates' point clouds.

The registration result is virtualized by the color maps in which the points with the displacement smaller than 5mm are all displayed in green color. The blue and red areas are with displacement bigger than 5mm. As shown in the Figure 9-8, the blue areas of these two point clouds in the green circles are both detected successfully as the areas with big displacement errors.

Since the defects in A-2 happens at the green area comparing from the result of A-1, the histograms of the displacement from the design surface have no big difference between A-1 and A-2.

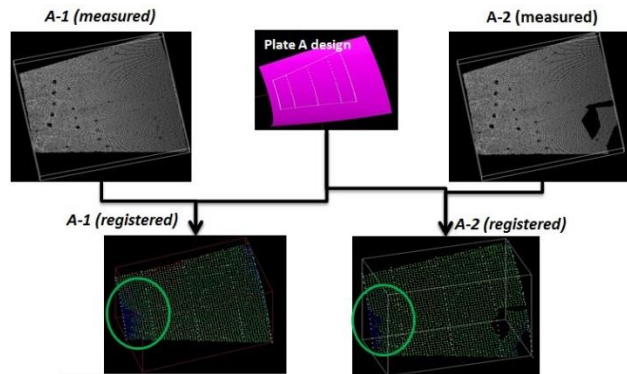


Figure 9-8 Registration result for plate A (defect rate 10.3%)

Table 9.11 Registration results of the plate A with and without defect

<i>Plate</i>	<i>Points On Plate</i>	<i>ICP Converging Times</i>	<i>ICP Error Converging</i>	<i>Max Displacement (+)</i>	<i>Max Displacement (-)</i>	<i>Standard Deviation</i>	<i>Execution Time</i>
(A-1)	57,807	42	2mm	+24mm	-11mm	3.6mm	50s
(A-2)	51,808	35	2mm	+31mm	-9mm	3.4mm	48s

The registration results of the plate A with and without defects are summarized in Table 9.11. The differences of ICP converging errors (the sum of the squares of all the points' displacements) between the last two times of converging are 2mm, which means that both of these two point clouds are registered well with the design surface. And standard deviations are 3.6mm and 3.4mm respectively showing no big difference from each other. The reason of the differences of the max displacements could be considered as that the defect of A-2 happens on the edge of the plate which caused the slight overlap differences during the registration.

No big difference on the execution time is detected between A-1 and A-2.

9.3.2.2. Registration of plate with big defects

Plate B is also measured twice and registered with the design surface. As shown in Figure 9-9, measured point cloud B-2 has obvious defects on all over the plate, while point cloud B-1 has the points covering all over the plate.

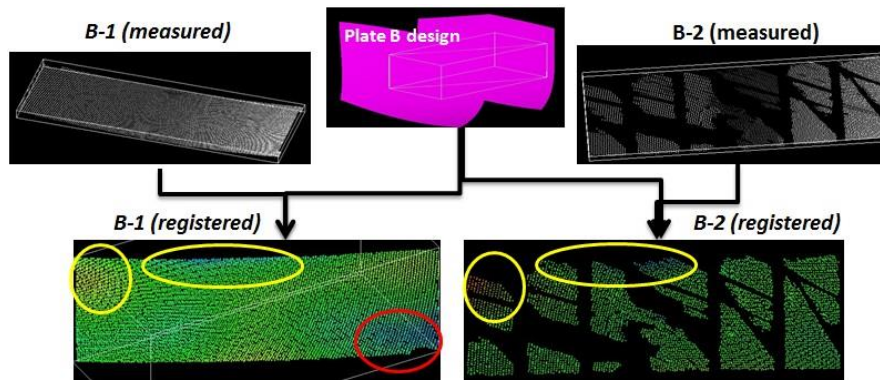


Figure 9-9 Registration result for plate B (defect rate 52.5%)

R_{defect} of point cloud B-2 is 52.5% which is relatively high in the 200 plates' point clouds. Usually, this kind of data will be required to be scanned once more with fewer obstacles. However, sometimes, especially close to the end of the manufacturing of a plate, workers usually have no time to remove all of the obstacles not only on the plate but also close to the plate. And when it is close to the end of the manufacturing, the displacement color maps are more expected than the frame's evaluation, so this kind of plates with big defects are still expected to be evaluated.

The registration result is virtualized by the color maps in which the points with the displacement smaller than 15mm are all shown in green color. The blue and red areas are with displacement bigger than 15mm. As shown in Figure 9-9, the red and blue areas of these two point clouds in the green circles are both detected successfully as the area with big displacement errors. The reason why the blue area in red circle is not detected on B-2 is considered as that large defects area on the edges which caused the overlap difference between these two data.

Due to the high defect rate of B-2, the distribution of the displacements after the registration has a big difference from the one of B-1, which can be observed from the histograms of the displacement from the design surface.

As summarized in Table 9.12, the differences of ICP converging errors (the sum of the squares of all the points' displacements) between the last two times of converging are 2mm and 1mm, which means that both of these two point clouds are registered well with the design surface. The standard deviations are 6.6mm and 5.4mm respectively showing no big difference from each other considering the high

defect rate in B-2.

The execution time of B-2 is 5 seconds shorter than B-1. This is because the points in B-2 are much less than that in B-1.

Table 9.12 Registration results of the plate B with and without defect

<i>Plate</i>	<i>Points On Plate</i>	<i>ICP Converging Times</i>	<i>ICP Error Converging</i>	<i>Max Displacement (+)</i>	<i>Max Displacement (-)</i>	<i>Standard Deviation</i>	<i>Execution Time</i>
(B-1)	23,336	43	2mm	+19mm	-15mm	6.6mm	41s
(B-2)	11,073	37	1mm	+23mm	-18mm	5.4mm	36s

9.4 Summary

This thesis presented a set of efficient point cloud processing methods in shipbuilding including the reformative component extraction method and the component registration method. These methods solved two common problems which arose when using the existing general methods including basic region growing method and ICP method directly in point cloud processing at shipyard, and are proved to be efficient according to experiments conducted in shipyard.

The proposed common domain recognition method is proved to be effective by successfully extracting a series of plates' point clouds which are divided by different kinds of obstacles. The section curves used in common domain recognition are discussed under different situations. The region growing candidate selecting is confirmed to be effective and efficient by comparing the growing time between the general region growing and the one with the proposed candidate selecting method. That some plates can only be extracted with high integrity using the proposed weighted region growing shows the effectiveness of the weighted region growing when dealing with the point clouds with varying densities.

The proposed registration method is proved to be effective by comparing the registration result of the same plate using the proposed method and the general method respectively. The experiment results show that not only the point clouds with high integrity, but also the point clouds with different levels of defects can be

registered with the design CAD surfaces using the proposed registration methods. The accuracies of the registration results are calculated and evaluated using the converging situation of ICP, the standard deviation of the displacements and the registration time.

Chapter 10 Cold forming support experiment

10.1. Overview of cold forming support experiment

In this chapter, the cold forming support experiments conducted in the shipyard will be illustrated. Plate Measurement System (MS) and Press Support System (PSS) are introduced with the Automation Engine (AE) into a shipyard S for the workers to grasp the manufacturing results of every manufacturing step. Multiple plates are evaluated in these experiments. After the cold forming manufacturing environment of the shipyard is introduced, the following items will be evaluated.

- a. Automation engine configuration
- b. Plate extraction
- c. Press evaluation
- d. Perimeter evaluation

The main objective of this experiment is to make sure that:

1. The evaluation process is efficient.
2. The evaluation results are effective.
3. All of the setting ups and customization according to the manufacturing environment are conducted by the administrators of the shipyards.
4. The measurement and analysis flow is completely automatized. The workers only need to select minimum information.

In this chapter, 2 plates, Plate “Regular 1” and Plate “Large 1” will be used as evaluation targets of the experiments. Laser scanner, server, input interface and display screen are set at the cold forming spot. The automation engine’s 4 configuration files are customized by the administrator in the shipyard according to the practical environment. Then the plate extraction results, evaluation results and perimeter measuring results are calculated automatically and displayed to the workers in the shipyard to help them recognize the situations of the plate during or after cold forming manufacturing.

At last the evaluation results will be summarized, and the supported cold forming manufacturing process will be reviewed by the selected experienced workers in the shipyard.

In this experiment, laser scanner Faro Focus 3D is used. The features are listed as below:

Table 10.1 Faro Focus 3D X series

<i>items</i>	<i>values</i>
Range Focus3D	0.6 – 130m
Measurement speed	up to 976,000 points/second
Ranging error	± 2mm
Integr. colour camera	Up to 70 mio. pixel
Laser class	Laser class 1
Weight	5,2kg
Multi-Sensor	GPS, Compass, Height Sensor, Dual Axis Compensator
Size	240 x 200 x 100mm
Scanner control	via touchscreen display and WLAN

The features of the server used in this experiment are as shown in the table below:

Table 10.2 Server features

<i>items</i>	<i>values</i>
CPU	Inter(R) Celeron CPU 2.16GHz
OS	Windows 7 64bit
Memory	4.00 GB
Hardware	500GB Hard disk

10.2. Experiment design

After the experiment environment is configured in the shipyard, the experiment is conducted following the flow shown in Figure 10-1. The workers select the design information of the plate being evaluated. Then the scan parameters are set according to the selected scan spot and the automation engine (introduced in appendix) sends the scan command to the scanner. After the scan, the scan results are sent to the server for analyzing. The plate's displacement errors and perimeters are calculated and used to judge if the plate reaches the designed press shape or not and if it has to be cut or not.

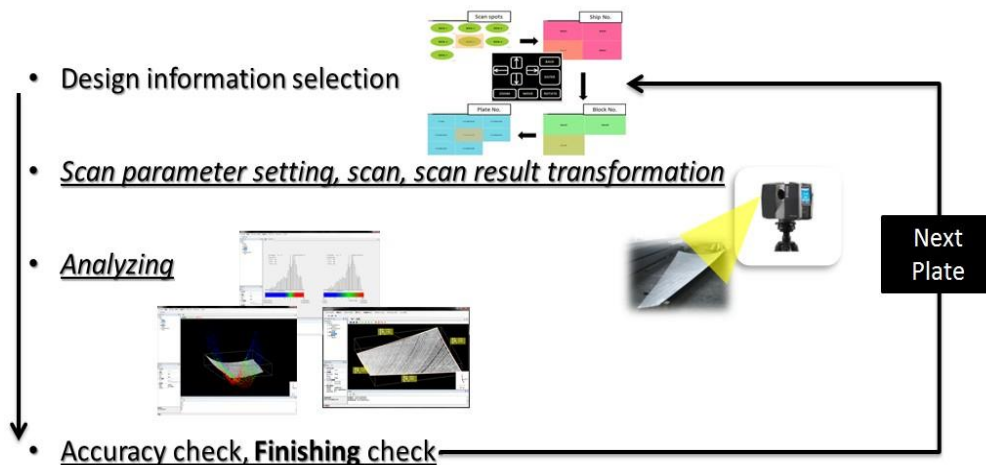


Figure 10-1 Cold forming experiment flow

The following aspects are checked during the experiment.

(1) Plate Extraction

When trying to introduce the cold forming support framework (MS + PSS + AE) into the cold forming manufacturing at the shipyard, at least 7 plates are scanned during or after the cold forming process. The main features of scanned plates during the cold forming process are as below:

- A lot of obstacles exist but the plates remain integrated because there are no obstacles on the plates.
- The density of the scanned point cloud is relatively high because the

scanner is located close to the plates.

Therefore, the Plate Measurement System (MS) is configured without common domain recognition (discussed in 5.5) to save the calculation time. Also, since the density of the scanned point cloud is high, so the configuration discussed in 5.3 - 5.4 is set to high sensitivity.

As the pre-process of the evaluation of the press and perimeter, in this sub section, the 2 kinds of plates “Bowl 1” and “Large 1” are extracted from the scanned raw point cloud during and after the cold forming process.

(2) Press Evaluation

As a conventional way to evaluate the plate during the cold forming process, workers put the wooden templates made for cold forming checking on the plates after each manufacturing step. The evaluation is not quantitative and has great individual differences. The cold forming manufacturing, as a critical pre-manufacturing of the heating forming manufacturing, is expected to be quantitatively evaluated and virtualized for the workers to grasp the shape of the plate after each manufacturing step.

In this sub section, the effectiveness of the Press Evaluation Engine discussed in 6.3 will be verified by conducting the evaluation towards the extracted 2 kinds of plates “Bowl 1” and “Large 1”. The design data and the extracted measured plate are registered together and the distance errors are calculated and visualized in the forms of color map, histograms.

In this experiment, the design data of the cold forming process is the DAT file which contains the 3D coordinates of the points representing the design shape of the cold forming target. Since the DAT file cannot be recognized directly by the 3D view system, it is converted to point cloud data before the analysis process.

The main objectives of this sub section are as below:

- Evaluate the plates' shapes without using the real templates
- Visualize the evaluation results in a comprehensible way
- Decide if the plate can be passed to the subsequent heating forming manufacturing

(3) Perimeter Evaluation

After the cold forming process and before the welding process, the perimeters are measured by measuring tape. However, since in this framework, the plate's point cloud has been scanned when evaluating the plate's shape, the method evaluating the plate's perimeters is also developed.

In this sub section, the effectiveness of the Perimeter Evaluation Engine discussed in 6.4 will be verified by conducting the evaluation towards the extracted 2 kinds of plates "Bowl 1" and "Large 1". The design data and the extracted measured plate are registered together and the lengths are calculated and visualized in the 3D view.

The main objectives of this sub section are as below:

- Evaluate the plates' perimeters without using the measuring tape
- Visualize the evaluation results in a comprehensible way

10.3. Experiment configuration in shipyard

The introducing layout of the cold forming support framework (MS, PSS and AE) in the shipyard S is as shown in Figure 10-2. One laser scanner (FARO) is installed beside the press machine (750 ton) and connected with the server through LAN. There are two scan spots of the cold forming manufacturing. Scan spot A is located just under the press machine which make sure that the curved shell plates can be evaluated during the manufacturing. Scan spot B is located beside the press machine where the finished curved shell plates are placed.

The pictures of these two scan spots taken by laser scanner are shown in Figure 10-3 and Figure 10-4. When switching from one scan spot to another, the scan scope parameters are automatically set by automation engine.

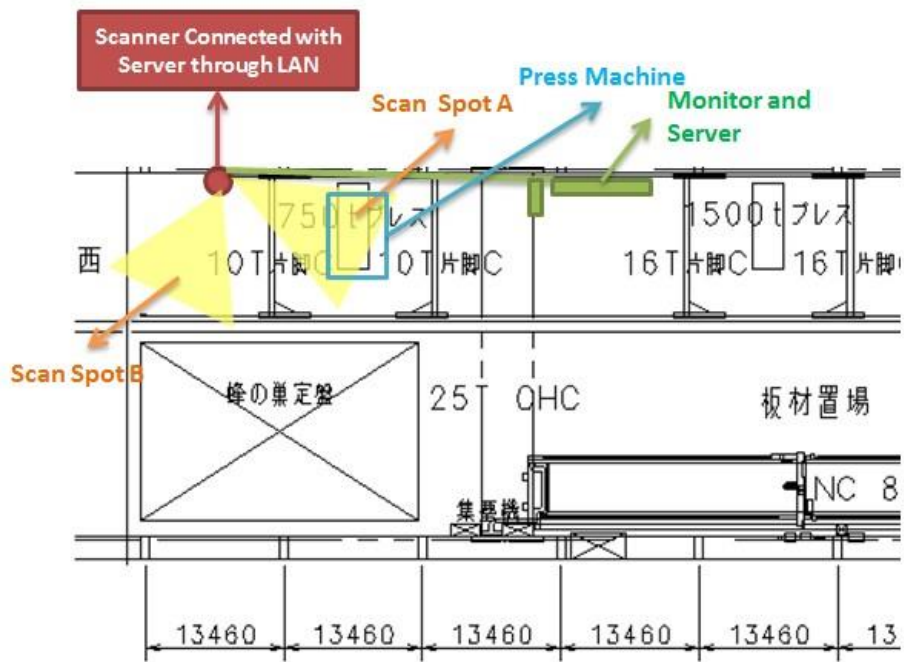


Figure 10-2 Layout of the experiment in the shipyard

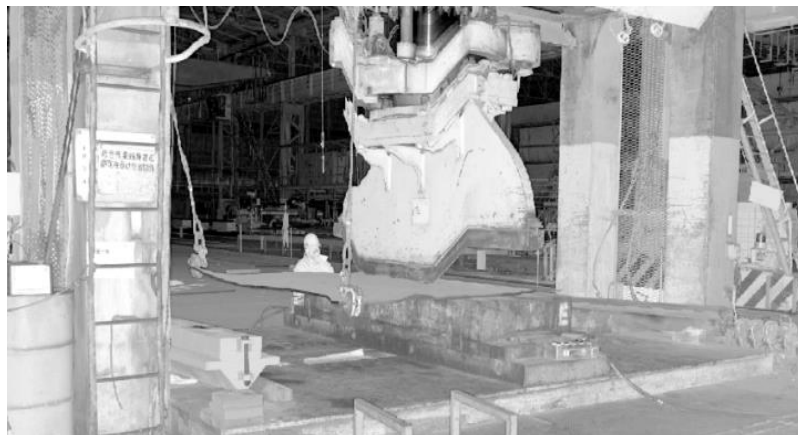


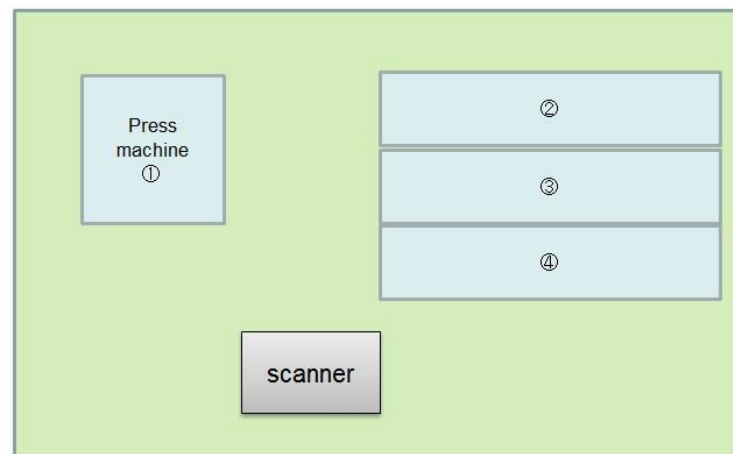
Figure 10-3 Scan spot A (Press machine)



Figure 10-4 Scan spot B (After every press step)

In the case of cold forming supporting, the laser scanner is fixed at one location. So the targets that are controlled by automation engine (AE) are as below:

- Laser scanner's scan scope
- Laser scanner's scan command
- Press design data's selection
- Press evaluation flow
- Perimeter evaluation flow



	Vertical (°)	Horizontal (°)
①	-10 ~ 0	110 ~ 140
②	-13 ~ -5	180 ~ 240
③	-20 ~ -5	180 ~ 245
④	-40 ~ -5	180 ~ 260

Figure 10-5 Scanner parameter setting

In practical use, the scan spot B is divided into 3 spots for different kinds of curved shell plates. The scanner parameter settings for the different scan spots are listed in Figure 10-5.

The experiment scenario of the cold forming support framework is illustrated in Table 10.3. After the automation configuration files are composed by the administrator of the cold forming in shipyard, as the operator of the framework, an experienced worker W operated the automatized framework by using the numeric keyboard as the curved shell plate's information selecting interface. The executed items and the average executing time of each item are also listed in the table.

The customized numeric keyboard used to control the automatic engine and the laser scanner located at the cold forming spot are as shown in the figures above.

Table 10.3 Experiment scenario of the cold forming support framework

<i>Automatized cold forming support experiment</i>			
Operator	Experienced worker W of the shipyard S		
Objective	Evaluation of the cold forming support framework (MS + PSS + AE)		
Interface	Customized numeric keyboard with buttons : “UP” “DOWN” “LEFT” “RIGHT” for scan spot and plate selecting “ENTER” “BACK” for confirmation or cancellation of the selection “ZOOM” “ROTATE” “MOVE” for result view operation		
Experiment Targets	Multiple curved shell plates which are manufacturing or manufactured in shipyard.		
Automation configuration files' composing	<ul style="list-style-type: none"> - Person in charge: Administrator of the cold forming in shipyard - Contents: scan spot, scan scope of each scan spot, region growing seed coordinates, ship number, block number, curved shell plate number, tolerance value etc... 		
Result display	Display screen connected with the server		
Period	From 2014.3		
Automatic executed items and executing time	<i>Executed items</i>	<i>Interface</i>	<i>Executing time</i>
	Scan spot selecting	Numeric	5 seconds
	Ship selecting	Keyboard (Manual)	
	Block selecting		
	Curved shell plate selecting		
	Scan scope setting	AE (Automatic)	2 seconds
	Scan command sending	AE (Automatic)	1 seconds
	Scan	AE (Automatic)	50 seconds ave
	Design file loading	AE (Automatic)	5 seconds
	Press evaluation	AE (Automatic)	20 seconds ave
	Perimeter evaluation	AE (Automatic)	12 seconds ave
	Result display	AE (Automatic)	-

The user interfaces of the cold forming support framework are generated based on the UI configuration files composed by the administrators in the shipyard. Not only are the items shown in the user interfaces but also the other necessary configuration features as below are set in the configuration file. Details are in the appendix.

For UI configuration “ui.conf”:

- Scan scope of each scan spot
- Region growing seed’s coordinates of each scan spot
- Tolerance value of every curved shell plate

For operation configuration “op.conf”:

- Normal vector similarity value
- Nearest neighbors’ count

In this sub-section, the following features of the Automation Engine (AE) when introduced into the cold forming manufacturing process are verified:

- a. The effectiveness of the automation engine

The measurement flow of Measurement System (MS) and the analysis flow of Press Support System (PSS) are well automatized from the plate selection to the evaluation result displaying within a relatively acceptable time cost.

- b. The flexibility of the automation engine

The parameters such as the scan scope, the tolerance values for evaluation, and the normal vector similarity values for analysis which are necessary for both the MS and PSS can be all pre-set by modifying the configuration files of automation engine.

10.4. Experiment 1 : Plate “Regular 1”

10.4.1. Plate measurement

As shown in Figure 10-6, the scanned raw point cloud data of the Plate “Regular 1” contains over 0.5 million points, the density of the points is less than 5 mm. The main obstacles of the scanned point cloud are the floors and the cranes’ shadows.

The extraction result of Plate “Regular 1” is as shown in Figure 10-6 (right). The points constituting the plate are about 0.2 million. The time used to extract the plate is 26 seconds which decreased substantially from over 12 minutes (the plain region growing method).

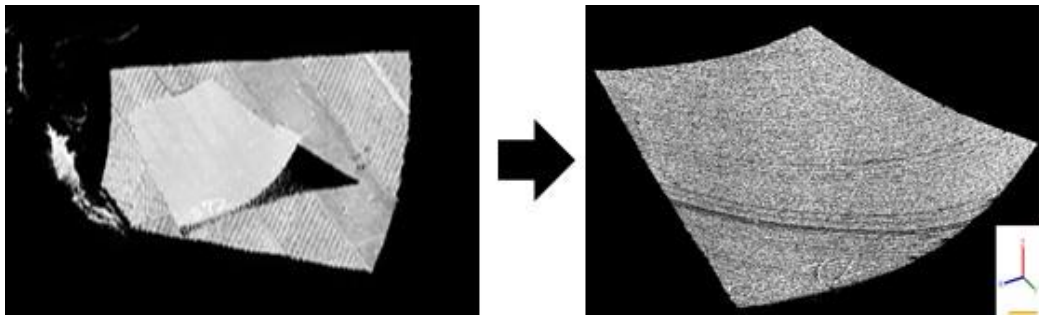


Figure 10-6 Measurement of Plate “Regular 1”

10.4.2. Press Evaluation Result

The converted design data of Plate “Regular 1” is as shown in Figure 10-7. The density of the design data is lower (about 100mm) than the measured data, thus the design data is configured as the moving point cloud and the measured data stays at the same position when doing the registration of these two data to save the calculation time.

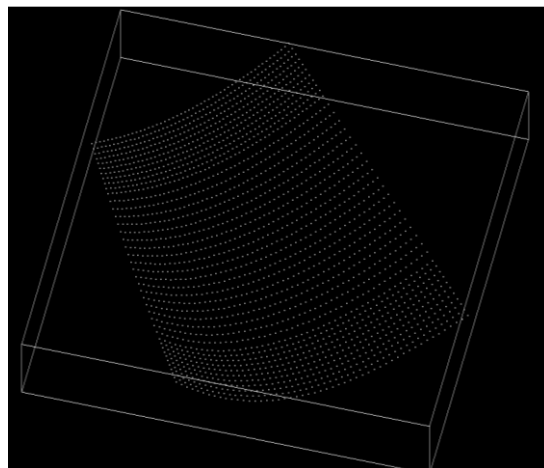


Figure 10-7 Press design data of Plate “Regular 1”

10.4.2.1. Plate 1

The evaluated distance errors between the design data and the measured data are visualized in form of color maps as shown in Figure 10-8. The red area is in the middle while the blue areas are distributed at both sides of the plate which means the plate has lower curvatures when compared with the design shape.

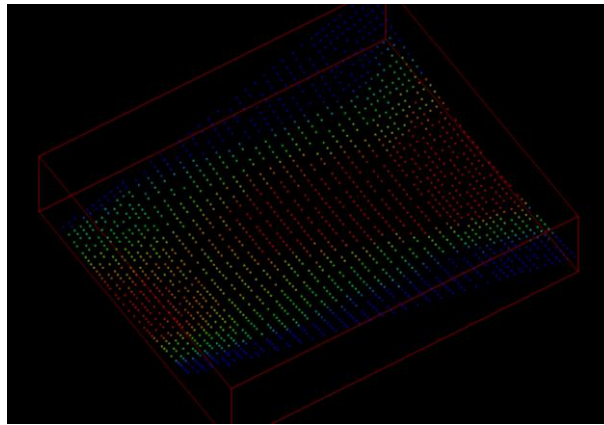


Figure 10-8 Evaluation result of Plate "Regular 1" (plate 1)

To make the errors more easily to be understood, the distance errors are magnified as shown in Figure 10-9. The blue areas (design data) are above the measured data while the red area (design data) is below the measured data. To achieve the final design shape, more press manufacturing steps are needed. However, this plate was still forwarded to the heating forming in this experiment.

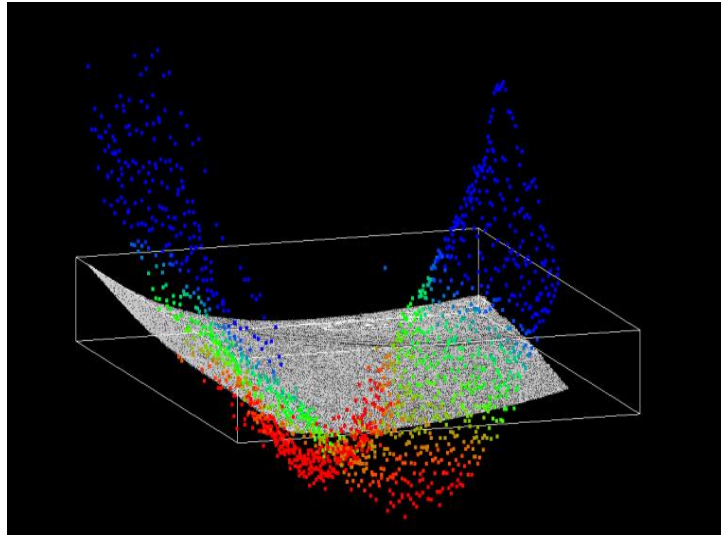


Figure 10-9 Exaggerative evaluation result of Plate “Regular 1” (plate 1)

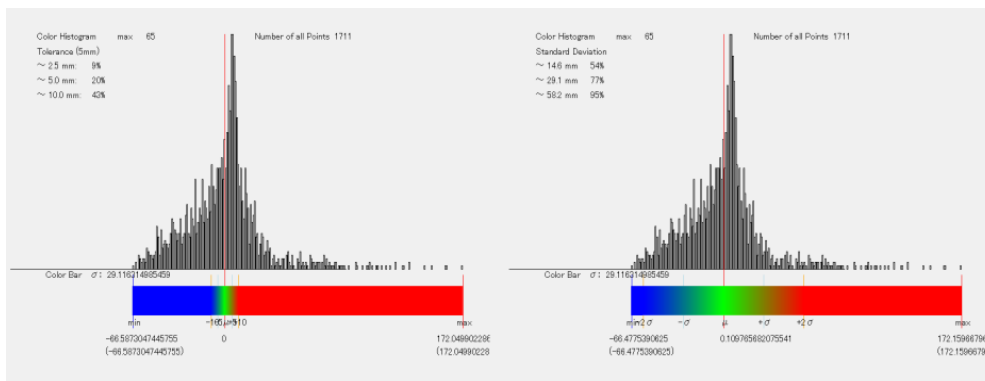


Figure 10-10 Evaluation histogram of Plate “Regular 1” (plate 1)

The histograms are as shown above. There is about 58% of the design points which are beyond the tolerance 10mm, thus the plate should be judged unfinished and deserving more manufacturing before being passed to the heating forming process. However, in this case, this plate was still passed to the heating forming stage.

For this plate, to achieve the final design shape, there were totally over 10 manufacturing steps for the heating forming, costing over 7 hours.

10.4.2.2. Plate 2

Another plate having the same design shape of plate “Regular 1” was measured after the cold forming. The evaluation results are as shown below:

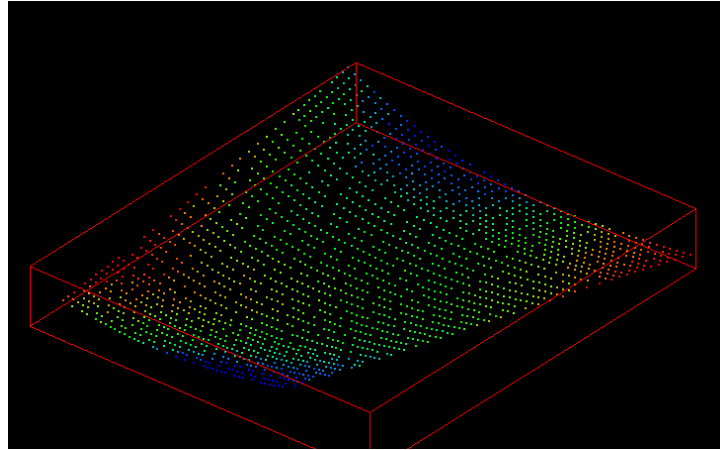


Figure 10-11 Evaluation result of Plate “Regular 1” (plate 2)

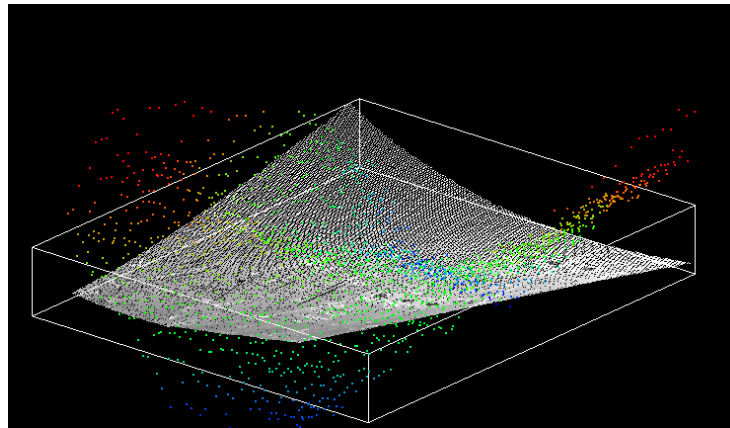


Figure 10-12 Exaggerative evaluation result of Plate “Regular 1” (plate 2)

According to the evaluation color map shown in Figure 10-11 and the exaggerated displayed color map shown in Figure 10-12, the points in green color increased and are distributed unsymmetrically to the wooden template’s perspective sticks.

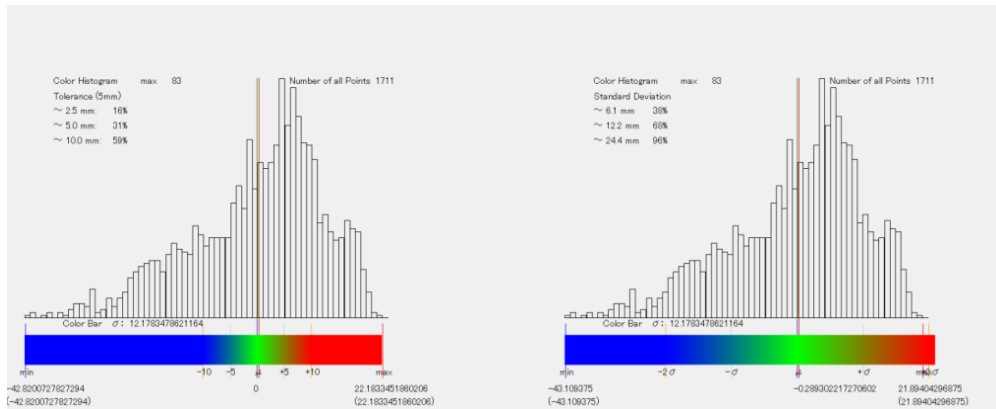


Figure 10-13 Evaluation histogram of Plate “Regular 1” (plate 2)

According to the histogram shown in Figure 10-13, there are about 60% of the design points which are within the tolerance 10mm, thus the plate should be judged finished can be passed to the heating forming process.

For this plate, to achieve the final design shape, there were totally 7 manufacturing steps for the heating forming, costing only 4.5 hours.

10.4.3. Perimeter Evaluation Result

The perimeter evaluation results of Plate “Regular 1” are shown in Figure 10-14 and Table 10.4. There are 3 perimeters have measured length bigger than the design length, therefore the plate need to be cut before the welding process.

However, the system measured lengths are all smaller than the real value measured by ruler; the biggest difference is over 6mm. The reason can be considered for this inaccurate result:

- The density of the point cloud is too low, that there are no points on the edges of the plate.

The solution for these problems is discussed in the discussion chapter.

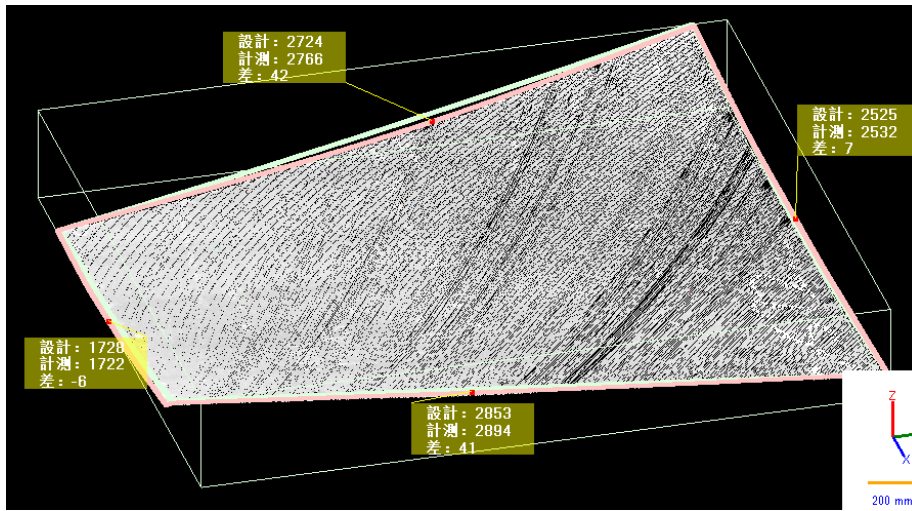


Figure 10-14 Perimeter evaluation result of Plate “Regular 1”

Table 10.4 Perimeters of Plate “Regular 1”

	<i>Design (mm)</i>	<i>System Measured (mm)</i>	<i>Manually Measured (mm)</i>
Edge 1	1727	1722	1727
Edge 2	2524	2532	2533
Edge 3	2723	2766	2765
Edge 4	2852	2894	2896
Total	9829	9914	9921

10.5. Experiment 2 : Plate “Large 1”

10.5.1. Plate measurement

As shown in Figure 10-15, the scanned raw point cloud data of the Plate “Large 1” contains over 1.2 million points, the density of the points is less than 10 mm. The main obstacles of the scanned point cloud are the floors and the shadow of the worker and the pipes located close to the plate.

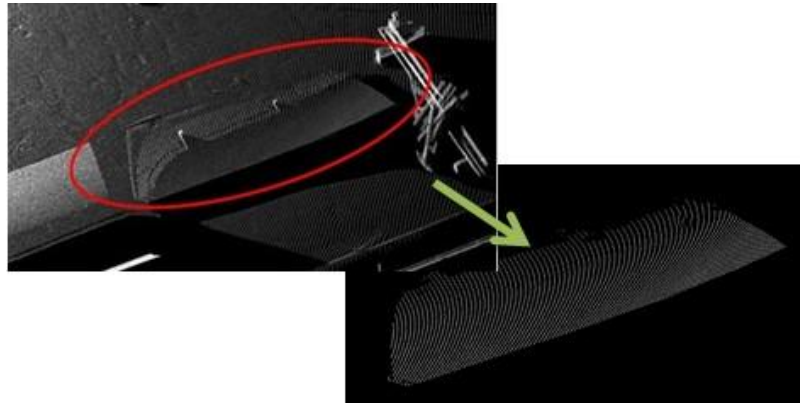


Figure 10-15 Measurement of Plate “Large 1”

The extraction result of Plate “Large 1” is as shown in Figure 10-15 (lower). The points constituting the plate are about 0.3 million. The time used to extract the plate is 34 seconds which decreased substantially from over 13 minutes (the plain region growing method).

10.5.2. Press Evaluation Result

The converted design data of Plate “Large 1” is as shown in Figure 10-16. The density of the design data is lower (about 100mm) than the measured data, thus the design data is configured as the moving point cloud and the measured data stays at the same position when doing the registration of these two data to save the calculation time.

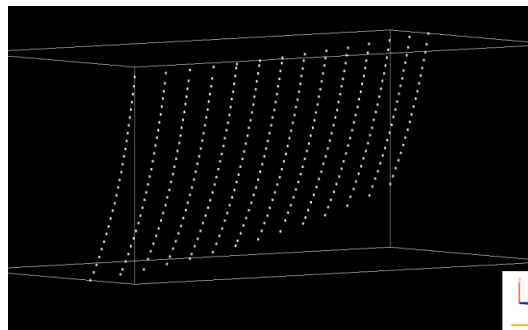


Figure 10-16 Press design data of Plate “Large 1”

10.5.2.1. 1st scan

The evaluated distance errors (during manufacturing) between the design data and the measured data are visualized in form of color maps as shown in Figure 10-17. The red area is in the middle while the blue areas are distributed at both sides of the plate which means the plate has lower curvatures when compared with the design shape.

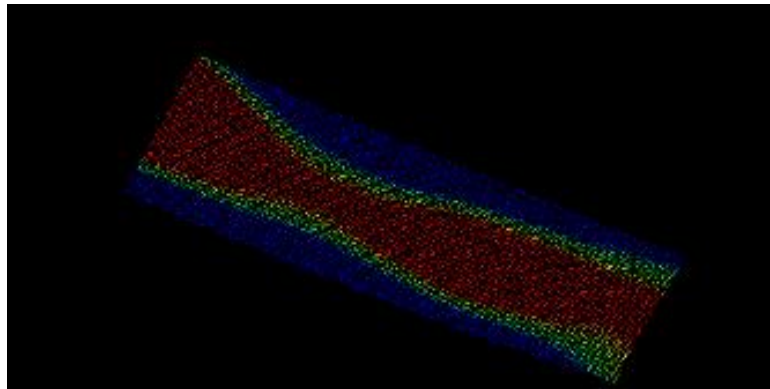


Figure 10-17 Evaluation result of Plate “Large 1” during manufacturing

10.5.2.2. 2nd scan

The evaluated distance errors (after manufacturing) between the design data and the measured data are visualized in form of color maps as shown in Figure 10-18. The distributions of the red areas and blue area changed in an irregular way. Besides, the histograms shown in Figure 10-19 show that over 75% of the design points are with the tolerance 10mm. Therefore, this plate is judged as a finished plate which can be passed to the following heating forming process.

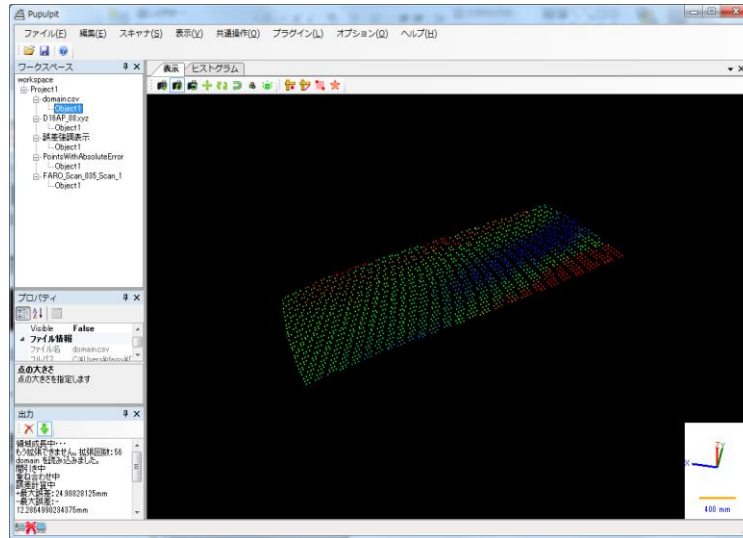


Figure 10-18 Evaluation result of Plate “Large 1” after cold forming

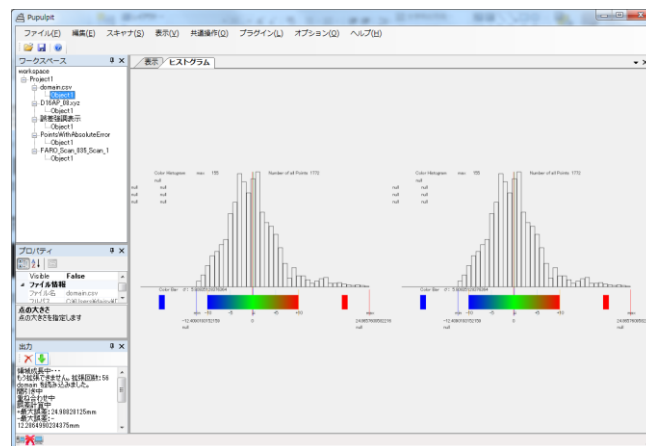


Figure 10-19 Evaluation histogram of Plate “Large 1” after cold forming

10.5.3. Perimeter Evaluation Result

The perimeter evaluation results of Plate “Large 1” are shown in Figure 10-20 and Table 10.5 Perimeters of Plate “Large 1” The measured length is larger than the design length, therefore the plate need to be cut before the welding process. Because the density of this point cloud is high enough, there are points laying on the edges of the plate. So the differences between the value measured by system and the manually measured value are all within 2mm which is permitted in the shipyard

daily usage.

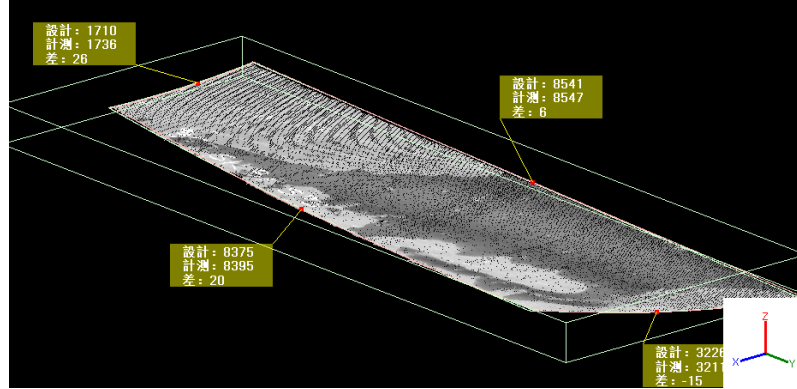


Figure 10-20 Perimeter evaluation result of Plate “Large 1”

Table 10.5 Perimeters of Plate “Large 1”

	<i>Design (mm)</i>	<i>System Measured (mm)</i>	<i>Manually Measured (mm)</i>
Edge 1	1710	1736	1738
Edge 2	3220	3217	3218
Edge 3	8375	8395	8396
Edge 4	8541	8547	8550
Total	21846	21895	21902

10.6. Summary

In this chapter, 2 plates are evaluated during the cold forming process by using the proposed cold forming support framework. The features are verified as below:

- ✓ The effectiveness of the plate extraction

The plates are successfully extracted from the measured raw point cloud data which contains relatively less obstacles on the plate within less than 1 minute which is a comparatively short time to the plain region growing method.

- ✓ The effectiveness of the plate evaluation

The effectiveness of the plate evaluation color map and histograms are verified. The plates with distance errors larger than the tolerance are judged as unfinished. The magnifying color maps tell the workers the relative position of the design data and measured data. 2 plates of the same design shape are passed to the heating forming stage with different evaluation results. According to Table 10.6, the following heating forming steps tell the plate should be evaluated first after the cold forming stage to enhance the heating forming efficiency.

Table 10.6 Cold forming support experiment result summary

<i>items</i>	Plate type “Regular 1”			Plate type “Large 1”	
	General	Proposed Case (1)	Proposed Case (2)	General	Proposed Case (1)
Perimeter within tolerance 8mm?	---	YES	YES	---	YES
Displacement over 10mm	---	58%	40%	---	25%
Heating forming manufacturing time	<i>5 hours</i>	<i>7 hours</i>	<i>4.5 hours</i>	11 hours	<i>8 hours</i>

- ✓ The effectiveness of the perimeter evaluation

The perimeters are evaluated and visualized in the 3D view as well to help workers grasp the situation of the plate. For the point cloud of low density the system measured perimeters may be smaller than the real values. The solutions are discussed in the following chapter.

The executive time of the automation engine for both the 2 plates is less than 30 seconds which is within the tolerance of the worker in shipyard.

Chapter 11 Heating forming support experiment

11.1. Overview of heating forming support experiment

In this chapter, the heating forming support experiments conducted in the shipyard will be illustrated. Plate Measurement System (MS) and Virtual Template System (VTS) are introduced with the Automation Engine (AE) into a shipyard S for the workers to grasp the manufacturing results of every heating forming step and design the next manufacturing plans (heating lines for next step). Multiple plates are manufactured without using the real wooden templates in these experiments. After the heating forming manufacturing environment of the shipyard is introduced, the following items will be evaluated.

- Automation engine configuration for heating forming environment
- Plate extraction
- Curvature error view
- Torsion evaluation view
- Heating plan suggestion (along with the roller lines)

The main objective of this experiment is to make sure that:

- ✓ The 2 views generated by the framework automatically are effective for the manufacturing plans' design.
- ✓ The manufacturing plans from the framework are effective.
- ✓ No real wooden template is used.
- ✓ All of the setting ups and customization according to the manufacturing environment are configured by the administrators of the shipyards.
- ✓ The measurement and analysis flow is completely automatized. The workers only need to select the minimum information.

In this chapter, 3 plates, Plate “Bowl 1” Plate “Bowl 2” and Plate “Hybrid 1” will be used as evaluation targets of the experiments. Server, input interface and display screen are set at the heating forming spot, and the laser scanner is located on a movable crane. The automation engine's 4 configuration files are customized by the administrator in the shipyard according to the practical environment. Then the curvature error view and the torsion evaluation view are calculated automatically and displayed to the workers in the shipyard to help them grasp the situations of

the plate and design the manufacturing plan for every manufacturing step.

At last the manufacturing results will be summarized, and the supported heating forming manufacturing process will be reviewed by the selected experienced workers in the shipyard.

In this experiment, laser scanner Faro Focus 3D is used. The features are listed as below:

Table 11.1 Faro Focus 3D 120 series

<i>items</i>	<i>values</i>
Range Focus3D	0.6 – 130m
Measurement speed	up to 976,000 points/second
Ranging error	± 2mm
Integr. colour camera	Up to 70 mio. pixel
Laser class	Laser class 1
Weight	5,2kg
Multi-Sensor	GPS, Compass, Height Sensor, Dual Axis Compensator
Size	240 x 200 x 100mm
Scanner control	via touchscreen display and WLAN

The features of the server used in this experiment are as shown in the table below:

Table 11.2 Server features

<i>items</i>	<i>values</i>
CPU	Inter(R) Celeron CPU 2.16GHz
OS	Windows 7 64bit
Memory	4.00 GB
Hardware	500GB Hard disk

11.2. Experiment design

After the experiment environment is configured in the shipyard, the experiment is conducted following the flow shown in Figure 11-1. The workers select the design information of the plate being evaluated. Then the scan parameters are set according to the selected scan spot and the automation engine (introduced in appendix) sends the scan command to the scanner. After the scan, the scan results are sent to the server for analyzing. The plate’s displacement errors and curvature errors at each frame and the automatically arranged virtual templates are provided to the workers for designing the manufacturing plan of the next manufacturing step. This loop repeats itself until the plate passes the finishing check by the system (Over 90% of the point are with the displacement error smaller than 5mm).

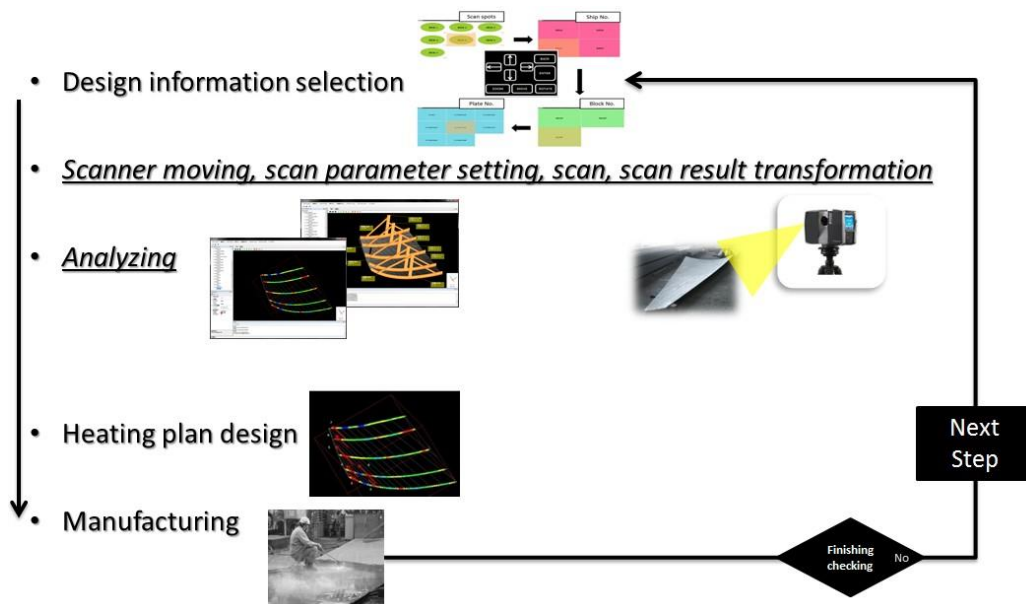


Figure 11-1 Heating forming experiment flow

11.3. Experiment configuration in shipyard

The introducing layout of the heating forming support framework (MS, VTS and AE) in the shipyard S is as shown in Figure 11-2. One laser scanner (FARO) is installed on the rail and connected with the server through LAN. The scanner can

be moved through the rail control system so that plates located in different spots can be scanned by only one scanner. And a big display consisting of 9 displays is used to display the analysis results of the framework as shown in Figure 11-3.

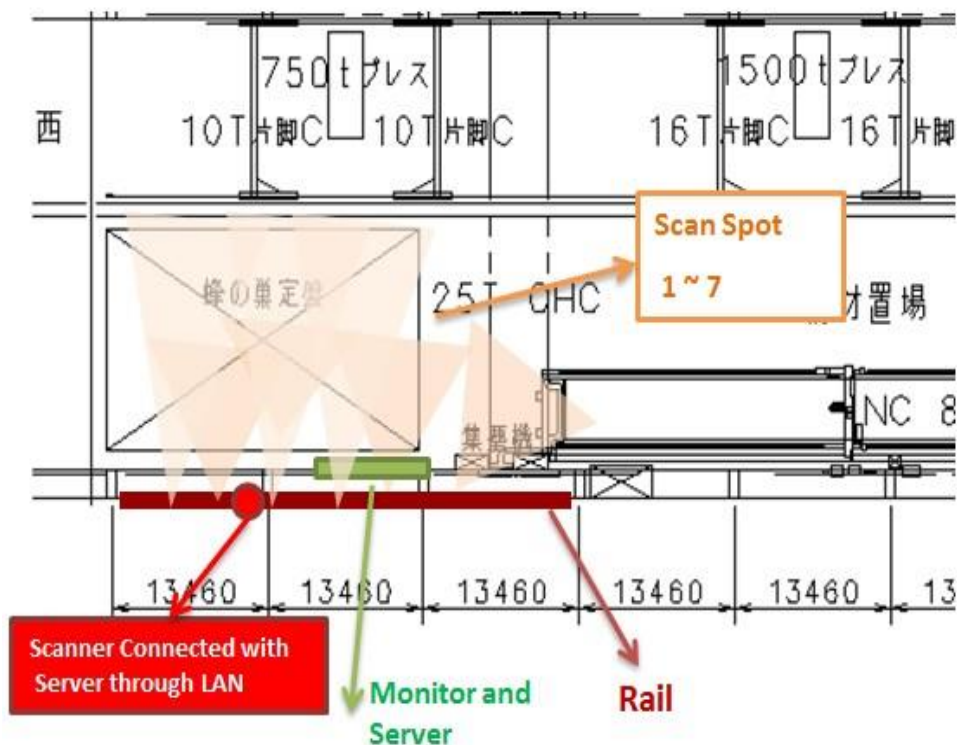


Figure 11-2 Heating forming support framework layout in shipyard

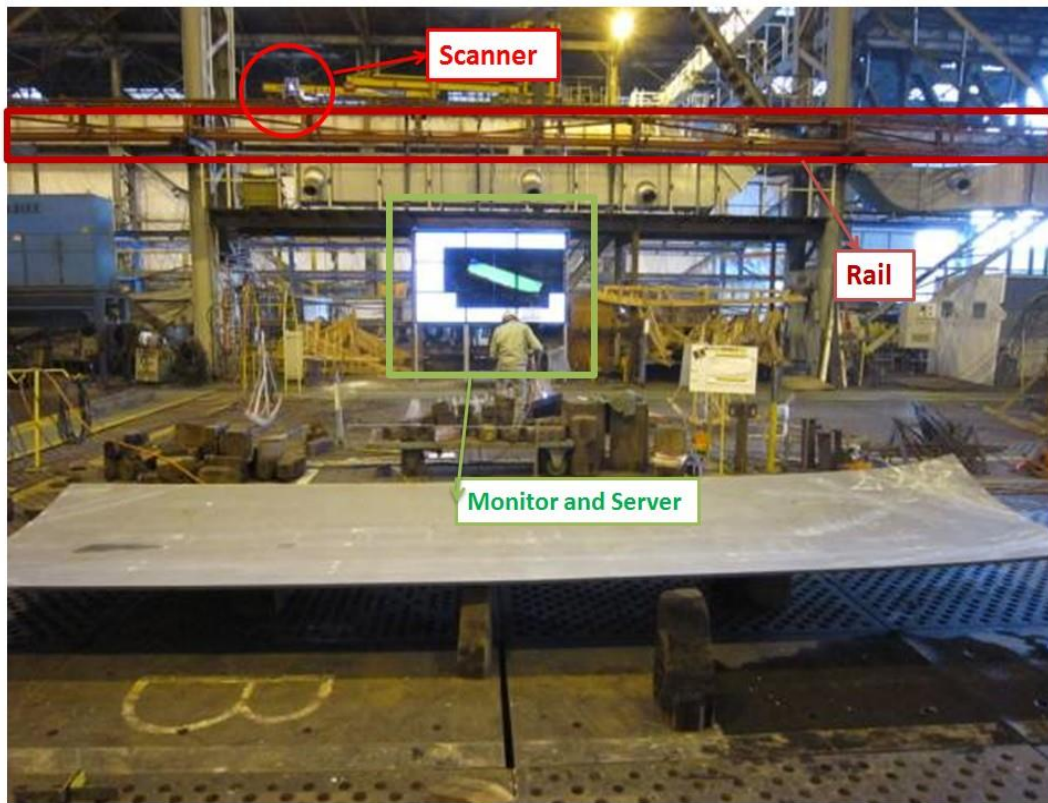


Figure 11-3 Heating forming process support scene in shipyard

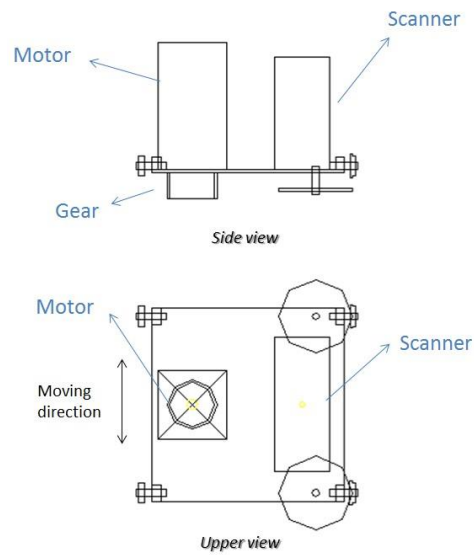


Figure 11-4 Scanner setting with motor and gear

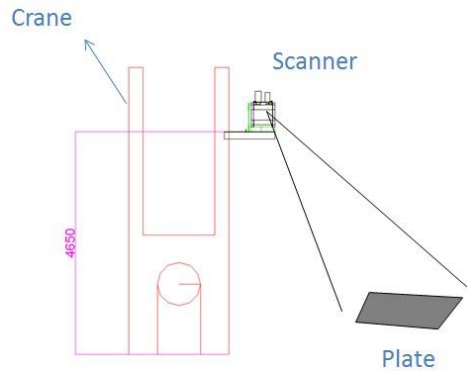


Figure 11-5 Scanner setting with crane (height 4650mm)

The scanner is fixed by the administrator in the shipyard with a motor that can move the scanner on the crane's rail as shown in the figures above.

As shown in Figure 11-6, there are totally 7 scan spots of the heating forming manufacturing area. 4 of them are located close to the rail with relatively small scan scope. The other 3 scan spots are located far away from the rail with large scan scope.

The pictures of these 7 scan spots taken by laser scanner are shown in Figure 11-7 ~ Figure 11-13. When switching from one scan spot to another, the scan scope parameters shown in these figures are automatically set by automation engine.

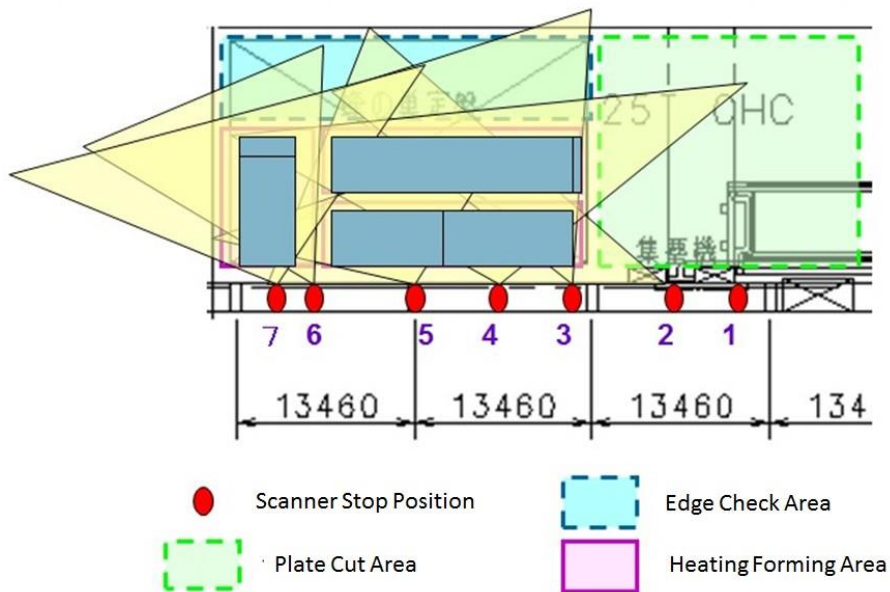


Figure 11-6 Scan spots at the heating forming area

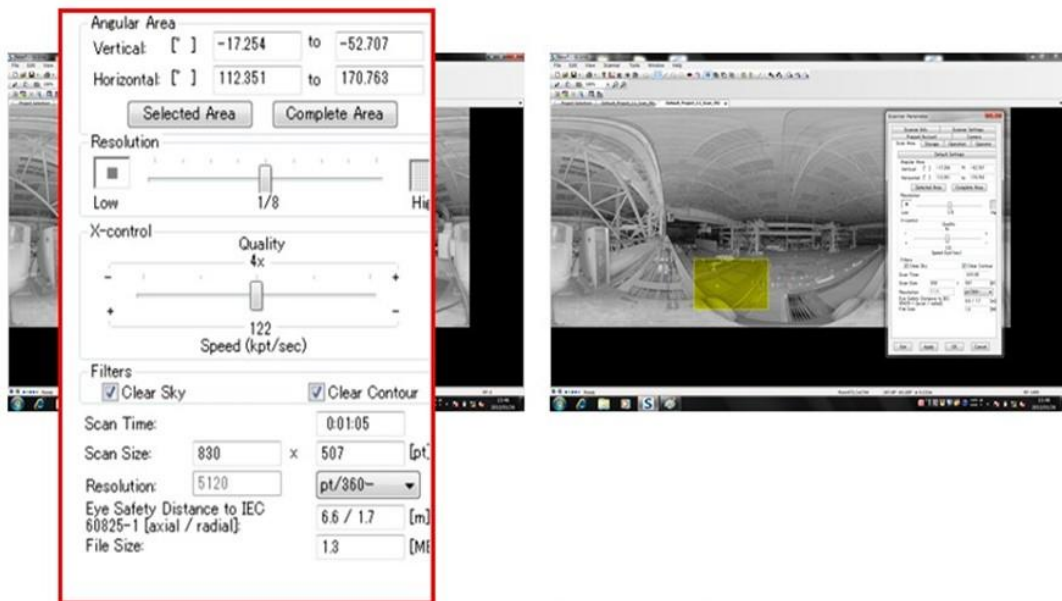


Figure 11-7 Scan spot 1



Figure 11-8 Scan spot 2

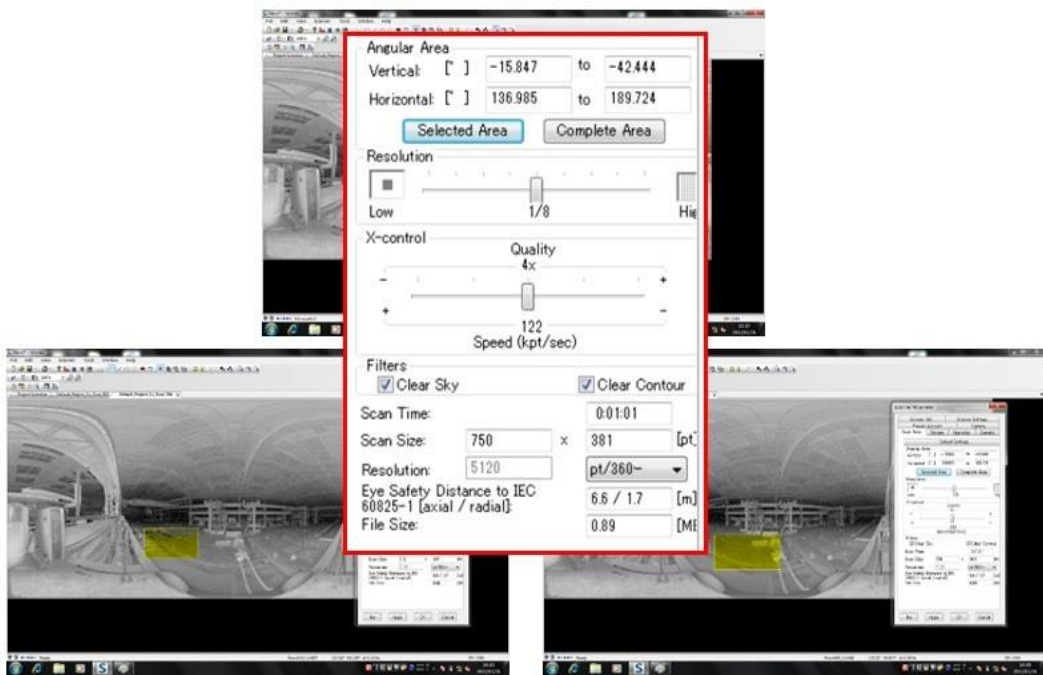


Figure 11-9 Scan spot 3



Figure 11-10 Scan spot 4

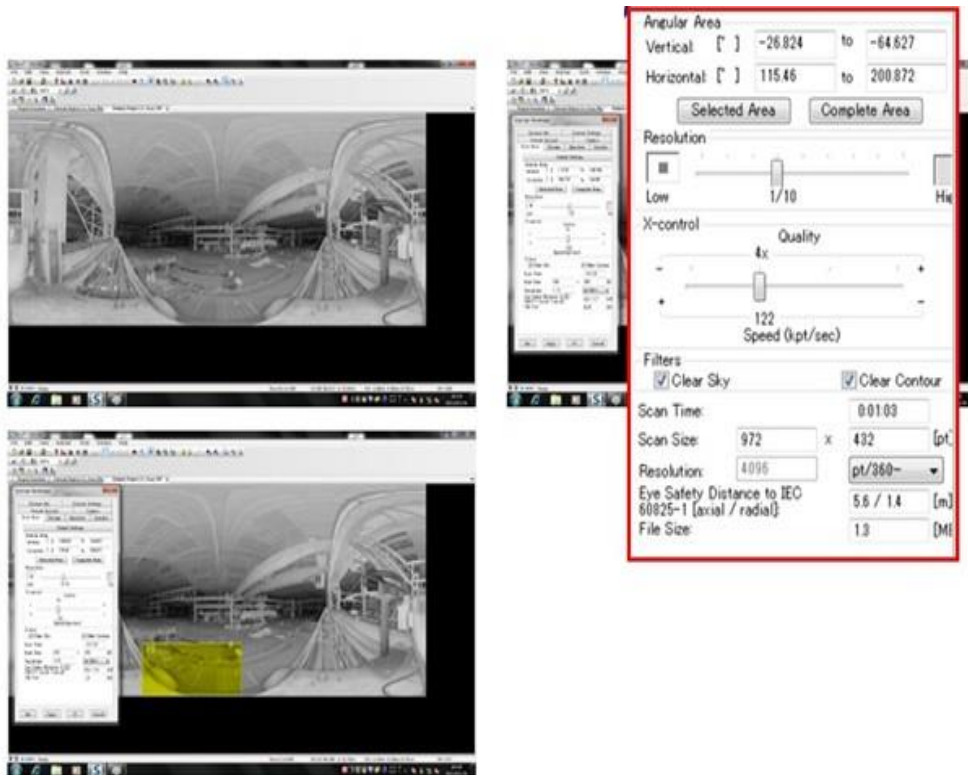


Figure 11-11 Scan spot 5

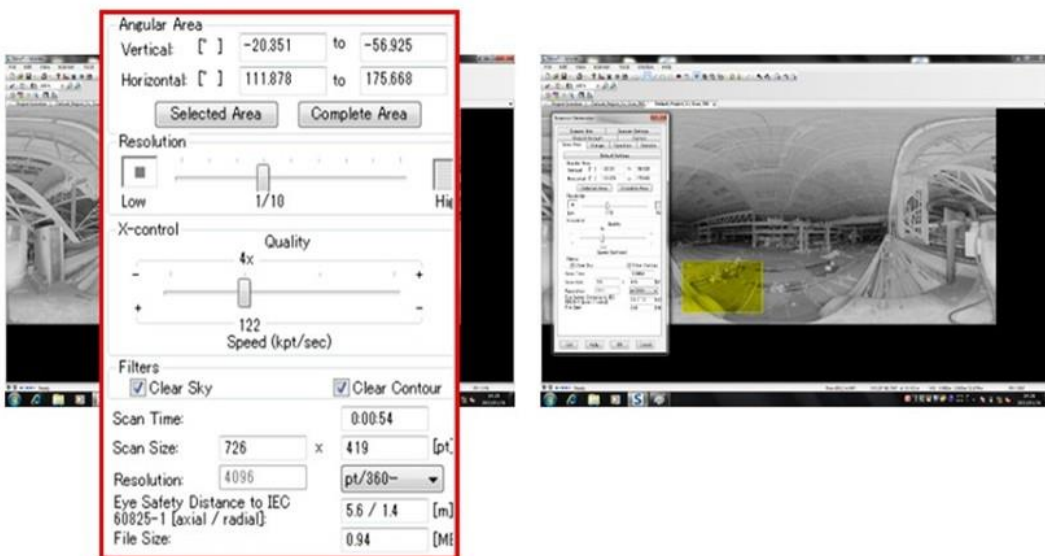


Figure 11-12 Scan spot 6

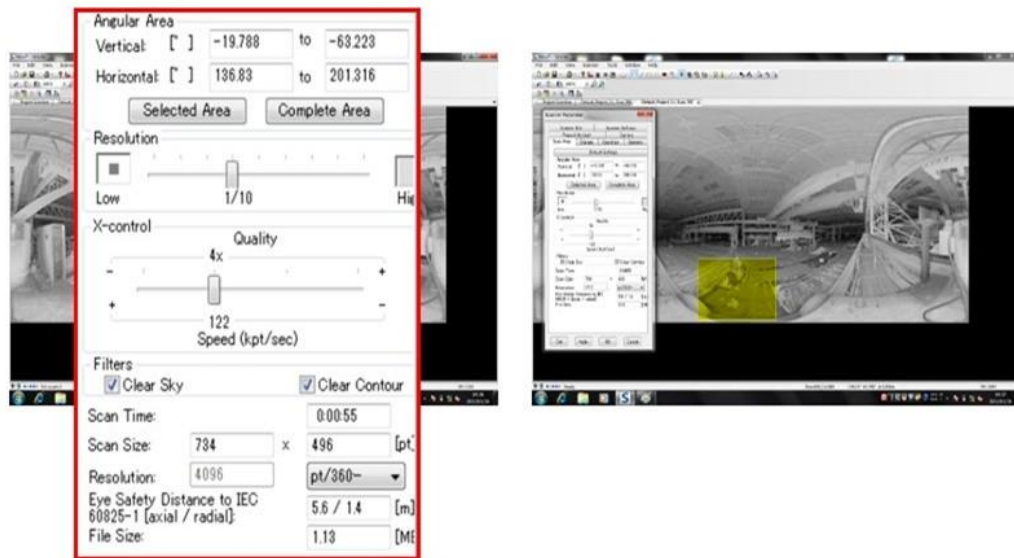


Figure 11-13 Scan spot 7

In the case of heating forming supporting, the laser scanner is located on the rail. So the targets that are controlled by automation engine (AE) are as below:

- Laser scanner stop location
- Laser scanner's scan scope
- Laser scanner's scan command
- Heating forming design data's selection
- Plate evaluation flow
- Curvature error view generation
- Torsion evaluation view generation

The experiment scenario of the heating forming support framework is illustrated in Table 11.3. After the automation configuration files are composed by the administrator of the cold forming in shipyard, as the operator of the framework, an experienced worker I operated the automatized framework by using the numeric keyboard as the curved shell plate's information selecting interface. The executed items and the average executing time of each item are also listed in the table.

Table 11.3 Experiment scenario of the heating forming support framework

<i>Automatized heating forming support experiment</i>			
Operator	Experienced worker W of the shipyard S		
Objective	Evaluation of the heating forming support framework (MS + VTS + AE)		
Interface	Customized numeric keyboard with buttons : “UP” “DOWN” “LEFT” “RIGHT” for scan spot and plate selecting “ENTER” “BACK” for confirmation or cancellation of the selection “ZOOM” “ROTATE” “MOVE” for result view operation		
Experiment Targets	Multiple curved shell plates which are manufacturing in shipyard.		
Automation configuration files' composing	- Person in charge: Administrator of the cold forming in shipyard - Contents: scanner location, scan spot, scan scope of each scan spot, region growing seed coordinates, ship number, block number, plate number, tolerance value etc...		
Result display	Display screen connected with the server		
Automatic executed items and executing time	<i>Executed items</i>	<i>Interface</i>	<i>Executing time</i>
	Scan spot selecting	Numeric	5 seconds
	Ship selecting	Keyboard (Manual)	
	Block selecting		
	Curved shell plate selecting		
	Scanner moving	AE (Automatic)	10 seconds
	Scanner scope setting	AE (Automatic)	2 seconds
	Scan command sending	AE (Automatic)	1 seconds
	Scan	AE (Automatic)	50 seconds ave
	Design file loading	AE (Automatic)	5 seconds
	Plate evaluation	AE (Automatic)	25 seconds ave
	Views' generation	AE (Automatic)	10 seconds ave
	Views' display and operation	AE (Automatic)	-

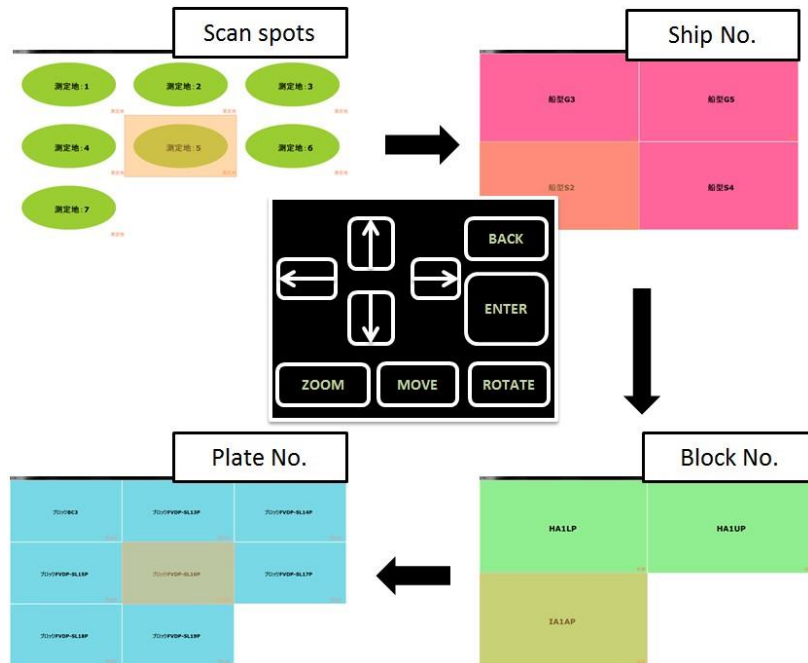


Figure 11-14 Generated UI of the heating forming support framework

Figure 11-14 shows the generated user interfaces of the heating forming support framework which are generated based on the UI configuration files composed by the administrators in the shipyard. Not only are the items shown in the user interfaces but also the other necessary configuration features as below are set in the configuration file as shown in Figure a1-13.

For UI configuration “ui.conf”:

- Scan scope of each scan spot
- Region growing seed’s coordinates of each scan spot
- Tolerance value of every curved shell plate

For operation configuration “op.conf”:

- Normal vector similarity value
- Nearest neighbors’ count

For control configuration of the rail system “color.conf”:

- Spot button color RGB
- Spot button area

In this sub-section, the following features of the Automation Engine (AE) when introduced into the heating forming manufacturing process are verified:

a. The effectiveness of the automation engine

The measurement flow of Measurement System (MS) and the analysis flow of Virtual Template System (VTS) are well automatized from the plate selection to the evaluation result displaying within a relatively acceptable time cost.

b. The flexibility of the automation engine

The parameters such as the scan scope, the tolerance values for evaluation, and the normal vector similarity values for analysis which are necessary for both the MS and VTS can be all pre-set by modifying the configuration files of automation engine. Besides, to control the rail where the laser scanner is located, the buttons detection information of the external system (rail control system) is also configured.

11.4. Design data used in the experiment

In this experiment, there are 3 different kinds of design data which are used for different evaluation purpose.

- SAT curved surface design data (3D)
- DXF roller line design data (2D)
- DAT frame line design data (3D)

The SAT (Standard ACIS Text) file is a kind of CAD files representing the shape of the curved shell plate in the form of NURBS (Non-Uniform Rational Basis Spline) curved surface. In the proposed framework, the SAT file is used to calculate the distance errors between the design surface and the measured surface after the registration of the design data and the measured data.

The DXF (Drawing Exchange Format File) file is also a kind of CAD files representing the relative locations of the designed roller lines. The DXF files used in this framework is in 2D (x, y, 0) by defining the Z coordinate as 0. The 2D roller lines have to be matched to the 3D SAT data to make them easier to be observed.

The DAT (Data File) is a generic data file created by a specific application; typically accessed only by the application that created the file; may contain data in text or binary format; text-based DAT files can be viewed in a text editor. The proposed framework uses DAT file to store the curved shell plate's designed frame line's points in 3D (x, y, z) and also the names of different frame lines. The DAT file has to be converted into the normal point cloud data format for the system to read.

In the following subsections, these design data and the converted input data of

the 3 plates, Plate “Bowl 1” Plate “Bowl 2” and Plate “Hybrid 1”, will be illustrated.

11.5. Preliminary experiment

The preliminary experiment validates the plate’s point cloud extraction in the shipyard, the basic performance of the VTS system by measuring two curved shell plates during manufacturing, and compares the system suggested heating areas and the heating areas actually used by the workers according to the check results of the real wooden templates at each manufacturing step. After that, the relations between the heating conditions and the consequent contractions of the plate are evaluated for both the point heating and line heating technics. At last the heating and refrigeration conditions are decided for the following general experiment to manufacturing the plate “Bowl 1”, “Bowl 2” and “Hybrid 1”.

11.5.1. Curved shell plate extraction

Two curved shell plates are extracted successfully using the proposed approach. Figure 11-15(left lower) shows the extracted point cloud data of curved shell plate A consisting of 119,431 points. While Figure 11-15(right lower) is the extracted results of curved shell plate B consisting of 231,321 points. Unlike curved shell plate A, curved shell plate B’s scan result is divided into many separate domains by obstacles’ shade. The proposed separated region recognition method extracted all of the divided regions and integrated them together into one curved shell plate.

In addition, the time to extract the separate domains like that of curved shell plate B increases with the separate domains’ number. But the total time of extraction in this case study is under 1 minute. When curved shell plate A is compared with curved shell plate B, an obvious decrease in extraction time cannot be seen for its larger point cloud’s density. In other words, by reducing the scan density to a proper degree and avoiding obstacles’ shade, the curved shell plate’s extraction time can be shortened.

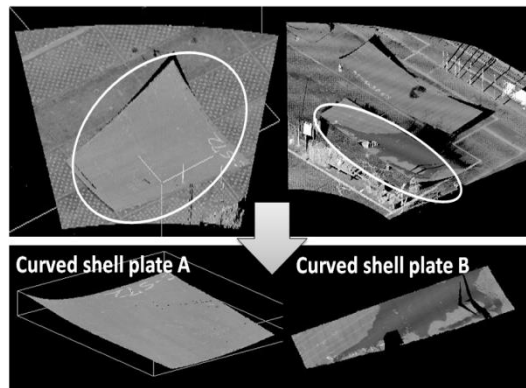


Figure 11-15 curved shell plate extraction in preliminary experiment

11.5.2. Evaluation results' comparison of one single processing step

The heating standard μ proposed in this thesis which shows the relative curvature errors of the 5 frames of curved shell plate A is calculated. As shown in Figure 11-16, if μ at a point has a value of 0.5 or more, the bending at this segment is insufficient and additional heating is required.

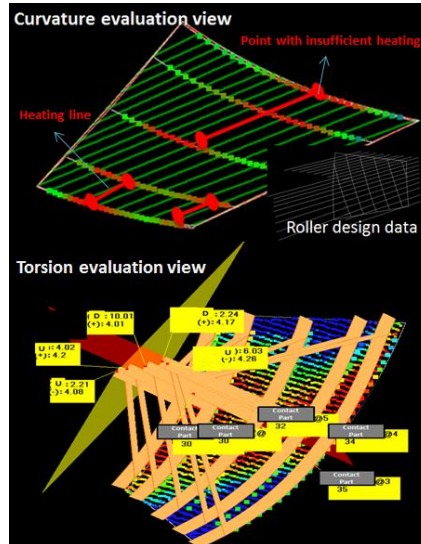


Figure 11-16 Curvature evaluation view and torsion evaluation view in preliminary experiment

Figure 11-16(upper) also gives the colour map results of the curvature error by this system. Six big solid circles show the positions having insufficient bending. As shown in the figure, the heating areas for the following manufacturing were also

shown as 3 lines combining the points with insufficient heating where the bending is insufficient and along with the parallel roller lines. The roller lines are also registered to the measured point cloud from the roller line design data as the parallel lines show in the figure. The workers provided the same heating lines exactly at the same areas as these 3 heating lines.

Table 11.4 Torsion evaluation for curved shell plate A

Torsion values measured by system v_{system} and (values measured by wooden template v_{wooden})						
	Contact location		Distance D_{upper} (mm)		Angle (°)	
	No.					
	v_{system}	v_{wooden}	v_{system}	v_{wooden}	v_{system}	v_{wooden}
Virtual template 1	@4	@4	+2.21	(+3)	-4.08	Middle
Virtual template 2	@2	@2	+4.02	(+5)	+4.2	Middle
Virtual template 3	@3	@3	-10.01	(-8)	+4.01	Middle
Virtual template 4	@4	@4	-2.24	(-2)	+4.17	Middle
Virtual template 5	@6	@5	+6.03	(+7)	-4.26	Middle

Figure 11-16(lower) shows the torsion evaluation view of curved shell plate A. Every frame is equally divided into 10 parts. The templates are rotated to every part on the measured frame, and the sums of the ends' distances between virtual templates and curved shell plate are calculated. Then the virtual templates are located at the positions as shown in Figure 11-16(lower) and the torsion evaluation result is shown in Table 11.4. It can be seen that the contact locations measured by the system and the ones measured by the wooden templates do not have big differences from each other. For the frame 5 though slight difference happens, the workers confirmed that the contact location measured by system could also be

considered effective because the shake extents of the wooden template from these two locations are the same.

It can be seen here the torsion almost complies the design because the angles between the perspective plane and the perspective sticks are all in $\pm 5^\circ$, but the big distance between upper plane and the endpoint of virtual template 3 shows that the heating along the portrait direction is insufficient. By using the wooden templates, the angles are not detected, while the differences between D_{upper} measured by system and D_{upper} measured by wooden templates are within 2mm which is considered acceptable.

From this preliminary experiment, the traditional way of deciding manufacturing plans were reproduced well in virtual environment though the torsion evaluation view. Besides, the basic performance of the proposed software system is evaluated by comparing the system suggested processing plans and the actually used processing plans. Strong correlation of these two plans confirmed the feasibility of the system. Some slight differences manifested the existing knowledge during processing which will be discussed in the following chapters.

Table 11.5 Experiment conditions in the general experiments

<i>Experiment conditions for point heating (refrigeration from upper side)</i>					
<i>Items</i>	<i>Plate Thickness (mm)</i>	<i>Refrigeration Method</i>	<i>Heating Time (s)</i>	<i>Heating Radius (mm)</i>	<i>Expected Contraction (mm)</i>
<i>Value</i>	14	By water	60	70	2.2 (upper heating) 1.6 (under heating)
<i>Experiment conditions for line heating (water refrigeration)</i>					
<i>Items</i>	<i>Plate Thickness (mm)</i>	<i>Refrigeration Method</i>	<i>Heating speed (mm/min)</i>	<i>Expected Contraction with heating line of 300mm (°)</i>	
<i>Value</i>	14	By water	170	-0.5 (upper refrigeration) 1.5 (under refrigeration)	
			260	1.5 (upper refrigeration)	

From the preliminary experiments in appendix for analyzing the relations between the heating conditions and the plate contraction, the manufacturing conditions for the following general experiment 1, 2 and 3 are decided as above.

11.6. Experiment 1 : Plate “Bowl 1”

11.6.1. Objective

In this experiment, a relatively small but complicated plate, Plate “Bowl 1”, is manufactured based on the analysis results of the proposed heating forming framework. The plate is scanned for 7 times before every manufacturing step including the final evaluation after the manufacturing. For every manufacturing step, the plate is scanned and registered to the design data, and the curvature errors and torsions are evaluated automatically. The worker W conducts the manufacturing based on the generated curvature error view and the torsion evaluation view. Another experiment assistant records the manufacturing plans (heating line set) for all the manufacturing steps.

11.6.2. Design data reforming and loading

The 3 different kinds of design data which is used for different evaluation purpose are listed as below.

- SAT curved surface design data (3D)
- DXF roller line design data (2D)
- DAT frame line design data (3D)

Figure 11-17 shows the SAT curved surface design data of the plate “Bowl 1”. As shown in this figure, the plate can be seen as a bowl type plate, and there are 190 points on the perimeter curve. The perimeters are designed as (1727mm, 2524mm, 2723mm, 2852mm).

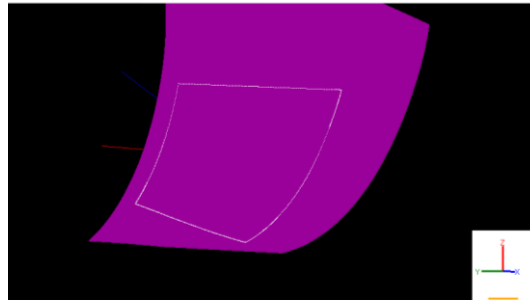


Figure 11-17 SAT design data of Plate “Bowl 1”

Figure 11-18 (left) shows the DXF file containing the 2D roller line design data of the plate “Bowl 1”. As shown in this figure, the 2D points existing on the roller lines are listed in the file and have to be extracted and matched to the 3D SAT files.

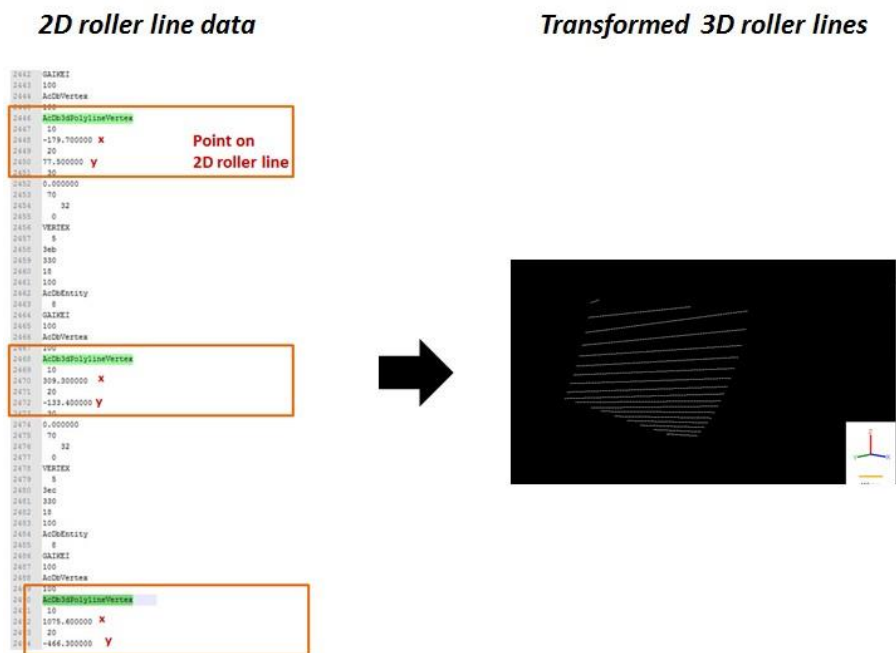


Figure 11-18 DXF file containing 2D roller line data of Plate “Bowl 1”

Figure 11-18 (right) shows the reformed roller lines in 3D. As shown in this figure, there are totally 18 different roller lines for this plate to help the workers keep the attention on the right torsion directions of the plate.

As shown in Figure 11-19, the 3D coordinates of the representative frame points of Plate “Bowl 1” are extracted from the DAT file which also containing the frames’ names such as “S4” and “S10”. The extracted 3D points are displayed in the 3D

virtual environment as shown in Figure 11-19 (right). There are totally 5 frames, 95 points representing the surface of plate “Bowl 1”. The average interval of the neighbor points is about 480mm.

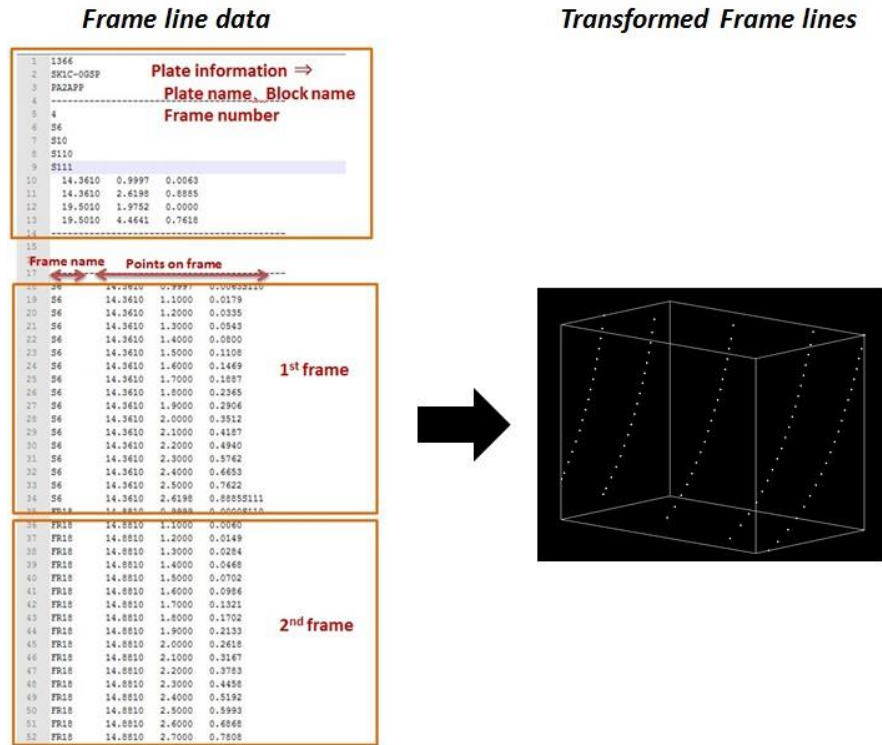


Figure 11-19 DAT file containing frame design data of Plate “Bowl 1”

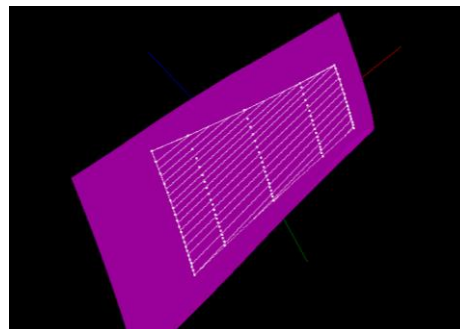


Figure 11-20 Registered design data of Plate “Bowl 1”

The roller lines’ point cloud, the CAD surface and the frame lines’ point cloud of the plate “Bowl 1” are all registered together as shown in Figure 11-20.

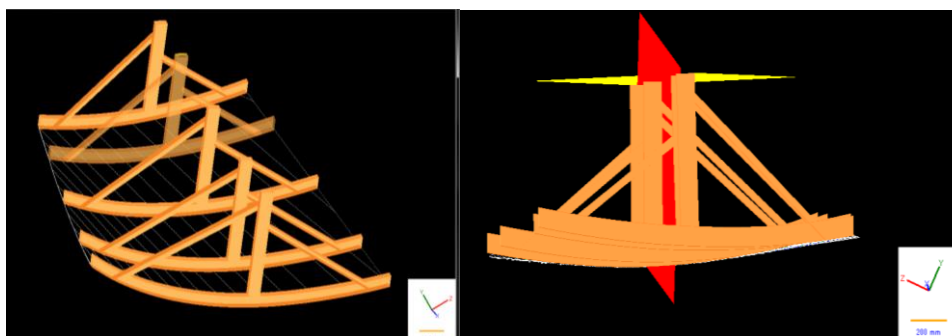


Figure 11-21 Virtual template generation of Plate “Bowl 1”

Figure 11-21 shows the generated virtual templates of the plate “Bowl 1”. The virtual templates are generated following the conventional wooden template’s producing tradition. The bottom lines of the generated virtual templates pass all of the frame design points. And the representative planes, perspective plane which passes all the wooden templates’ sticks and upper plane which passes all the upper points of the wooden templates are also painted as shown in Figure 11-21 (right).

11.6.3. Analysis results for one manufacturing step

The workers totally run the automation engine and manufactured plate “Bowl 1” for 6 times. For every manufacturing step, the plate is extracted from the measured data automatically and registered to the design data prepared in 11.6.2 for the following analysis.

The sample plate analysis result of plate “Bowl 1” (for the first manufacturing step) is illustrated in this subsection. The executive time and the manufacturing plan suggested by the proposed framework are explained too.

11.6.3.1. Plate measurement

As shown in Figure 11-22, the plate is measured with the obstacles including the floor, the shadows of the wooden templates and water. The plate is extracted from these obstacles by the reformed region growing method.

There are totally 350 thousand points existing in the raw measured point cloud. The average interval between the points is about 5mm.

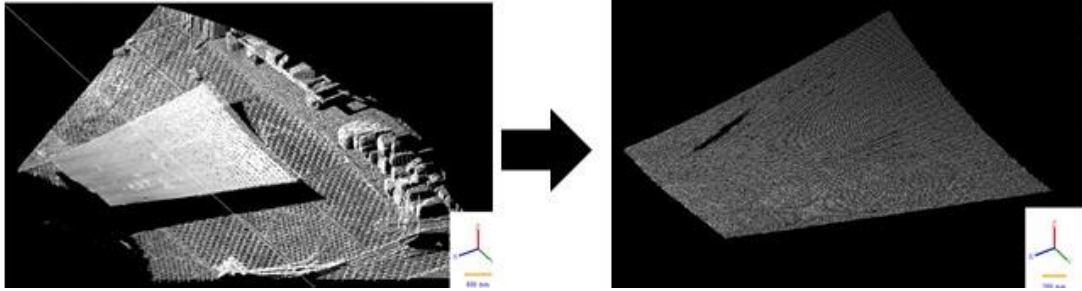


Figure 11-22 Extraction of Plate “Bowl 1” (Step1)

Figure 11-22 (right) shows the extraction result of plate “Bowl 1”. 50 thousand points representing the measured shape of plate are extracted within 50 seconds.

After plate “Bowl 1” is extracted from the raw measured point cloud, it is registered to the design data prepared in 11.6.2 for the following analysis. Figure 11-23 (left) illustrates the registration result of the virtual templates and the extracted plate. All of the relative data are registered together for the curvature comparison and virtual template rotation. On this occasion, the virtual templates still keep the designed locations without being rotated respectively. This process cost only 18 seconds.

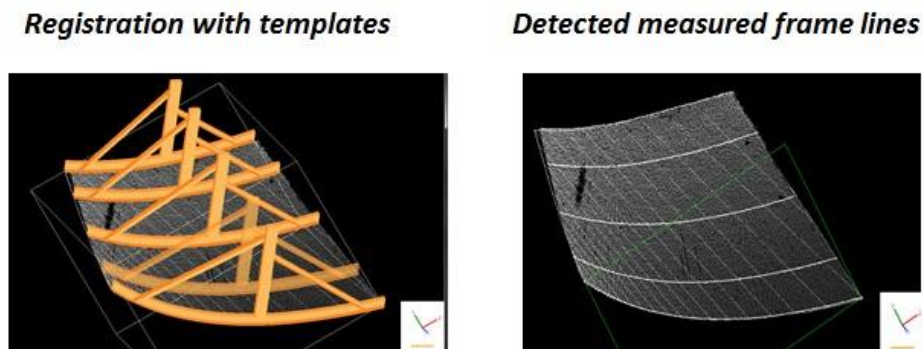


Figure 11-23 Registration result of Plate “Bowl 1” (Step1)

After all of the measured data and the designed data of plate “Bowl 1” are registered together, just as the conventional way to use wooden template, the corresponding frame line of each virtual template on the measured plate are calculated and painted on the plate as shown in Figure 11-23 (right). This process cost only 10 seconds.

11.6.3.2. Plate analysis

Figure 11-24 shows the distance error analysis result of Plate “Bowl 1”. The threshold is set to 5mm. As shown in the figure, there are over 50% of the points out of the threshold range which means the plate has to be deformed to achieve the design shape. Moreover, since the blue areas where the measured points are below the designed surface are at the two sides of the plate, the curvatures of the 3 frames in the middle of the plate are smaller than the designed curvatures. The red areas where the measured points are above the designed surface are on the two sides of the plate (vertical direction).

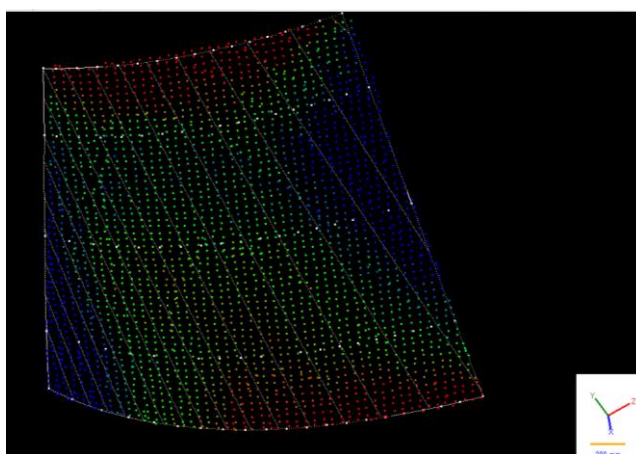


Figure 11-24 Distance error analysis result of Plate “Bowl 1” (Step1)

Then the torsion situation of the plate is evaluated as shown in Figure 11-25. The virtual templates are rotated automatically to the proper locations to help the worker check the plate’s torsion. The angles between the virtual templates’ sticks and the perspective plane are calculated and displayed in the half-transparent message box. The angles are (0, 0, 0, 0, 0) which means there are not yet improper torsions in this occasion, while the distance between the endpoints of the virtual templates’ sticks and the upper plane are (10, -7, -7 -3, 7) (mm) which means the vertical curvatures should be changed too to achieve the designed shape. The distances between the ends of the virtual templates’ bottom lines and the measured plate are {(13, 20), (8, 16), (20, 12), (20, 1), (9, 12)} (mm).

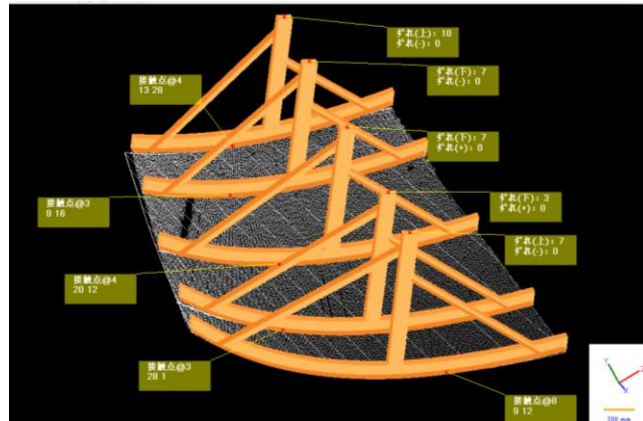


Figure 11-25 Torsion analysis results of Plate “Bowl 1” (Step1)

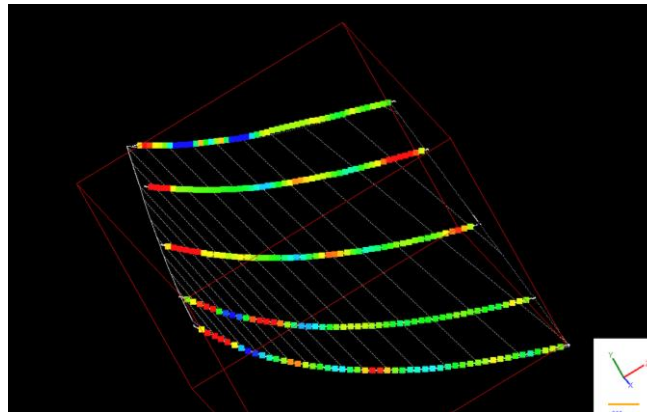


Figure 11-26 Curvature error analysis results of Plate “Bowl 1” (Step1)

The curvature errors at the frame points are calculated and displayed as shown in Figure 11-26. The red areas are that have smaller curvatures and have to be applied deforming on the upper side of the plate. In this case, because the torsion of the plate is still normal, the heating lines can be applied along with the roller lines passing the red areas.

11.6.3.3. Manufacturing plan design and manufacturing

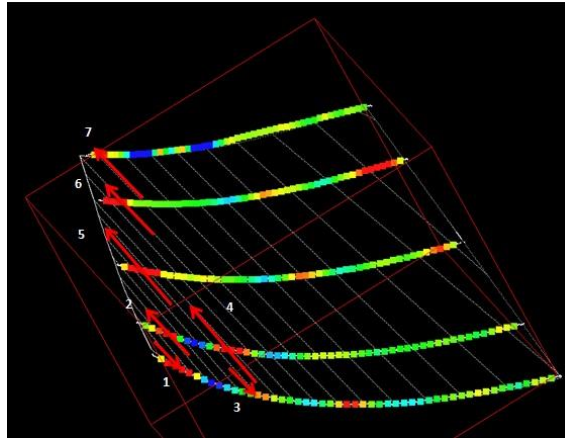


Figure 11-27 Designed manufacturing plan for “Bowl 1” (Step1)

The manufacturing plan designed for this step is as shown in Figure 11-27. There are totally 7 heating lines designed for this manufacturing step. These heating lines are all applied along with the roller lines passing the red areas (the areas with insufficient curvatures). In this experiment, the plate is manufactured without considering the heating grades which lead to the over bending at the last 2 steps.

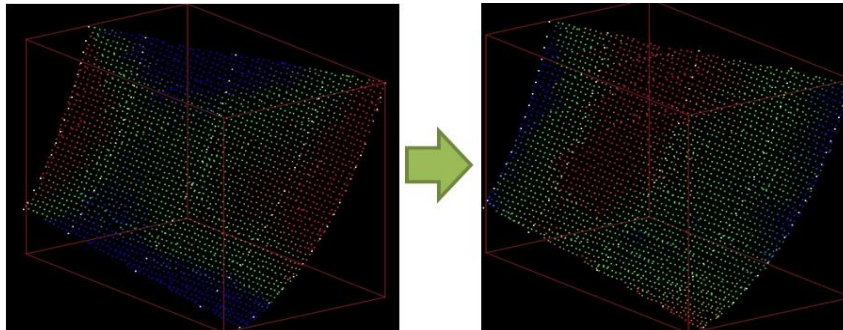


Figure 11-28 Displacement color map before and after this manufacturing step (“Bowl 1”)

The plate’s displacement color map’s change is as shown in Figure 11-28, the blue areas are reduced by applying the heating lines along with the roller lines; while the plate’s displacement error histogram before and after this manufacturing step is as below. It can be seen that the displacement error decreased after this manufacturing step. The points with displacement within 5mm increased from 47% to 63%. And the standard deviation σ also decreased from 8.9mm to 6.2mm.

Table 11.6 Plate evaluation results before and after this manufacturing step (A1*S)

<i>Step</i>	<i>Ratio of the points with (displacement < 5mm)</i>	<i>Standard deviation</i>
Before Step 1	47%	8.9mm
After Step 1	63%	6.2mm

11.6.4. Manufacturing plans for all the steps

The manufacturing plans used to manufacture plate “Bowl 1” is as shown in Figure 11-29. All of the heating lines in this figure are based on the analysis results generated by the proposed framework. In this case, for the last 1 step, the blue heating points in this figure are applied because the right part of the plate is found over bended. The manufacturing process cost totally 3.5 hours including the scanning, measurement, analysis and manufacturing. The average manufacturing time of this plate using the real wooden template (expert workers) is about 5 hours. Here some heating steps are applied on points; the point heating plan’s design will

be discussed in the discussion chapter.

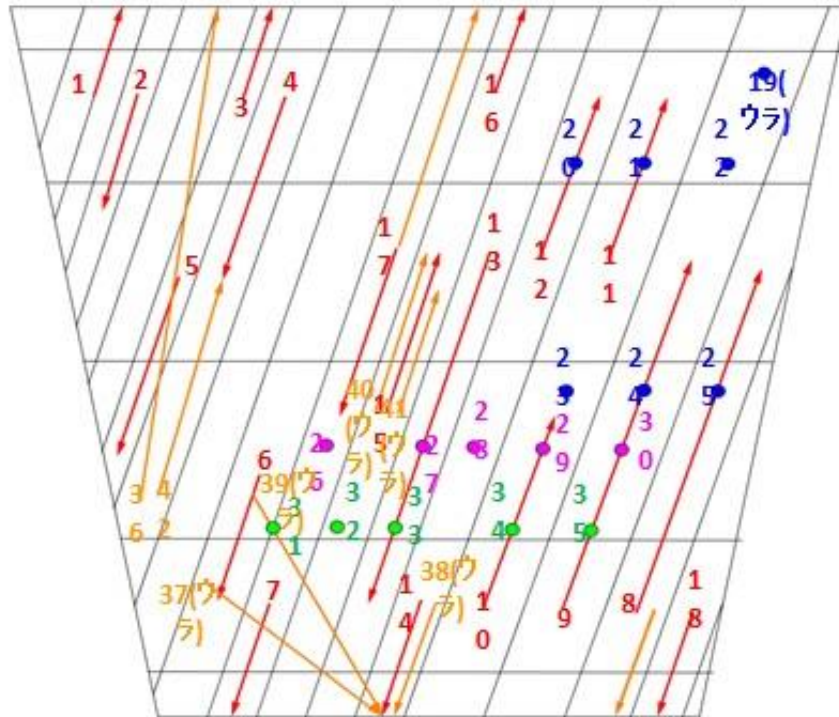


Figure 11-29 Manufacturing actions of Plate “Bowl 1” (all the steps)

11.6.5. Manufacturing results

The manufacturing results (the distance errors between the measured plate and the design surface) of all the manufacturing steps are as shown in Figure 11-30. The green areas are that have the error within 5mm. At last over 90% points are within the threshold.

Unlike plate “Bowl 2” and “Hybrid 1”, this plate is just test piece so that it was not passed to the heat sealing process. The final shape was checked by the expert workers using the real wooden templates.

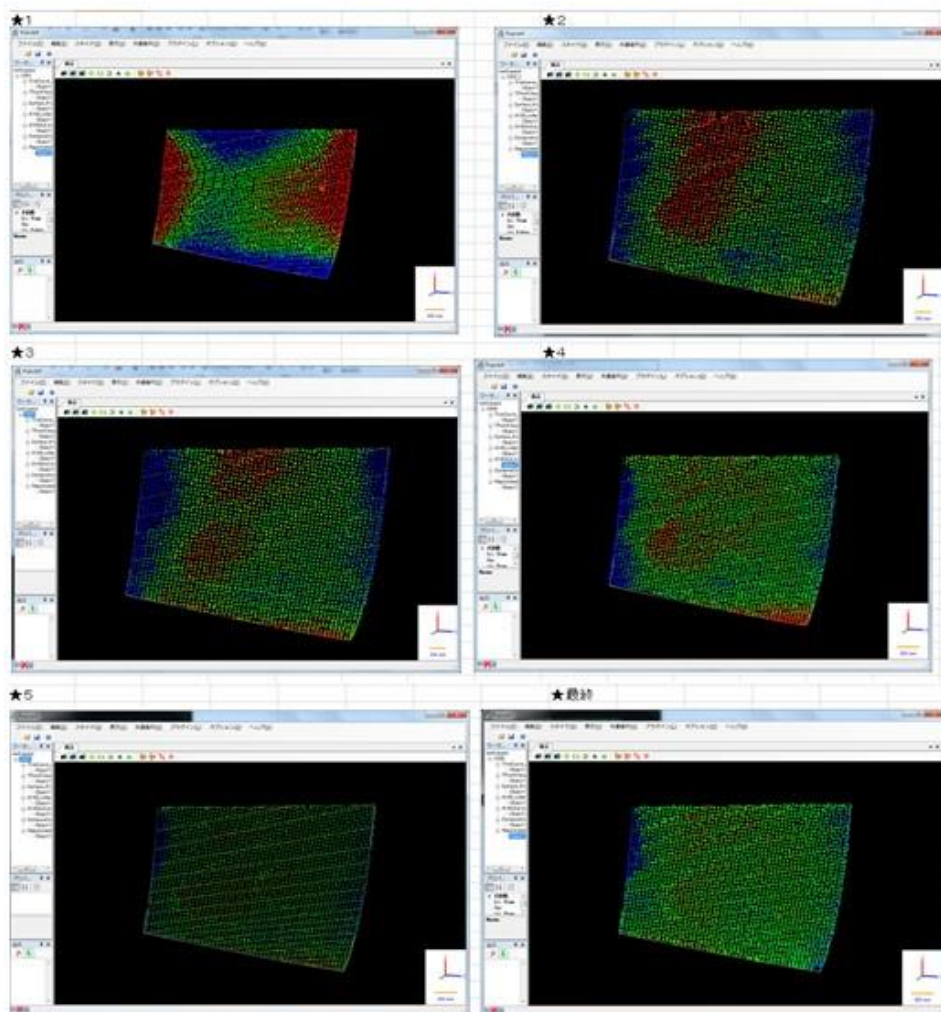
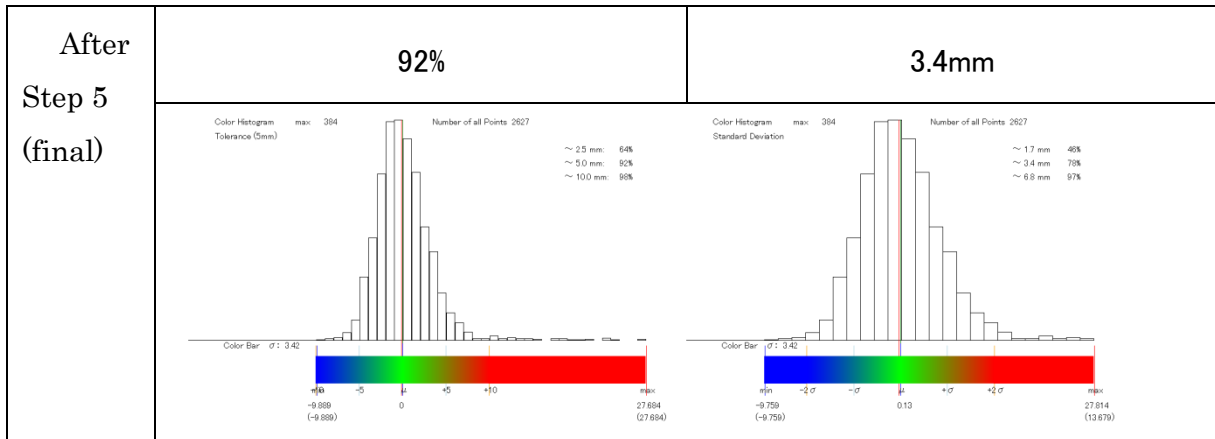


Figure 11-30 Manufacturing result of Plate “Bowl 1” (all the steps)

Specifically, the distance error histograms from the 1st manufacturing step till the last one are as shown in the following table.

Table 11.7 Plate evaluation results after each manufacturing step (“Bowl 1”)

Step	Ratio of the points with (displacement < 5mm)	Standard deviation
After Step 2	61%	5.9mm
After Step 3	76%	4.8mm
After Step 4	86%	4.3mm



As shown in Figure 11-31, the ratio of points with displacement smaller than 5mm increases after most of the manufacturing steps; while the points' displacement standard deviation decreased after every manufacturing step. This proved that the manufacturing plans designed based on the proposed framework are effective.

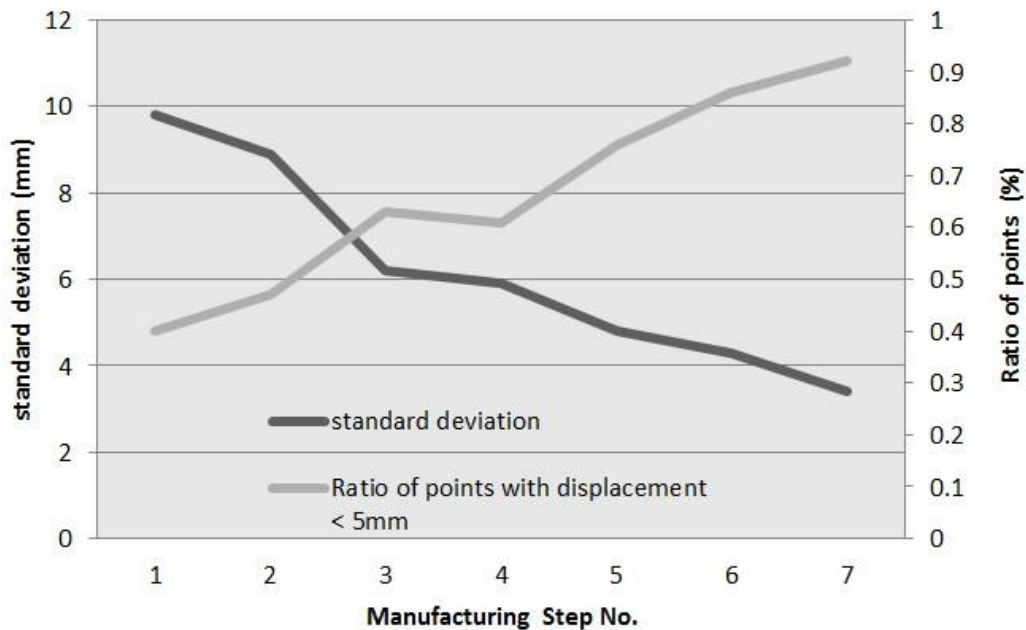


Figure 11-31 Plate's evaluation results for all the manufacturing steps ("Bowl 1")

11.7. Experiment 2 : Plate “Bowl 2”

11.7.1. Objective

In this experiment, a relatively small but complicated plate, Plate “Bowl 2” which is the symmetrical side plate of the Plate “Bowl 1”, is manufactured based on the analysis results of the proposed heating forming framework. The plate is scanned for 10 times before every manufacturing step including the final evaluation after the manufacturing. For every manufacturing step, the plate is scanned and registered to the design data, and the curvature errors and torsions are evaluated automatically. The worker W conducts the manufacturing based on the generated curvature error view and the torsion evaluation view. Another experiment assistant records the manufacturing plans (heating line set) for all the manufacturing steps.

11.7.2. Design data reforming and loading

The 3 different kinds of design data which is used for different evaluation purpose are listed as below.

- SAT curved surface design data (3D)
- DXF roller line design data (2D)
- DAT frame line design data (3D)

Figure 11-32 shows the SAT curved surface design data of the plate “Bowl 2”. As shown in this figure, the plate can be seen as a bowl type plate, and there are 190 points on the perimeter curve.

Since plate “Bowl 2” is symmetrical of plate “Bowl 1”, so they share the DXF file containing the 2D roller line design data with the plate “Bowl 1”. As shown in this figure, there are totally 18 different roller lines for this plate to help the workers keep the attention on the right torsion directions of the plate.

The 3D coordinates of the representative frame points of Plate “Bowl 2” are extracted from the DAT file which also containing the frames’ names such as “S4” and “S10”. The extracted 3D points are displayed in the 3D virtual environment. There are totally 5 frames, 95 points representing the surface of plate “Bowl 2”. The average interval of the neighbor points is about 480mm.

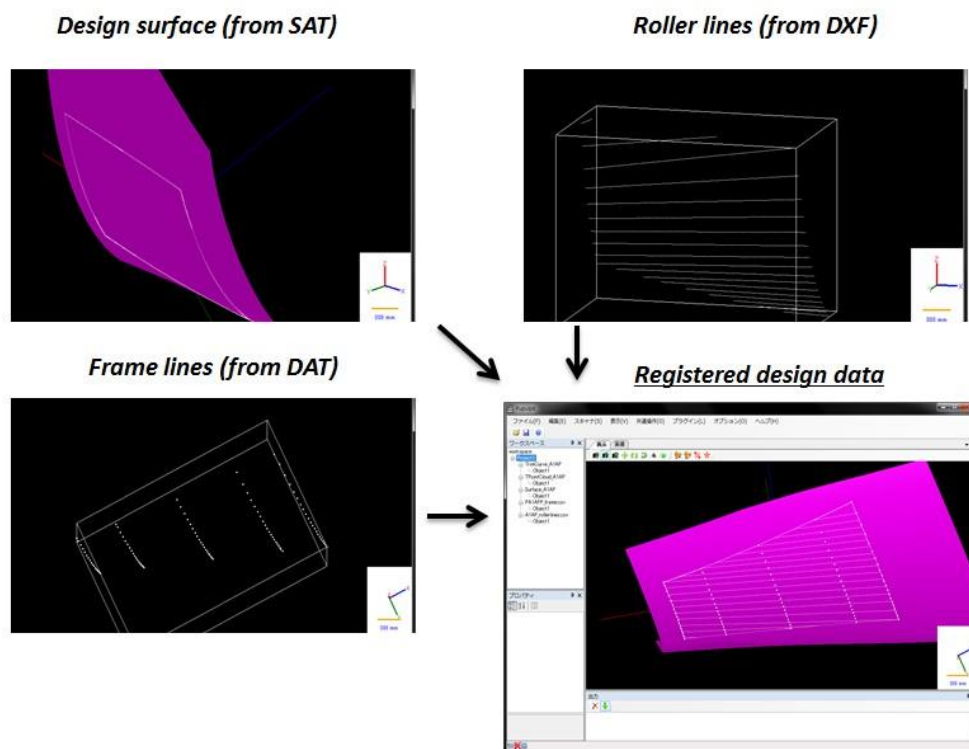


Figure 11-32 design data of Plate “Bowl 2”

As the last step of the preparation of the design data, the roller lines’ point cloud, the CAD surface and the frame lines’ point cloud of the plate “Bowl 2” are all registered together.

Figure 11-33 shows the generated virtual templates of the plate “Bowl 2”. The virtual templates are generated following the conventional wooden template’s producing tradition. The bottom lines of the generated virtual templates pass all of the frame design points. And the representative planes, perspective plane which passes all the wooden templates’ sticks and upper plane which passes all the upper points of the wooden templates are also painted on computer. As shown in this figure, this plate is symmetrical with the plate “Bowl 1” used in prior experiment 1.

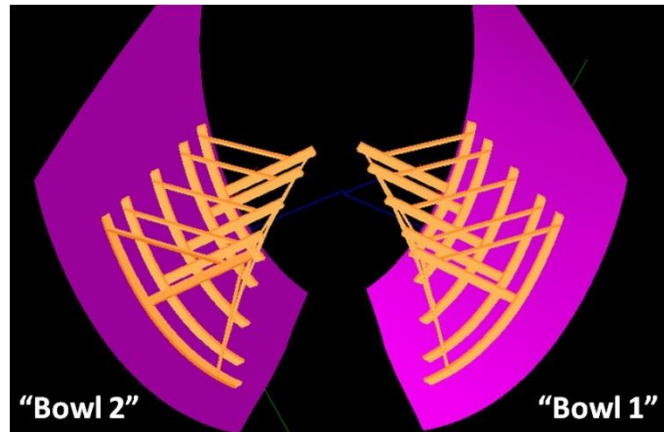


Figure 11-33 Virtual template generation of Plate “Bowl 2”

11.7.3. Analysis results for one manufacturing step

The workers totally run the automation engine and manufactured plate “Bowl 2” for 8 times. For every manufacturing step, the plate is extracted from the measured data automatically and registered to the design data prepared in 11.7.2 for the following analysis.

The sample plate analysis result of plate “Bowl 2” (for the first manufacturing step) is illustrated in this subsection. The executive time and the manufacturing plan suggested by the proposed framework are explained too.

11.7.3.1. Plate measurement

As shown in Figure 11-34 (left), the plate is measured with the obstacles including the floor, the support wood, the shadows of the wooden templates and water. The plate is extracted from these obstacles by the reformed region growing method.

There are totally 215 thousand points existing in the raw measured point cloud. The average interval between the points is about 6mm.

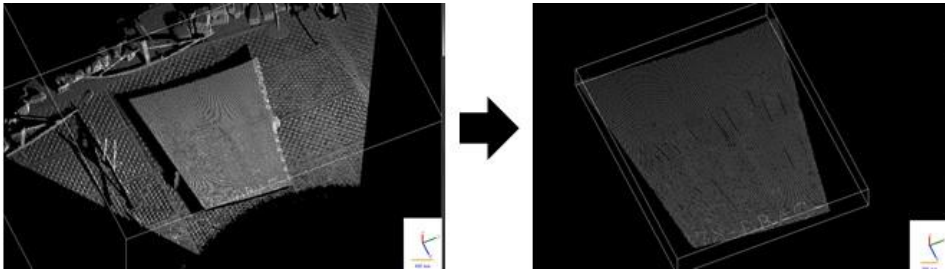


Figure 11-34 Extraction of Plate “Bowl 2” (Step1)

Figure 11-34 (right) shows the extraction result of plate “Bowl 2”. 53 thousand points representing the measured shape of plate are extracted within 52 seconds.

After plate “Bowl 2” is extracted from the raw measured point cloud, it is registered to the design data prepared in 11.7.2 for the following analysis. Figure 11-35 (left) illustrates the registration result of the virtual templates and the extracted plate. All of the relative data are registered together for the curvature comparison and virtual template rotation. On this occasion, the virtual templates still keep the designed locations without being rotated respectively. This process cost only 20 seconds.

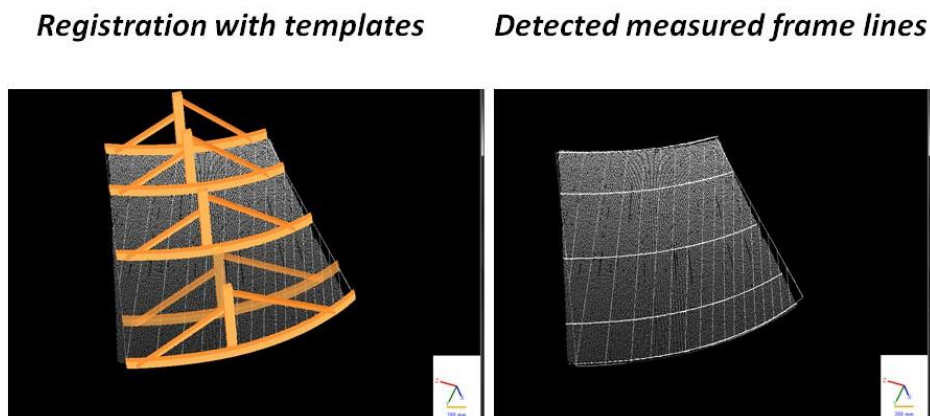


Figure 11-35 Registration result of Plate “Bowl 2” (Step1)

After all of the measured data and the designed data of plate “Bowl 2” are registered together, just as the conventional way to use wooden template, the corresponding frame line of each virtual template on the measured plate are calculated and painted on the plate as shown in Figure 11-35 (right). This process cost only 9 seconds.

11.7.3.2. Plate analysis

Figure 11-36 shows the distance error analysis result of Plate “Bowl 2”. The threshold is set to 5mm. As shown in the figure, there are over 60% of the points out of the threshold range which means the plate has to be deformed to achieve the design shape. Moreover, since the blue areas where the measured points are below the designed surface are at the two sides of the plate, the curvatures of the 3 frames in the middle of the plate are smaller than the designed curvatures. The red areas where the measured points are above the designed surface are on the two sides of the plate (vertical direction) and spread to the middle of the plate.

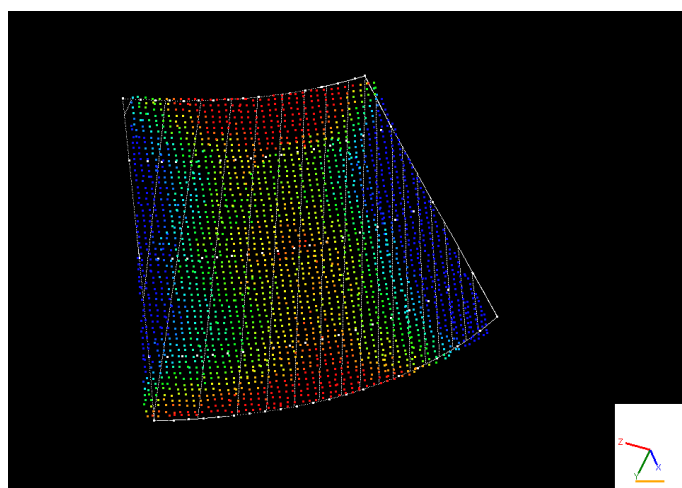


Figure 11-36 Distance error analysis results of Plate “Bowl 2” (Step1)

Then the torsion situation of the plate is evaluated as shown in Figure 11-37. The virtual templates are rotated automatically to the proper locations to help the worker check the plate’s torsion. The angles between the virtual templates’ sticks and the perspective plane are calculated and displayed in the half-transparent message box. Since the threshold of the angles are set to 5° . The calculated angles are (0, 0, 1, 1, -2) which means there are not yet improper torsions in this occasion. The distance between the endpoints of the virtual templates’ sticks and the upper plane are (4, -3, -1, -2, 3) (mm) which means the vertical curvatures should be changed too to achieve the designed shape. The distances between the ends of the

virtual templates' bottom lines and the measured plate are $\{(12, 24), (31, 5), (34, 16), (50, 15), (26, 13)\}$ (mm).

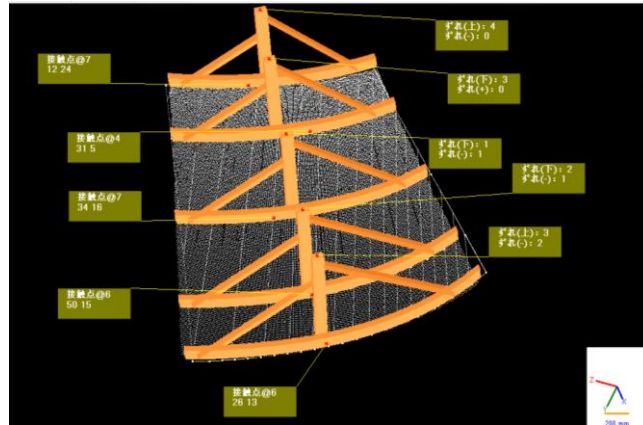


Figure 11-37 Torsion analysis results of Plate “Bowl 2” (Step1)

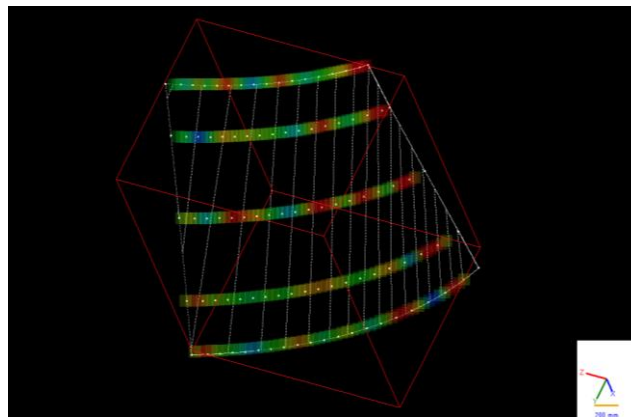


Figure 11-38 Curvature error analysis results of Plate “Bowl 2” (Step1)

The curvature errors at the frame points are calculated and displayed as shown in Figure 11-38. The red areas are that have smaller curvatures and have to be applied deforming on the upper side of the plate. In this case, because the torsion of the plate is still normal, the heating lines can be applied along with the roller lines passing the red areas.

11.7.3.3. Manufacturing plan design and manufacturing

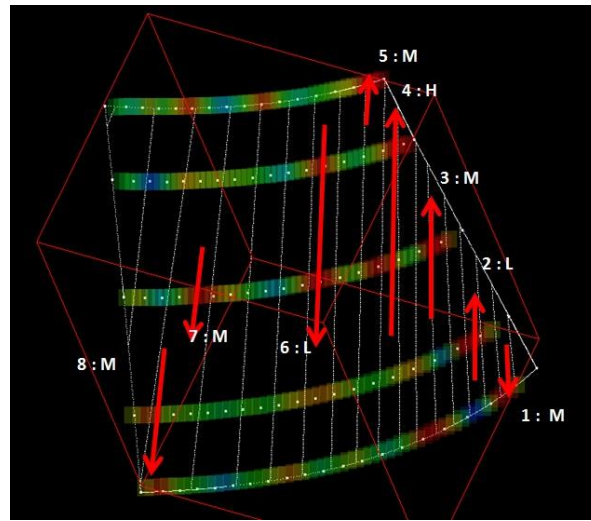


Figure 11-39 Designed manufacturing plan for “Bowl 2” (Step1)

The manufacturing plan designed for this step is as shown in Figure 11-39. There are totally 8 heating lines designed for this manufacturing step. These heating lines are all applied along with the roller lines passing the red areas (the areas with insufficient curvatures). In this experiment, the plate is manufactured considering the 3 heating grades (H, M, L).

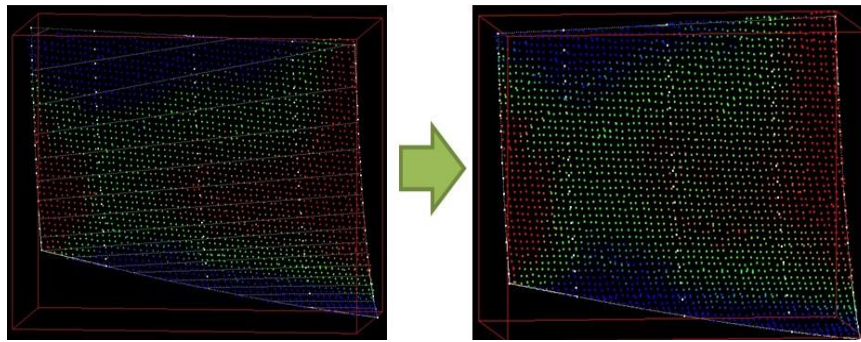


Figure 11-40 Displacement color map before and after this manufacturing step (“Bowl 2”)

The plate’s displacement color map’s change is as shown in Figure 11-40; while the plate’s displacement error histogram before and after this manufacturing step is as below. It can be seen that the displacement error decreased after this manufacturing step. The points with displacement within 5mm increased from 38% to 48%. And the standard deviation σ also decreased from 10mm to 7.9mm.

Table 11.8 Plate evaluation results before and after this manufacturing step (“Bowl 2”)

Step	<i>Ratio of the points with (displacement < 5mm)</i>	<i>Standard deviation</i>
Before Step 1	38%	10.0mm
After Step 1	48%	7.9mm

11.7.4. Manufacturing plans for all the steps

The manufacturing plans used to manufacture plate “Bowl 2” is as shown in Figure 11-41. All of the heating lines in this figure are based on the analysis results generated by the proposed framework. In this case, no over bending is found, thus all of the heating lines and heating points are applied from the upper side of the plate. The manufacturing process cost totally 4.5 hours including the scanning, measurement, analysis and manufacturing. The average manufacturing time of this plate using the real wooden template (expert workers) is about 5 hours.

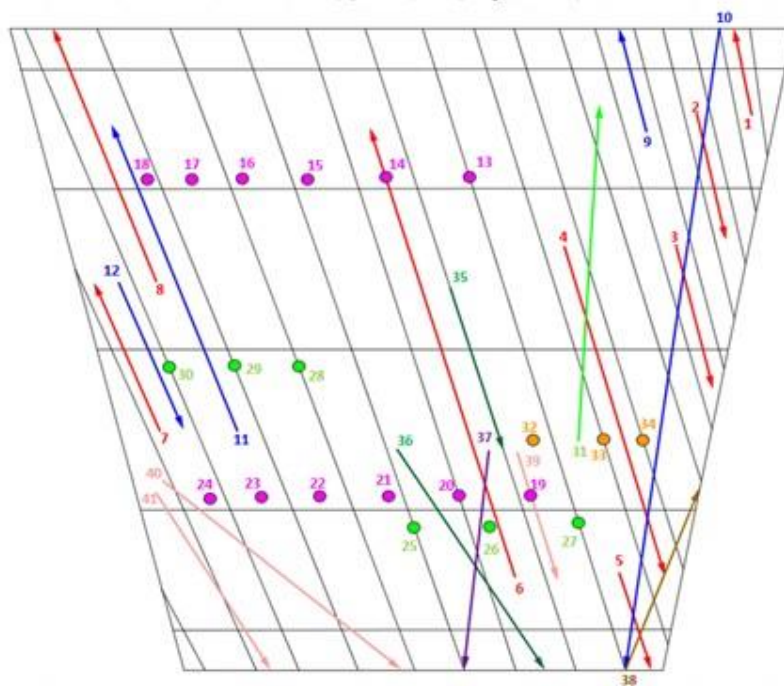


Figure 11-41 Manufacturing actions of Plate “Bowl 2” (all the steps)

11.7.5. Manufacturing results

The manufacturing results (the distance errors between the measured plate and the design surface) of all the manufacturing steps are as shown in Figure 11-30. The green areas are that have the error within 5mm. At last over 90% points are within the threshold.

This plate is a real plate which is supposed to be used on the ship. Before being passed to the heat sealing process, the final shape was checked by the expert workers using the real wooden templates.

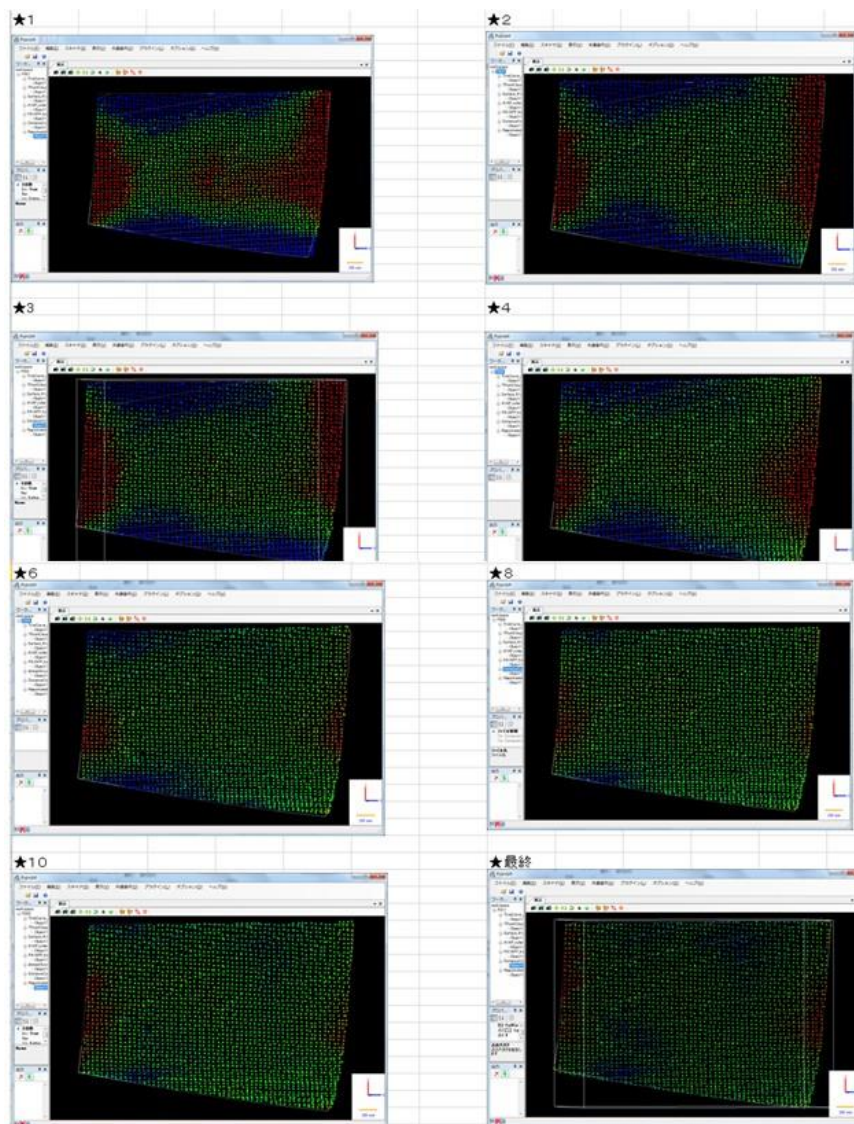
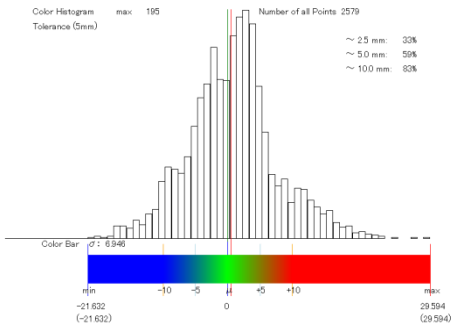
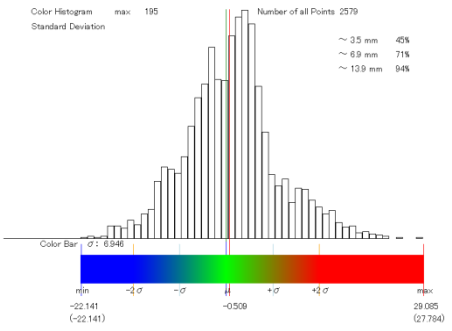
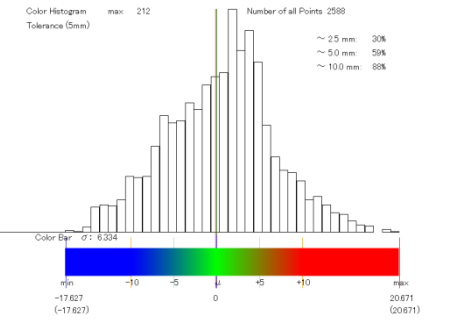
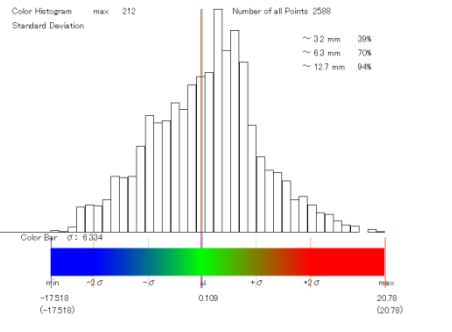
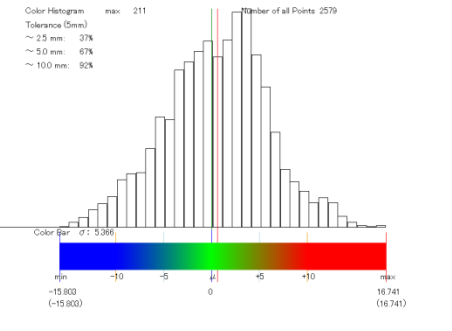
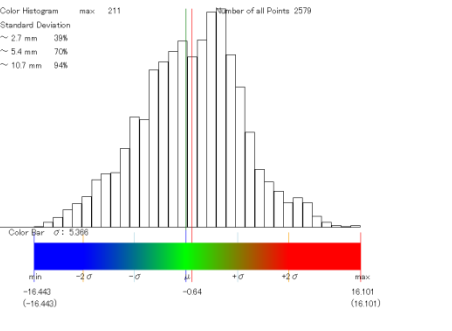
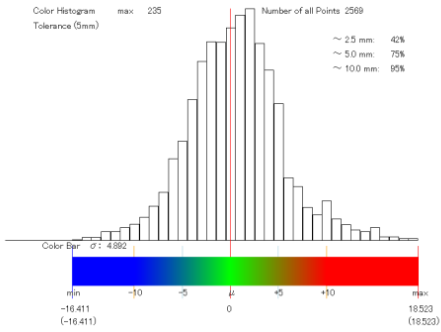
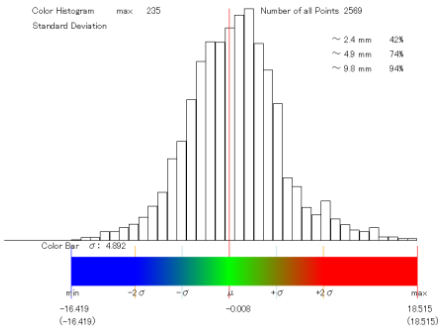
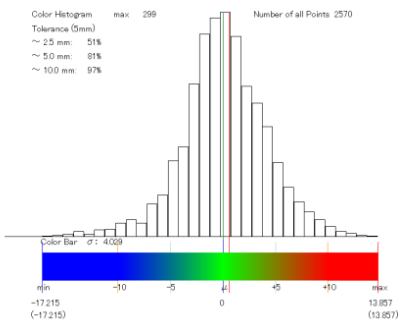
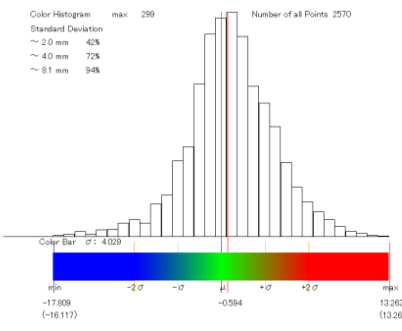
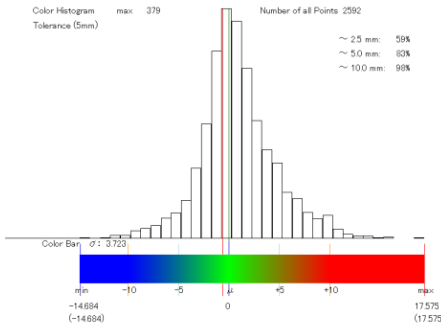
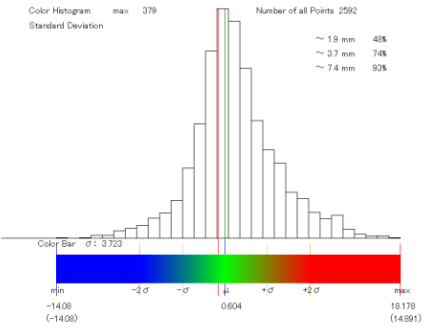


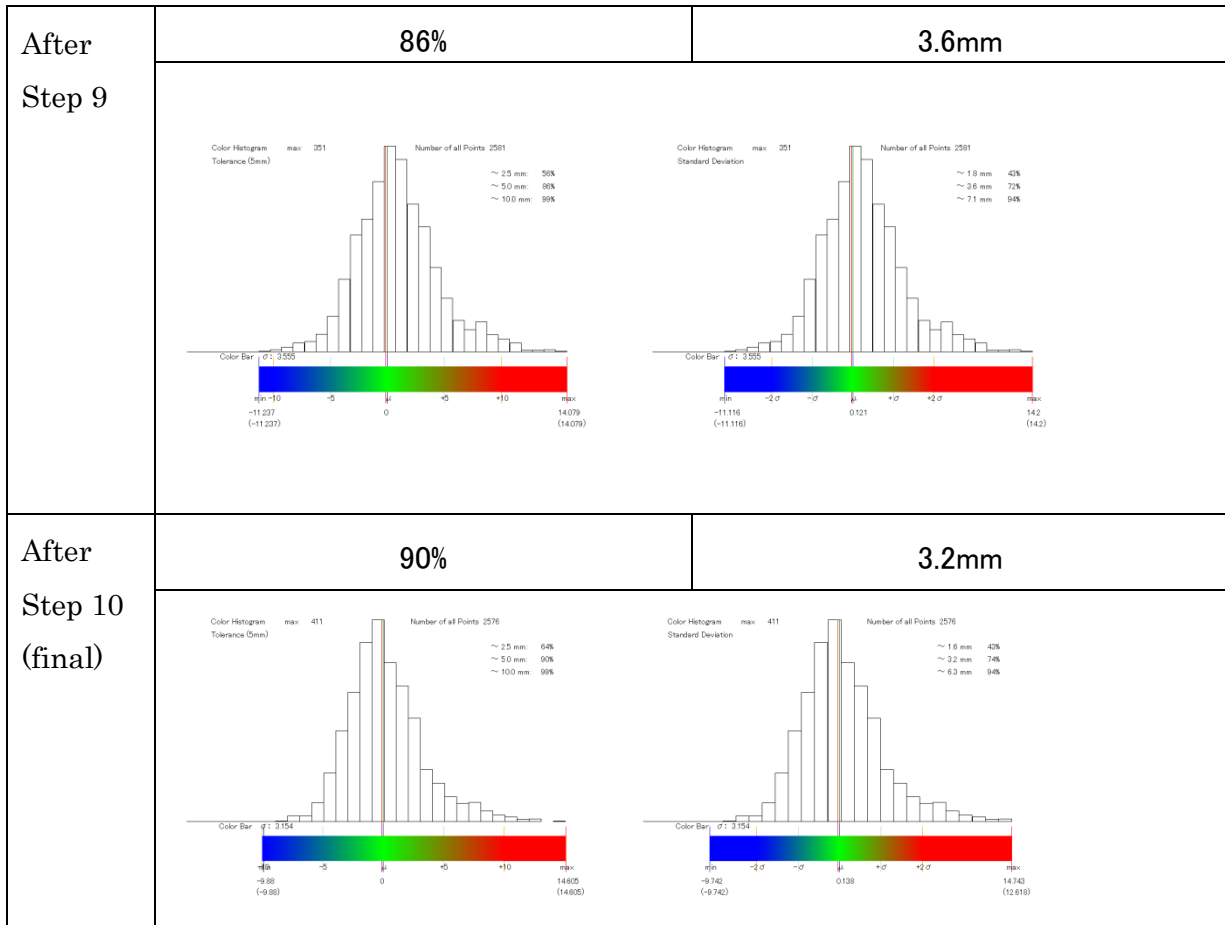
Figure 11-42 Manufacturing result of Plate “Bowl 2” (all the steps)

Specifically, the distance error histograms from the 1st manufacturing step till the last one are as below.

Table 11.9 Plate evaluation results after each manufacturing step (A1*P)

Step	Ratio of the points with (displacement < 5mm)	Standard deviation
After Step 2	<p style="text-align: center;">59%</p> 	<p style="text-align: center;">6.9mm</p> 
After Step 3	<p style="text-align: center;">59%</p> 	<p style="text-align: center;">6.3mm</p> 
After Step 4	<p style="text-align: center;">67%</p> 	<p style="text-align: center;">5.4mm</p> 

<p>After Step 6</p>	<p style="text-align: center;">75%</p> 	<p style="text-align: center;">4.9mm</p> 
<p>After Step 7</p>	<p style="text-align: center;">81%</p> 	<p style="text-align: center;">4.0mm</p> 
<p>After Step 8</p>	<p style="text-align: center;">83%</p> 	<p style="text-align: center;">3.7mm</p> 



As shown in Figure 11-43, the ratio of points with displacement smaller than 5mm increases after most of the manufacturing steps; while the points' displacement standard deviation decreased after every manufacturing step. This proved that the manufacturing plans designed based on the proposed framework are effective.

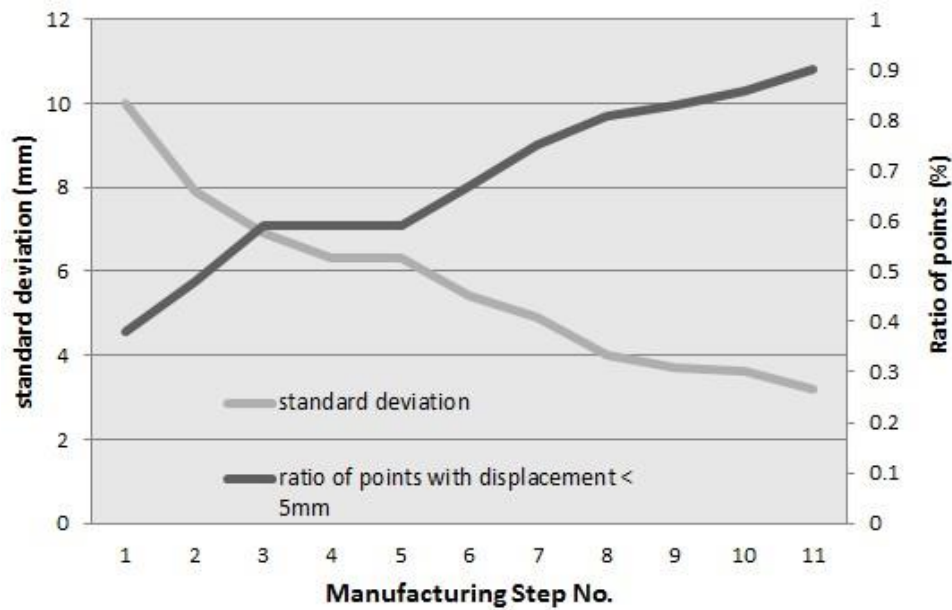


Figure 11-43 Plate's evaluation results for all the manufacturing steps ("Bowl 2")

11.8. Experiment 3 : Plate "Hybrid 1"

11.8.1. Objective

In this experiment, a relatively small but very complicated plate with both the features of the bowl type plate and the saddle type plate, Plate "Hybrid 1", is manufactured based on the analysis results of the proposed heating forming framework. The plate is scanned for 8 times before every manufacturing step including the final evaluation after the manufacturing. For every manufacturing step, the plate is scanned and registered to the design data, and the curvature errors and torsions are evaluated automatically. The worker W conducts the manufacturing based on the generated curvature error view and the torsion evaluation view. Another experiment assistant records the manufacturing plans (heating line set) for all the manufacturing steps.

11.8.2. Design data reforming and loading

The 3 different kinds of design data which is used for different evaluation purpose are listed as below.

- SAT curved surface design data (3D)
- DXF roller line design data (2D)
- DAT frame line design data (3D)

Figure 11-44 shows the SAT curved surface design data of the plate “Hybrid 1”. As shown in this figure, the plate can be seen as a bowl type plate, and there are 190 points on the perimeter curve. The size of this plate is about 1750mm × 1420mm (adjacent edges). The relative positions of this plate and the plates used in experiment 1 and 2 are also shown in the figure. It is close to the starboard of the ship and with great importance to have the high accuracy. The average manufacturing time for this plate is about 11 hours.

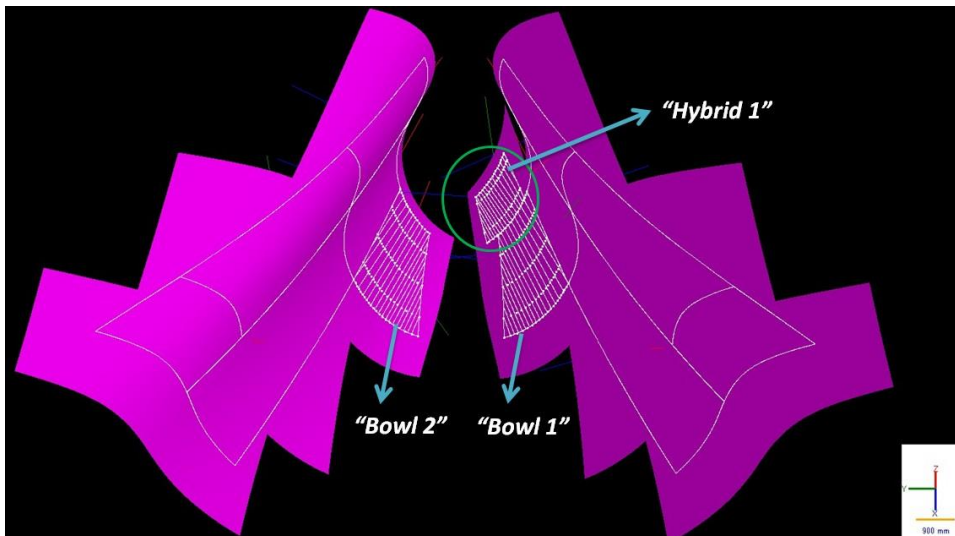


Figure 11-44 NURBS design data of Plate “Hybrid 1”

Figure 11-45 shows the DXF file containing the 2D roller line design data of the plate “Hybrid 1”. As shown in this figure, the 2D points existing on the roller lines are listed in the file and have to be extracted and matched to the 3D SAT files.

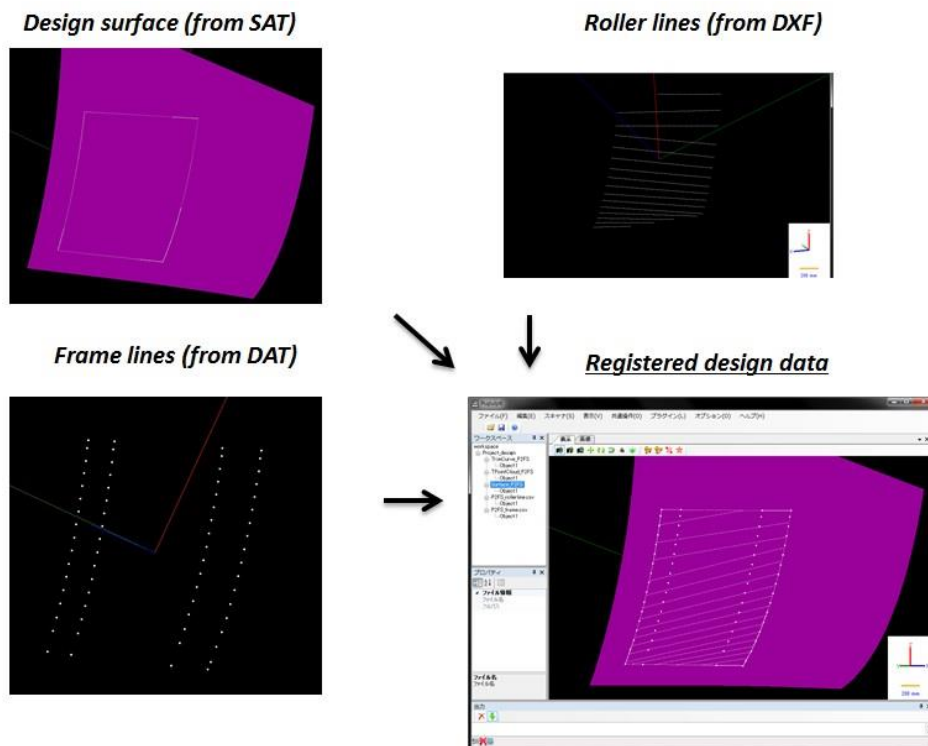


Figure 11-45 Design data of Plate “Hybrid 1”

According to the reformed roller lines in 3D shown in this figure, there are totally 16 different roller lines for this plate to help the workers keep the attention on the right torsion directions of the plate.

The 3D coordinates of the representative frame points of Plate “Hybrid 1” are also extracted from the DAT file. There are totally 4 frames, 69 points representing the surface of plate “Hybrid 1”. The average interval of the neighbor points is about 520mm. The roller lines’ point cloud, the CAD surface and the frame lines’ point cloud of the plate “Hybrid 1” are all registered together.

Figure 11-46 shows the generated virtual templates of the plate “Hybrid 1”. The virtual templates are generated following the conventional wooden template’s producing tradition. The bottom lines of the generated virtual templates pass all of the frame design points.

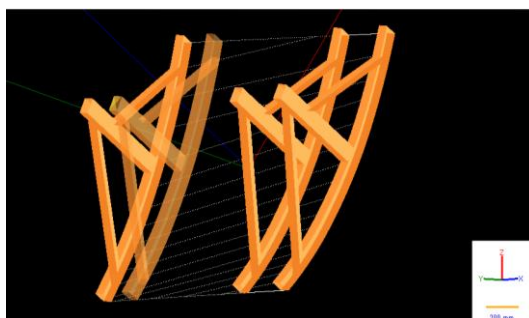


Figure 11-46 Virtual template generation results of Plate “Hybrid 1”

11.8.3. Analysis results for one manufacturing step

The workers totally run the automation engine and manufactured plate “Hybrid 1” for 10 times. For every manufacturing step, the plate is extracted from the measured data automatically and registered to the design data prepared in 11.8.2 for the following analysis.

The sample plate analysis result of plate “Hybrid 1” (for the first manufacturing step) is illustrated in this subsection. The executive time and the manufacturing plan suggested by the proposed framework are explained too.

11.8.3.1. Plate measurement

As shown in Figure 11-47 (left), the plate is measured with the obstacles including the floor, the support wood, the shadows of the crane and the water. The plate is extracted from these obstacles by the reformed region growing method.

There are totally 950 thousand points existing in the raw measured point cloud. The average interval between the points is about 5mm.

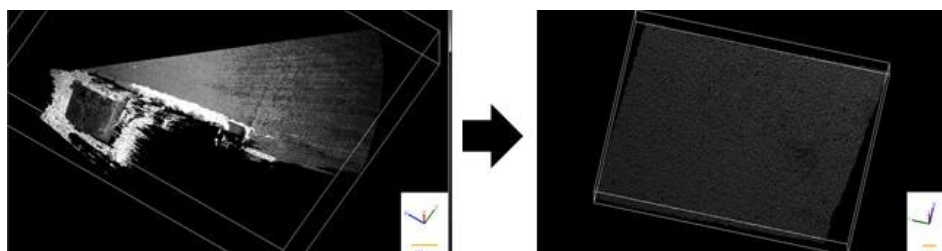


Figure 11-47 Extraction of Plate “Hybrid 1” (Step1)

Figure 11-47 (right) shows the extraction result of plate “Bowl 2”. 28 thousand points representing the measured shape of plate are extracted within 49 seconds.

After plate “Hybrid 1” is extracted from the raw measured point cloud, it is registered to the design data prepared in 11.8.2 for the following analysis. Figure 11-48 (left) illustrates the registration result of the virtual templates and the extracted plate. All of the relative data are registered together for the curvature comparison and virtual template rotation. On this occasion, the virtual templates still keep the designed locations without being rotated respectively. This process cost only 21 seconds.

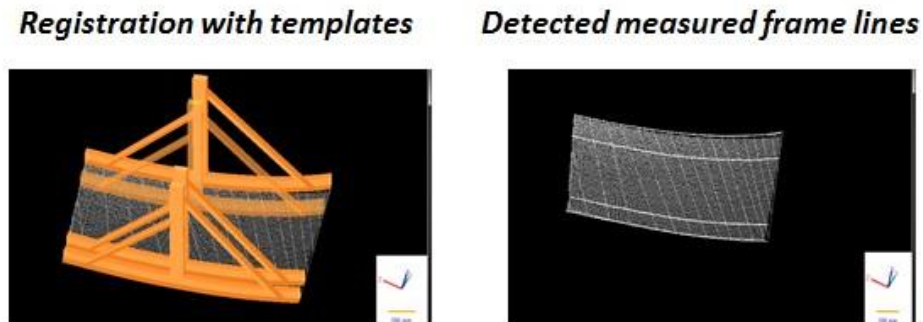


Figure 11-48 Registration result of Plate “Hybrid 1” (Step1)

After all of the measured data and the designed data of plate “Hybrid 1” are registered together, just as the conventional way to use wooden template, the corresponding frame line of each virtual template on the measured plate are calculated and painted on the plate as shown in Figure 11-48 (right). This process cost only 9 seconds.

11.8.3.2. Plate analysis

Figure 11-49 shows the distance error analysis result of Plate “Hybrid 1”. The threshold is set to 4mm. As shown in the figure, there are over 62% of the points out of the threshold range which means the plate has to be deformed to achieve the design shape. Moreover, since the blue areas where the measured points are below the designed surface are at the two sides of the plate, the curvatures of the 5 frames

in the middle of the plate are smaller than the designed curvatures. The red areas where the measured points are above the designed surface are distributed irregularly on the plate.

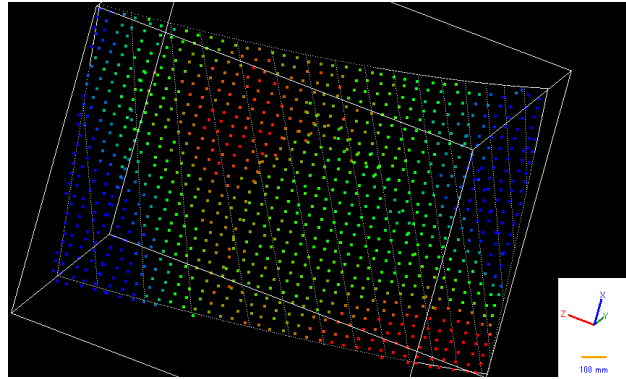


Figure 11-49 Distance error analysis results of Plate “Hybrid 1” (Step1)

Then the torsion situation of the plate is evaluated as shown in Figure 11-50. The virtual templates are rotated automatically to the proper locations to help the worker check the plate’s torsion. The angles between the virtual templates’ sticks and the perspective plane are calculated and displayed in the half-transparent message box. The angles are (1, 1, 0, 0) which means there are not yet improper torsions in this occasion, while the distance between the endpoints of the virtual templates’ sticks and the upper plane are (4, -4, -3, 4) (mm) which means the vertical curvatures should be changed too to achieve the designed shape. The distances between the ends of the virtual templates’ bottom lines and the measured plate are {(23, 21), (25, 7), (9, 5), (4, 14)} (mm).

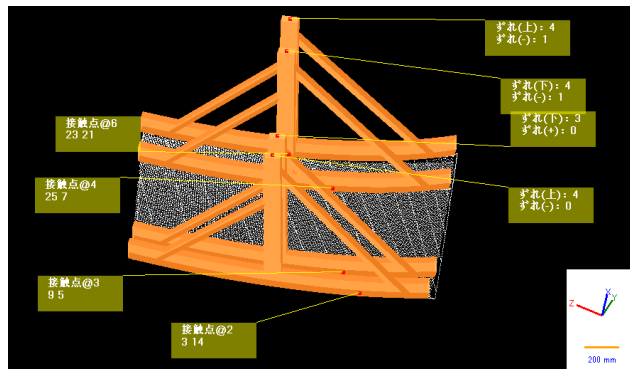


Figure 11-50 Torsion analysis results of Plate “Hybrid 1” (Step1)

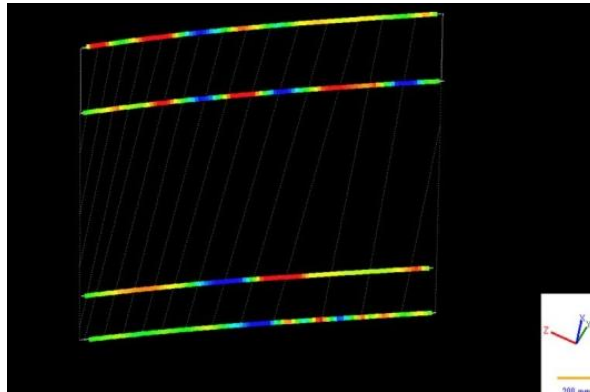


Figure 11-51 Curvature error analysis results of Plate “Hybrid 1” (Step1)

The curvature errors at the frame points are calculated and displayed as shown in Figure 11-51. The red areas are that have smaller curvatures and have to be applied deforming on the upper side of the plate. In this case, because the torsion of the plate is still normal, the heating lines can be applied along with the roller lines passing the red areas.

11.8.3.3. Manufacturing plan and manufacturing results of this step

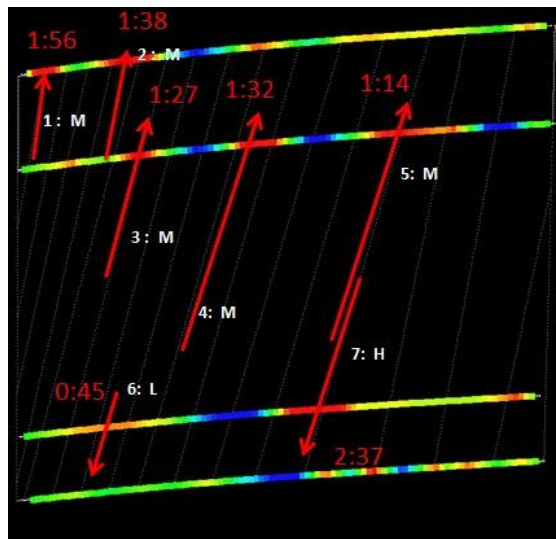


Figure 11-52 Designed manufacturing plan for “Hybrid 1” (Step1)

The manufacturing plan designed for this step is as shown in Figure 11-52. There are totally 7 heating lines designed for this manufacturing step. These heating lines are all applied along with the roller lines passing the red areas (the areas with insufficient curvatures). In this experiment, the plate is manufactured considering the 3 heating grades (H, M, L).

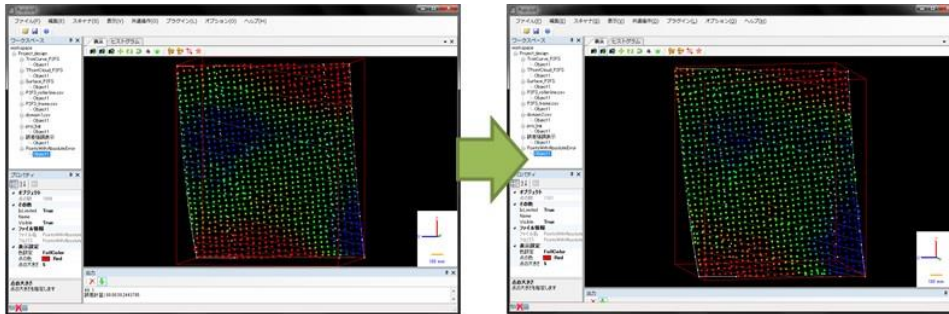


Figure 11-53 Displacement color map before and after this manufacturing step (“Hybrid 1”)

The plate’s displacement color map’s change is as shown in Figure 11-40; while the plate’s displacement error histogram before and after this manufacturing step is as below. It can be seen that the displacement error decreased after this manufacturing step. The points with displacement within 5mm increased from 50% to 58%. And the standard deviation σ also decreased from 8.3mm to 6.2mm.

Table 11.10 Plate evaluation results before and after this manufacturing step (“Hybrid 1”)

Step	Ratio of the points with (displacement < 5mm)	Standard deviation
Before Step 1	50%	8.3mm
After Step 1	58%	6.2mm

11.8.4. Manufacturing plans for all the steps

The manufacturing plans used to manufacture plate “Hybrid 1” is as shown in Figure 11-54. All of the heating lines in this figure are based on the analysis results generated by the proposed framework. The manufacturing time of each heating line is recorded in the figure. Except for the last two heating lines in blue, all of the heating lines and heating points are applied from the upper side of the plate. The manufacturing process cost totally 5.5 hours including the scanning, measurement, analysis and manufacturing. The average manufacturing time of this plate using the real wooden template (expert workers) is about 11 hours.

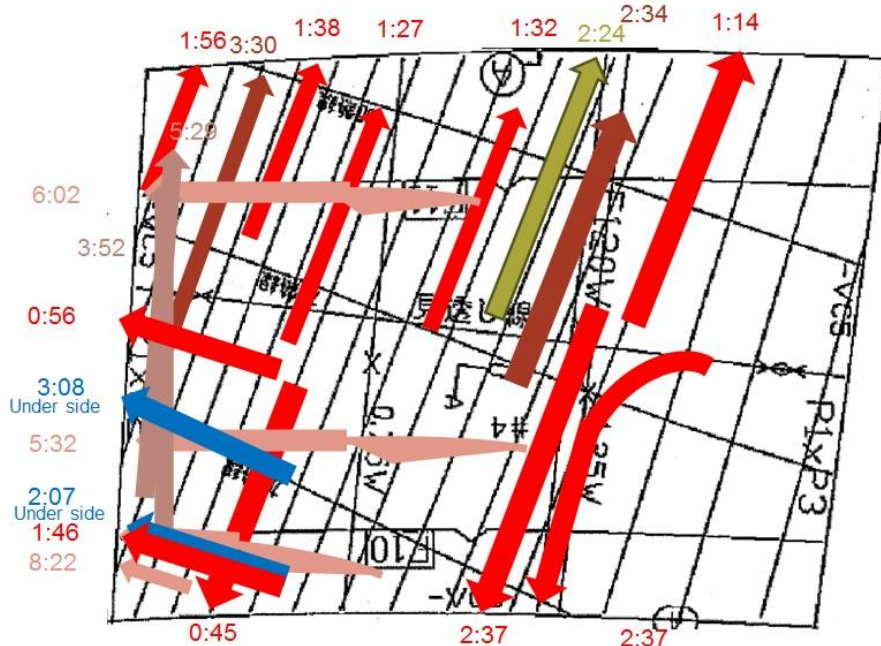


Figure 11-54 Manufacturing actions of Plate “Hybrid 1” (all the steps)

11.8.5. Manufacturing results

The manufacturing results (the distance errors between the measured plate and the design surface) of all the manufacturing steps are as shown in Figure 11-55. The green areas are that have the error within 5mm. At last over 90% points are within the threshold.

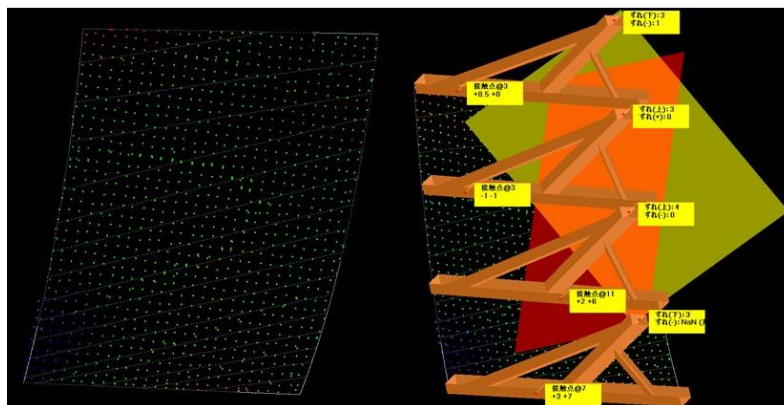


Figure 11-55 Final manufacturing result of Plate “Hybrid 1” (checked by system)

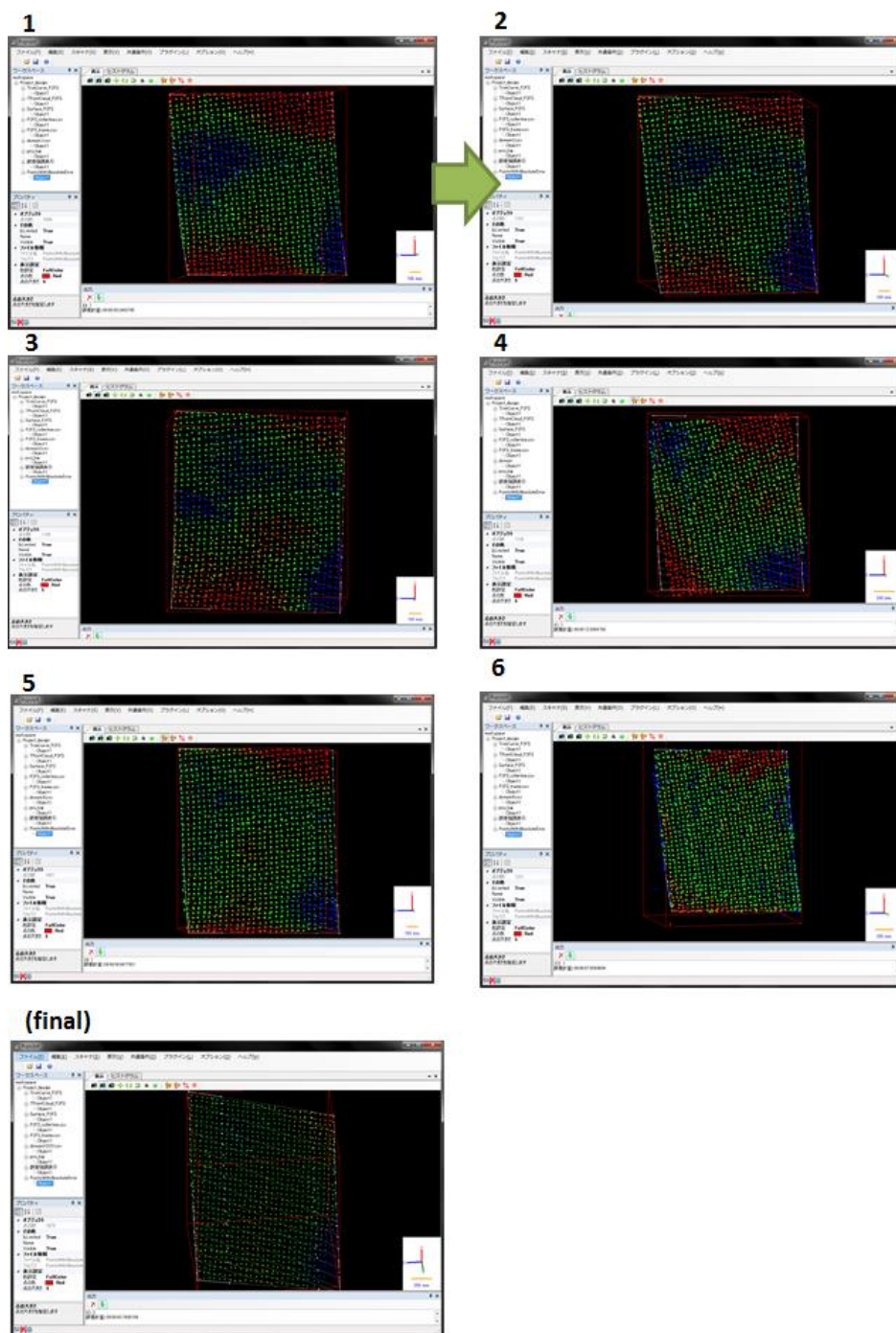
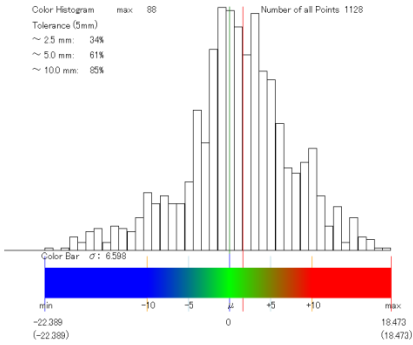
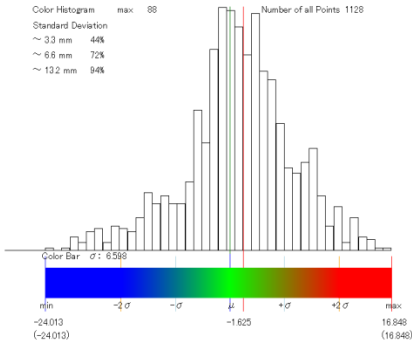
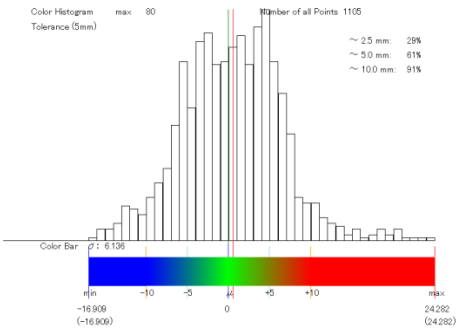
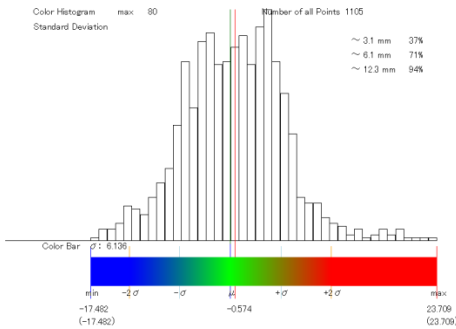
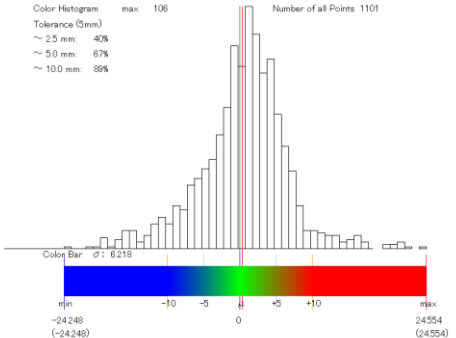
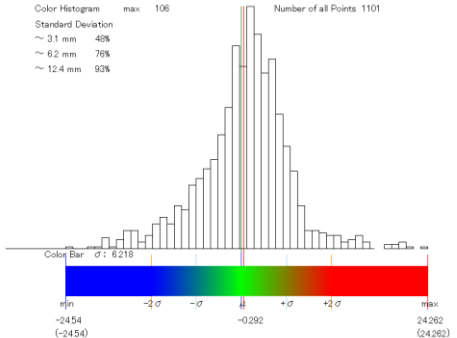
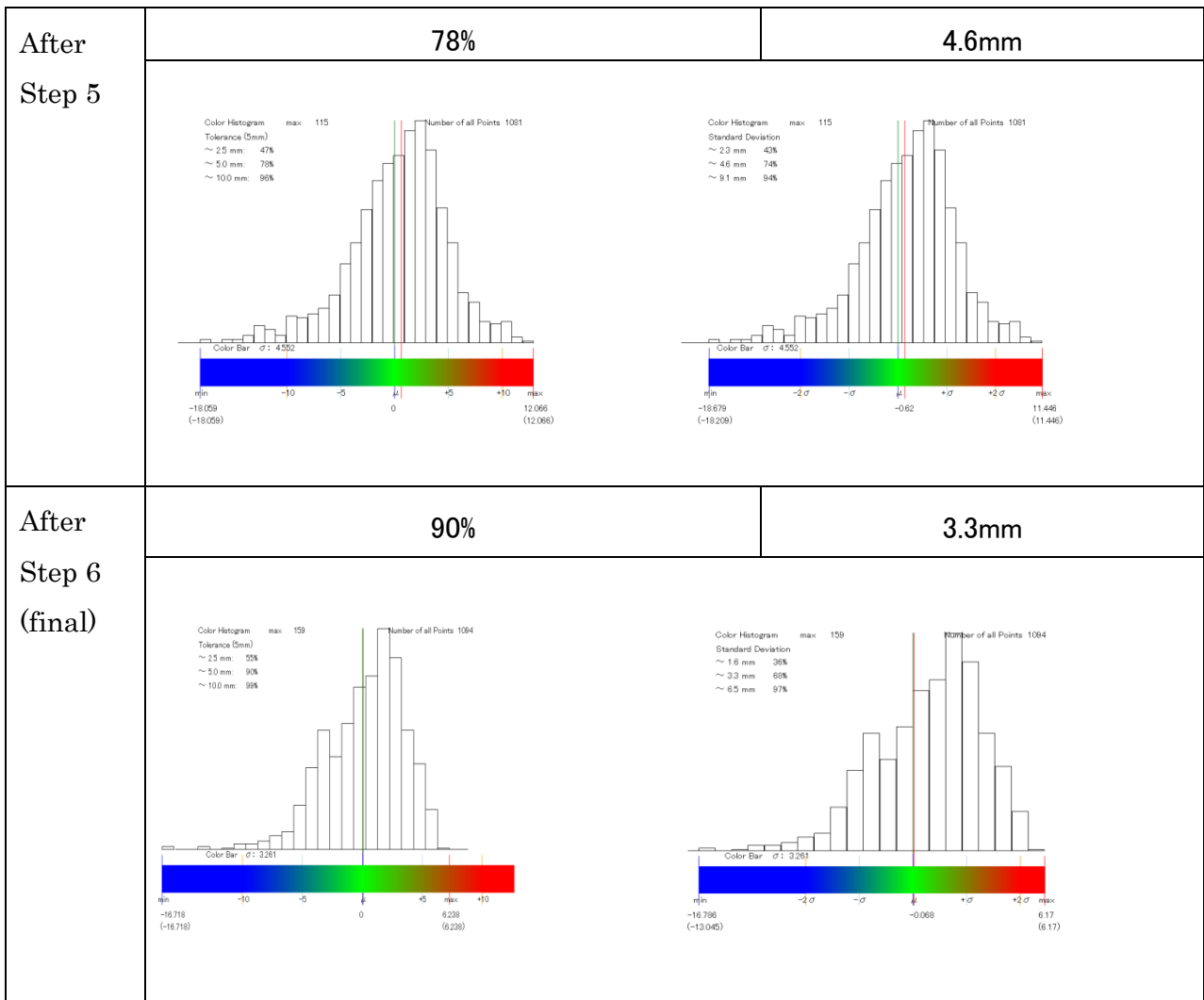


Figure 11-56 Manufacturing result of Plate “Hybrid 1” after every step

Specifically, the distance error histograms from the 1st manufacturing step till the last one are as shown in below.

Table 11.11 Plate evaluation results after each manufacturing step (“Hybrid 1”)

Step	Ratio of the points with (displacement < 5mm)	Standard deviation
After Step 2	<p style="text-align: center;">61%</p> 	<p style="text-align: center;">6.6mm</p> 
After Step 3	<p style="text-align: center;">61%</p> 	<p style="text-align: center;">6.1mm</p> 
After Step 4	<p style="text-align: center;">67%</p> 	<p style="text-align: center;">6.2mm</p> 



As shown in Figure 11-57, the ratio of points with displacement smaller than 5mm increases after most of the manufacturing steps; while the points' displacement standard deviation decreased after every manufacturing step. This proved that the manufacturing plans designed based on the proposed framework are effective.

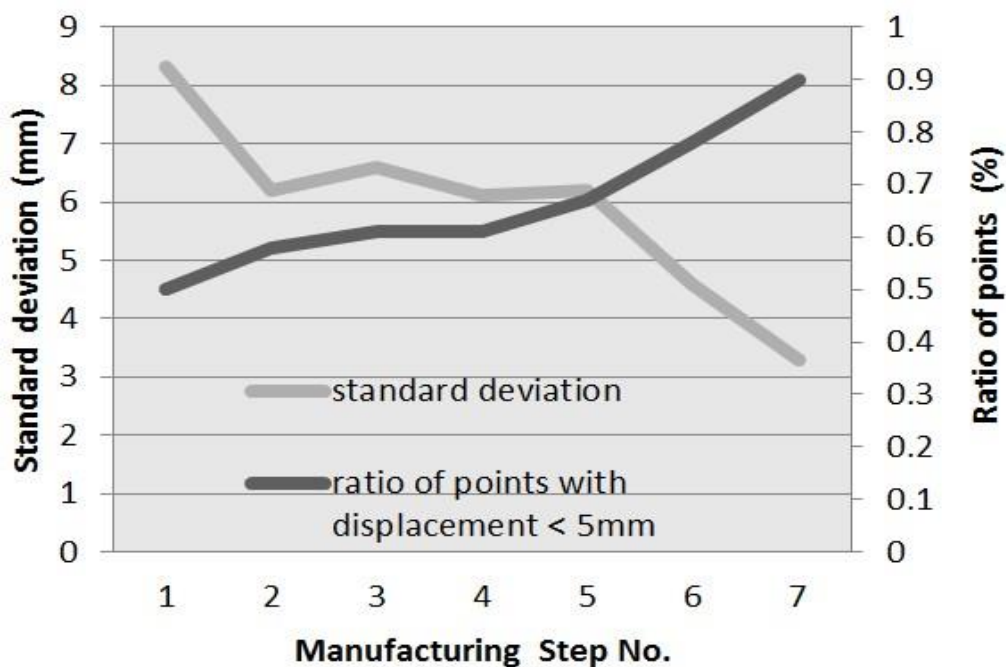


Figure 11-57 Plate's evaluation results for all the manufacturing steps ("Hybrid 1")

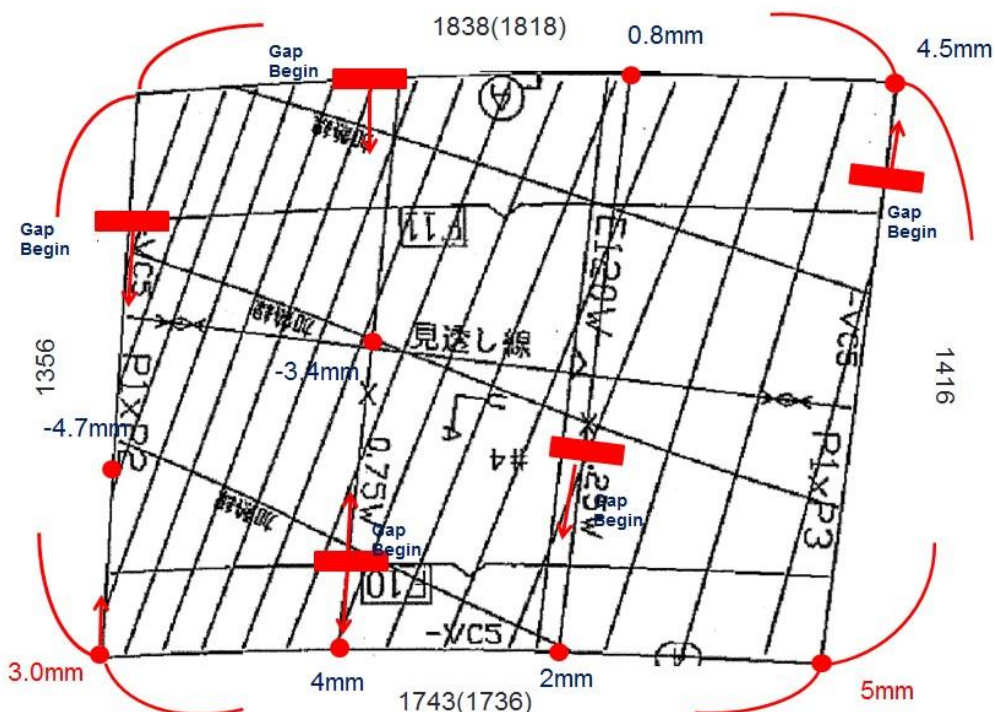


Figure 11-58 Final manufacturing result of Plate "Hybrid 1" (checked by real wooden template)

This plate is a real plate which is supposed to be used on the ship. Before being passed to the heat sealing process, the final shape was checked by the expert workers using the real wooden templates. The result is as shown in Figure 11-58. After the real wooden templates are located at the proper positions on the plate, the biggest gap between the bottom lines of the wooden templates and the plate is about 5mm which is much smaller than the error threshold 10mm of the heating forming.

11.9. Summary

In this chapter, the heating forming support experiments conducted in the shipyard are illustrated. Plate Measurement System (MS) and Virtual Template System (VTS) are introduced with the Automation Engine (AE) into a shipyard S for the workers to grasp the manufacturing results of every heating forming step and design the next manufacturing plans (heating lines for next step). Multiple plates are manufactured without using the real wooden templates in these experiments.

The following items are evaluated.

- Plate extraction
- Curvature error view
- Torsion evaluation view
- Heating plan suggestion (along with the roller lines)

Though these experiments, the following items are verified:

- ✓ The 2 views generated by the framework automatically are efficient.
- ✓ The manufacturing plans from the framework are effective.
- ✓ No real wooden template is used.
- ✓ All of the setting ups and customization according to the manufacturing environment are configured by the administrators of the shipyards.
- ✓ The measurement and analysis flow is completely automatized. The workers only need to select the minimum information.

Three plates, Plate “Bowl 1” Plate “Bowl 2” and Plate “Hybrid 1” are manufactured using the proposed framework. The manufacturing results are summarized as below, and the supported heating forming manufacturing process is

reviewed by the selected experienced workers in the shipyard.

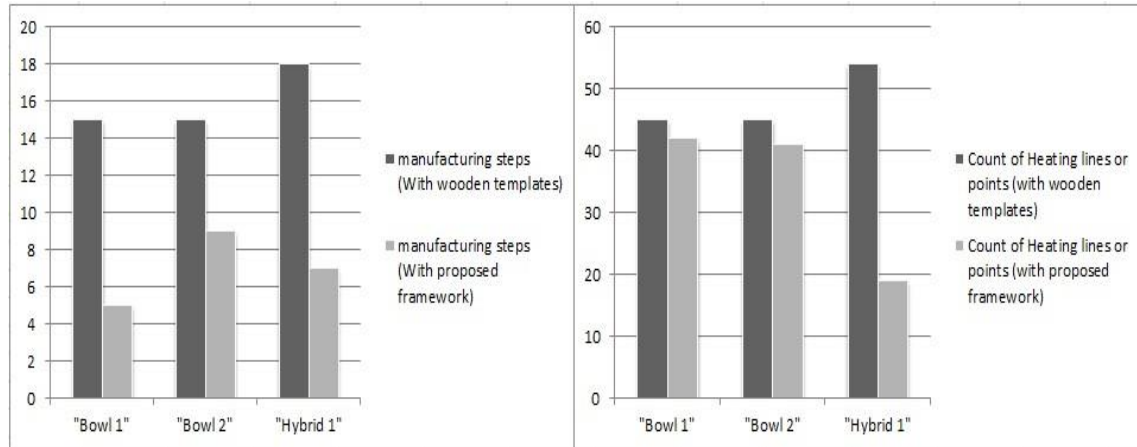


Figure 11-59 Manufacturing steps and count of heating actions under real wooden templates and the proposed framework

The manufacturing steps' change from the manufacturing with real wooden templates to the manufacturing with the proposed framework is shown in Figure 11-59 (left). The manufacturing steps decreased almost to 50% averagely by using the proposed framework. Besides the average wooden template fixing and observing time for each step is about 7 - 12 minutes depending on the manufacturing difficulty of each plate. However, with the proposed framework, the evaluation result with the virtual templates is outputted within 2 - 3 minutes in average.

Besides, as shown in Figure 11-59 (right), with the accurate evaluation results from the proposed framework, the total count of the heating actions (lines or points) also decreased, which means not only the evaluation time but also the manufacturing time itself is reduced.

Table 11.12 Heating forming experiment result summary (Sun, J.Y., JASNAOE, 2014)

<i>items</i>	“Bowl 1”	“Bowl 2”	“Hybrid 1”
Manufacturing time when using real wooden templates	5 hours	5 hours	11 hours
Manufacturing time when using heating forming support framework	3.5 hours	4.5 hours	5.5 hours
Modification manufacturing?	Yes (last 6 heating lines)	No	No
Fitness with the design shape	<i>good</i>	<i>good</i>	<i>good</i>

According to the table summarized above and the interviews with the workers who actually used the proposed framework to manufacture the plates, the framework is proved to be both effective and efficient comparing with the manufacturing process which uses the real wooden templates. Considerable time and physical effort are saved and the manufacturing results are beyond the expectations with the real wooden templates.

Chapter 12 Evaluation of knowledge elicitation and dissemination

12.1. Overview of knowledge based system evaluation

This thesis proposed an interview based NRDR knowledge model to deal with the explicit knowledge and the implicit knowledge existing in the curved shell plate's manufacturing process.

The objective of this chapter is as below:

- ✓ To elicit rules for the knowledge models based on the interviews or recorded data referring to the manufactured plates.
- ✓ To confirm if the rule set is correct or not by the interviews with the expert workers after the rule set is constructed.
- ✓ To use the generated rule set to provide the common manufacturing guidelines based on the plate's shape information or to provide the detailed instructions based on the plate's full situation.

In this chapter, all the evaluation and demonstration are based on the experiments from the interviews conducted towards the expert workers or the recorded 3D manufacturing data.

12.2. Line heating analysis with curvature error view

The trace experiments which includes approximately 27 times of bending heating are conducted during a curved shell plate's whole manufacturing cycle for constructing the basic guidelines' rule base. The main steps are shown in Figure 12-1. Every time distinction between the manufacturing plan suggested by system and the actually used manufacturing plan is discovered and the distinction could not be explained by the existing rules' set, the parameters representing the plate's situation are calculated and analyzed in a virtual environment and the exclusive

features of the plate's situation are coded as a new rule which is added into the existing KB.

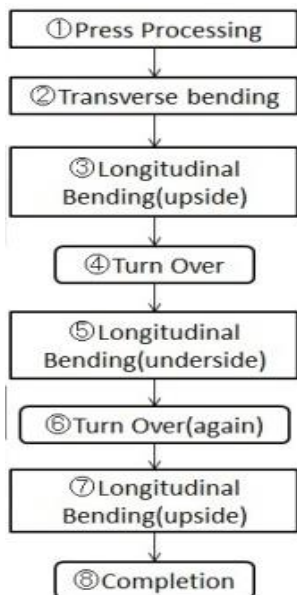


Figure 12-1 Manufacturing steps of the curved shell plate

12.2.1. Original rule base

The original knowledge base is initialized as shown in Figure 12-2. If the curved shell plate belongs to the types the system can deal with, the heating should be conducted along with the lines which connect the adjacent frame's points which have big curvature errors. This rule is also representing how the proposed VTS makes the suggestion automatically for the manufacturing plans.

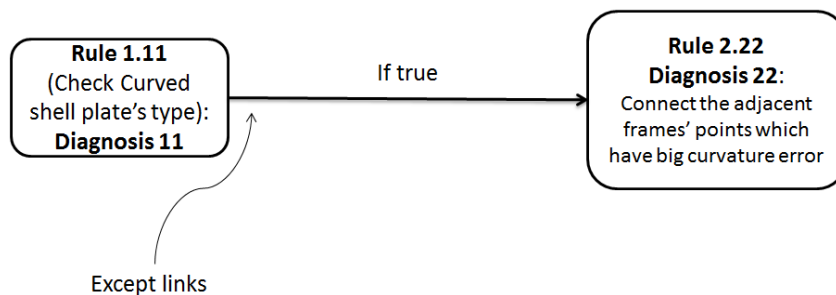


Figure 12-2 The original rule base

12.2.2. Knowledge elicitation process and results

The manufacturing plan (left) automatically generated by the proposed system and the manufacturing plan (right) which the worker actually used are shown in Figure 12-3 (only the step where expert’s knowledge appeared). It can be seen that the arrangement of the heating line are mostly the same except some slight differences including the heating line 1, 4, 5, 20 and 21, which were also verified as appropriate heating lines by workers using the output analysis result of VTS. In addition, the distinction existing in step 3 and step 7 are also successfully classified by adding new rules.

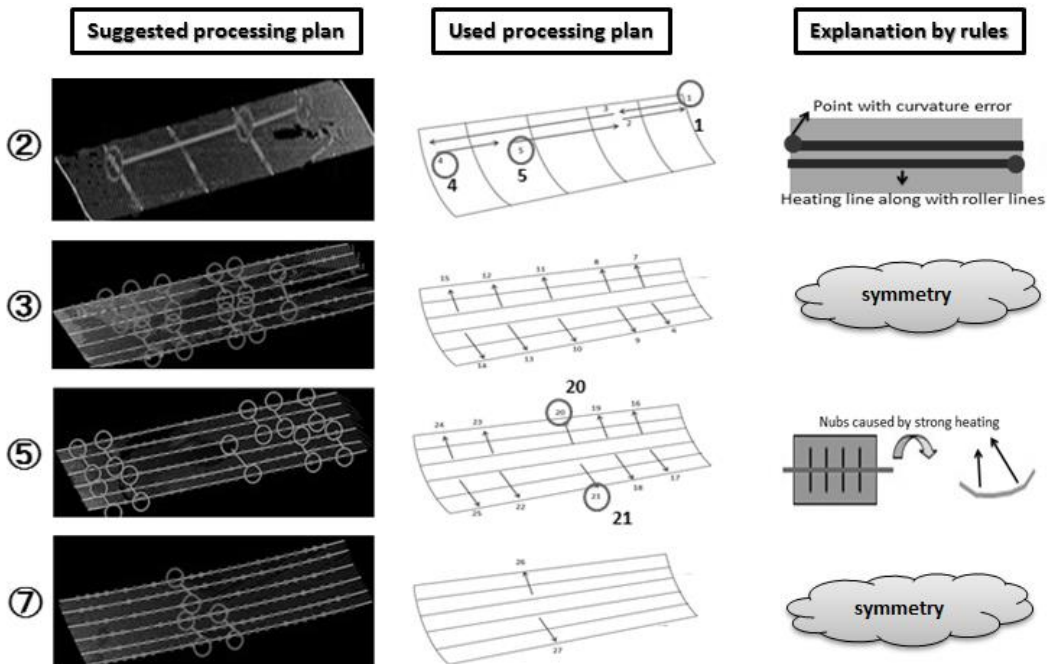


Figure 12-3 Plan comparison

In this case study, the knowledge during this curved shell plate’s manufacturing process is extracted and represented by adding rules into a set of independent rules.

Based on the interview after step 2, when the generated heating line intersects the roller line which is decided based on the curvature distribution at the beginning of the heating processing, the heating line is usually located along with the roller line in order to avoid improper torsion (Rule 5.51 in Figure 12-4).

For example, correction heating was performed at the heating lines 1, 4, and 5 in two straight parallel lines(along with the roller lines) as shown in Figure 12-3 (center) instead of single lines connecting the points with big error as shown in Figure 12-3 (left).

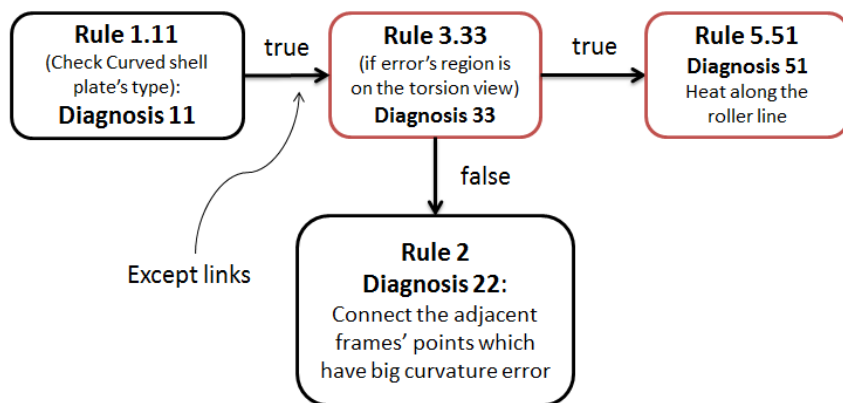


Figure 12-4 Knowledge base after step 2

Based on the interview, after step 3 and step 7, when the error's region is not symmetrical relative to the torsion, the heat can also be applied symmetrically relative to the torsion as shown in Figure 12-5.

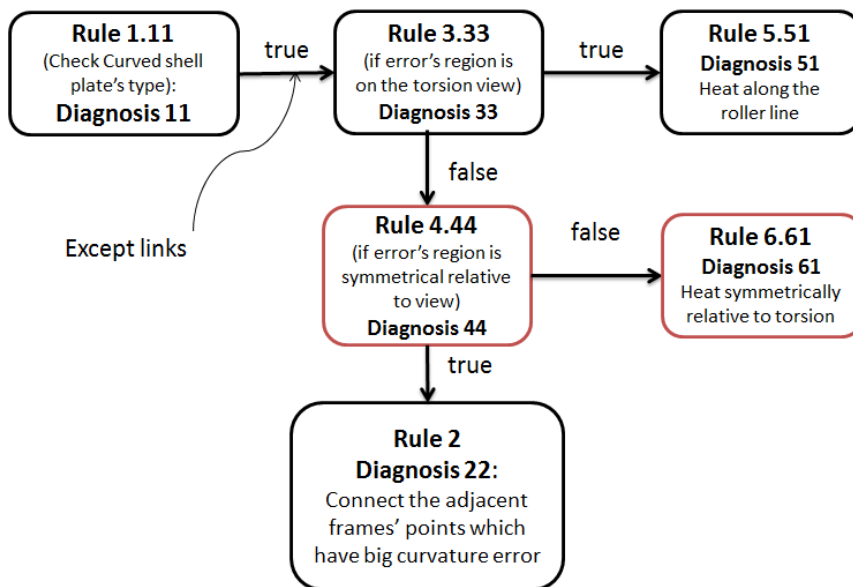


Figure 12-5 Knowledge base after step 3

Based on the interview after the step 5, when a nub (relatively small region) occurs because of improper heating, correction heating is needed for the same position from the opposite of the curved shell plate (Rule 7.71 in Figure 12-6).

For example, at the step of back heating after reversal, in order to correct the place of the nub, the line heating was performed between the points which have no obvious curvature errors in large region (heating lines 20 and 21 in Figure 12-3).

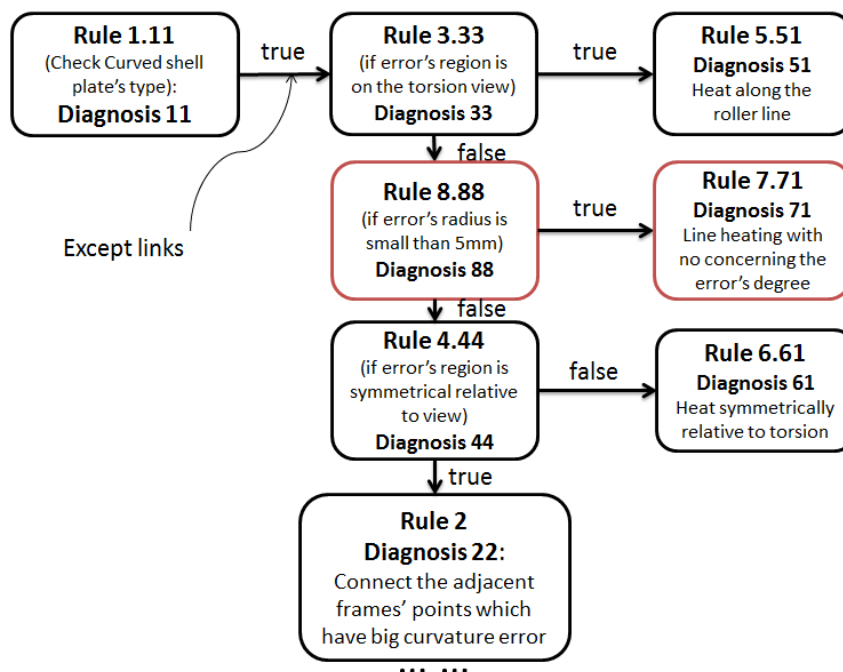


Figure 12-6 Knowledge base after step 5

In this experiment, the measured data facilitate the rule base to elicit the general basic knowledge in the curved shell plate's manufacturing process. The ripple down rule is proved to be a good approach for perfectly describing the situations in which the basic rules that heating should be applied to where the curvature error is relatively large are not applicable. All of the experimental data can be recorded automatically for the following analysis. With interview based on the accurate data stored, the expert's knowledge can be extracted efficiently and revised properly.

12.3. Complicated heating technic analysis with torsion evaluation view

This experiment is the subsequent experiment of that from the prior RDRs model as shown in Figure 12-8 which is constructed from the common guidelines in the curved shell plates' manufacturing. By the manufacturing using the generated RDRs rule set, 85% points of the curved shell plate's measured point cloud were within 5mm from the design shape; and the distance between each virtual template's bottom line (the endpoint) and the curved shell plate is within 15mm. However, when the workers continued trying to minimize the error, new knowledge turn out which means new rules had to be added; within them, some duplicated and difficult rules existed and caused the inefficiency of both the knowledge base's construction and the knowledge dissemination.

The main objective of the experiment in this sub-section is to evaluate the proposed knowledge elicitation approach for the complicated heating technic's analysis based on NRDRs that it can better capture the manufacturing knowledge during the knowledge elicitation and make the knowledge base easier to understand during knowledge dissemination.

12.3.1. Plate analysis

The bending situation on both the horizontal frame and the vertical frame are measured, evaluated and stored as shown in Figure 12-7 (left and middle). As shown in the right of Figure 12-7, the 2 straight lines are the manufacturing areas suggested by the system, but as the result, neither the errors on the horizontal frame on the upper area nor the ones on the vertical frames in the middle of the plate reduced. The expert suggested doing the manufacturing along with the rounded areas shown in the middle of the plate after checked the plate's vertical frame and horizontal frame. Result proved this theory. The idea that both the errors on the horizontal frames and the ones on the vertical frames should be considered together was taken into the knowledge base as the rules C6 and C101 in the Figure 12-8(right).

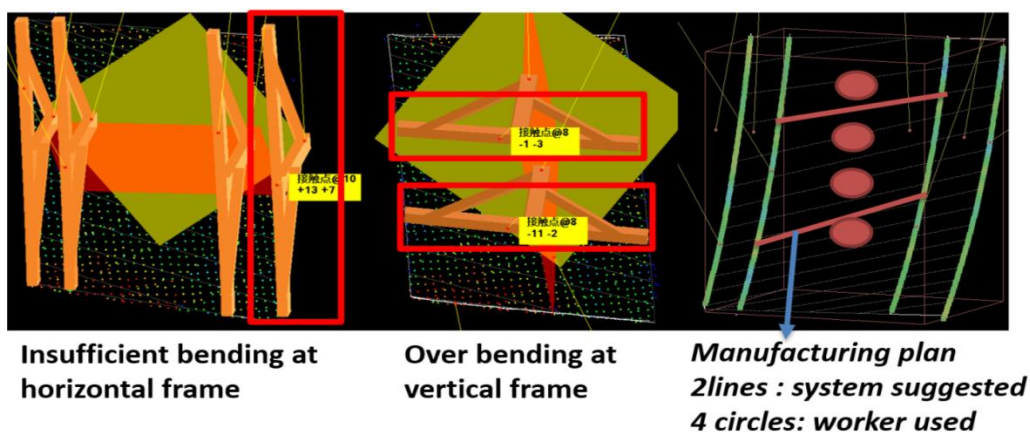


Figure 12-7 The Situation and Manufacturing Area of the Curved Shell Plate

12.3.2. Elicited rules

Also, before and after this manufacturing step, the errors' region distribution and the errors' radius should be taken into consideration which means the rules in the dashed lines in Figure 12-8 should be executed. Therefore, these rules which is considered to be reused in the following knowledge elicitation are arranged into a new lower level RDRs tree C3, and be referred from the Rule3.33 and Rule 10.101.

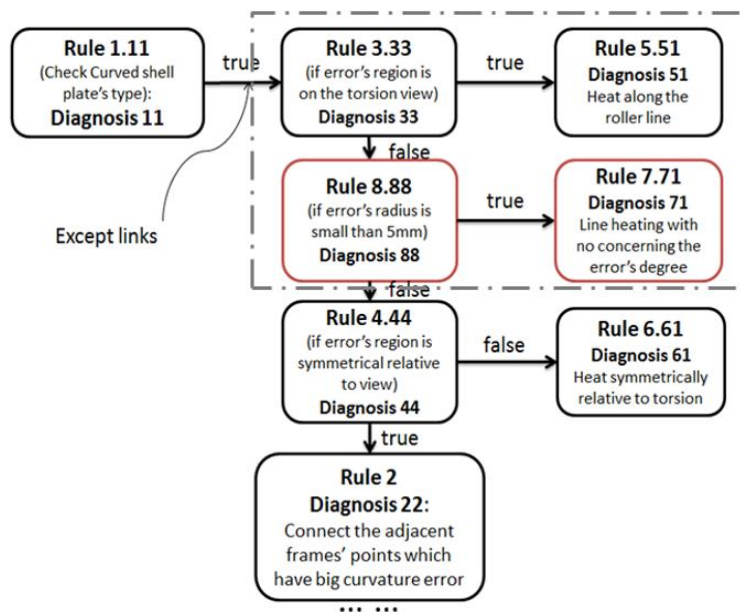


Figure 12-8 Rule base for line heating (Sun, J.Y, ISPE2013)

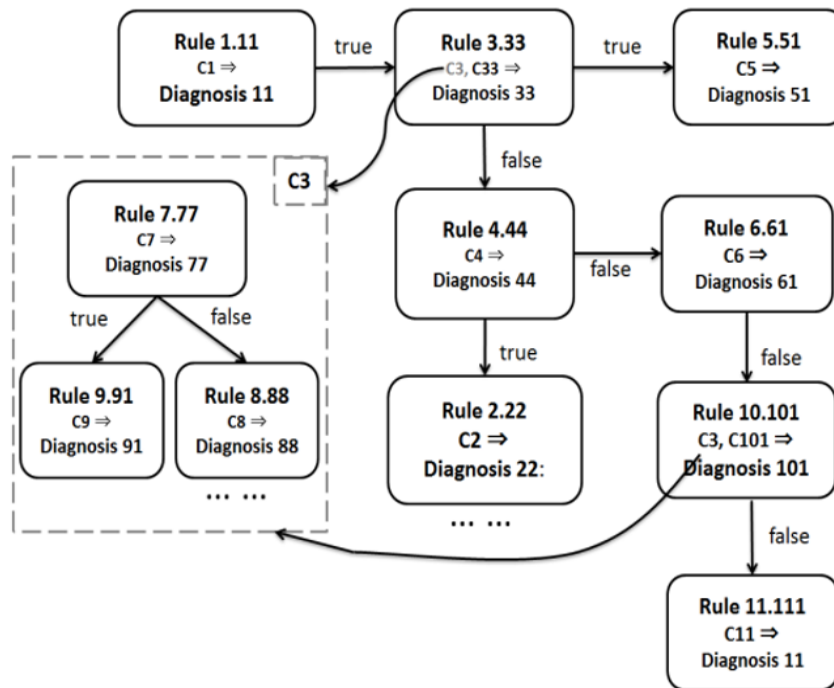


Figure 12-9 Nested ripple down rule base (Sun, J.Y, ISPE2014)

The rules in Figure 12-9 is illustrated as below.

- C3: Same as the rule set in dashed lines of Figure 12-8 (left) reused twice (rule 3.33 and 11.111).
- C1: Can the curved shell plate be processed by this system or not.
- C33: Is the errors' region symmetrical relative to the view or not.
- C5: Can the heating line be arranged symmetrically to the torsion (physically).
- C4: Is here no multiple errors (insufficient/over relative to the design) existed both in the horizontal and vertical directions.
- C2: Can the adjacent frames' points which have relatively big error be connected physically.
- C6: Can point/line heating arranged along with the single frame's points which have relatively big curvature error cause extra errors belonging to other frames.
- C101: Would the point/line heating mentioned in C6 overcorrect the

errors existing.

- C11: Is the point/line heating executable physically.

12.3.3. Elicited rules' adaption

In this experiment, another curved shell plate's manufacturing step is analyzed using the constructed Knowledge Base above.

The plate analysis result is as below:

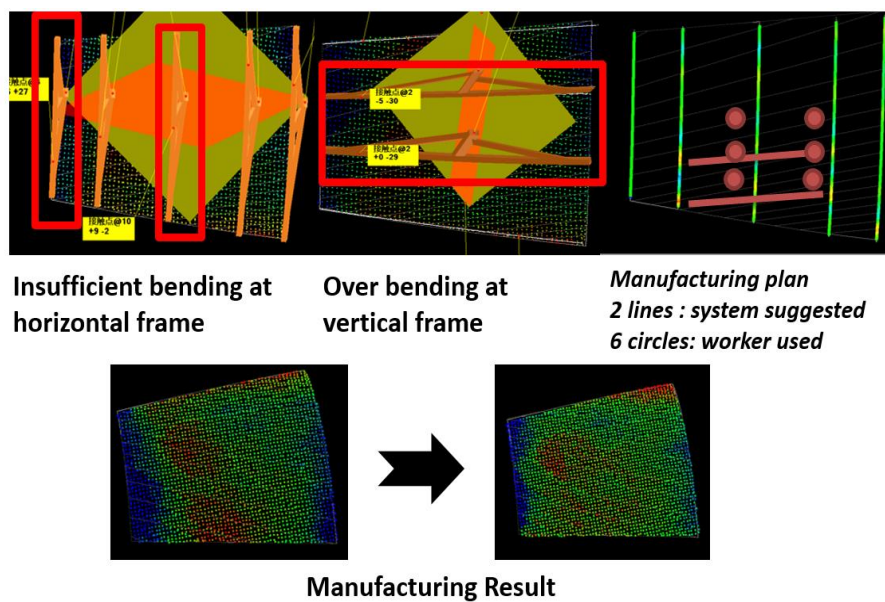


Figure 12-10 Manufacturing based on constructed Knowledge Base

As shown in Figure 12-10(upper), the situation of the plate is similar as the one from experiment A. The bending on the horizontal frame is inefficient while the one on the vertical frame is over.

The rule set constructed in experiment A is searched as below:

- C1: TRUE (Plate type can be processed)
- C3: TRUE (the errors' region distribution and the errors' radius checked)
- C33: FALSE (the errors' region is not symmetrical)
- C4: FALSE (errors of multiple types exist)
- C6: FALSE (point heating arranged along with single frame's points)

causes no extra error)

- C3: TRUE (the errors' region distribution and the errors' radius are checked again)
- C101: FALSE (Point heating mentioned in C6 would not overcorrect the errors existing)
- C11: TRUE (Point heating is executable physically)
- Diagnosis: do point heating between the single frame's points which has relatively big error

After this manufacturing step, as shown in Figure 12-10 (below), the areas of error (the red and blue areas) reduced. Also, with the virtualized environment, the details of the plate's information is more clear and specific to help the worker make decision, and with the constructed knowledge base in experiment A, even a beginner worker can do make the correct manufacturing decision following the rules' set introduction.

12.4. Knowledge model with different views

In this sub-section, the examples about the usage of the proposed knowledge models and the Virtual Template System are introduced. The effectiveness of these models is proved through these examples.

12.4.1. Usage of knowledge model with curvature evaluation view

When trying to decide the manufacturing plan for a plate, the first thing comes to the workers is which area has relatively bigger curvature errors because they want to do the heating along with these areas to reduce the curvature errors at these areas. However, the method they used to find these areas are too inefficiency:

- By touching the plate to find the areas with obvious insufficient curvatures
- By comparing the plate and the wooden templates to find the positions which cannot match each other.

The procedures above for only one plate (about 2 frames at once) could cost over 5 minutes.

The curvature evaluation view outputted by VTS is here to solve this problem.

The curvature errors as shown in Figure 12-11 is automatically calculated within only 2 minutes, and the red areas means where more heating is needed, while the blue areas means there are already over bending. It cost much less time by using the virtual template to evaluate the curvatures rather than the real ones. And the evaluation results are more intuitionistic and comprehensible.

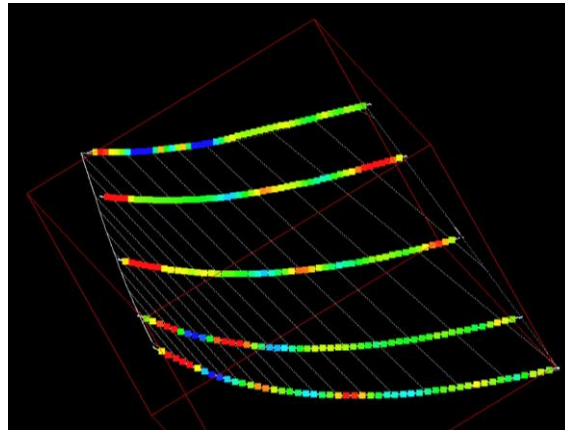


Figure 12-11 Curvature evaluation view for one manufacturing step

When the workers design the heating lines based on the known areas with big curvature errors, they just need to arrange the heating lines passing the red areas and along with the roller lines shown as the white lines in Figure 12-12.

Here different combinations and precise locations exist in the heating lines from different workers. worker can design the heating lines as shown in Figure 12-12, while another worker can connect the heating line (a) (b) and (c) (d) as shown in Figure 12-13.

It is hard to decide which one would be better without a quantitative evaluation of the subsequent manufacturing of these 2 kinds of manufacturing plans. The data-based knowledge model introduced in Chapter 16 can give answer to this question by comparing the subsequent manufacturing steps of these different heating lines' design quantitatively.

Two different manufacturing plans (one with the separated heating lines and the other with the connected heating lines) are evaluated by taking the subsequent manufacturing as the evaluation standards. It tells that if possible the heating should be applied depressive instead of joint heating of multiple heating lines in a

torture direction even the torture degree is only small.

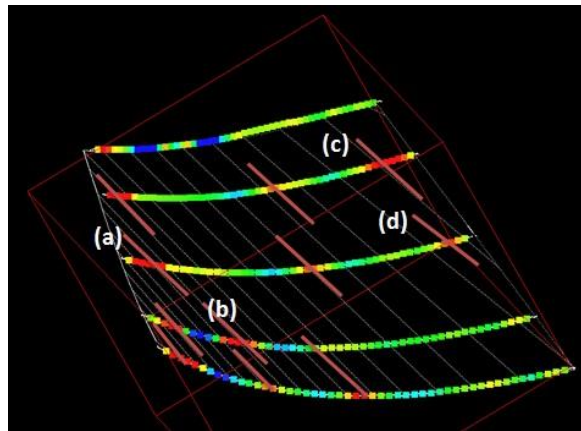


Figure 12-12 Heating lines' designed by a worker

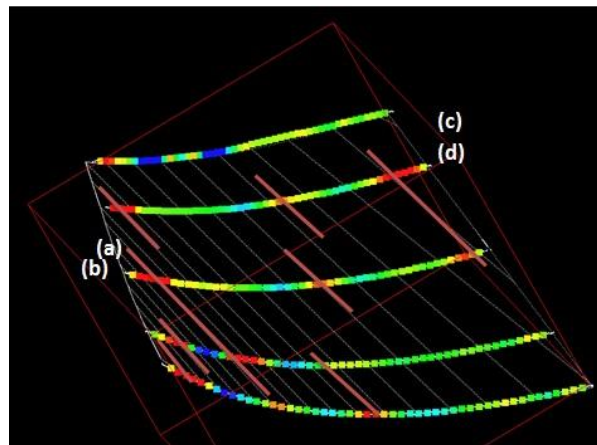


Figure 12-13 Heating lines' designed by another worker

12.4.2. Usage of knowledge model with torsion evaluation view

In some case, the curvature errors of all the frames seems to be all right, however the displacements between the plate and the NURBS design surface are still observable as shown in Figure 12-14. The workers start to consider about other heating technics such like the point heating.

In the experiment 11.6.4, from the heating action 26 to 30 marked in Figure 11-29, the workers did the heating at 5 points instead of any heating lines. Here we are going to discuss how he designed these 5 heating points based on the torsion

evaluation view. Also the design process of these heating points follows the elicited rules of the interview-based knowledge model too.

That has to be mentioned is this manufacturing design process was of great difficulty when the workers try to do it using the real wooden templates because the perspective sticks' observation is too inaccurate and time cost. Sometimes, after they found the curvatures at each frames are good (the wooden templates matches well at the plate's frames), they declare the plate is finished, however a lot of problems are found and the plate can be sent back to the heating forming stage again after it is forwarded to the subsequent stage like the heating sealing stage. Only some expert workers insist that the curvatures at the vertical direction should be check again, and if it does not matches with the design shape, some special heating technics such as the point heating or curve heating should be applied.

(1) Rule C1

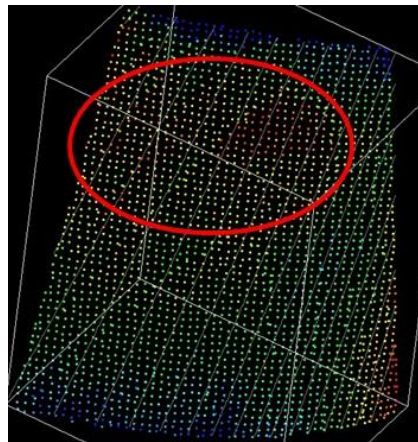


Figure 12-14 Displacement color map

When the workers try to use the torsion evaluation view to design the heating plans, they first need to check “if the curved shell plate can be processed by this framework or not “(**Rule C1** in Figure 12-9), as mentioned before, this framework can only deal with the first three types in the list below:

- [1] Trumpet type: No vertical bending in the plate's width direction
- [2] Bowl Type: vertical bending, center falls

- [3] Saddle Type: vertical bending, center rises
- [4] Twist Type: diagonal areas are higher / are lower than the other diagonal area

(2) Rule C3 and Rule C33

Then whether “the straight line heating is not available” (Joint **Rule set C3** in Figure 12-9) should be asked. Here the obvious curvature errors cannot be found on the frames according to the curvature color map in Figure 12-15, thus the heating technics besides line heating should be considered.

According to the displacement color map shown in Figure 12-14, the region of the errors (red area) is not symmetrical to the torsion direction (**Rule C33** in Figure 12-9); otherwise some heating lines (curve) may be arranged symmetrically to the torsion without destroying the torsion situation.

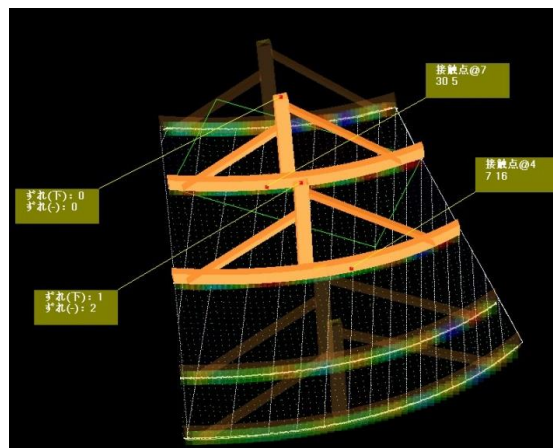


Figure 12-15 Horizontal virtual templates (plate view)

(3) Rule C4

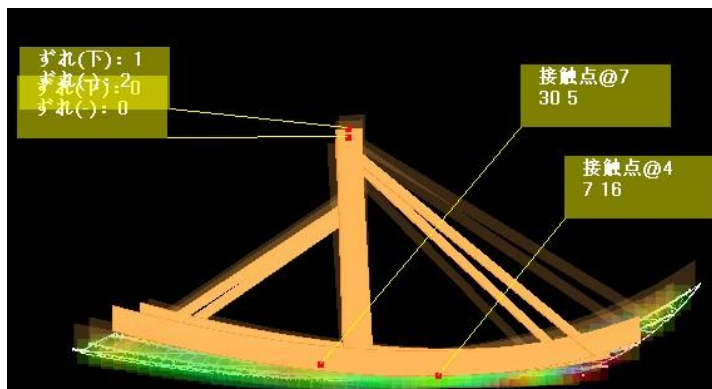


Figure 12-16 Horizontal virtual templates (perspective view)

Obviously, **Rule C4** in Figure 12-9 is false for there are 2 kinds of errors exist on this plate according to Figure 12-16, (insufficient bending at horizontal frame) and Figure 12-17 (over bending at vertical frame). The displacements between the horizontal virtual templates' ends and the plate are (30mm, 5mm) and (7mm, 16mm); while the displacements between the vertical virtual templates' ends and the plate are (-11mm, -3mm), (-6mm, -3mm) and (-3mm, -12mm). The 2 horizontal virtual templates in the middle of the plate are “below 0mm and 1mm” from the calculated upper plane; while the 1 vertical virtual template is “above 4mm” from the calculated upper plane.

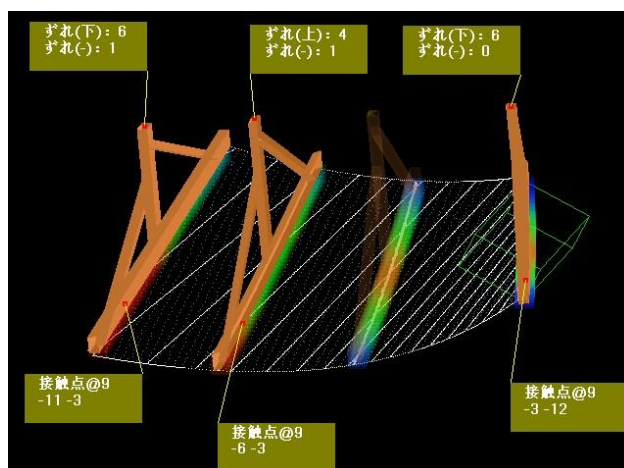


Figure 12-17 Vertical virtual templates (plate view)

(4) Rule C6 and Rule C101

Then because the areas around the red area in Figure 12-14 are blue or light blue, means the displacement direction of these areas are opposite. When the red area goes downward in the horizontal direction, the blue area will goes upward relatively. Therefore, applying point heating at the red area will cause no extra errors or over correct the errors existing here (**Rule C6** and **Rule C101** in Figure 12-9).

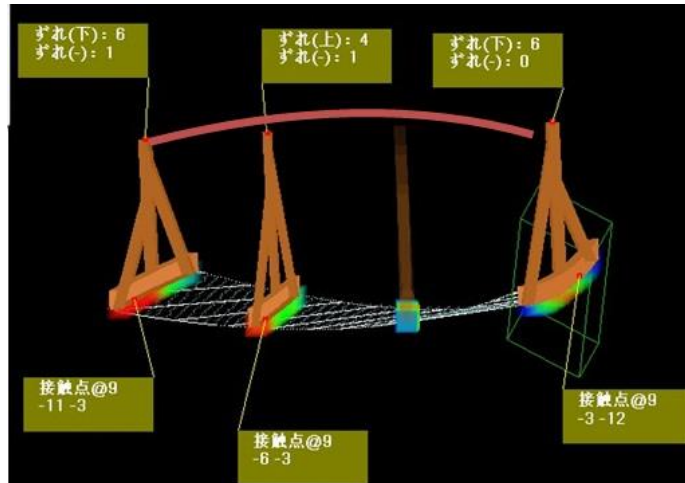


Figure 12-18 Horizontal virtual templates (side view)

(5) Rule C11

At last, physically, since the plate is relatively thick, self-weight is also considered in this case, so that the point heating is judged physically effective in this case (**Rule C11** in Figure 12-9). The expected plate deformation is as shown in Figure 12-19 (the blue arrows go downward due to the self-weight, and the green arrows go upward relatively). Eventually, the workers designed the heating action at the 5 points in the figure.

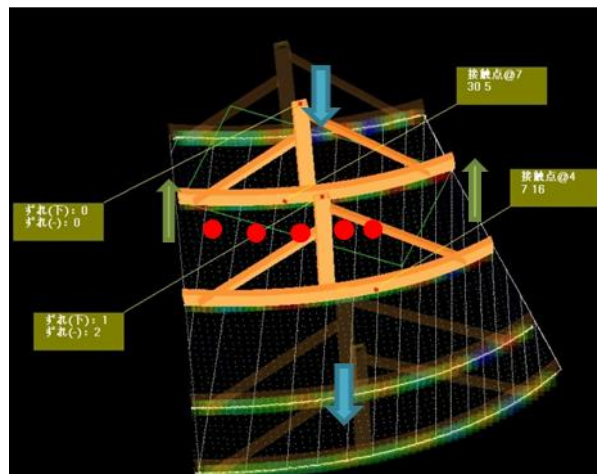


Figure 12-19 Horizontal virtual templates (perspective view)

(6) Manufacturing result

The result of this manufacturing action is as shown in Figure 12-20. Comparing with the displacement evaluation result before this action in Figure 12-14, the red area dramatically decreased; the plate become much closer to the designed shape which proved this manufacturing action is effective.

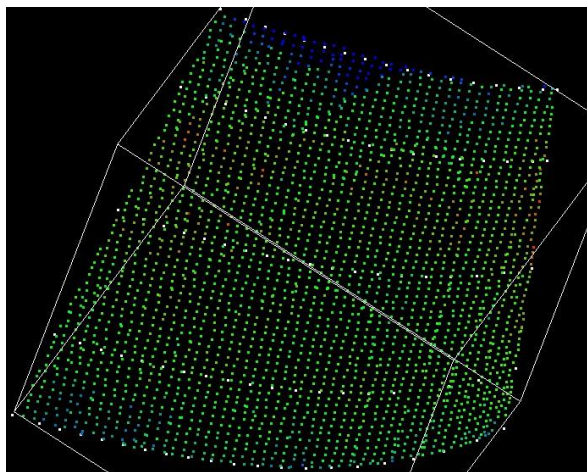
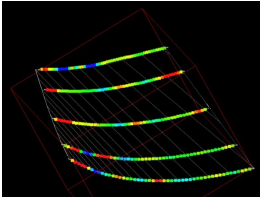
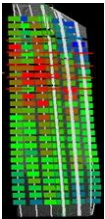
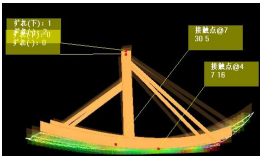
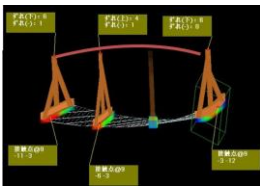
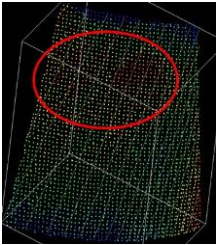


Figure 12-20 Result of the designed manufacturing action

12.5. Views for different observation purposes

According to the results of the multiple experiments and the analysis after manufacturing, the degrees of views for different observation purposes are shown in Table 12.1.

Table 12.1 Importance of views for different purposes

		Observations Purposes			
		Heating Areas	Heating Technics	Heating Grade	Heating Finishing
Curvature Evaluation View	Horizontal 	High	Low	High	Low
	Vertical 	Low	Low	Low	Low
Torsion Evaluation View	Perspective 	Medium	High	Medium	Medium
	Side 	Low	High	Low	Low
Displacement Color Map View		Low	Medium	Low	High

For deciding where to do the heating, the heating areas, the horizontal curvature

evaluation views are usually observed first, and then the displacements of the virtual templates and the plate showing in the perspective torsion view are used to confirm the decisions. For deciding the heating technics, the torsion situations of the plate are observed as well as the displacement color maps. As introduced before, the curvature evaluation view is used to decide the heating grade. At last, to check if a plate is finished or not, the displacement color map and the histogram showing the percentage of the points with different displacements is usually used first, and then the perspective plane showing the torsion situation of the plate is checked.

12.6. Summary

This thesis proposed an interview based NRDR knowledge model to deal with the explicit knowledge and the implicit knowledge existing in the curved shell plate's manufacturing process respectively.

In this experiment, the knowledge was articulated in NRDR (Nested Ripple Down Rules) tree format and a software system was developed for facilitating the captured knowledge for reuse. The virtualized environment by the VTS system provided information about the plate efficiently. The interview-based knowledge model proposed in this paper was evaluated by conducting a series of experiments in the shipyard. The common guidelines such as which heating technic should be selected is elicited based on the level separated Nested Ripple Down Rules by evaluating a couple of parameters' combination. Also the experiment showed that the knowledge base can help workers make decision during the knowledge dissemination.

PART IV DISCUSSION AND CONCLUSION

PART IV	DISCUSSION AND CONCLUSION	290
Chapter 13	Discussion	292
13.1.	Overview.....	292
13.2.	Problems existing in the proposed framework	292
13.2.1.	Imprecise perimeter evaluation with low density.....	292
13.2.2.	Scanner failure under high temperature	295
13.3.	Innovations in the proposed framework.....	296
13.3.1.	Manufacturing on vertical direction.....	296
13.3.2.	Knowledge dissemination's innovation	298
13.3.3.	Discussions on the proposed framework and the renovated manufacturing process	299
13.4.	Values of this work.....	306
13.4.1.	Cost impact	306
13.4.2.	Academic values.....	307
Chapter 14	Conclusion	310
14.1.	Conclusion	310
14.2.	Future work.....	313

Chapter 13 Discussion

13.1. Overview

In this chapter, the problems existing in the proposed curved shell plate's framework and the possible solutions, and the innovations of the proposed curved shell plate's manufacturing process are discussed.

13.2. Problems existing in the proposed framework

Two problems exist in the proposed framework when we try to introduce it into the shipyard.

- When the density of the point cloud is low (intervals are larger than 10mm), the perimeters measured by the system is not precise enough.
- In summer when the temperature around the scanner is too high (over 40 degrees), the scanner failure may happen and cause the imprecise measured results.

In this sub-section, the possible solutions of these two problems will be discussed.

13.2.1. Imprecise perimeter evaluation with low density

In this existing method introduced in 6.4, the points of edges are directly extracted from point cloud data based on the distance from a curved shell plate. However, it is difficult to obtain the accurate shape and the length of edges from the measured point cloud due to intervals existing especially in low density point cloud data of the large component.

As a possible solution for this problem, a high accuracy edge measurement method of components using 3D laser scanner could be applied (Hiekata, K., Yamato, H., Sun, J., Matsubara, H., Toki, N 2014). Concretely, the method for edge's shape measurement using the point cloud of the component's side face and the method for edge's length measurement using the feature points of the 3D targets are explained.

First, the component is measured by 3D laser scanner and point cloud data including the surface part and the side faces of the component are obtained. An

arbitrary point on the surface of the component is selected from the measured data and only the points of surface part are extracted by region growing method. The point cloud except for the extracted surface part including the component's side face is detected at following process.

In order to reduce computational complexity in the following process, the point cloud of the surface part is thinned. The concrete procedure of thinning is described following.

1. Principal component of the surface part is analyzed and it is divided into two equal parts by a plane which is vertical to the first principal component vector.
2. The operation 1 is repeated for the other divided parts until the number of points from each separated part becomes less than a fixed threshold.
3. A set of each part's gravity center is considered as thinned points of the surface part.

Next, the points on the boundary are detected from the thinned point cloud of the surface using edge detecting method from Kalogerakis (2009).

Using the points on boundary (\mathbf{E}), the shape of edges is acquired. Figure 13 illustrates how points of edges are fitted. The procedure of edge fitting is described as following.

1. The neighborhood of \mathbf{E} ($\{\mathbf{P}_{surf}\}$) is searched by k-NN BBF method from the point cloud of the surface part.
2. The gravity center of $\{\mathbf{P}_{surf}\}$ (\mathbf{G}) is calculated and an approximate plane α is fitted to $\{\mathbf{P}_{surf}\}$.
3. The projection point of \mathbf{E} to plane α (\mathbf{E}_{proj}) is calculated. The line segment GE_{proj} is extended toward \mathbf{E}_{proj} and a point on the line (\mathbf{E}') is obtained. The neighborhood of \mathbf{E}' ($\{\mathbf{P}_{side}\}$) is searched from the points except the surface in the same way as step 1.
4. An approximate plane β is fitted to $\{\mathbf{P}_{side}\}$ and the intersection of the line GE' and plane β is calculated. It is one of the points describing the edge.

The above procedure is conducted for each point on the boundary and the shape of the edge is obtained.

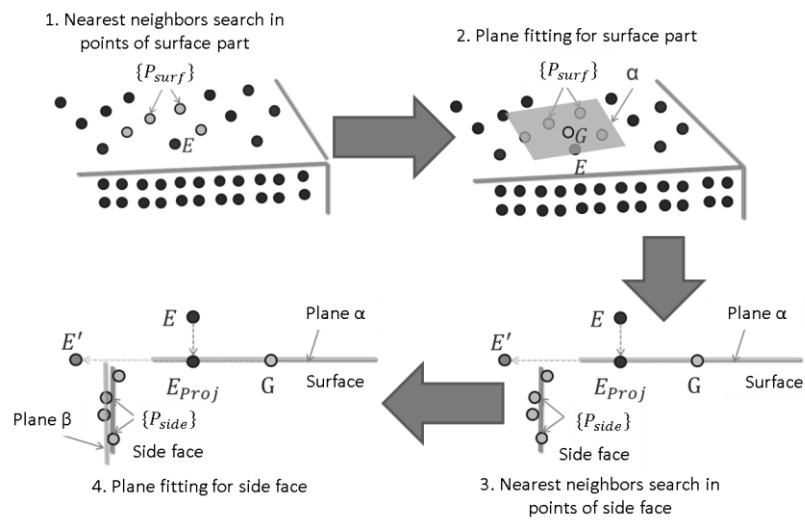


Figure 13-1 Procedure of edge fitting (Hiekata, K., Yamato, H., Sun, J., Matsubara 2014)

As an example of this solution, a panel's perimeter is measured as shown in Figure 13-2

The length of the edge 1 was calculated ten times. The result is shown in Table 13.2. The average of error is -0.15mm compared with the measured value by tape measure and standard deviation is 0.56mm . Two-sigma range is included from -1.27mm to 0.97mm . The accuracy of the error of length measured by the proposed method is less than 2mm .

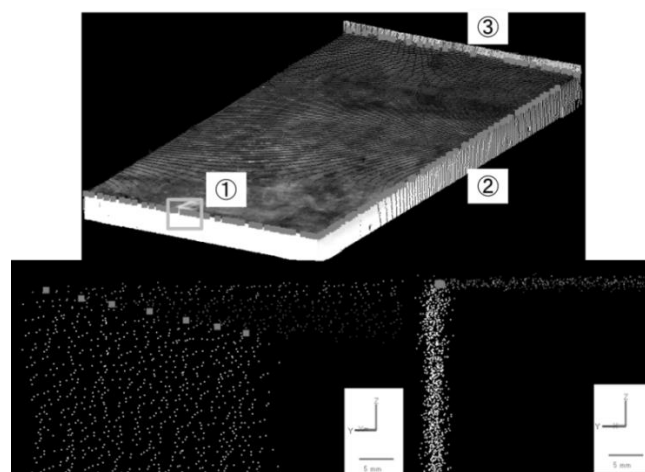


Figure 13-2 Result of measurement of edge shape in an experiment with a surface plate

Table 13.2 Result of measurement of edge length in an experiment with a surface plate (mm)

Average value by proposed method	Standard deviation	Value by tape measure	Average of error
1501.85	0.56	1502.0	-0.15

13.2.2. Scanner failure under high temperature

Considering the practical manufacturing environment in the shipyard, especially around the heating forming spot, in summer, the temperature could be over 40 degrees when doing the heating. And because the scanner is set on the crane about 5 meters above the heating forming spot where the cooling spray cannot reach, the temperature around the scanner can be kept about 50 degrees.

Because the scanner is not designed for long use under this serious situation, there is a high possibility for the scanner failure. Here gives some samples scan results when facing a scanner failure. These samples are scanned under about 48 degrees.

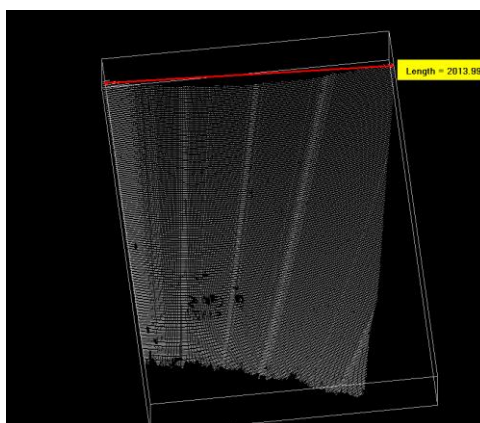


Figure 13-3 Scanner failure example (a)

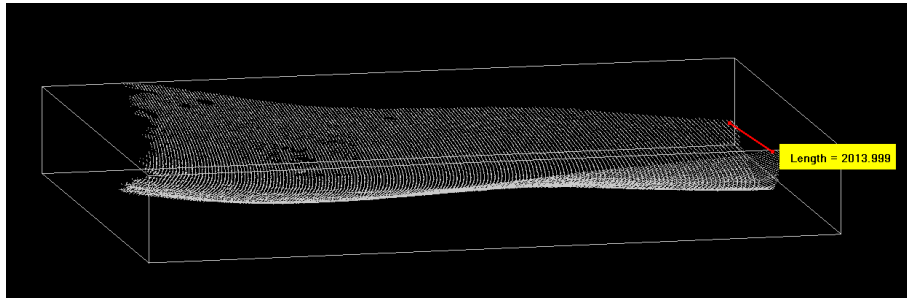


Figure 13-4 Scanner failure example (b)

As shown in Figure 13-3, there are some obvious flabellate noises distributed on the plate, and the measured length shown in the figure is about 50 mm shorter than the real length. Figure 13-4 illustrates another example about the scanner failure under high temperature, the undulated noise existing on the perimeters of the plate can be observed.

As a possible solution of this problem, the administrator of the shipyard is advised to set a fan under the scanner even there is already one built inside of the scanner. And to reduce the temperature of the scanner during the manufacturing, it is suggested that the workers can take a 10 minutes rest between two manufacturing steps to give the scanner enough time to cool off when the outdoor temperature is over 30 degrees.

13.3. Innovations in the proposed framework

In this sub-section, the innovation points of the proposed framework and the new manufacturing environment are discussed, and then the discussion about the proposed framework and the renovated manufacturing process will be summarized.

13.3.1. Manufacturing on vertical direction

Another difference between the conventional manufacturing process and the renovated manufacturing process is that the vertical templates are also no longer needed. Conventionally, the vertical templates have to be produced too before the

manufacturing of the plate. In this thesis, the vertical virtual templates can be generated at the same time from the same design data as the horizontal virtual templates. An example is the last manufacturing step of the plate “Hybrid 1”. As shown in Figure 13-5, the virtual templates are located on the plate automatically, and the gaps between the templates and the plate are also calculated and displayed on computer. Based on the vertical curvature analysis result from the system, the workers applied several heating lines to the plate as shown in Figure 13-6.

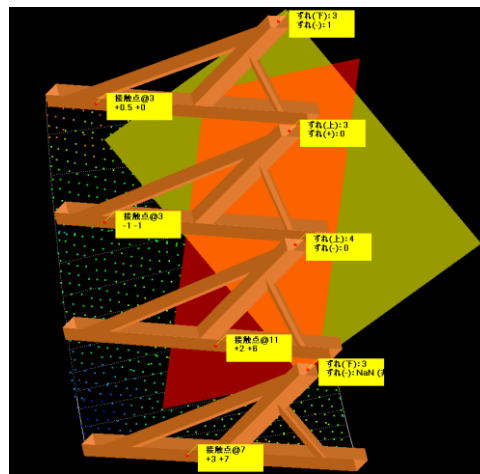


Figure 13-5 Vertical curvature evaluation using the vertical virtual templates

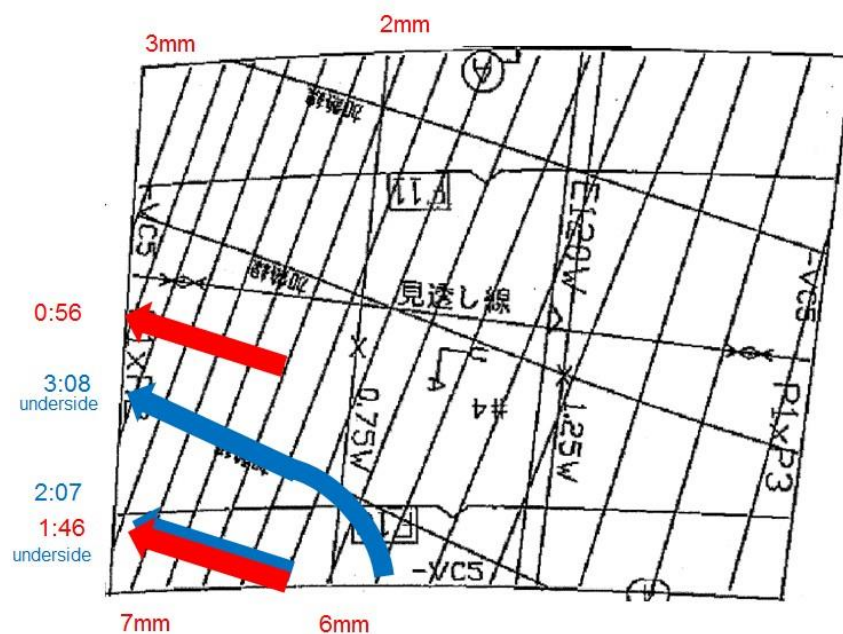


Figure 13-6 Heating lines on the vertical directions

13.3.2. Knowledge dissemination's innovation

A major problem in the curved shell plates' manufacturing is that the design of the manufacturing plan heavily depends on the implicit knowledge, habits and experience of the workers. Manufacturing plans varies according to the knowledge and skills of the craftsman in charge of the plate even for the same design shape. In other words, the current practice highly depends on the individuals and there is a risk to lose the knowledge and skills at the time of their retirement. Also to avoid inaccurate distorted output shapes and troubles in the subsequent heat sealing process, the tacit knowledge and skills for bending plates must be elicited, shared and reused in daily operation.

A conventional way to disseminate the knowledge existing in curved shell plates' manufacturing process is to make some introductions consisting of some independent rules based on the interviews with the expert workers.

However, some points making the conventional introduction manual ineffective and inefficient exist:

- The rules are all independent without considering the relationships with the former situations of the plate and the connections with the other rules.
- Some of the knowledge is tacit and unexplainable without the examples in the real practical environment.

The two knowledge models proposed in this thesis solved the problems above respectively. The interview-based NRDR knowledge model makes the relationships and the context of the independent rules clear enough for the beginner workers to follow step by step. On the other hand, the data-based knowledge model facilitates the elicitation of the tacit knowledge which can only be disseminated OJB.

Because all of the manufacturing data and the manufacturing scenario can be recorded on computer, the knowledge elicitation and dissemination can be done whenever the expert workers are available. And by using the virtualized rule base, the elicited knowledge is more comprehensible and easier to be modified when the new rules are found.

13.3.3. Discussions on the proposed framework and the renovated manufacturing process

The perspective plane and the contact points of the wooden templates and the plate are observed as shown in Figure 13-7 when trying to manufacturing the plates using the wooden templates. Specifically, in the conventional way of designing the heating lines, firstly, the wooden template A and wooden template B are put on the frame lines of the plate respectively. Then if the perspective plane cannot be confirmed (with strong angles between the two perspective sticks), the heating will be applied along with the vertical direction of the plate (the frame line's direction). The strength of the heating and the density of the heating lines are designed based on the angles between the wooden templates' sticks.

On the other hand, when trying to design the heating lines in the horizontal direction (crossing the frame lines), the steps below are followed to find out the points which need more heating:

- The degrees of the distances beside the contact points a and b.
- How much the wooden templates A and B can be swayed around the contact points.

Then the heating will be applied along with the roller lines painted on the plane and passing the points a and b.

Therefore, a lot of time and physical effort are cost in this process when trying to fix the wooden templates on the plate and observe the results. And because the observed results cannot be quantitative precise, the designed heating lines are usually different due to the different individual decisions.

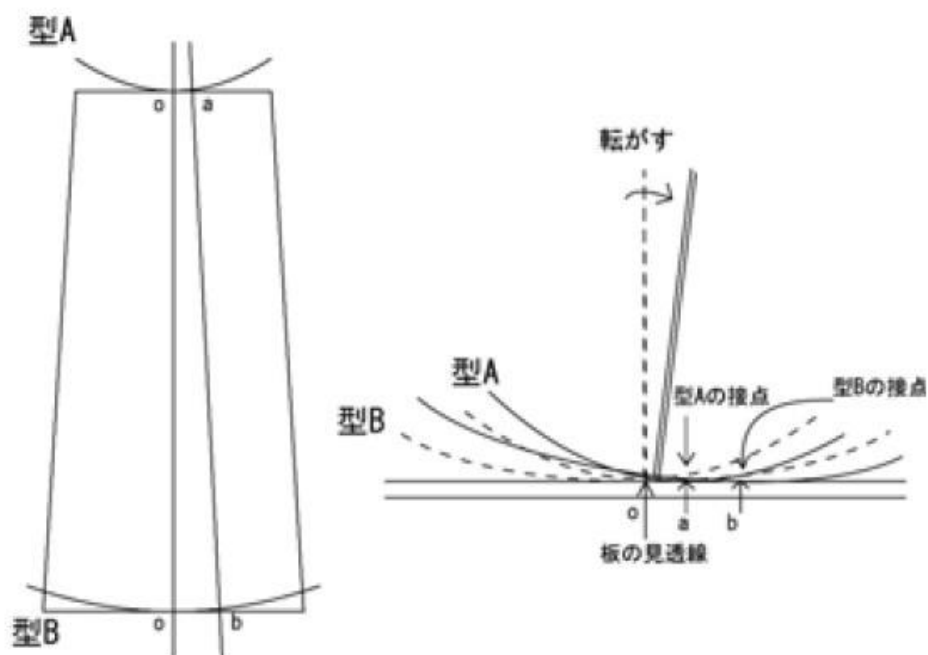


Figure 13-7 Conventional manufacturing method (Tanaka, Y., 2004)

According to this thesis, as shown in Figure 13-8, the conventional manufacturing process is renovated as follows:

- A) The production of the real wooden templates is no longer required.
- B) The completion judgment and the evaluation are performed on computer.
- C) The basic design of the manufacturing plans for every manufacturing step is performed on computer automatically.
- D) The advanced design of the manufacturing plans for some difficult manufacturing steps can be made by the expert workers based on the control and observation of the automatically arranged virtual templates.
- E) During D), the knowledge is elicited and modeled to facilitate the manufacturing by beginner workers.
- F) All of the measurement and analysis are performed automatically.
- G) Not only the horizontal curvature can be evaluated, but also the vertical virtual templates can be generated from the design data too.

In summary, both the manufacturing time and the physical effort can be saved to some extent by using the proposed framework.

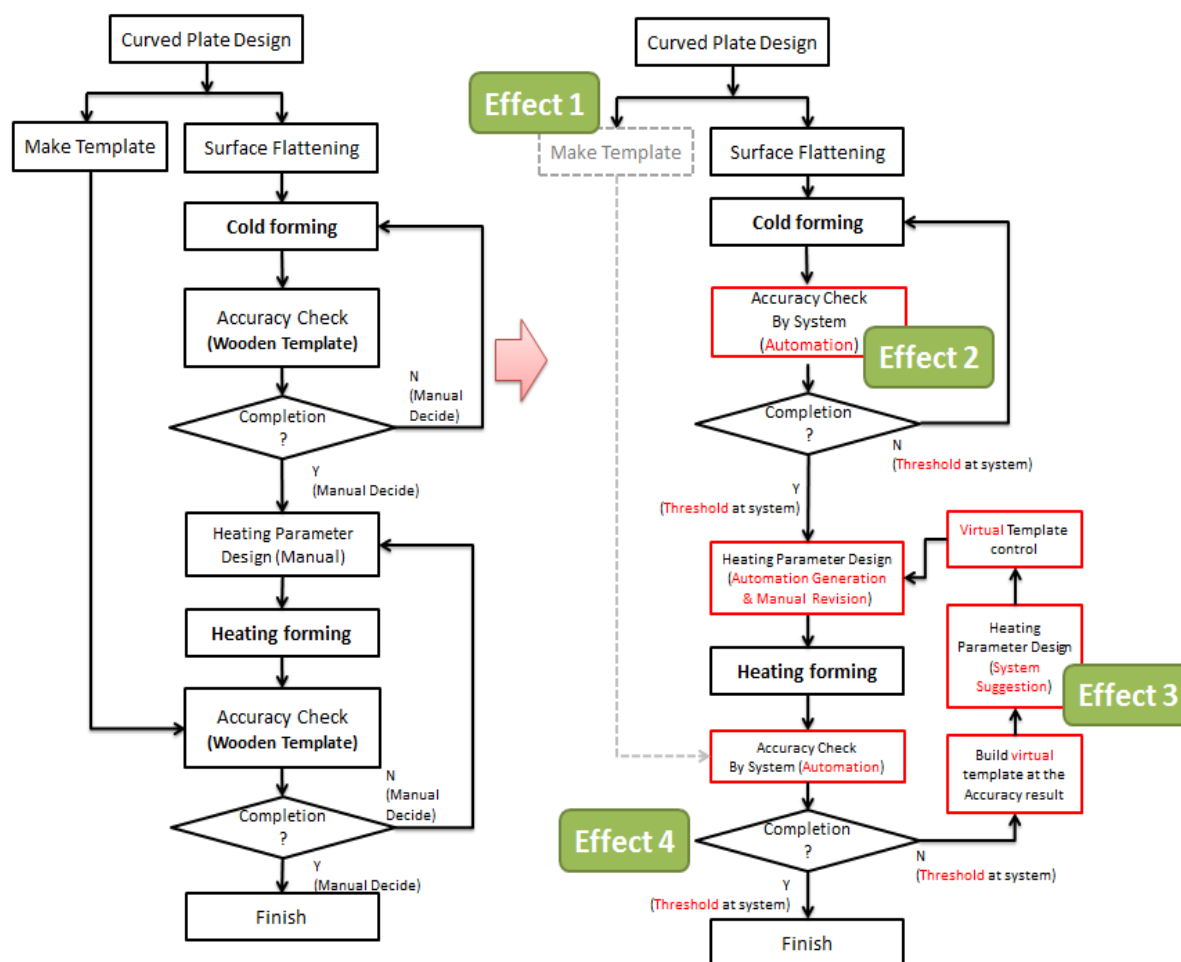


Figure 13-8 Renovated manufacturing process and the effects

The effects by introducing the proposed framework into the shipyard are evaluated as below:

Effect 1. Economic and environmental effect:

- ✓ The wooden templates (one set for about 1 million Yen) are no longer needed for most of the plates. The money can be saved for the new ship's design and the automation research of the curved shell plates. Besides, the production of wooden templates cost too much wood, about 5kg for one wooden template, and 4 – 8 wooden templates for 1 plate, and then about 200 plates for one ship. The proposed framework can also be considered as environment conscious.

Effect 2. Decrease of the setback on cold forming

- ✓ The experiments conducted to the plates with the same design shape proved that with the support of the proposed framework on the cold forming stage, the plates are seriously evaluated and judged if can be forwarded to the subsequent processing or not. This contributes to the decrease of the subsequent manufacturing time and the setback on cold forming. As shown in Figure 13-9, the plates passed the PSS check averagely are manufactured 2.5 hours less than which didn't. This is also because the press machine has the high deformation effect than the heating forming, thus the workers should try their best to achieve the press design shape during the cold forming instead of passing them to the heating forming stage regardless of their press accuracy.

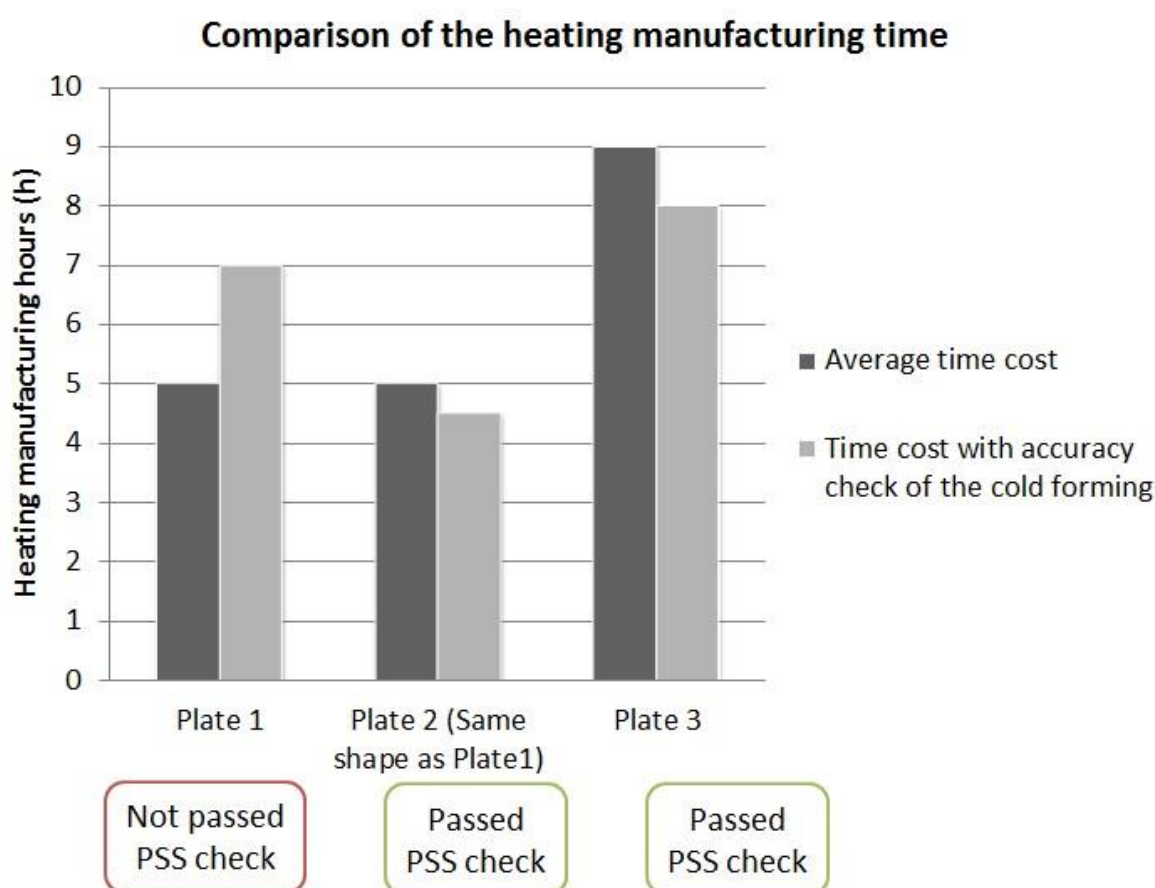


Figure 13-9 Decrease of the setback (long heating manufacturing time) on cold forming

Effect 3. Decrease of time cost and physical effort on heating forming

- ✓ The experiments conducted in the shipyard using the proposed VTS instead of the real wooden templates shows that the manufacturing time is dramatically reduced averagely 30% from the one under conventional manufacturing as shown in Figure 13-10. This is partly because the workers do not need to put the wooden templates on the plate for every manufacturing step any more, and the plate is evaluated more accurately. Also, instead of just evaluating 2 or 3 frames one time during the conventional manufacturing, VTS can evaluate all the frames at one time which are also considered an important reason for the decrease of the time cost.
- ✓ The physical effort is proved to be reduced, too. This is partly because the effort for putting and fixing the wooden templates are saved, as well as the total manufacturing time decreased.

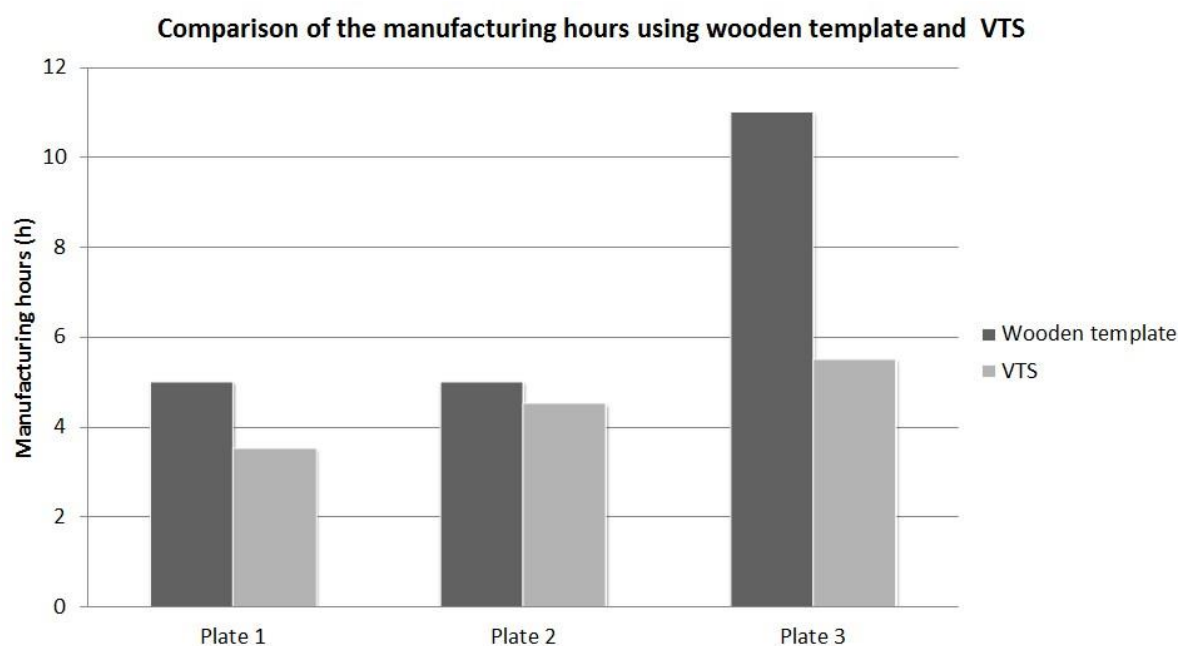


Figure 13-10 Decrease of time cost and physical effort on heating forming

Effect 4. Decrease of the failures and setback on heating forming

- ✓ The effectiveness of the developed automatic accuracy evaluation part of the proposed framework became clear in 5 months after introduction to shipyard. After each manufacturing step, the accuracy is evaluated using the system. Judging from the evaluation result, the workers decide whether to do the

modification manufacturing or pass the plate to subsequent heat sealing process. The result is shown in Figure 13-11 and Figure 13-12.

- ✓ By adopting the developed system, as shown in Figure 13-11, the rate of the finished plates which fell out of the fixed accuracy's tolerance range decreased from 75% to 45% within just 5 months. And as shown in Figure 13-12, the range of error (the distances from design data and measured data) decreased dramatically too.

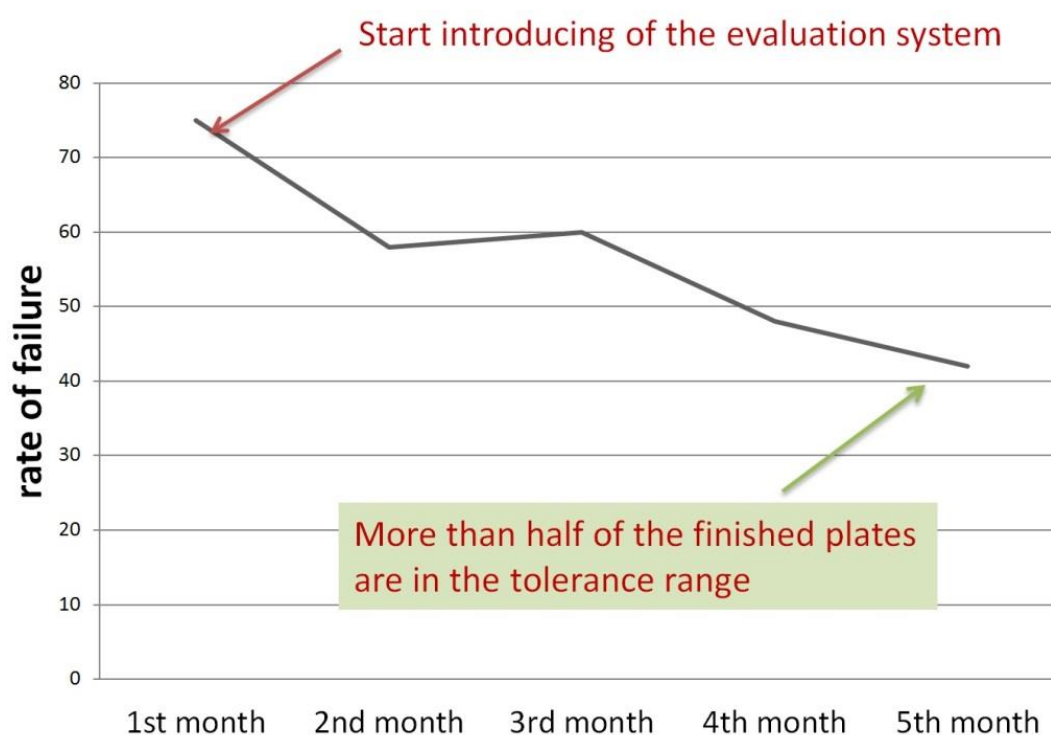


Figure 13-11 Rate of failure (%) on heating forming

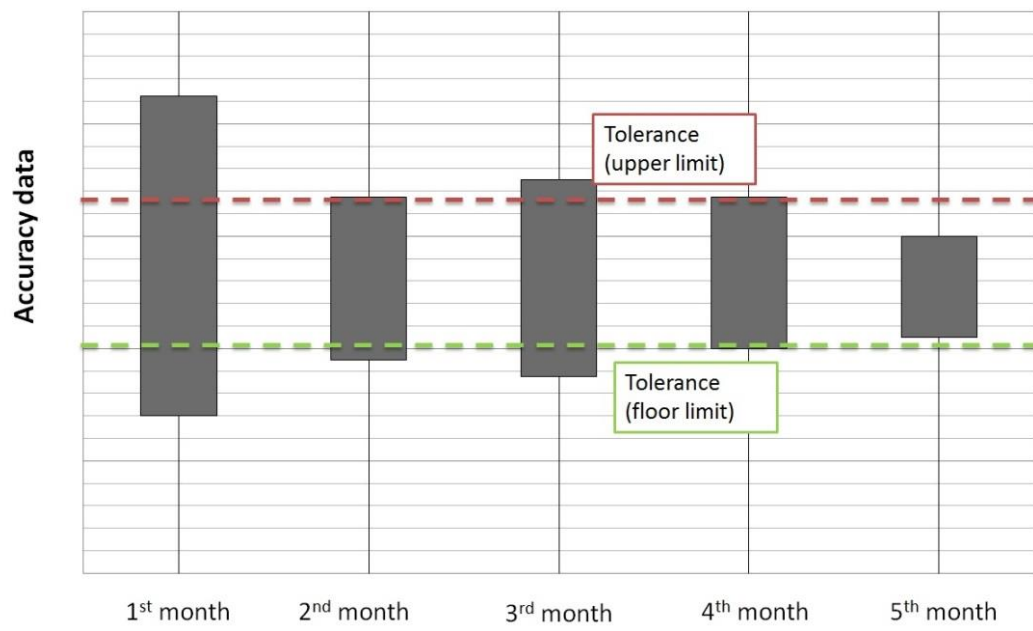


Figure 13-12 Change of accuracy distribution on heating forming

13.4. Values of this work

13.4.1. Cost impact

Based on the interview with the shipyard's administrator, a 10 years' scenario on the curved shell plates' manufacturing in shipyard S can be summarized as below:

Table 13.3 Curved shell plates' manufacturing scenario in shipyard S

<i>No</i>	<i>items</i>	<i>value</i>
(1)	Wooden templates' producing money per ship	5,000,000 ~ 8,000,000 JPY (average 6,500,000 JPY)
(2)	Life of wooden templates	about 2.5 years
(3)	Produced ship types at the same time	2 different types
(4)	Produced ships per year	4 ships
(5)	New ship type	every 4~6 years (average 5 years)
(6)	Curved shell plates per ship	about 180 plates per ship
(7)	Manufacturing time	7 hours / plate
(8)	Readjustment due to poor quality	200 hours / ship
(9)	Labor cost per hour	5500 JPY/ hour

Therefore, for the next 10 years, under current situation, the cost of the wooden template's producing should be around $C_{Wood} = (1) \times (3) \times 10 / (2)$. The cost for the normal manufacturing for this 10 years should be about $C_{Manufacturing} = (6) \times (7) \times (9) \times (4) \times 10$. And the readjustment cost due to the poor manufacturing quality should be about $C_{readjustment} = (8) \times (9) \times (4) \times 10$.

The impact of this work is evaluated based on the scenario above. The only extra cost for introducing the proposed framework is the cost of buying laser scanner which is about 5,000,000 JPY. Dramatic support effects have been observed in the experiments conducted in the shipyard. The evaluation and the measurement

during the whole manufacturing process of curved shell plate are totally automatically performed on computer. Real wooden templates are no longer needed; the time cost and physical effort on using them are also saved. What the workers need to do is just push some buttons to select the plate they want to evaluate, and then just wait no longer than 3 minutes for the analysis result.

The high accurate evaluation results after the cold forming and heating forming manufacturing tell the workers if the plate is ready for the subsequent processing or not. The cold forming and the heating forming repeat themselves until the plate passes the system check which contributes to the decrease of the setbacks from the subsequent processing.

The computer-calculated parameters for the manufacturing plan design help the workers design more effective and efficient heating actions. The high measurement and calculation speed and the accurate virtual templates' parameters contribute to the decrease of the manufacturing time comparing to the conventional manufacturing. Knowledge learning is no longer restricted to OJT. Since the 3D manufacturing scenarios are recorded by the proposed framework, the knowledge elicitation and dissemination for the beginner workers can be conducted at any time they want. The knowledge is no longer a set of independent obscure introductions, but a series of well-constructed rules which can facilitate the beginner worker's manufacturing.

Based on the experiments' results, the heating manufacturing time is averagely reduced to about 70% by introducing the proposed framework. The readjustment time due to poor quality is also reduced to about 55%.

Therefore, the manufacturing cost, the readjustment cost, as well as the hardware cost can all be reduced dramatically by introducing the proposed framework into shipyard during this 10 years' scenario.

13.4.2. Academic values

The academic values of this work can be demonstrated from two aspects: the point cloud processing when facing data with irregular obstacles and the knowledge engineering during the active manufacturing process.

For the point cloud processing of the data containing irregular obstacles which is obviously not only an identical problem in shipyard, the pre-processing methods proposed in Chapter 5 can give chances to remove these obstacles and register them with the design data.

Not only can curved shell plates be extracted from the measured point cloud using the proposed algorithm, other components, such as the panel or the block's lateral surface can use the proposed method. Figure 13-13 shows the extraction results of a panel component.

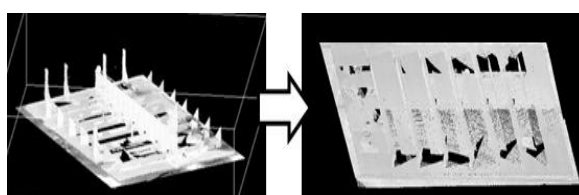


Figure 13-13 Panel extraction result

For the knowledge engineering during the active manufacturing processes, this work firstly proposed a framework which can record every single manufacturing step and suggest the manufacturing plans in real time.

The figure below shows the values of the proposed framework comparing doing the interviews during the manufacturing for knowledge extraction. The reproducibility of the manufacturing process enables the interviews after a plate is finished. More accuracy of the evaluation results leads to the identical answer even from multiple experts. Rules and guidelines can be obtained by comparing multiple plates under the similar situation.

Thanks to this framework, it becomes easier to do the interview with existing rule base. And the rules can be confirmed after being extracted.

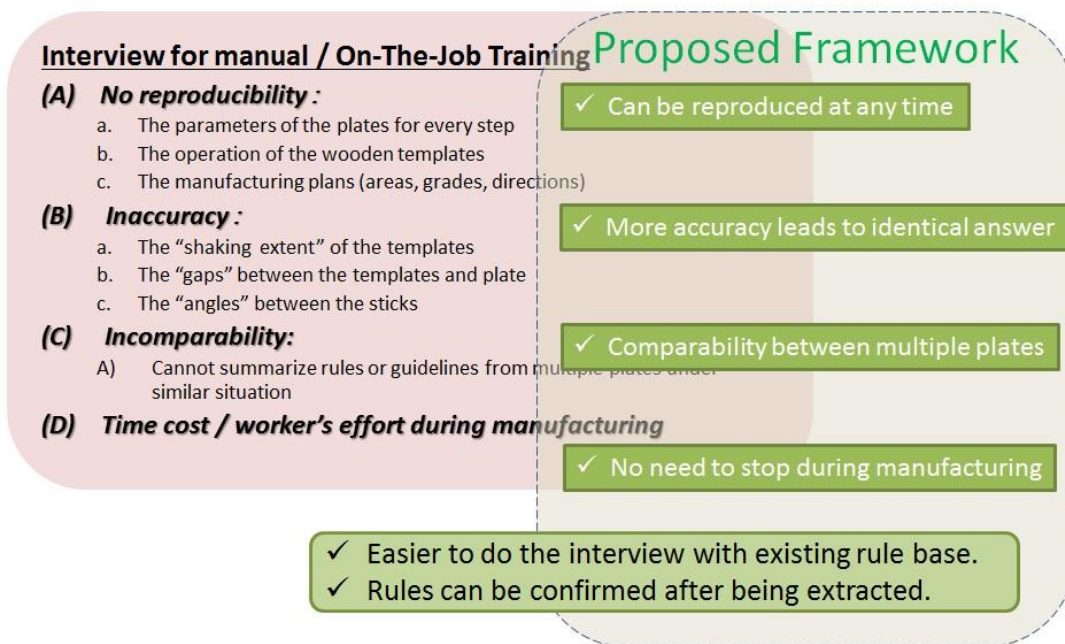


Figure 13-14 Improvement in knowledge engineering

Chapter 14 Conclusion

14.1. Conclusion

A practical framework for facilitating the whole manufacturing process of the curved shell plate was proposed. Necessary original innovations for realizing the proposed framework were introduced:

- (1) Interfaces for facilitating the curved shell plates' manufacturing and preserving the manufacturing convention were proposed and developed with high accuracy and high usability. Efficient method for eliciting and disseminating the knowledge existing in the manufacturing processes based on the data recorded by the proposed interfaces was proposed.
- (2) Original point cloud processing methods supporting (1) for extracting the plates' point clouds which are separated by irregular obstacles and for registering them with the design data were developed.

Multiple experiments evaluating and manufacturing the curved shell plates were conducted in the shipyard S to verify the methods proposed in the framework. The conclusions can be summarized as below:

- (A) The manufacturing convention preserving interfaces and knowledge elicitation and dissemination methods

The cold manufacturing support interface was generated by comparing the press design data and the measured point cloud of the plate to calculate and virtualize the distance errors and the perimeters of the plate. The plate's areas which the real wooden templates cannot check were also evaluated and visualized by the proposed color map interface. The heating forming support interface was generated by virtualizing the conventional manufacturing process in which the wooden template was used. The wooden templates were virtualized and the manufacturing parameters supporting the conventional

manufacturing are calculated on computer. The workers could operate and observe the virtual template in the conventional way to reserve the conventional manufacturing skills and habits.

The knowledge elicitation and dissemination method using Nested Ripple-Down-Rules was proposed. By updating the existing rule base according to the differences between the system-suggested manufacturing plan shown on the proposed interfaces and the worker-used manufacturing plan, the knowledge elicitation process from the expert workers was introduced. By visualizing both the existing rule base and the details of the plate's information, the knowledge can be efficiently disseminated to the beginner workers.

According to the experiments eliciting knowledge using 3 different kinds of plate during totally over 20 manufacturing steps, it showed that the knowledge about the line heating and point heating was successfully elicited. These two can be used to manufacture over 90% of the plates in the shipyard. The elicited rule base was verified though the interviews with the expert workers. The beginner worker successfully manufactured 2 plates using the manufacturing plans suggested by the system in the dissemination experiment. The effectiveness of the proposed method is confirmed.

(B) The point cloud processing methods

As common pre-processing for both the cold forming and the heating forming supporting, the general region growing method was redesigned for achieving high extraction speed and reducing the extraction errors. The method for recognizing the separated parts of the plates' point clouds caused by the obstacles existing in the raw data was developed by proposing the common domain judging standard based on the edges of the extracted domains. The registration method of the measured data and the design data was proposed by pre-setting the registration directions.

In the preliminary experiments conducted in the shipyard, over 200 plates were extracted and registered using the proposed methods. The average extraction time (about 38 seconds per million points without separations)

showed that the reformed extraction method can satisfy the practical usage in the shipyard. Besides, about 120 plates separated by different kinds of obstacles were also extracted successfully which demonstrated the effectiveness of the common domain recognition standard. Finally, all of these 200 plates were successfully registered with design data automatically, and the calculated displacement color maps were verified by using the real wooden templates at the end of the manufacturing.

According to the experiment results of the whole framework, the high and stable quality of the cold forming was achieved. The contribution of the cold forming support system for the decrease (average 1.5 hours per plate) of the subsequent manufacturing time and the setback on cold forming was confirmed.

With the proposed interface for heating forming, the manufacturing time was dramatically reduced averagely 30% from that under conventional manufacturing. The interviews with the workers who used the proposed virtual template interface showed that the physical effort was reduced, too. The heating manufacturing time was averagely reduced to about 70% by introducing the proposed framework. The readjustment time due to poor quality was also reduced to about 55%. That the interface outputted by the proposed system can facilitate different kinds of curved shell plate's manufacturing following the conventional manufacturing technics was confirmed.

14.2. Future work

The automation of the curved shell plate's manufacturing is always a dream of not only the workers but also the whole shipbuilding industry.

(1) In the future, experiments about other types of curved shell plates will be carried out, and a complete knowledge database is to be constructed. Based on a complete knowledge database, the virtualized manufacturing process proposed in this paper can be expected to be optimized, more and more knowledge will be elicited from the experts not only for the beginners but also for our future automation machine.

(2) After about several years manufacturing plates using the proposed framework, the different ideas between multiple expert workers can be compared, evaluated and scored by using the recorded subsequent manufacturing processes. The possible usage of the accumulated data in the future is discussed in the Appendix A.2.

Finally, the design of the manufacturing plan can be standardized and the automatic machining technic is becoming mature which will absolutely give all of us an adequate ground to continue aiming higher, and higher.

REFERENCES

Araki, M., Inoue, N., Horioka, M., Ando, M. (1973) : “On Angular Distortion of Hull Steel Plates by Line Heating Methods”. *Journal of Zosen Kyokai*, , 133 : 343-348.

Arias, P., Armesto, J., Lorenzo, H., Ordóñez, C. (2007): “Terrestrial Laser Technology in Sporting Craft 3D Modelling”. *Proceedings book of the International Symposium CompIMAGE 2006. Computational Modelling of Objects Represented in Images: Fundamentals, Method and Applications*. ISBN 978-0-415-43349-5, Vol. 1, 63-69.

Besl, P. and McKay, N. (1992): “Method for Registration of 3-D Shapes”, *IEEE Transactions on Pattern Analysis and Machine Intelligence*, 14(2), 239-256.

Beyer, H., Holtzblatt, K. (1998): “Contextual Design: Defining Customer-Centered Systems”, *Morgan Kaufmann Publishers*. 1998.

Bindoff, I., Curtain, C., Peterson, G., Westbury, J., Ling, T.(2014): “Problems Detected by a Ripple-Down Rules Based Medication Review Decision Support System: Are They Relevant?”, *Knowledge Management and Acquisition for Smart Systems and Services Volume 8863 of the series Lecture Notes in Computer Science* pp 59-68

Bisgaard, C. H. (2000) : “Plate Forming by Line Heating”. *Denmark : Technical University of Denmark*.

Biskup, K. (2007): “Application of Terrestrial Laser Scanning for Shipbuilding”, *ISPRS Workshop on Laser Scanning 2007 and SilviLaser 2007*, pp56-61.

Catlett, J. (1992): "Ripple-Down-Rules as a mediating representation in interactive induction". Proceedings of the Second Japanese Knowledge Acquisition for Knowledge-Based Systems Workshop, Kobe, Japan,

Catmull, E. and Clark, J (1978): "Recursively generated B-spline surfaces on arbitrary topological meshes", Computer-aided design

Caversan F.L. (2009): "Fuzzy Computing: Basic Concepts" .
http://www.aforgenet.com/articles/fuzzy_computing_basics/

Cheung, C.F., Lee, W.B., Wang, W.M., Wang, Y., Yeung, W.M. (2011): "A multi-faceted and automatic knowledge elicitation system (MAKES) for managing unstructured information", Journal of Expert Systems with Applications 38 (2011) 5245–5258

Clancey, W. J. (1985): "Heuristic classification." Artificial Intelligence 27(3):289-350.

Clancey, W. J. (1992): "Model construction operators." Artificial Intelligence 53: 1-115.

Compton, P., Horn, K. et al. (1989): "Maintaining an expert system. Application of Expert Systems" Ed. J. R. Quinlan. London, Addison Wesley. 366-385.

Compton, P. and Jansen, R. (1990): "A philosophical basis for knowledge acquisition." Knowledge acquisition 2: 241-257.

Compton, P., Edwards, G. et al. (1992). "Ripple down rules: turning knowledge acquisition into knowledge maintenance." Artificial Intelligence in Medicine 4:47-59.

- Compton, P., Kang, B. H. et al. (1993): "Knowledge acquisition without analysis. Knowledge Acquisition for Knowledge Based Systems", Lectures Notes in AI (723) Eds. G. Boy and B. Gaines. Berlin, Springer Verlag. 278-299.
- Compton, P., Preston, P. et al. (1994): "Local patching produces compact knowledge bases". A Future for Knowledge Acquisition Eds. L. Steels, G. Schreiber and W. V. d. Velde. Berlin, German, Springer-Verlag. 104-117.
- Cristobal, G., Schelkens, P. and Thienpont, H. (2011): "Optical and Digital Image Processing", John Wiley & Sons, Hoboken, New Jersey, US.
- Enomoto, M., Oguri, S., Masuda, H., Tanaka, I. (2012): "Accuracy assessment of Mid-Range Laser Scanners by measuring a flat board", The Japan Society of Precision Engineering, 2012 Autumn Conference
- FARO (2011), "FARO Laser Scanner Focus 3D", Available at<<http://www.globalspec.com/datasheets/579/FARO/F7DD1C91-CE09-4A0A-AB9C-71EC273AC1FA>>, Accessed on March. 28th.
- Forsyth, D. and Ponce, J. (2007): "Computer Vision : A Modern Approach", Prentice Hall Professional Technical Reference .Upper Saddle River, New Jersey, US
- Fujimura, K. (2009): "Efficiency Improvement of Automated Line Heating for Plate Forming Using IHI-ALPHA System", JASNAOE, The Japan Society of naval Architects and Ocean Engineers, 2009. Vol. 49, 2009, pp. 43-46 (in Japanese)
- Gabriel, A. (2001) : "Lagrange and average interpolation over 3D anisotropic elements", Journal of computational and applied mathematics , vol 135 , pp91 – 109
- Gaines, B.R, Compton, R. (1995): "Induction of Ripple-Down Rules Applied to Modeling Large Databases", Journal of Intelligent Information Systems, 5, 211-228.

Gordon, S., Lichti, D., Franke, J., Stewart, M., (2004): “Measurement of Structural Deformation using Terrestrial Laser Scanners”. Archives of 1st FIG International Symposium on Engineering Surveys for Construction Works and Structural Engineering.

Gross, M. and Pfister, H (2007), “*Point-based Graphics*”, Morgan Kaufmann, Burlington, Massachusetts, US.

Hayashi, S., Sunagawa, Y., Matsuoka, K., Tomisawa, S., Katsumata, K., Iwata, T.(2004): “State-of-the-art of Plate Forming in Japan”; JASNAOE, The Japan Society of naval Architects and Ocean Engineers, Vol. 3, 2004, pp. 107-108 (in Japanese)

Hiekata, K., Yamato, H., Oida, Y., Enomoto, M., Furukawa, Y. (2011): “Development and Case Studies of Accuracy Evaluation System for Curved Shell Plates by Laser Scanner”, Journal of Ship Production and Design, vol.27, (2), pp.84-90.

Hiekata, K., Yamato, H., Rojanakamolpan, P. (2007): “Ship Design Educational Framework Using ShareFast: A Case Study of Teaching Ship Design With CAD Software”, Journal of Ship Production, Vol. 23, No. 4, November 2007, pp. 202–209

Hiekata, K., Yamato, H., Sun, J., Matsubara, H., Toki, N (2014): “Study on Improving Accuracy for Edge Measurement Using 3D Laser Scanner” ; Product Lifecycle Management for a Global Market IFIP Advances in Information and Communication Technology, 2014, p.427-434 Vol. 442

Hiekata, K., Yamato, H., Sun, J. Y., Matsubara, H., Toki, N (2014): “Development of Method for High Accuracy Edge Measurement Using 3D Laser Scanner”; PLM International Conference on Product Lifecycle Management, July 2014

Hiekata, K., Yamato, H., Sun, J.Y., Nakagaki, N., Sugawara, A. (2012): "Utility of Accuracy Evaluation System for Curved Shell Plates Using Laser Scanners"; JASNAOE, The Japan Society of naval Architects and Ocean Engineers, 2012. Vol. 15, 2012, pp. 117-120 (in Japanese)

Hiekata, K., Yamato, H., Sun, J.Y., Nakagaki, N., Sugawara, A. (2011): "Development of Extraction Algorithm of Curved Shell Plates from 3D Point Cloud Data"; JASNAOE, The Japan Society of naval Architects and Ocean Engineers, 2011. Vol. 13, 2011, pp. 159-162 (in Japanese)

Hill, M. (1990): "K-d trees for semidynamic point sets", SCG '90 Proceedings of the sixth annual symposium on Computational geometry, 1990, pp. 187-197

Ikeda, Y. (2009): "Everything About The Ship", NATSUME publisher, 2009

Jeffrey, S. B. and David G. L. (1997) : "Shape Indexing Using Approximate Nearest-Neighbour Search in High-Dimensional Spaces", In Conference on Computer Vision and Pattern Recognition, pp1000-1006

Kakuta, R., Yamato, H., Ando, H., Koyama, T., Nakamura, S.(2007): "A study on analysis of BRM Simulator Training Scenario by Using of Simulation", The Japan Society of Naval Architects and Ocean Engineers, 2007, Volume 6, 99-107

Kalogerakis, E., Nowrouzezahrai, D., Simari, P., Singh, K. (2009): "Extracting lines of curvature from noisy point clouds", pp282-292, Computer-Aided Design.

Kobayashi, Y. (2008): "Useful Application of a Non-contact 3D Measuring System for Nissan's Monodukuri", Nissan Technical Review, 62, pp56-60.

Levin, D. (2003): "Mesh- independent surface interpolation", Geomertic modeling for Scientific Visualization, pp37-49, 2003

Liu, M., Chen, D. G., Wu, C (2002): “The continuity of Mamdani method, Machine Learning and Cybernetics”, 2002. Proceedings. 2002 International Conference on (Volume:3)

Makoto, S., Seira, N., Ayumi, T. (2008): “Attempt of Cloth Animation by OpenGL”, Memoirs of the Faculty of Engineering, Miyazaki University 37, 299-304 (in Japanese)

Makoto, S., Seira, N., Ayumi, T. (2010): “Attempt of Cloth Animation by OpenGL II”, Memoirs of the Faculty of Engineering, Miyazaki University 41, 291-294 (in Japanese)

Makoto, S., Seira, N., Ayumi, T. (2012): “Attempt of Cloth Animation by OpenGL III”, Memoirs of the Faculty of Engineering, Miyazaki University 39, 327-332 (in Japanese)

Masaki, M., Kazuyoshi, K., Jyunichi, K. (1993) : “A Preliminary Study on the Angular Distortion by Line-heating”. NASA no. 19980223034 Reports of the Faculty of Engineering, Nagasaki University(ISSN 0286-0902), 23(40) : 55-63.

Matsuoka, K., Sunagawa, Y., Tanaka, Y., Tomisawa, S., Takagi, E., Asari, E. (2004): “New Plane Development Method Considering Plate Forming Process”; JASNAOE, The Japan Society of naval Architects and Ocean Engineers, Vol. 3, 2004, pp. 103-104 (in Japanese)

Monserrat, O., Crosetto, M. (2008): “Deformation measurement using terrestrial laser scanning data and least squares 3D surface matching”, ISPRS Journal of Photogrammetry & Remote Sensing 63 (2008) 142–154

Nakagaki, N., Sugawara, A., Hiekata K., Yamato, H., Enomoto, M.; Takahashi, K, (2011): “Development of the Algorithm for Accuracy Evaluation System for Curved Shell Plates by Laser Scanner”. the 15th International Conference on Computer Applications in Shipbuilding (ICCAS 2011),

Nakagaki, N., Sugawara, A., Hiekata, K., Yamato H., and Sun, J.Y. (2013): “Development of Accuracy Evaluation System for Curved Shell Plates Using Laser Scanners (2nd Report)”. Journal of the Japan Society of Naval Architects and Ocean Engineers, 17, 169-176 (in Japanese)

Nguyen, D. Q., Pham, D. D., Pham, S. B.(2015): “A Robust Transformation-Based Learning Approach Using Ripple Down Rules for Part-of-Speech Tagging”, Computer Science - Computation and Language, 1412.4021

Okuda, H., Kitaaki, Y., Hashimoto, M., Kaneko, S. (2004): “Fast and High-precision 3-D Registration Algorithm using Hierarchical M-ICP”, THE INSTITUTE OF ELECTRONICS, INFORMATION AND COMMUNICATION ENGINEERS, TECHNICAL REPORT OF IEICE, PRMU2003-54, pp1-8.

Okumoto, T. (2009): “Shipbuilding Technology And Production System”, SEIZANDO publisher, 2009.

Park, H. S., Lee, H. M.(2007): “A New Approach for Health Monitoring of Structures: Terrestrial Laser Scanning”, Computer-Aided Civil and Infrastructure Engineering 22 (2007) 19–30

Park, J.S, Shin, J.G, Ko, K.H. (2007): “Geometric assessment for fabrication of large hull pieces in shipbuilding”, CAD, 39, pp.870-881.

Pauly,M., Gross,M., Kobbelt,L.(2002): “Efficient simplification of point-sampled surfaces”, Proceedings of the conference on Visualization,02,163-170, Boston, US, October.

Piegl, L., Tiller, W. (1996): “The NURBS Book 2nd Edition”, Springer.

Pu, S., Vosselman, G. (2009): “Knowledge based reconstruction of building models from terrestrial laser scanning data”, ISPRS Journal of Photogrammetry and Remote Sensing 64 (2009) 575–584

Rabbania, T., Heuvelb, F. A., Vosselmanc, G.(2006): “Segmentation of point clouds using smoothness constraint”, ISPRS Commission V Symposium 'Image Engineering and Vision Metrology' Volume XXXVI, Part 5, 248-253

Robinson, S., Lee, E.P.K., Edwards, J.S. (2012): “Simulation based knowledge elicitation: Effect of visual representation and model parameters”, Expert Systems with Applications 39 (2012) 8479–8489

Scully, K.(1987): “Laser Line Heating. Journal of Ship Production”, 3(4) : 237–246.

Shin, J.G., Ryu, C.H., Nam, J.H. (2004): “A Comprehensive Line-Heating Algorithm for Automatic Formation of Curved Shell Plates”, Journal of Ship Production, Volume 20, Number 2, pp. 69-78(10)

Sithole, G., Vosselman, G.(2003): “Automatic structure detection in a point-cloud of an urban landscape”. 2nd Joint Workshop on Remote Sensing and Data Fusion over Urban Aereas (Urban 2003)

Sun, J.Y., Hiekata, K., Yamato, H., Nakagaki, N., Sugawara, A.(2014) : “Efficient Point Cloud Data Processing in Shipbuilding” : Reformative Component Extraction

Method and Registration Method ; IJCC, Journal of Computational Design and Engineering Volume 1, Number 3, July 2014, pages 202-212

Sun, J.Y., Hiekata, K., Yamato, H., Nakagaki, N., Sugawara, A. (2014):
“Virtualization and automation for knowledge extraction in curved shell plates’
machining plan design process” ; IJASM, International Journal of Agile Systems
and Management, 2014, p.282-303 Vol.7

Sun, J.Y., Hiekata, K., Yamato, H., Maret, P., Muhuhlenbach, F. (2015): “Process
Knowledge Model For Facilitating Industrial Components’ Manufacturing” ; 22th
ISPE International Conference on Concurrent Engineering, 2015.07, p.406-415

Sun, J.Y., Hiekata, K., Yamato, H., Nakagaki, N., Sugawara, A. (2014); “A
Knowledge-Based Approach for Facilitating Design of Curved Shell Plates’
Machining Plans”; 21th ISPE International Conference on Concurrent Engineering,
2014.09, p.143-152

Sun, J.Y., Hiekata, K., Yamato, H., Nakagaki, N., Sugawara, A. (2013) : “Automatic
Generation of Curved Shell Plates’ Processing Plan Using Virtual Templates for
Knowledge Extraction” ; 20th ISPE International Conference on Concurrent
Engineering, 2013.09, p.441-450

Sun, J.Y. (2014): “Knowledge-based Approach for Facilitating Design of Curved
Shell Plates’ Manufacturing Plans in 3D Virtual Environment”; PLM International
Conference on Product Lifecycle Management, July 2014

Sun, J.Y., Hiekata, K., Yamato, H., Nakagaki, N., Sugawara, A. (2013):
“Development of Software System For Generating Curved Shell Plate's Processing
Plan Using Virtual Templates”; ICCAS, International Conference on Computer
Applications in Shipbuilding, 2013, Busan, Korea, 2013.09, p.131-138 Vol.2

Sun, J.Y., Hiekata, K., Yamato, H., Nakagaki, N., Sugawara, A. (2014):
“Development And Evaluation of Curved Shell Plate’s Processing Plan Generation System Using 3D Measured Data and Virtual Templates”; JASNAOE, The Japan Society of naval Architects and Ocean Engineers, 2014. Vol. 19, 2014, pp.603-606 (in Japanese)

Sun, J.Y., Hiekata, K., Yamato, H., Nakagaki, N., Sugawara, A. (2013):
“Development And Evaluation of Curved Shell Plate’s Processing Plan Generation System Using 3D Measured Data and Virtual Templates”; JASNAOE, The Japan Society of naval Architects and Ocean Engineers, 2013. Vol. 16, 2013, pp. 563-566 (in Japanese)

Tanaka, Y., Matsuoka, K., Hayash, S., Ando, T. (2004): “Data Bases for Plate Forming Process”; JASNAOE, The Japan Society of naval Architects and Ocean Engineers, 2004. Vol. 16, 2004, pp. 105-106 (in Japanese)

Tango, Y., Ishiyama, M., Suzuki, H. (2011): ““IHIMU-alpha" A Fully Automated Steel Plate Bending System for Shipbuilding”, IHI Engineering Review, 44(1), pp.6-11,

Varady, T., Benko, P.(2000) Reverse engineering B-rep models from multiple point, in: Proceedings of Geometric Modeling and Processing, April 2000, IEEE, Hong Kong, pp. 3–12.

Wang, Z., Liu, Y.J., Ji, Z.Y. (2007) : ”Research on Pivotal Techniques for Automatic Line-Heating Process; Design and manufacture of ships and marine structures”, Dalian University of Technology, Doctoral Thesis, 2007

Wani, M. A., Arabnia, H. R., (2003): “Parallel edgeregion-based segmentation algorithm targeted at recon-figurible multiring network”. Journal of

Supercomputing 25(1), pp. 43–62.

Weingarten, J., Gruener, J., and Siegwart, R. (2004): “Probabilistic Plane Fitting in 3D and an Application to Robotic Mapping”, *Robotics and Automation (ICRA)*, 1, 927-932.

Yang, M., Lee, E. (1999): “Segmentation of measured point data using a parametric quadric surface approximation”, *Journal of Computer-Aided Design*, Volume 31, Issue 7, June 1999, 449–457

Yun, D., Kim, S., Heo, H., Koa, K.H. (2015): “Automated registration of multi-view point clouds using sphere targets”, *Journal of Advanced Engineering Informatics*, 2015, 1-10.

Zhang, X. P., Li, H. J., Cheng Z. L. (2008): “Curvature Estimation of 3D Point Cloud Surfaces Through the Fitting of Normal Section Curvatures”, *ASIAGRAPH 2008 PROCEEDINGS*

Zhang, Z. (1994): “Iterative Point Matching for Registration of Free-Form Curves and Surfaces”, *International Journal of Computer Vision*, 13(2), 119-152.

ACKNOWLEDGE

I would like to show my sincerest gratitude to the people who have helped and supported me during my Master and PHD study in The University of Tokyo. Foremost, I would like to give my sincere thankfulness to my academic supervisor, Associate Professor Kazuo Hiekata, for his precious instructions and uncountable enlightenments on my academic study, and also for his edification to my cognition of the laboratory in Japan. Without him, I could get lost a million times facing various obstacles of my research life during the 5 years' study. I also want to express my super appreciations to Professor Hiroyuki Yamato, specifically for his advices when I faced troubles, and also for his extremely valuable support in my research. Appreciations to professor Shinichi Warisawa for the kind advices and comments at the preliminary review meeting. And great thanks to Associate Professor Susumu Shirayama, for his kind support at the joint meeting of the design engineering lab and the preliminary review meeting. Super thanks to Associate Professor Bryan Moser too for his kind supports when I did presentations abroad in Netherlands and in the regular meetings of my lab. Also, I want to especially thank Assistant Professor Taiga Mitsuyuki, for his kind support, sharing time with my research at any time despite being so busy.

A lot of thanks to Professor Pierre Maret, for his instructions on the knowledge model part of my research during the 6 months' study in France.

Sincere appreciation goes to Mr Norito Nakagaki and Mr Akiyoshi Sugawara from Sumitomo Heavy Industries Marine and Engineering Co. ,Ltd.. They were in

charge of the administration in the shipyard during my experiments and gave a lot of valuable advices and suggestions on the experiment configurations. They shared a lot of time for supporting the practical usage of my systems in the shipyard. Besides, a lot of help is from worker Mr Ito who conducted the manufacturing in the experiments under severe manufacturing conditions in August, cooperated very well while being interviewed and gave a lot of opinions

Great appreciations to Associate Researcher Isaac Okada who always has brilliant advices whenever I faced problems no matter in my study or my life, and provides me with a lot of chances to know Japanese culture. Thanks to Mr. Masakazu Enomoto for his kind advices and supports for my experiments and meetings in the shipyard, even when the experiment conditions are so severe, he has always been with me. Thanks to Ms. Junko Mizuno, Ms. Kazuko Yamamoto, Ms. Mieko Uemura, Ms. Tomoko Otsuka, MS. Fumiko Samejima for their kind supports of administrative affairs.

I appreciate supports from my lab members. To my seniors who have already graduated from my lab: Mr. Kohta Tsubouchi, who gave me many valuable advice. Ryu Yanagisawa, who was very kind in my memory; Yoshiaki Oida, who also did the research in the same area as me, and was always generous for sharing his brilliant ideas with me, giving very valuable suggestions on my research; Jae Youl Kim, who used to be the other international student of the only two foreign students in my lab after I started my PHD course sharing a lot of common joys and culture shocks with me.

I am grateful to the graduated lab members who have been accompany with me since the beginning: Huanan Cao, who shared my troubles and joys, I felt stronger

with his support; Shunsuke Kado, who had a lot of manliness and confidence and somehow thankfully transferred to me; Takashi Hasegawa, who was so brilliant and insightful; Shogo Kimura, who also worked in the same research area with me and always shared his super smart opinions with me.

I cannot forget my great respect to the diligent and intelligent juniors in my lab : Satoru Nakamura, who is now also a PHD student in my lab and never had hesitation whenever I need any help; Takaaki Hiroi, who is the most diligent student I ever met and must have a bright future; Hiroya Matsubara, who has both the intelligence and the great composure which is rare in his age, playing an exceedingly important role in my research team; Tomoki Saito, who is a real gentleman helping me with the experiments in the shipyard disregarding the extremely bad conditions; Shinnosuke Wanaka, who holds exceptional mature opinions in the common research life and never had hesitation to share them with others; Yoshihiro Mizubayashi, who is so expert in Math sharing computational ideas. Sincere thanks also go to Ryuji Ueno, Takuya Goto and Nobuhito Manome who are very nice to share their ideas and organize a lot of seminars inspiring me a lot; and thanks to Kodai Ito, Kota Okada, Yasuyuki Kin and Shoji Morooka.

Thanks also should go to the juniors who has already graduated from my lab: Kei Ishiguro, Yu Kawano, Saki Ando, Kyohei Koyama and Masaru Isonuma, who were so kind and ready to give me help any time I needed. They let me recognize how wonderful to learn things when trying to instruct the juniors.

I learned and experienced a lot during my Master and PHD study. I will definitely benefit a lot from these 5 years in the future.

Thanks to my friends who have been there for me.

Thanks to my family who gave me the biggest support for my pursuit of the overseas study.

APPENDIX**A.1 Automation engine and configurations in shipyard**

A1.1 Overview of the automation engine

Systems for supporting both the cold forming process and the heating forming process are introduced. However, when trying to introduce these systems into the shipyard, it is almost impossible to have the workers use these systems directly due to the complicated operation of all the measurement and analysis steps.

Besides, in practical use, not only the systems mentioned above, but also the scanner and the scanner moving crane should be automatically controlled for facilitating the whole measurement and analysis flow.

On the other hands, there are usually multiple manufacturing spots in the shipyards, while only one or two scanners are available at once for each manufacturing process (cold forming or heating forming). Therefore, for all the manufacturing spots, there should be specialized measurement parameters such as the scope of one scan shot, the scan density and the region growing seed's location of every spot. And the measurement parameters should be automatically modified when trying to scan curved shell plates at another manufacturing spots.

Especially, because the manufacturing environments of the cold forming and the heating forming are different, the automation engine should be flexible enough to be adopted in both of these environments.

The basic concept of the automation engine developed in this research is to operate the Press Support System, Virtual Template System, the necessary external systems and the scanner automatically instead of the manual operation. And to satisfy different manufacturing environments in shipyards, all the parameters varying in different environments should be able to be customized by the administrators of the shipyards.

The overview of the automation engine is as shown in Figure a1-1. Four kinds of configuration files are designed to be customized as below:

- AE user interface configuration file – ui.conf
- Operation configuration file – op.conf
- Path configuration file – path.conf
- External system configuration file – exui.conf

Two threads work together to operate the systems automatically according to the workers' requirements.

- UI paint thread
- System operation thread

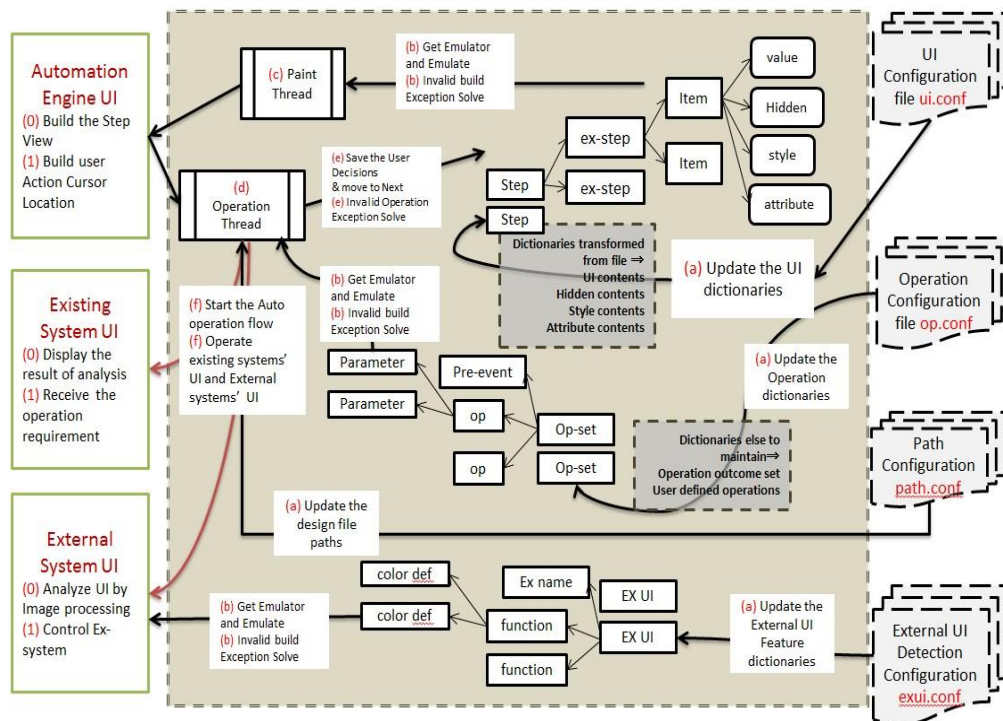


Figure a1-1 Overview of automatic engine

There are three UIs in this overview.

- Automation engine UI
- Existing systems' UI (VTS and PSS)
- External systems' UI

The automation engine UI is generated and painted on computer based on the UI configuration file in real time. The Existing systems' UIs and the External systems' UIs are evoked when necessary based on the Operation configuration file. And by

using the functions of the operation system, automation engine can control the mouse to move and click on these UIs imitating the human operation.

A1.2 Automation flow setting

Sun also developed an automation flow setting system in 2013. This system had two configuration files:

- AE user interface configuration file – ui.conf
- Operation configuration file – op.conf

The virtual template prototype introduced in 7.1.1 was automatized by this system. However, there are two problems existing in this system:

- The design files' path and some of the operation flow was hard coded, therefore it can only automatize one expected system such as the VTS. When trying to automatize another system, only the modification of the two configuration files is not enough.
- When trying to control some external systems, the locations of the buttons and flags have to be pre-set manually which cost a lot of time during the system introducing to shipyards.

A1.3 Macro design for multiple system detection and control

In this research, four configuration files are used to satisfy different requirements in the environment of the shipyards. These configuration files are written in the form of XML and are read on run time. Therefore, without recompile the system, only by modifying these XML files, the automatic flow of the measurement and analysis for both the cold forming process and the heating forming process can be changed whenever necessary.

Automatic UI configuration

As shown in Figure a1-1, three trees including the UI tree, operation tree and external system UI tree are generated based on these configuration files. The data

format for the automation engine UI configuration files is designed as shown in Figure a1-2. Multiple steps representing different user selection steps are customized in this file. After the UI is generated and painted based on this configuration file, the workers can select the necessary information as they want.

```
1 <UI>
2 <Step type="select">
3   <name>測定地</name>
4   <style>
21   <sound>Step1.mp3</sound>
22   <items ex-step="0">
28 </Step>
29
30 <Step type="select">
31   <name>船型</name>
32   <style>
49   <sound>Step2.mp3</sound>
50   <items ex-step="0">
54 </Step>
55
56 <Step type="select">
57   <name>ブロック</name>
58   <style>
75   <sound>Step2.mp3</sound>
76   <items ex-step="1">
80   <items ex-step="2">
83 </Step>
84
85 <Step type="select">
86   <name>外板</name>
87   <style>
104   <sound>Step3.mp3</sound>
105   <items ex-step="1">
109   <items ex-step="2">
114 </Step>
115
116 <Step type="confirm">
117   <name>確認</name>
118   <style>
135   <sound>Confirm.mp3</sound>
136   <items ex-step="0">
139 </Step>
140
141
142 <Step type="loop-option">
166
167 </UI>
```

Figure a1-2 Automation engine UI configuration file

The details of each user interface are shown in Figure a1-3. Every step has a name, ex-step's number, display style settings and the display items. Every step of the user interface is painted on computer based on the information from this file.

```

56 <Step type="select">
57   <name>ブ ロ ッ ク</name>
58   <style>
59     <color comment="A,R,G,B">255,173,216,230</color>
60     <shape comment="eclipse | rectangle">rectangle</shape>
61     <padding comment="left, right, up, down">2,2,2,2</padding>
62     <font>
63       <font-item>
64         <color comment="A,R,G,B">255,0,0,0</color>
65         <bold>true</bold>
66         <size>16</size>
67       </font-item>
68       <font-item>
69         <color comment="A,R,G,B">255,255,127,80</color>
70         <bold>false</bold>
71         <size>18</size>
72       </font-item>
73     </font>
74   </style>
75   <sound>Step2.mp3</sound>
76   <items ex-step="1">
77     <item id="1">BC3</item>
78     <item id="2">FVDP-SL13P</item>:
79   </items>
80   <items ex-step="2">
81     <item id="1">TEST1</item>
82   </items>
83 </Step>

```

Figure a1-3 Details of automation engine UI configuration

Figure a1-4 illustrates the generated user interfaces of the automation engine. The items shown on these user interfaces and the styles of these items are all based on the UI configuration files customized by the administrators of the shipyards. And the workers only need to select from these items to choose the target they want to measure and analyze.

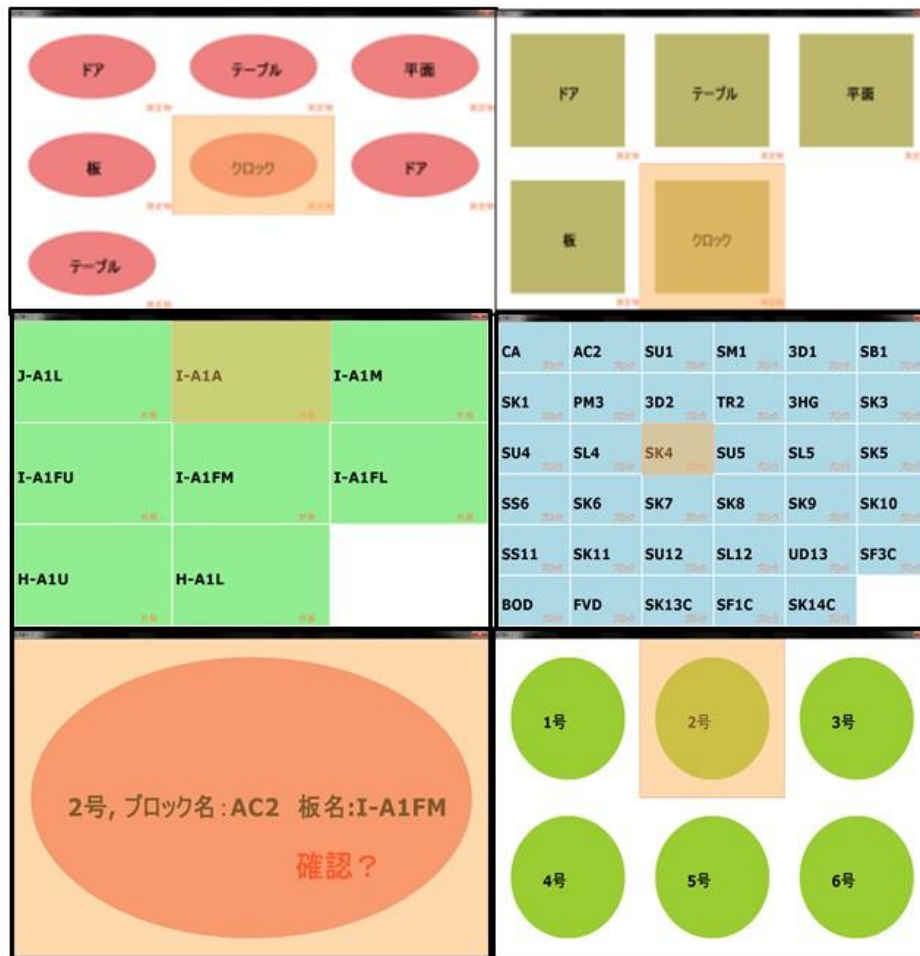


Figure a1-4 Generated user interface

Operation configuration

As shown in Figure a1-5, every single operation step which was used to be operated manually is defined as an “op-set” in the operation configuration files. Automation engine automatically conducts the operation one by one according to this file. Every “op-set” has an attribute “comment” to clarify the main purpose of this operation step.


```

1  <operation>
2  +  <op-set comment="adjustScreen">
27
28 +  <op-set comment="setSymbol">
50
51 +  <op-set comment="openDialog">
68
69 +  <op-set comment="setTexttoDialog">
93
94 +  <op-set comment="pushOKButton">
112
113 +  <op-set comment="openDialog">
130
131 +  <op-set comment="setTexttoDialog">
155
156 +  <op-set comment="pushOKButton">
174
175 +  <op-set comment="openDialog">
192
193 +  <op-set comment="setTexttoDialog">
217
218 +  <op-set comment="pushOKButton">
236
237 +  <!--
392
393 +  <op-set comment="Analyze">
423
424 +  <op-set comment="showResult">
447
448 +  <op-set comment="beginLoop">
480 </operation>

```

Figure a1-5 Operation configuration file

The details of each operation step are illustrated in Figure a1-6. Every single operation step has a “pre-event” which declare the former operations and the expected “time-out” scale of this step.

In practical use, every single operation of human accurately contains multiple steps when operated by computer. Thus, every “op-set” contains multiple “op” in the majority of cases. Each single “op” has attributes of an operation name, operation target object, and parameters obtained from the UI configuration.

The parameters selected for each UI step are passed to the operation flow using the special identifications “UIVALUE_X”. “X” means the index of the referred UI

step.

```

131 | <op-set comment="setTexttoDialog">
132 |   <pre-event object="thread" type="sleep">
133 |     <timeout>1500</timeout>
134 |   </pre-event>
135 |   <op type="FindWindow" level="window">
136 |     <name>Handle_1</name>
137 |     <object></object>
138 |     <classname></classname>
139 |     <windowname>開 <</windowname>
140 |   </op>
141 |   <op type="FindWindowEx" level="control">
142 |     <name>Handle_2</name>
143 |     <object>Handle_1</object>
144 |     <strclass>ComboBoxEx32</strclass>
145 |     <FrmText></FrmText>
146 |   </op>
147 |   <op type="SendMessageGroup" level="control">
148 |     <object>Handle_2</object>
149 |     <name></name>
150 |     <Msg>WM_SETTEXT</Msg>
151 |     <wParam>0</wParam>
152 |     <lParam>UIVALUE_2,UIVALUE_3,UIVALUE_4;_rollerlines.csv</lParam>
153 |   </op>
154 | </op-set>

```

Figure a1-6 Details of operation configuration

Path configuration and external system configuration

The external system such as the crane control system is analyzed using the colors of the buttons which are supposed to be clicked manually. As shown in Figure a1-7, the colors of different buttons are recorded in the external system configuration file. Automation engine analyzes these colors and the area these colors occupy to identify the controls of these external systems such as buttons or dropdown lists. After that, according to the operation configuration, automation engine operates these controls automatically.

At last, the path configuration file as shown in Figure a1-8 enables the administrators in the shipyards to customize their own folders to store the input design files, scanned files and the output analysis files such as the histograms and color maps.

```

1  <External>
2  <Externalsys content = "scanner moving crane">
3      <GreenColor>ff1ea801</GreenColor>
4      <Yellow>ffffff02</Yellow>
5      <GrayYellow>ffc3ca01</GrayYellow>
6      <LightOn>ff57ffed</LightOn>
7      <LightOff>ff857f76</LightOff>
8  </Externalsys>
9
10 <Externalsys content = "connection checking">
11     <GreenColor>ff1ea801</GreenColor>
12     <Yellow>ffffff02</Yellow>
13     <GrayYellow>ffc3ca01</GrayYellow>
14     <LightOn>ff57ffed</LightOn>
15     <LightOff>ff857f76</LightOff>
16 </Externalsys>
17 <!--
24 </External>

```

Figure a1-7 External system configuration

```

1  <Path>
2  <workspace content= "design main">C:\Users\daisy\Desktop\Workspace</workspace>
3
4  <workspace content= "roller line">C:\Users\daisy\Desktop\Workspace\roller</workspace>
5
6  <workspace content= "CAD files">C:\Users\daisy\Desktop\Workspace\cad</workspace>
7
8  <workspace content= "DXF files">C:\Users\daisy\Desktop\Workspace\dxfl</workspace>
9
10 <workspace content= "output">C:\Users\daisy\Desktop\Workspace\output</workspace>
11
12 </Path>

```

Figure a1-8 Path configuration

Tolerance value setting for different plates

The tolerance value setting for different plates follows the width and the thickness of the plates. The relationship is as shown in the following table.

Table a1.1 Correlation between tolerance setting and the plate thickness

Plate Width \ Plate Thickness	~ 15mm	15~20 mm	20~25 mm	35mm ~
~ 1000mm	none	Normal tolerance value	Normal tolerance value	Strict tolerance value
1000~ 3000mm	Normal tolerance value	Normal tolerance value	Normal tolerance value	Strict tolerance value
3000mm~	Flexible tolerance value	Flexible tolerance value	none	none

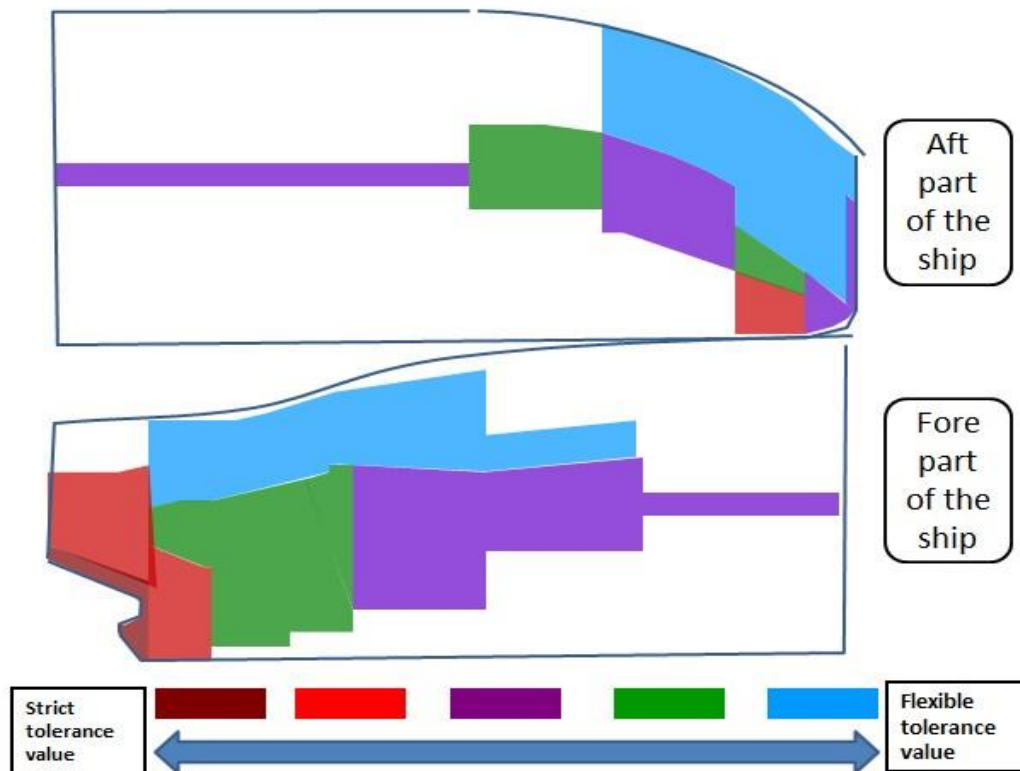


Figure a1-9 Correlation between tolerance setting and the ship part



Figure a1-10 Customized numeric keyboard



Figure a1-11 Laser scanner located at the cold forming spot

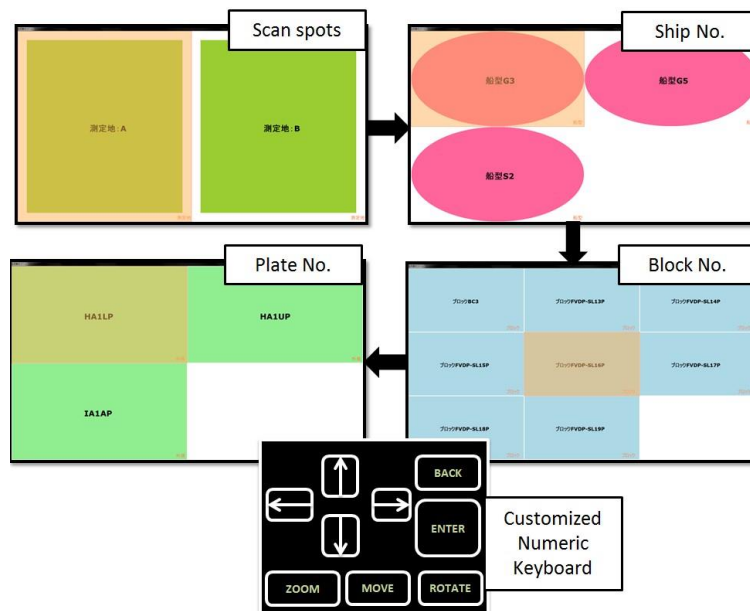


Figure a1-12 Generated UI of the cold forming support framework

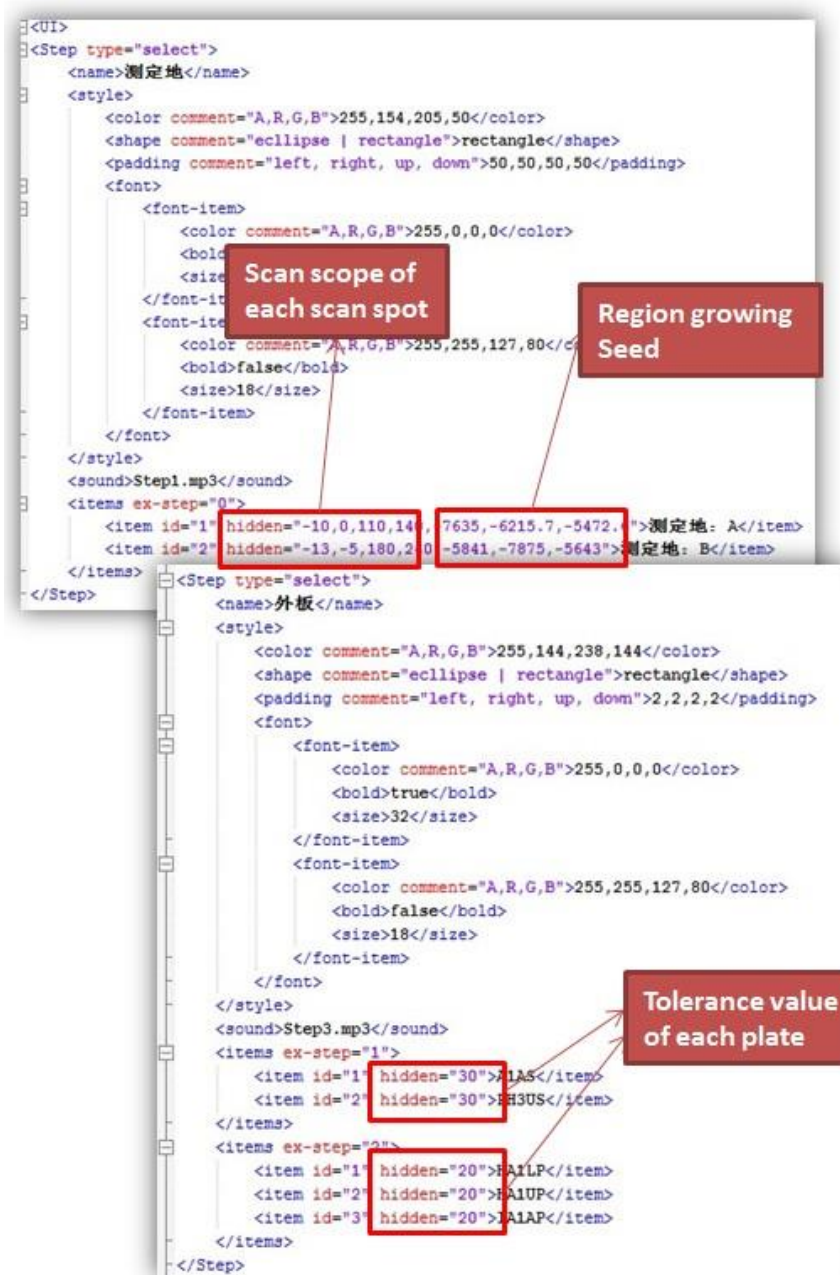


Figure a1-13 Scan scope setting and tolerance value setting

Relations between the heating conditions and the contraction

Though the heating grades and heating areas are outputted by the proposed framework, the manufacturing conditions which change when manufacturing different kinds of plates are also expected to be decided based on the evaluation. Therefore, in this preliminary experiment, the relations between the following

heating and refrigeration conditions and the plate's contraction will be indicated through some experiments.

(1) Point heating

- Refrigeration method (by water / by air)
- Heating direction (from upper side / from underside)
- Plate thickness (mm)

(2) Line heating

- Heating speed
- Refrigeration direction (from upper side / from underside)
- Plate's thickness (mm)

Table a1.2 Experiments in different manufacturing conditions

<i>Plates for point heating (refrigeration from upper side)</i>					
<i>No</i>	<i>Plate Thickness (mm)</i>	<i>Plate Size (mm)</i>	<i>Temperature before heating (°C)</i>	<i>Temperature after heating (°C)</i>	<i>Refrigeration Method</i>
1	14	470 × 470	7	1030	Water
2	17	470 × 470	17	1056	Water
3	22	470 × 470	15	1050	Water
4	14	470 × 470	8	1018	Air
<i>Plates for line heating (water refrigeration)</i>					
<i>No</i>	<i>Plate Thickness (mm)</i>	<i>Plate Size (mm)</i>	<i>Temperature before heating (°C)</i>	<i>Temperature after heating (°C)</i>	<i>Heating Speed (mm/min)</i>
1	14	470 × 470	17	934	170
2	22	470 × 470	15	926	170
3	14	470 × 470	22	875	210
4	14	470 × 470	16	832	260

The plate conditions used in this preliminary experiment are listed in Table a1.2. And the result will be summarized in the following sub-sections.

(1) Point heating

All of the plates used to evaluate the point heating contraction have the refrigeration done from upper side of the plate. And the heating time is 60s. The heating point's radius is 70mm.

Figure a1-14 shows that under the same heating time and heating speed, the plate which is relatively thicker will get less contraction than other plates. In the following general experiments, the plates used are all 14mm.

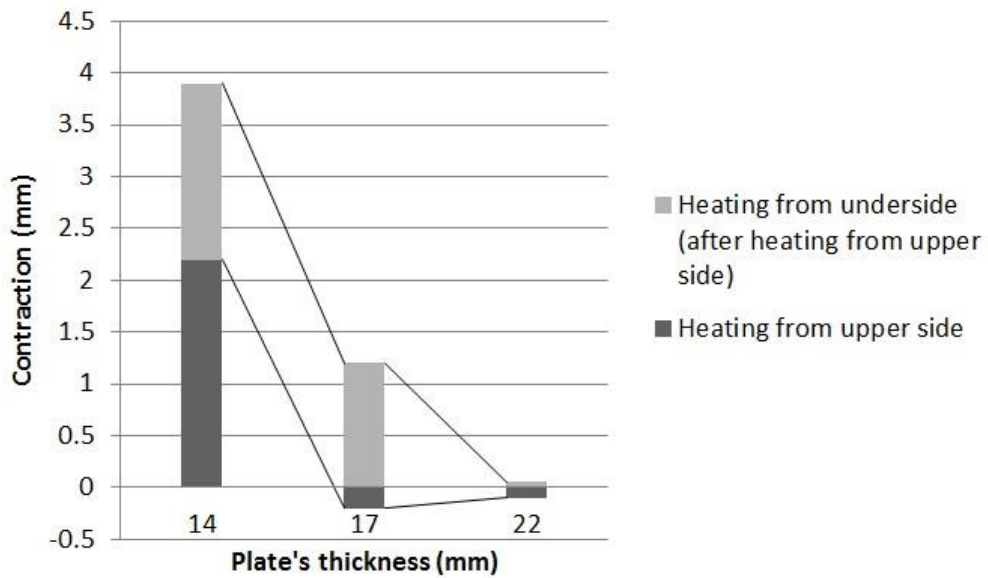


Figure a1-14 Relation between the plate's thickness and the contraction of the plate (Refrigeration by water)

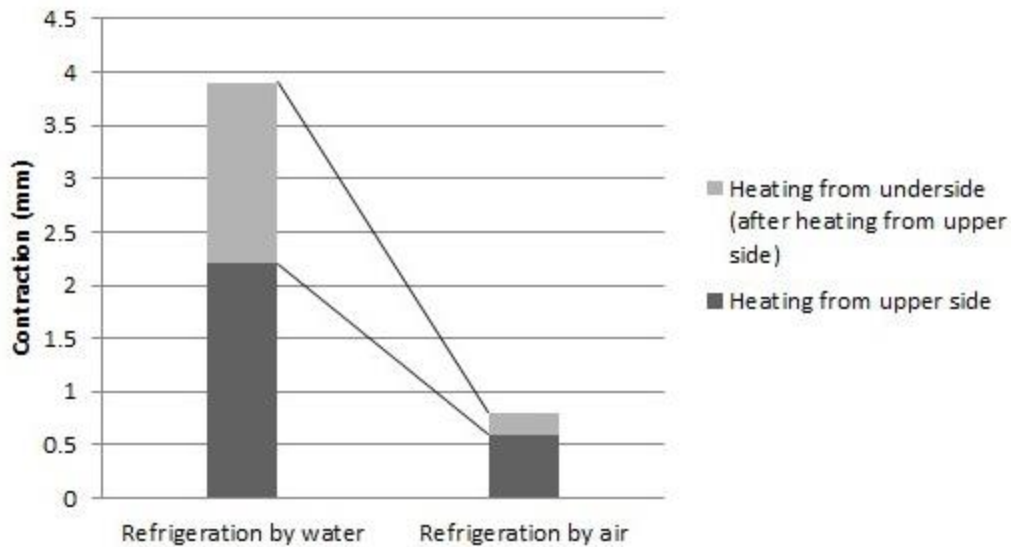


Figure a1-15 Relation between the refrigeration method, heating direction and the contraction of the plate (Plate's thickness: 14mm)

Figure a1-15 shows that refrigeration using water can lead to more contractions than that using air. In the following general experiments, the plates will all be refrigerated by water.

(2) Line heating

All of the plates used to evaluate the line heating contraction have the refrigeration done using water. The heating line's length is about 300mm.

Figure a1-16 shows the contraction results after the heating of 170mm/min from the upper side of the plate. It can be seen that the contraction direction can be changed by doing the refrigeration from the other side of the plate when the plate thickness is 14mm which gives the workers an option to modify the over bending without upturning the plate.



Figure a1-16 Relation between the plate's thickness and the contraction of the plate (Heating speed: 170mm/min; Heating from upper side)

Figure a1-17 shows the relation between the heating speed and the contraction of the plate when doing the heating from upper side. In the following general experiments the heating speed are all set to 170mm/min or 260mm/min.

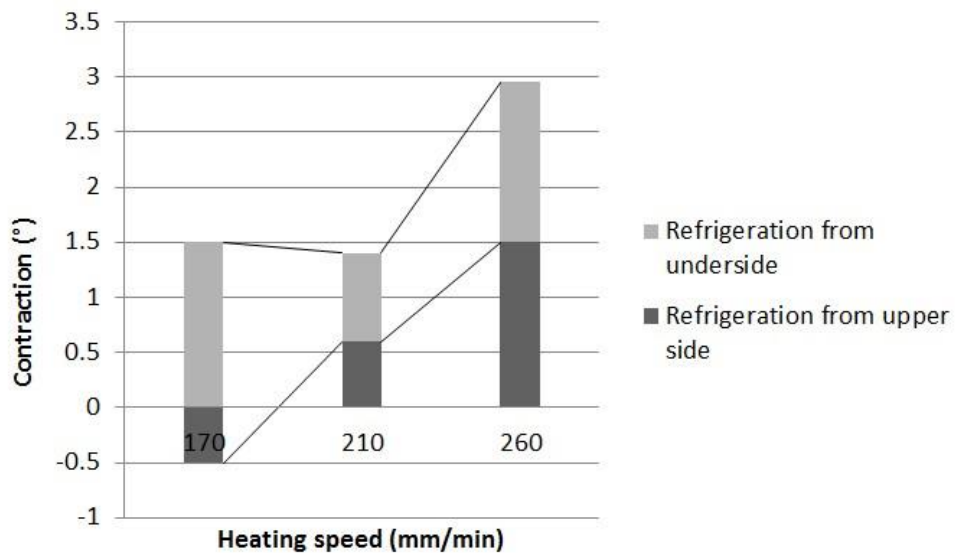


Figure a1-17 Relation between the heating speed and the contraction of the plate (Plate's thickness: 14mm; Heating from upper side)

From this preliminary experiment, the manufacturing conditions for the following general experiment 1, 2 and 3 are decided as below:

Table a1.3 Experiment conditions in the general experiments

<i>Experiment conditions for point heating (refrigeration from upper side)</i>					
<i>Items</i>	<i>Plate Thickness (mm)</i>	<i>Refrigeration Method</i>	<i>Heating Time (s)</i>	<i>Heating Radius (mm)</i>	<i>Expected Contraction (mm)</i>
<i>Value</i>	14	By water	60	70	2.2 (upper heating) 1.6 (under heating)
<i>Experiment conditions for line heating (water refrigeration)</i>					
<i>Items</i>	<i>Plate Thickness (mm)</i>	<i>Refrigeration Method</i>	<i>Heating speed (mm/min)</i>	<i>Expected Contraction with heating line of 300mm (°)</i>	
<i>Value</i>	14	By water	170	-0.5 (upper refrigeration) 1.5 (under refrigeration)	
			260	1.5 (upper refrigeration)	

A.2 Possible usage of the accumulated data in the future

In this section, we assume that there are already enormous manufacturing data recorded by VTS, and within them, different workers hold different manufacturing opinions on the same situation of the plate sometimes. The data-based model introduced in this chapter cannot be totally verified currently because the data is not abundant enough yet, but is expected to be able to play a positive role in picking the right instructions from these arguments for the beginner workers.

The reason why the tacit knowledge existing in these manufacturing processes is difficult to be explained sometimes is because there is not yet an efficient way to describe the manufacturing processes especially with multiple expert workers because sometimes they have different opinions on the same plate's situation. Therefore, it is not possible to analyze these processes efficiently even there is enough data recorded. Besides, the knowledge provided by different expert workers should be properly evaluated and restructured before being used in the future daily manufacturing.

This sub-section proposes a process knowledge model for facilitating the complicated industrial components' manufacturing supposing that there are already enormous data recorded by the VTS. The manufacturing process of the complicated component is modeled as a sequence of the situations under which the experienced workers made their manufacturing decisions and the actions which the workers took under the given situation. Every situation and action can be broken down into a set of elements representing the detailed items constituting this manufacturing step. Then the element pair of the situation and action is evaluated using the recorded manufacturing data and stored in the knowledge model. When manufacturing a new component under the similar situation, the most efficient action is suggested by the constructed knowledge model in the form of a combination of the action elements which are fuzzily inferred to be the most effective ones under the given situation.

At first, a process model regarding the generalized manufacturing process as a sequence of the situations and actions as shown in Figure a2- which could represent the most generalized manufacturing process existing in today's industry is built.

Facing one group of the similar given situation S of the component, multiple experts or one experts in different periods may use different manufacturing plans A , and based on different manufacturing plans, there are different subsequent manufacturing steps until the component reaches the designed target situation S_{target} .

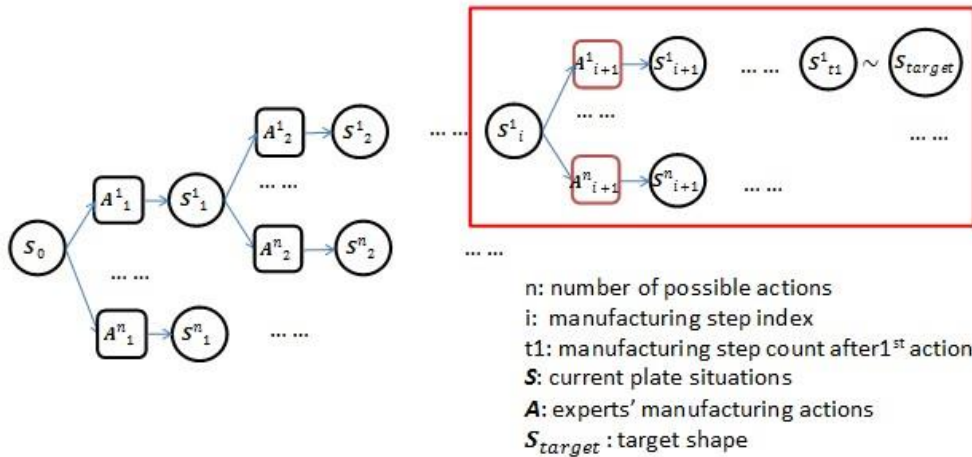


Figure a2-1 Process modeling (Sun, J.Y, ISPE, 2015)

To analyze how proper each action (from $A^{1_{i+1}}$ to $A^{N_{i+1}}$) is when facing the situation S^1_i (or similar situations' group), the subsequent manufacturing from S^1_i as shown in Figure a2-2 should be evaluated. Multiple representative milestones (M_1, \dots, M_D) are set. The count of the total subsequent manufacturing steps d and the count of the subsequent milestones D are found out. The concept is that the better action is that make the manufacturing steps numerical less (smaller d) and more comprehensible (smaller D).

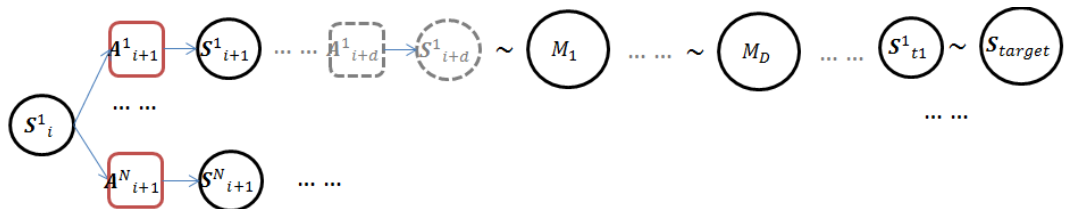


Figure a2-2 Subsequent manufacturing analyzing (Sun, J.Y, ISPE, 2015)

The structure of the whole knowledge modeling process which implemented the

proposed approach is illustrated in Figure a2-3. The recording data to be analyzed representing the manufacturing situations and the multiple actions took by experienced workers is recorded in the manufacturing scenario DB. After a series of processes which will be introduced later, an expert knowledge model with a set of elicited rules is constructed. Then an effective inference process is instituted facilitating the using of the constructed knowledge model.

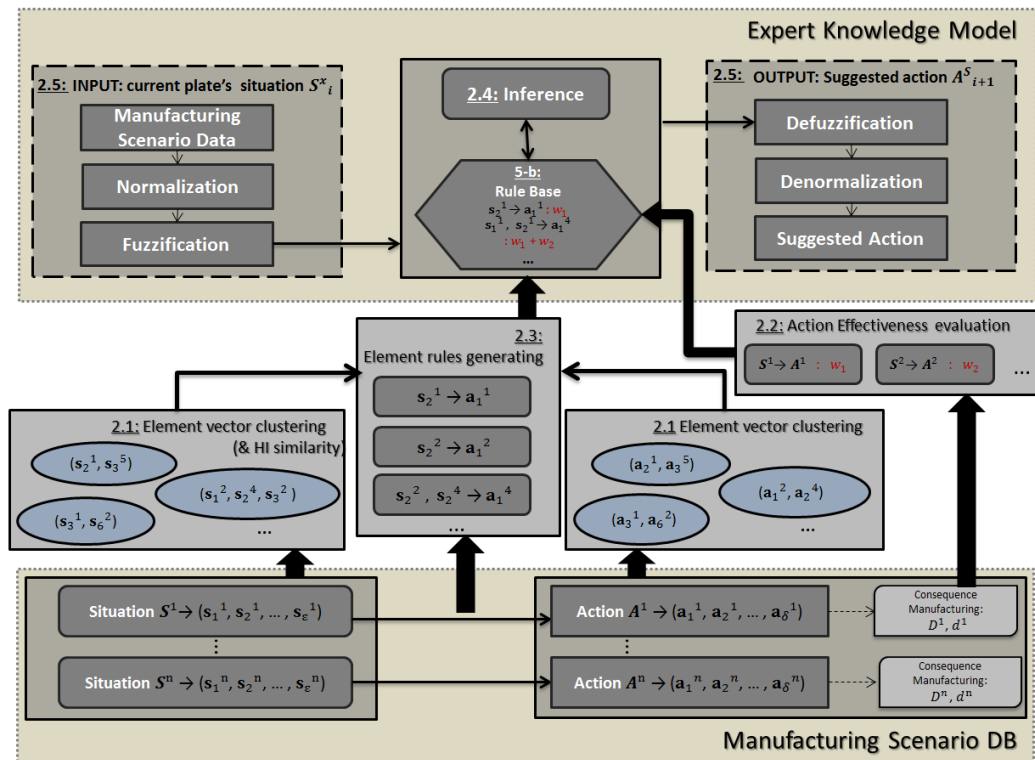


Figure a2-3 Process knowledge model (Sun, J.Y, ISPE, 2015)

A.2.1 Element storing of situation and action

Assuming both the situations and actions can be broken down in to a series of elements, the basic inferences from the situation to action and the clustering of different situations and actions are conducted towards these elements. When there are multiple data pairs, clustering method such as K-means is used to cluster these element situations and element actions based on the vector distances between them.

a. $S^x \rightarrow (s_1^x, s_2^x, \dots, s_\varepsilon^x)$

- b. Cluster situation elements based on the similarity between them
- c. $A^x \rightarrow (a_1^x, a_2^x, \dots, a_\delta^x)$
- d. Cluster action elements based on the similarity between them

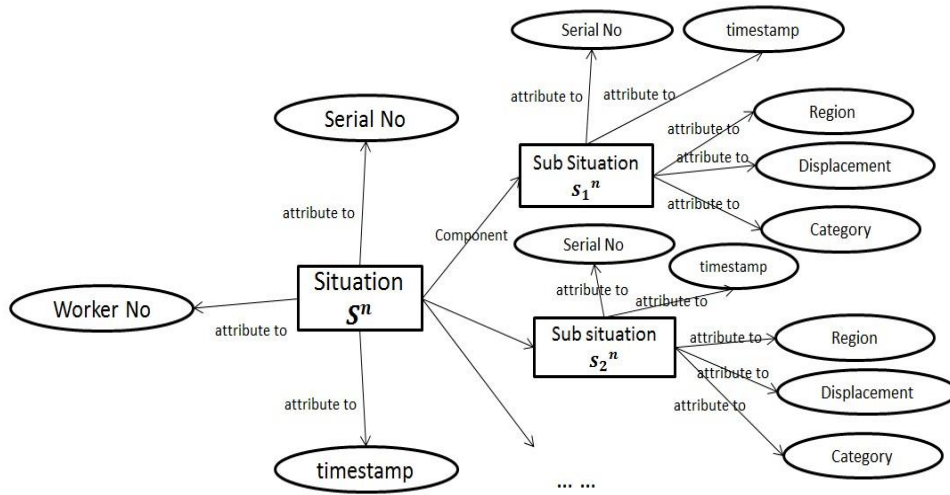


Figure a2-4 Ontology of situations

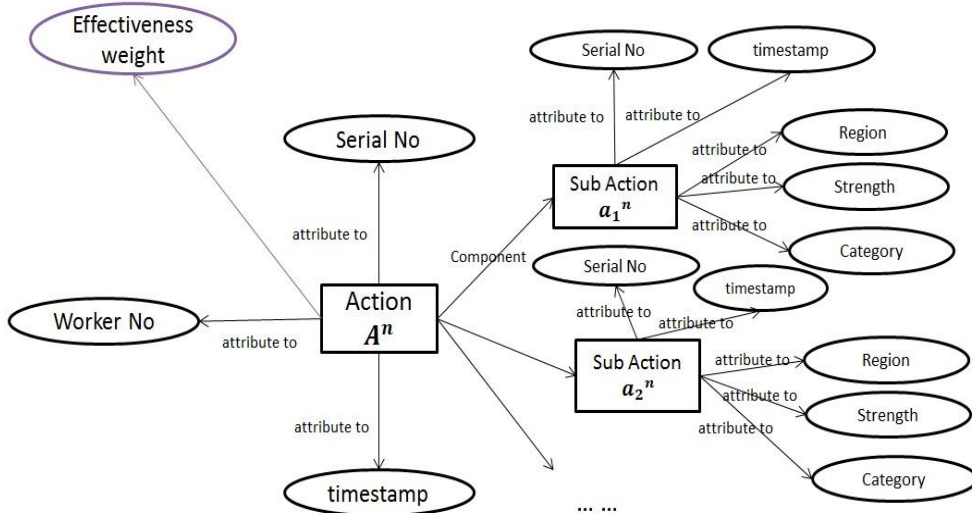


Figure a2-5 Ontology of actions

The ontologies of the situations and actions are shown in Figure a2-4 and Figure

a2-5. There are multiple ways to construct these situations and actions for different analysis purpose. One simple example is : Suppose that there are n frame points on the heating line (or n frame points around the heating point), the vector of situation usually has the element value for each dimension including the locations of the curvature error region, the grade of the error (X1: error grade of frame point1, X2: error grade of frame point2, ..., Xn: error grade of frame pointN); while the vector of the actions has the element value for each dimension including the heating area's region (X : the relative location comparing to the roller lines, Y: the relative location comparing with the frame lines of the plate, Z: the heating line's length or the heating point's area).

A.2.2 Knowledge elicitation after data accumulation

This knowledge model is mainly used to handle the cases in which different workers have different manufacturing ideas. Assuming they are dealing with the plates with extremely high similarity, the effectiveness of the actions they took can be evaluated based on the subsequent manufacturing steps' count d and the subsequent manufacturing milestones' count D .

- a. Find / Estimate count d of milestones from M_1 to M_D
- b. Find / Estimate count D of necessary manufacturing steps from S^1_i to S^1_{i+d}
- c. Set 2 weights to each A^x_{i+1} using D and d and a general weight ω^x_{i+1} , γ_1 and γ_2 can be changed when being applied to different components.

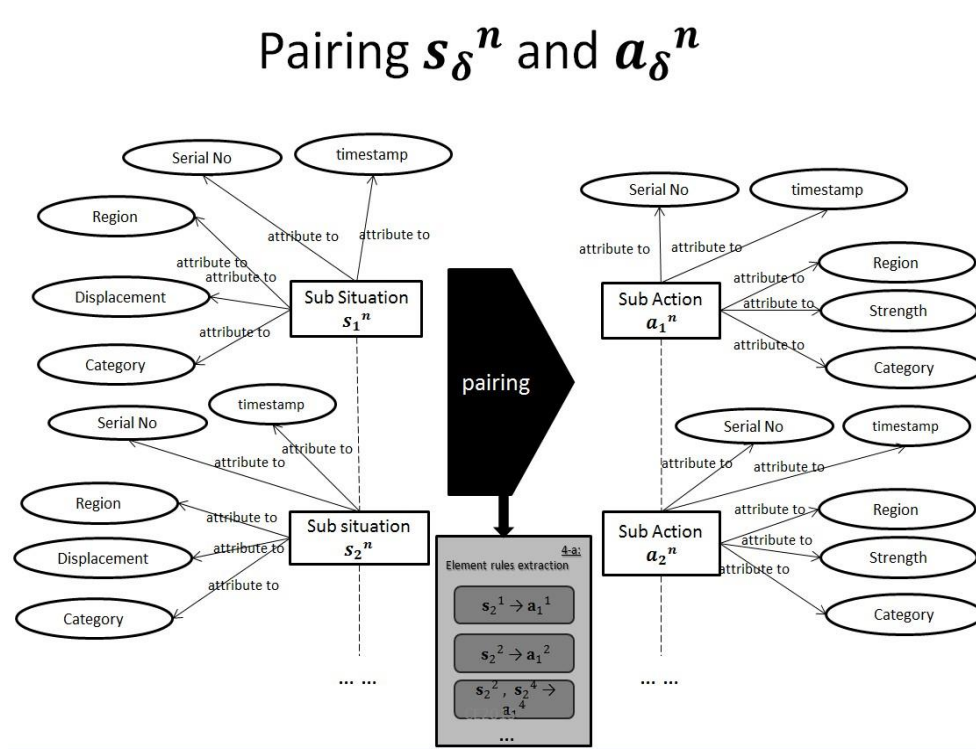
$$W^x_{i+1} = \frac{1}{2\pi\sigma^2} e^{-\frac{(D^x)^2}{2\sigma^2}} \quad w^x_{i+1} = \frac{1}{2\pi\sigma^2} e^{-\frac{(d^x)^2}{2\sigma^2}} \quad (3)$$

$$\omega^x_{i+1} = \frac{\gamma_1 \times W^x_{i+1} + \gamma_2 \times w^x_{i+1}}{\gamma_1 + \gamma_2} \quad (4)$$

The knowledge model constructed by the evaluated weighted rules is built according the following steps:

- a. Generate element rules like (If s_l , then a_k). When both the similarities (the clustering result) of the situation and action elements are big enough, the two element rules can be seen as the same rule.

- b. Decide Fuzzification and Defuzzification regulations according to the specific manufacturing process.
- c. Give calculated weight to the generated element rules.



A.2.3 Knowledge dissemination after data accumulation

When using the knowledge model to try to get an instruction (especially when there are controversial opinions) under certain situation, the inference process of the knowledge model is as below:

- a. Substitute the component's situations $S_f = (f_1, f_2, \dots, f_{\delta})$ into the generated rule base.
- b. Get every inferred element actions : $A_{inf} = (a_{inf_1}, a_{inf_2}, \dots)$
- c. Give each element actions a_{inf_z} in A_{inf} the weight

$$\overline{\omega}_{inf} = \frac{\sum(\gamma_1 \times W_{i+1}^X + \gamma_2 \times w_{i+1}^X)}{\gamma_1 + \gamma_2} \quad (5)$$

(W_{i+1}^X and w_{i+1}^X are the weights of the actions A in which a_{inf_1}

exists)

d. Choose the top δ element actions ranked by $\overline{\omega_{inf}}$ and build the result Action :

- $A_r = (a_{\sigma_1}, a_{\sigma_2}, \dots)$

Besides, because not all the situation elements match perfectly with the former ones used to construct the knowledge model, and a rule should not be fully followed when it has a low strength, the whole inference process should be fuzzed as the following figure when generate the output suggested actions. The Fuzzification of the input data is as below: W_N is the general weight of each rule and VT_N is the situations' similarity between the known rule and the input rule. O is the output strength of each selected rule.

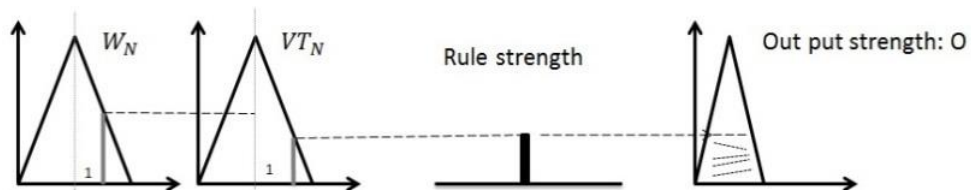


Figure a2-7 Fuzzification process (Sun, J.Y, ISPE, 2015)

PUBLICATIONS

Overview

- A) *Awards*: 2
- B) *Contributed Article*: 1
- C) *Journals*: 4
- D) *International Conferences (With peer reviews)*: 3
- E) *International Conferences (Without peer reviews)*: 3
- F) *National Conferences*: 6

A) Awards

- [1] 日本船舶海洋工学会奨学褒賞, 社団法人日本船舶海洋工学会, 2013
- [2] Best Student Paper Award, 20th ISPE International Conference on Concurrent Engineering, 2013.09

B) Contributed Article

- [1] Kazuo Hiekata , Jingyu Sun, Junichi Hirata: Innovative Technologies And Products Applied For Marine Industry, Computer-aided approach for manufacturing in shipyard; SNAME, The International Community For Maritime And Ocean Professionals ; 2015 Oct. 11-14

C) Journals

- [1] Kazuo Hiekata, Hiroyuki Yamato, Jingyu Sun, Hiroya Matsubara, Naoji Toki: Study on Improving Accuracy for Edge Measurement Using 3D Laser Scanner ; Product Lifecycle Management for a Global Market IFIP Advances in Information and Communication Technology, 2014, p.427-434 Vol. 442
- [2] Jingyu Sun, Kazuo Hiekata, Hiroyuki Yamato, Norito Nakagaki, Akiyoshi Sugawara : Efficient Point Cloud Data Processing in Shipbuilding : Reformative Component Extraction Method and Registration Method ; IJCC,Journal of Computational Design and Engineering Society of CAD/CAM Engineers Volume 1, Number 3, July 2014, pages 202-212
- [3] Jingyu Sun, Kazuo Hiekata, Hiroyuki Yamato, Norito Nakagaki, Akiyoshi Sugawara : Virtualization and automation for knowledge extraction in curved shell plates' machining plan design process ; IJASM, International Journal of Agile Systems and Management, 2014, p.282-303 Vol.7
- [4] 中垣憲人, 菅原晃佳, 稗方和夫, 大和裕幸, 孫晶鈺 : レーザスキャナによる曲がり外板の工作精度評価システムの研究開発 (第2報) ; 日本船舶海洋工学会論文集 2013. Vol. 17, 2013, pp. 169-176

D) International Conferences (With peer reviews)

- [1] Jingyu Sun, Kazuo Hiekata, Hiroyuki Yamato, Pierre Maret Fabrice Muhuhlenbach : Process Knowledge Model For Facilitating Industrial

Components' Manufacturing ; 22th ISPE International Conference on
Concurrent Engineering, 2015.07, p.406-415

- [2] Jingyu Sun, Kazuo Hiekata, Hiroyuki Yamato, Norito Nakagaki, Akiyoshi Sugawara ; A Knowledge-Based Approach for Facilitating Design of Curved Shell Plates' Machining Plans; 21th ISPE International Conference on Concurrent Engineering, 2014.09, p.143-152

- [3] Jingyu Sun, Kazuo Hiekata, Hiroyuki Yamato, Norito Nakagaki, Akiyoshi Sugawara : Automatic Generation of Curved Shell Plates' Processing Plan Using Virtual Templates for Knowledge Extraction ; 20th ISPE International Conference on Concurrent Engineering, 2013.09, p.441-450

E) International Conferences (Without peer reviews)

- [1] Kazuo Hiekata, Hiroyuki Yamato, Jingyu Sun, Hiroya Matsubara, Naoji Toki : Development of Method for High Accuracy Edge Measurement Using 3D Laser Scanner ; PLM International Conference on Product Lifecycle Management, 2014.07

- [2] Jingyu Sun : Knowledge-based Approach for Facilitating Design of Curved Shell Plates' Manufacturing Plans in 3D Virtual Environment ; PLM International Conference on Product Lifecycle Management, 2014.07

- [3] Jingyu Sun, Kazuo Hiekata, Hiroyuki Yamato, Norito Nakagaki, Akiyoshi Sugawara : Development of Software System For Generating Curved Shell Plate's Processing Plan Using Virtual Templates ; ICCAS, International Conference on Computer Applications in Shipbuilding, 2013, Busan, Korea, 2013.09, p.131-138 Vol.2

F) National Conferences

- [1] 孫晶鈺, 稗方和夫, 大和裕幸, 中垣憲人, 菅原晃佳 : 3D 計測データとバーチャル木型を用いた曲がり外板加工方案生成システムの開発と評価; 日本船舶海洋工学会講演会論文集 2014. Vol. 19, 2014, pp.603-606
- [2] 稗方和夫, 大和裕幸, 孫晶鈺, 中垣憲人, 菅原晃佳 : 3D 計測データとバーチャル木型を用いた曲がり外板加工方案生成システムの開発; 日本船舶海洋工学会講演会論文集 2013. Vol. 16, 2013, pp. 563-566
- [3] 稗方和夫, 大和裕幸, 孫晶鈺, 中垣憲人, 菅原晃佳: バーチャル木型による曲がり外板加工方案生成手法の開発; SIG-KST 知識・技術・技能の伝承支援研究会(人工知能学会 第2種研究会) 2013, SIG-KST-2012-03-05
- [4] 稗方和夫, 大和裕幸, 孫晶鈺, 中垣憲人, 菅原晃佳 : レーザスキャナによる曲がり外板工作精度評価システムの実用化; 日本船舶海洋工学会講演会論文集 2012. Vol. 15, 2012, pp. 117-120
- [5] 稗方和夫, 大和裕幸, 孫晶鈺, 中垣憲人, 菅原晃佳 : 3次元計測データによる曲がり外板加工方案設計プロセスのバーチャル化と知識抽出; SIG-KST 知識・技術・技能の伝承支援研究会(人工知能学会 第2種研究会) 2012, SIG-KST-2012-02-08
- [6] 稗方和夫, 大和裕幸, 孫晶鈺, 中垣憲人, 菅原晃佳 : 三次元計測点群データからの曲がり外板抽出アルゴリズムの開発; 日本船舶海洋工学会講演会論文集 2011. Vol. 13, 2011, pp. 159-162